

DEVELOPMENT OF A TSUNAMI FORECAST MODEL FOR SAND POINT, ALASKA

Yong Wei

January 30, 2009

Contents

Abstract	3
1. Background and Objectives.....	3
2. Forecast Methodology	4
3. Model development.....	5
3.1 Study Area	5
3.2. Historical events and water level data	5
3.3. Bathymetry and Topography in Alaska	7
3.4 Model Setup and Parameters	8
4. Results and Discussions.....	9
4.1 Model Validation	9
4.2 Modeling and Assessment of Artificial Mega Tsunamis.....	10
5. Potential Tsunamis Originated in Seismic Gaps in the Aleutians.....	11
5.1 Shumagin Seismic Gap and Unalaska Seismic Gap	11
5.2 Impact Assessment of Tsunamis Originated in the Shumagin and Unalaska Seismic Gaps	12
6. Summary and Conclusions	14
6. References.....	14

Abstract

As part of NOAA's Short-term Inundation Forecast of Tsunami (SIFT), this study addresses the development, model validation, and stability tests of the tsunami forecast model for Sand Point, Alaska. Based on the Method of Splitting Tsunami (MOST), the forecast model is constructed at a spatial resolution up to 50-60 m in the finest grid to accomplish 4-hr simulation of wave inundation onto dry land in only minutes of CPU time. A referenced inundation model is developed in parallel using grids of higher resolution up to 8.3 m to provide modeling references for the forecast model. The model validations using historical tsunami events show good agreement between the model computation and observations in spite of background noise, and provide quantitative estimation of the inundation, runup and computed maximum values for these events. The model stability is evaluated based on 43 hypothetical scenarios generated in all subduction zones of the Pacific Rim at different levels of M_w 9.3. This shows the robustness of the forecast model under the strike of 14-m-high waves.

1. Background and Objectives

The National Oceanic and Atmospheric Administration (NOAA) Center for Tsunami, Research (NCTR) at the NOAA Pacific Marine Environmental Laboratory (PMEL) has developed a tsunami forecasting capability for operational use by NOAA's two Tsunami Warning Centers located in Hawaii and Alaska (Titov *et al.*, 2005). The system is designed to efficiently provide basin-wide warning of approaching tsunami waves accurately and quickly. The system, termed Short-term Inundation Forecast of Tsunamis (SIFT), combines real-time tsunami event data with numerical models to produce estimates of tsunami wave arrival times and amplitudes at a coastal community of interest. The SIFT system integrates several key components: deep-ocean observations of tsunamis in real time, a basin-wide pre-computed propagation database of water level and flow velocities based on potential seismic unit sources, an inversion algorithm to refine the tsunami source based on deep-ocean observations during an event, and high-resolution tsunami forecast models.

Alaska has a greater earthquake and tsunami potential than any other state because of its proximity to one of the most seismically active regions in the world. The Alaskan-Aleutian Subduction Zone, where the Pacific Plate is subducting under the North America Plate, has the potential to generate both local and basin-wide tsunamis that threaten coastal communities in Alaska and the Pacific Basin. Distant and local earthquakes along subduction zones in the Pacific account for 80% of the origins of tsunamis that have impacted Alaskan coastlines. Historically, the highest tsunami water level measured at Sand Point is 61 cm from the 11 March 2011 Japan tsunami. However, potentially destructive tsunamis generated in the two major seismic gaps of Alaska, the Shumagin and Unalaska gaps, need special attention.

The main objective of this work is to develop a tsunami forecast model for Sand Point to maximize the length of time that the community has to react to a tsunami threat by providing accurate information quickly to emergency managers and other officials responsible for the community and infrastructure. An additional goal is minimization of false alarms that ultimately erode system credibility with the resident and fishing populations. Discussion of the details of the individual components of the Sand Point

forecast model, including the development of grids using bathymetry and topography, model validation using historical tsunami cases, model stability and robustness, sensitivity testing using synthetic tsunami events, the basic model setup, and model parameters are provided in this report.

2. Forecast Methodology

A high-resolution inundation model was used as the basis for development of a tsunami forecast model to operationally provide an estimate of wave arrival time, wave height, and inundation at Sand Point following tsunami generation. All tsunami forecast models are run in real time while a tsunami is propagating across the open ocean. The Sand Point model was designed and tested to perform under stringent time constraints given that time is generally the single limiting factor in saving lives and property. The goal of this work is to maximize the length of time that the community of Sand Point has to react to a tsunami threat by providing accurate information quickly to emergency managers and other officials responsible for the community and infrastructure.

The general tsunami forecast model, based on the Method of Splitting Tsunami (MOST), is used in the tsunami inundation and forecasting system to provide real-time tsunami forecasts at selected coastal communities. The model runs in minutes while employing high-resolution grids constructed by the National Geophysical Data Center. MOST is a suite of numerical simulation codes capable of simulating three processes of tsunami evolution: earthquake, transoceanic propagation, and inundation of dry land. The MOST model has been extensively tested against a number of laboratory experiments and benchmarks (Synolakis *et al.*, 2008) and was successfully used for simulations of many historical tsunami events. The main objective of a forecast model is to provide an accurate, yet rapid, estimate of wave arrival time, wave height, and inundation in the minutes following a tsunami event. Titov and González (1997) describe the technical aspects of forecast model development, stability, testing, and robustness, and Tang *et al.*, 2009 provide detailed forecast methodology.

A basin-wide database of pre-computed water elevations and flow velocities for unit sources covering worldwide subduction zones has been generated to expedite forecasts (Gica *et al.*, 2008). As the tsunami wave propagates across the ocean and successively reaches tsunameter observation sites, recorded sea level is ingested into the tsunami forecast application in near real-time and incorporated into an inversion algorithm to produce an improved estimate of the tsunami source. A linear combination of the pre-computed database is then performed based on this tsunami source, now reflecting the transfer of energy to the fluid body, to produce synthetic boundary conditions of water elevation and flow velocities to initiate the forecast model computation.

Accurate forecasting of the tsunami impact on a coastal community largely relies on the accuracies of bathymetry and topography and the numerical computation. The high spatial and temporal grid resolution necessary for modeling accuracy poses a challenge in the run-time requirement for real-time forecasts. Each forecast model consists of three telescoped grids with increasing spatial resolution in the finest grid, and temporal resolution for simulation of wave inundation onto dry land. The forecast model uses the most recent bathymetry and topography available to reproduce the correct wave dynamics during the inundation computation. Forecast models, including the Sand Point model, are constructed for at-risk populous coastal communities in the Pacific and

Atlantic oceans. Past and present development of forecast models in the Pacific have validated the accuracy and efficiency of each forecast model currently implemented in the real-time tsunami forecast system (Tang *et al.*, 2009 & 2012; Titov *et al.*, 2005 & 2009; Wei *et al.*, 2008 & 2012). Models are tested when the opportunity arises and are used for scientific research. Tang *et al.* (2009) provide forecast methodology details.

3. Model development

3.1 Study Area

The Alaska Peninsula is a peninsula extending about 800km to the southwest from the mainland of Alaska and ending in the Aleutian, separating the Pacific from Bering Sea. The southern-most side of the Alaska Peninsula is rugged and mountainous, created by the uplifting tectonic activity of the North Pacific Plate subsiding under a western section of the North American Plate; whereas the northern side is generally flat and marshy, a result of millennia of erosion and general seismic stability.

As shown in Figure 1a and 1b, Sand Point is a city located on the northwestern coast of Popof Island, southeast of the Alaska Peninsula, with a small population of 952 according to census of 2000. Sand Point was founded by a San Francisco company in 1898 and since then fishing remains an important industry, as Sand Point is home to one of the largest fishing fleets in the Aleutian Chain.

3.2. Historical events and water level data

Tsunami forecast models coupled with deep-ocean observations play an important role in protecting vulnerable communities, including Sand Point, by providing timely forecasts of tsunami impacts on Alaska's seismically active, populated coastlines. Figure 2 shows the locations of 15 historical tsunamigenic earthquakes in the Pacific and the proximity of the DART systems along with the location of the 100- by 50-km unit sources as defined in the Pacific Marine Environmental Laboratory (PMEL) tsunami propagation database.

Historical tsunamis had a devastating impact on the Alaskan coastline. Lander (1996) documented 100 tsunami events that had affected Alaskan coastlines between 1737 and 1996, including 43 distant-, 31 local-, 14 landslide-, 10 volcanic- and 2 meteorological-generated tsunamis. The 1946 Unimak event generated a destructive transoceanic tsunami that became the milestone event for establishing a basin-wide tsunami warning and forecast system in the Pacific. Between 1940s and 1960s, the five destructive tsunamis including 1946 Unimak, 1952 Kamchatka, 1957 Andreanov, 1960 Chile and 1964 Alaksa represented an era of tsunami hazards and led to intensive efforts in tsunami monitoring and modeling. These events were recorded by tide gages throughout the Pacific (U.S. Coast and Geodetic Survey, 1952, Berkman *et al.*, 1960, Spaeth *et al.*, 1964) and provided valuable datasets for tsunami research. There have been 122 fatalities due to tsunamis in Alaska since 1900. The distant tsunamis, except for the great 1960 Chilean tsunami, hardly produced any damage, the locally generated tsunamis have resulted serious damage and loss of lives on Alaskan coastlines. The 1946 Unimak event caused five fatalities and the 1964 Prince William Sound event resulted in \$84 million in damages and 106 fatalities. Since 1994, 15 distant and local tsunamis have been observed at tide stations in Alaska, including the devastating 26 December 2004 Sumatra tsunami and 11 March 2012 Japan tsunami (NGDC Historical Tsunami Database). No damages or

fatalities on Alaskan coastlines have been reported for events since 1996.

The earthquakes along subduction zones in the Pacific account for 80% of the origins of the tsunamis that have impacted Alaskan coastlines. Attention is needed for the potential local tsunamis generated in the two major seismic gaps of Alaska, Shumagin gap and Unalaska gap. The Shumagin gap (Figure 3) is a segment of the Alaskan-Aleutian arc that has not ruptured in a great earthquake since at least 1899-1903 (Davies et al, 1981). To the west of the 1946 rupture area is the 200-km-long Unalaska seismic gap (House et al., 1981), which has not generated a large earthquake in a century. Boyd and Jacob (1986) suggested a major seismicity gap exists for events of magnitudes greater than at least 4.6 in the forearc region near Unalaska Island. Davis et al. (1981) described a “worst-case scenario” of an earthquake, which nucleates in the Shumagin Gap could also rupture the Unalaska Gap with a resultant magnitude of up to M_w 9.0. A tsunami induced by such an earthquake could be devastating for many communities not only along the Alaska-Aleutian coast, but also as far as Hawaii and the U.S. West Coast. Figure 3 depicts the approximate locations of Unalaska and Shumagin seismic gaps and the historically destructive earthquakes in Alaska-Aleutian Subduction Zone.

The Sand Point tide station was established in 1972 and upgraded to its present installation in 1991. The tide station is situated on the tip of the public dock attached to the western breakwater of small boat harbor at Sand Point (Figure 1b). The coordinates of the tide gage are (160.504333°W , 55.331722°N). In the Sand Point models, we use the coordinates (160.504167°W , 55.331111°N) to approximately represent the tide station location since the model grids cannot pinpoint the tide gage location. The mean tide range at Sand Point is about 1.6 m and the diurnal range is 2.2 m. The mean sea level is increasing at a rate of 0.07mm/year with a standard error of 0.93mm/year based on monthly mean sea level data from 1972-1999. Lying in the maritime climate zone, Sand Point is notorious for the high winds caused by the meeting of cold airflows from the Bering Sea with the warm air over the Japan Currents.

Table 1 listed the maximum observed tsunami water elevation at the Sand Point tide station for 15 historical events, most within the last three decades. Although the maximum of the observed tsunami water level is about 61 cm from the 11 March 2011 Japan tsunami, the destructive tsunamis in the 1940s – 1960s may have produced higher waves along the coastline of Sand Point but were not recorded due to the lack of a tide gage. The computational results from the present study show that the maximum tsunami amplitude at the tide station could have reached 2 m elevation during the 1946 Unimka tsunami, and produced some inundation in the Sand Point harbor area (Figure 33). In this study, 12 of the historical events in Figure 2 were used to validate the developed tsunami forecast model, and three destructive tsunamis, of 1946 Alaska, 1960 Chile and 1964 Alaska, were computed to provide an estimation of the tsunami impact along the coastline of Sand Point. Table 2 listed the detailed information of the tsunami source for the events.

The most noticeable feature of the observed time series at tide station is they are mostly masked by the background noises affecting long waves as a result of instrument errors and improper sampling of swell waves. These noises usually have magnitude of centimeters and period of long waves, making them hardly distinguished from tsunami signals within the same level. This side effect becomes especially serious at locations, such as Sand Point, in the shadow of tsunami wave energy, but experiencing significant

swell waves. One can have an idea how significant the noise level is by observing the recorded time series preceding the arrival of the tsunami waves during each event (Figure 4). In particular, events occurring during winter time, such as Oct. 1994 Kuril, Nov. 2006 Kuril and Jan. 2007 Kuril, turn out to be noisier than summer events, Jun. 2001 Peru, May 2006 Tonga and Apr. 2007 Solomon because of stronger interference of winter swell waves.

3.3. Bathymetry and Topography in Alaska

Accurate bathymetry and topography in offshore and coastal regions play the key role in tsunami generation, propagation and inundation. Marks and Smith (2006) conducted an evaluation of 6 publicly available global bathymetry grids: DBDB2 (Digital Bathymetric Data Base by Naval Research Laboratory), ETOPO2 (Earth Topography by National Geophysical Data Center), GEBCO (General Bathymetric Charts of the Oceans by British Oceanographic Data Center), GINA (Geographic Information Network of Alaska), Smith and Sandwell (1997) and S2004. They concluded the original Smith and Sandwell grid might be the best source among these global bathymetric grids. Walter Smith developed a new 1-min global topography grid S2004 that combines the Smith and Sandwell below 1000m depth and equatorward of 72° and GEBCO grids in shallow water and polar region. NOAA Center for Tsunami Research (NCTR) developed a Pacific-Basin 30sec grid, derived primarily the Smith and Sandwell grid and the SRTM30_PLUS grid, with amendments in areas where NCTR has better bathymetry. This comprehensive dataset covers the entire Pacific Ocean and part of the Arctic Ocean from E120° to W68°, and S80° to N80°.

While developing bathymetric and topographic grids for coastal sites, NOAA Center for Tsunami Research (NCTR) at PMEL has been collaborating with National Geographic Data Center (NGDC) in the NGDC Tsunami Inundation Gridding Project

since 2005 to build high-resolution digital elevation models (DEMs) for more U.S. coastal regions. This satisfies the needs of forecast model development in the near future. The datasets are downloadable, along with the associated documentation, in ESRI ArcGIS ASCII grid format at

http://www.ngdc.noaa.gov/mgg/inundation/tsunami/tsun_view_griddies.html. The sources and features of the individual dataset in this study will be addressed in detail in the model setup section. It needs to be pointed out that the topography data of NGDC's DEM was obtained from a combination of USGS NED 2 arcsec data and NGDC 2006 3 arcsec data. The DEM has an estimated vertical accuracy of 7-20 meters for the topographic features (Taylor et al., 2008). The lack of Lidar data in the DEM may cause errors in the model computation, especially when onshore flooding occurs.

The objective of a forecast model is to provide an estimate of wave arrival time, height, and inundation immediately after the generation of a tsunami. Forecast models are run in real time while a tsunami is propagating in the open ocean, and consequently they are designed to perform under very stringent time limitations. Given the time constraints, the process of computing the three stages of tsunami modeling, wave generation, propagation and inundation, has been expedited by generating a basin-wide database of pre-computed water elevations and flow velocities for unit sources covering subduction zones. As the tsunami wave propagates across the ocean and successively reaches the tsunameters, the recorded sea level information is reported back to the forecast system and processed by the inversion algorithm to produce an improved forecast of the tsunami

source. A linear combination of the pre-computed database is then performed based on the tsunami source to produce synthetic boundary conditions of water elevation and flow velocities to initiate the forecast model computation.

Each forecast model consists of three telescoped grids with increasing spatial and temporal resolution for simulation of wave inundation onto dry land. The forecast model utilizes the most recent bathymetry and topography developed by National Geophysical Data Center (NGDC) and the NOAA Center for Tsunami Research (NCTR) in order to reproduce the correct wave dynamics during the inundation computation. However, it is worth noting that NGDC's DEM is subject to updates when more accurate data becomes available. The forecast model developed in this study reflects the best available DEM at the time when the model was developed. The bathymetry and topography used in the development of this forecast model was based on a digital elevation model provided by the National Geophysical Data Center and the author considers it to be an adequate representation of the local topography/bathymetry. As new digital elevation models become available, forecast models will be updated and report updates will be posted at http://nctr.pmel.noaa.gov/forecast_reports/.

3.4 Model Setup and Parameters

Figure 5 shows the coverage of data sources that NGDC used to develop the high-resolution grids for Sand Point. Taylor et al. (2008) describes detailed procedure, data sources and analysis of the Digital Elevation Model (DEM) for Sand Point. This DEM was delivered in 2006 and is fully implemented for Sand Point forecast model development in this study.

The outermost grid of the Sand Point forecast model has an extent from 163°W to 158°W (~ 318 km) in longitudinal and 52.5°N to 57.0°N (~ 500 km) in latitudinal direction. The southern portion of the grid in the Pacific covers the entire Shumagin seismic gap while the northern portion includes a small area of the Bering Sea. The southern boundary of grid A goes offshore of Alaska-Aleutian trench and adapts the boundary conditions over a flat, and deep bathymetry. Figure 6 and 7 demonstrate the bathymetry and topography of grid A at the grid resolution of 36" for reference model and 2' for the forecast model. Both grids are interpolated from the Pacific 30-sec dataset. The red frame in each plot indicates the coverage of B grid, which is slightly smaller in reference model than in forecast model. The entire Shumagin Islands are situated on the edge of the Alaska-Aleutian trench, surrounding by water less than 100m deep. In addition to the contribution from the aforementioned strong tectonic activities, the rugged landscape of the southeast Alaska Peninsula is also owing to the scouring and grinding of the ice sheet of a Pleistocene ice cap. While the tsunami wave propagation is slowed down over the shallow bathymetry, the wave energy in the mean time is also scattered in different directions by the jagged sea floor and serrated coastline.

Figures 8 and 9 show the computational domain of the intermediate grid B, which has an extent from 161°W to 160°W (~ 63 km) in longitudinal and 0.845° (~ 94 km) in latitudinal direction. Figure 8 shows the 6-arcsec grid B of the reference model. Figure 9 depicts the bathymetry and topography grid with a 18-arcsec resolution for the forecast model. Both grids are interpolated from the Sand Point 1/3 arcsec dataset developed by NGDC (Taylor et al, 2008). The red frame in each plot indicates the coverage of C grid. The southern part of grid B shows much smoother sea bottom than the rest of this area. Popof Island is separated from other islands by Popof Strait to its the west and south,

Korovin Strait to the east and Unga Strait to the north. Compared to the other two, the sea bottom in Popof Strait is especially uneven with scattered submerging islets. As the strait goes north, the sea floor slopes up from 150-m deep and to its top near Sand Point, where Popof Island and Unga Island are connected by water shallower than 20m.

Figures 10 and 11 show the computational domain of the innermost grid C, for the forecast model with grid resolution of 3 arcsec (~ 53 m) in longitudinal and 2 arcsec (~ 62 m) in latitudinal direction (Figure 11) and for the reference model with grid resolution of $\frac{1}{2}''$ (~ 9 m) in longitudinal and $1/3''$ (~ 10 m) in latitudinal direction (Figure 10). The high-resolution grids show clearly the rocky bottom resulted from ice scouring and grinding in the Papof Strait. This feature spreads over the south entrance of the strait and intensifies between the southwest of Popof Island and east of Unga Island, where the strait turns northeast from northwest. The northern part of the strait has a less uneven but sloping bottom. The water depth becomes shallower than 20 m at the northern entrance, where it connects to Unga Strait. Steep topography runs along the coastlines on both islands, as low-lying areas below 10-m elevation occupy only minor portion of the land. However, the residential community of Sand Point is mostly located in the low-lying area next to Humboldt Harbor, as is the airport outhwest of downtown Sand Point.

The model setup and input parameters for the forecast and the reference models are given in Table 3. The three telescoping grids of the reference model cover slightly different areas than the forecast model, but with much higher grid resolution. A single reference model run takes approximately 30 hours for a 4-hour simulation while the forecast model only takes about 11 minutes.

4. Results and Discussions

4.1 Model Validation

Sand Point had no tide station, thus observations, until it was established in 1972, and since then each basin-cross tsunami has been registered at the station. These events provide valuable water-level data that are used for model validation. This study also includes the modeling results of several destructive tsunami events between 1946 and 1972 to assess the tsunami wave impact on the coast at Sand Point.

Figures 12 - 25 show the comparison of the computed and observed waveforms at the tide station of Sand Point for tsunami events, also shown are the plots of the maximum wave amplitude and flow speed computed by the forecast model and the reference model. In general, the computed first wave agrees with the observations in wave amplitude and arriving time, but underestimates the maximum wave amplitude when it arrives with late waves. One can see that when the signal-to-noise ratio is relatively large, such as 2011 Japan and 2010 Chile tsunamis (Figure 12 and 13), the Sand Point forecast model and reference model will both give good estimate of the time series at the tide gage. For events with small signal-to-noise ratio, the computed results of both models show significantly smaller wave amplitudes than observations, and the wave period is not comparable either. These background noises are a result of instrument errors and improper sampling of swell waves. They usually have magnitude of centimeters and period of long waves, making them hardly distinguished from tsunami signals within the same level. This effect becomes particularly serious at locations, such as Sand Point, in the shadow of tsunami wave energy, but experiencing significant swell waves. The forecast model computational results for tsunamis originated from Japan and Kuril (13

January 2007 Kuril, 15 November 2006 Kuril, 25 September 2003 Hokkaido and 14 October 1994 Kuril), shows discrepancies when comparing to the observations, with small amplitude but longer wave period (Figures 16,17,19 and 22). However, the excellent agreement between modeling results and observations at Dutch Harbor excludes the possibility of incorrect tsunami sources (Wei, 2008). It is noticeable that these 4 events all occur during fall and winter season when the tide gage at Sand Point records more interference of the swell waves, which dominates the tsunami signals and leads to less favorable comparison to forecast model results. One can clearly see the level of the noise shown in the observed time series before tsunami arrival during these events. The computational results of 2006 Tonga (Figure 18) and 2001 Peru (Figure 20) events show good agreement with the observations up to the first 8 waves in period and phase, and comparable amplitudes given the interference of background noise.

Also shown in each figure are the results computed by the reference model, which employs high-resolution grids to provide model reference on the computational accuracy of the forecast model. Figures 12 - 25 show that the reference model generally produces higher wave amplitudes than the forecast, except for the 2003 Hokkaido tsunami (Figure 19) and 2001 Peru tsunami (Figure 20). The difference of wave amplitude, wave period and phase is nearly negligible for the first couple of waves in every case. The difference in wave amplitude becomes noticeable in the late waves, but not much in wave period and phase lag. The phase lag in the time series is minor until 4 or 5 hours after the tsunami arrives, when the local effects become more dominant in the wave field as the reference model grids contain more bathymetric and topographic features.

The computed maximum wave amplitude and flow speed are shown in Figures 12 – 25 for the forecast model and the reference model. The bathymetry in the Shumagin Islands in Figures 6 - 11 shows tsunami waves may approach Sand Point from several different routes: one through Popof Strait from the south, one through Korovin Strait from the east, and another through Unga Strait from the north. Tsunami waves from all these different directions meet at a shallow sloping area between the coast of Sand Point and northeast of Unga Island, which works as a trap of high tsunami waves and fast flow currents in all the case studies. However, in the 1960 and 1964 tsunami events, the waves mainly approached Sand Point from the east and the north entrance of Popof Strait and induced higher water elevation in Unga and Korovin Straits than in the Popof Strait.

Three destructive tsunamis, 1946 Unimak, 1960 Chile and 1964 Alaska, resulted in tsunami flooding to the coasts of Unalaska, AK, a nearby Aleutian coastal community (Wei, 2008). However, the plots of maximum wave amplitude and flow speed in Figures 23 to 25 show the inundation was insignificant and the flooded area was limited to the segment at Humboldt Harbor due to the steep topography in Sand Point. The computational results obtained in the reference model are generally larger than those of the forecast model. The discrepancies are mainly due to the difference of the grid resolutions - the 10-m grid used by the reference model describes the local bathymetry and topography more precisely, especially the two jetties embracing the Humboldt Harbor.

4.2 Modeling and Assessment of Artificial Mega Tsunamis

The tsunami unit source is an important component of NOAA's tsunami forecast system in defining the tsunami source through real-time data assimilation with a pre-computed propagation database during an event in progress (Gica et al., 2008). A

combination of tsunami unit sources makes full use of the linearity of the tsunami wave in the deep ocean and the pre-computed propagation database to provide offshore tsunami scenarios for the modeling assessment of impact at identified sites. More than a thousand tsunami unit sources have been developed in NOAA's tsunami forecast system along the subduction zones to prepare for future events. A 1-m uplift on each tsunami source function represents a basic scenario of Mw 7.5. Varying combinations of uplift and source functions create synthetic tsunami scenarios with energy levels and equivalent magnitudes greater than the basic scenario. A suite of scenarios ranging from the basic Mw 7.5 to Mw 9.3 was used in this work to assess the potential tsunami impact on Unalaska. Table 5 provides source and uplift information for a total of 44 M_w 9.3 artificial scenarios in the Pacific, which are used in this study to evaluate the Sand Point tsunami forecast model under the strike of mega tsunami waves.

Figure 27 illustrate the computed results for M_w 9.3 scenario ACSZ 21-30, which is located just offshore of Sand Point. Nor surprisingly, ACSZ 21-30 generates the largest tsunami water level at Sand Point among all the tested scenarios. The maximum computed wave amplitude at the Sand Point tide station is 8 m, and its largest trough reaches 4 m below the referenced zero water level (MHW). Figure 28 show that this scenario, if happens, could lead to catastrophic impact to Sand Point. Models results indicate extensive flooding over the entire Sand Point harbor and residential area with > 10 m water elevation. The airport and its vicinity located at the southwestern tip of Popof Island may also be inundated with 6-7 m water elevation. Figure 28b shows that the maximum flow speed is greater than 8 m in the channel between Popof Island and Unga Island, as well as at the entrance of Humbolt Harbor.

Figure 29 illustrates the computed time series for all other artificial scenarios at the Sand Point tide station. These scenarios are much less significant comparing to ACSZ 21-30 with a maximum wave amplitudes less than 1 m. One can see that SCSZ 1-10 and NTSZ 30-39 can generate tsunami impact that is comparable with what is caused by ACSZ 31-40, although the latter source is much closer to Sand Point. Figures 30 to 42 show that the modeled wave amplitude and flow speed for selected mega scenarios are stable without singularities or spreading instability. The developed tsunami forecast model demonstrates excellent robustness under extreme wave conditions, meaning it is a reliable modeling tool for tsunami warning and forecast at Sand Point.

5. Potential Tsunamis Originated in Seismic Gaps in the Aleutians

5.1 Shumagin Seismic Gap and Unalaska Seismic Gap

Popof Island, along with 19 volcanic islands to its east and south, makes up the Shumagin Islands. Unga Island, the largest in the Shumagin Islands, is separated from Popof Island by Popof Strait. The Schumagins lie 40 to 120 km from the active Aleutian volcanic arc and are situated in the Shumagin gap. This seismic gap is a segment of the Alaskan-Aleutian arc that has not ruptured in a great earthquake since at least 1899-1903 (Davies et al, 1981) and that accordingly may have a high seismic potential. Previous studies (Davies et al. 1981; Johnson, 1999) have shown the rupture zones of Aleutian earthquakes of 1938, 1946 and 1948 did not break the interplate boundary beneath the Shumagin Islands, but did define the boundaries of the Shumagin seismic gap. Davis et al (1981) and Beaven et al. (1983) suggested the possibility of a major earthquake occurrence within this gap within the next two decades. The May 13, 1993 Shumagin

Islands earthquake, M_w 6.8, occurred at an expected location in the seismic gap, but the magnitude was too small to fill the gap (Tanioka et al, 1994). This earthquake did not generate a tsunami large enough to be observed at Sand Point tide station or at the ocean bottom pressure gages at distances of 100 and 300 km. Nishenko and Jacob (1990) and Nishenko (1991) suggested a gap-filling event will have an expected magnitude of 7.4, with conditional probabilities of 27%, 48% and 75% of occurring during the 5-, 10-, and 20-year periods that end in 1994, 1999, and 2009 respectively. Since a gap-filling event is still missing in this gap, a great event is due soon and makes this study an important evaluation of the potential tsunami hazards induced by the failure of the seismic gaps.

To the west of the 1946 rupture area is the 200-km-long Unalaska seismic gap (House et al., 1981), which has not generated a large earthquake in a century. A review of the historic record about 1770 by Boyd and Jacob (1986) reveals that the Unalaska region may have ruptured in a great earthquake in 1878 and a large earthquake in 1902. They suggested a major seismicity gap exists for events of magnitudes greater than at least 4.6 in the forearc region near Unalaska Island. The study of 1957 Aleutian tsunami by Johnson (1999) showed low moment release in the eastern half of the aftershock zone, which further confirmed the existence of the Unalaska Gap.

Davis et al. (1981) described a “worst-case scenario” of an earthquake that nucleates in the Shumagin Gap rupturing the possible Unalaska Gap to the west, the 1938 aftershock zone to the east, or both, with a resultant magnitude of up to M_w 9.0. Tsunamis induced by such an earthquake could be devastating for many communities not only along the Alaska-Aleutian coast, but also as far as Hawaii and the U.S. West Coast.

Figure 3 depicts the approximate locations of Unalaska and Shumagin seismic gaps and the historical destructive earthquakes in Alaska-Aleutian Subduction Zone. Also shown in the map is the layout of the unit sources, which gives us a better idea of how the seismic gaps can be represented in SIFT. Based on above analysis of the potential earthquakes in Unalaska and Shumagin seismic gaps, a full numerical modeling study using the forecast model is conducted to assess the tsunami impact on communities of Unalaska and Sand Point subject to all these possible scenarios at different levels of M_w = 7.5, 8.0, 8.5, 8.7 and 9.0.

5.2 Impact Assessment of Tsunamis Originated in the Shumagin and Unalaska Seismic Gaps

Figure 3 shows Unalaska gap covers area of four unit sources, ACSZ 23-24, and Shumagin gap covers area of 6 unit sources, ACSZ 26-28. Each unit source with a 1-m slip represents a M_w 7.5 earthquake, and with a 6.4-m slip represents a M_w 8.0 earthquake. As both gaps are bounded by the earthquake source of April 1, 1946 event, M_w = 8.5 (Lopez and Okal, 2006), five synthetic scenarios imitating the 1946 tsunami, an averaged 23-m slip applied on a pair of unit sources, are used to evaluate the tsunami impact along the coastline of Sand Point. Three M_w 8.7 synthetic scenarios are also used with 18-m slip on four unit sources and two M_w 9.0 scenarios with 34-m slip on all six unit sources. Including the ACSZ 21-30 scenarios (M_w 9.3) in section 4.2 (Figure 27 and 28), this study uses a total of 19 synthetic scenarios generated in the seismic gaps to evaluate the tsunami impact on Sand Point coastline.

Figure 43 plots the time series at Unalaska and Sand Point tide stations for tsunamis generated by synthetic scenarios in the Unalaska seismic gap. Located at the depression side of the initial deformation, Unalaska tide station first experienced an earthquake

subsidence, then the following one-hour-long leading tsunami wave and the second wave with shorter period but the highest wave amplitude. It takes about 1.5 hours for tsunami waves to arrive at Sand Point station, with no leading depression but a leading crest with highest wave amplitude in entire time series. The wave amplitude at Sand Point station is comparable with that at the Unalaska station in most of the synthetic cases, and slightly higher for the M_w 9.0 scenario.

Figure 44 shows the time series at both stations for tsunamis originated by synthetic scenarios in the Shumagin seismic gap. All these scenarios suggest the second wave at Unalaska station is the highest one in the entire time series. However the time series at the Sand Point station shows different pattern depending on the location of tsunami source. The leading wave has the highest amplitude in scenarios originated from row b of the unit sources, such as 26b, 27b or 28b, while the second wave is the highest in scenarios generated by row a, such as 26a and 27a. In scenarios involved with source 28a, the computed time series indicates the forth wave to be the highest one, which could be the results of the interference of rugged bathymetry and topography in Shumagin Islands. Compared with the time series at Unalaska station, the computed tsunami amplitudes at Sand Point are generally greater than those at Unalaska and suggest Sand Point is more vulnerable to tsunamis originated in the seismic gaps.

Figure 45 is a summary plot of the tsunami impact at both Unalaska and Sand Point for all synthetic scenarios originated in the seismic gaps, including the maximum computed runup, maximum computed tsunami height and maximum computed wave amplitude at the tide station.

- Each location is more vulnerable to tsunamis originated in the nearby seismic gap. However, Sand Point is more sensitive to these local tsunamis than Unalaska.
- Local tsunami in the seismic gaps at the level of M_w 9.0 can produce tsunami runup as high as 14 m in Sand Point and 9 m in Unalaska.
- Scenarios with a M_w greater than 8.5 should be considered as hazardous events for both Unalaska and Sand Point. Most of these scenarios create at least 2-m tsunami heights and runup heights at both locations.
- M_w 8.0 scenarios in Unalaska seismic gap cause a moderate impact to both locations with a maximum tsunami runup height less than 1 m. M_w 8.0 scenarios in Sand Point seismic gap have a minor impact in Unalaska, however they strike Sand Point as hard as M_w 8.5 scenarios do, especially if they are originated from unit sources 27a and 27b.
- Tsunami impact caused by M_w 7.5 scenarios in both gaps is negligible with maximum tsunami heights smaller than 0.1m for most cases with the exception for scenarios of 27a or 27b, which may flood areas lower than 0.6 m in Sand Point.
- The tsunami impact in Unalaska with respect to tsunami sources in the seismic gaps is given in descent order as following: 24, 23, 26, 27 and 28, and row a is more hazardous than row b.
- The tsunami impact in Sand Point with respect to tsunami sources in the seismic gaps is given in descent order as following: 27, 28, 26, 24 and 23, and row a is more hazardous than row b.
- Unit sources 27a and 27b are the most hazardous tsunami sources for Sand Point. The tsunami impact initiated by the two sources can be comparable with that caused by other sources with an earthquake magnitude of 0.5 larger.

- Most scenarios show the maximum amplitude at tide station follows the same trend as that of the maximum tsunami height and maximum tsunami runup, meaning the time series at the tide station is a good indication of the wave field of each computational domain.

6. Summary and Conclusions

This study developed the tsunami forecast model for Sand Point, which is being implemented into NOAA's tsunami forecast system for real-time model forecast of the water elevation, runup and inundation at Sand Point, Alaska. This study has discussed the details of each individual component of the forecast model and the reference model, including the bathymetry and topography, the basic model setup and model parameters. The tsunami forecast model accomplishes 4-hr simulation after tsunami arrival in 13 minutes of CPU time.

Model validation has been carried out using 12 historical tsunami events by comparing the modeling results and the observation at the tide station, and 3 destructive events to evaluate the tsunami impact at the coastline. Tsunami signals registered at the Sand Point tide station are mostly within the range of noises as a result of instrument errors and improper sampling of swell waves. The model validation shows good comparison with observations for events occurring during the seasons that are less affected by winter swells, but demonstrates some discrepancies when the tide gage records contain serious noises.

Synthetic mega events at the level of M_w 9.3 are used to ensure the stability of the forecast model. The developed tsunami forecast model showed excellent stability with 13 m waves generated locally from the Aleutians.

5. Acknowledgments

This research is funded by the NOAA Center for Tsunami Research (NCTR). The author would like to thank the modeling group of NCTR for help suggestions and discussions. This publication is also partially funded by the Joint Institute for the Study of the Atmosphere and Ocean (JISAO).

6. References

- Beavan, J.E., Hauksson, E., McNutt, S.R., Bilham, R. and Jacob, K.H. (1983). Tilt and Seismicity Changes in the Shumagin Seismic Gap. *Science*, 222, 322-325.
- Berkman, S.C. and Symons, J.M. (1960): The tsunami of May 22, 1960 as recorded at tide stations. *Coastal Geodetic Survey, U. S. Department of Commerce*, 79p.
- Boyd, T.M. and Jacob, K. (1986): Seismicity of the Unalaska region, Alaska. *Bulletin of Seismological Society of America*, 76, 463-481.
- Davies, J., Sykes, L., House, L., and Jacob, K. (1981): Schumagin seismic gap, Alaska Peninsula: history of great earthquakes, tectonic setting, and evidence for high seismic potential. *Journal of Geophysical Research*, 86(B5), 3821-3856.

- Eble, M.C. and Gonzalez, F.I. (1991). Deep-Ocean Bottom Pressure Measurements in the Northeast Pacific. *Journal of Atmospheric and Oceanic Technology*, 8, 221-233.
- Gica, E., M. Spillane, V.V. Titov, C. Chamberlin, and J.C. Newman (2008): Development of the forecast propagation database for NOAA's Short-term Inundation Forecast for Tsunamis (SIFT). *NOAA Tech. Memo. OAR PMEL-139*, 89 pp.
- House, L.S., Sykes, L.R., Davis, J.N., and Jacob, K.H. (1981). Identification of a possible seismic gap near Unalaska Island, eastern Aleutians, Alaska. Earthquake prediction – an international review. *American Geophysical Union, Washington D.C.*, 81-92.
- Lopez, A.M., and E.A., Okal (2006): A seismological reassessment of the source of the 1946 Aleutian ‘tsunami’ earthquake. *Geophysical Journal International*, 165, 835-849.
- Marks, K.M., and Smith, W.H.F. (2006): An evaluation of publicly available global bathymetry grids. *Marine Geophysical Researches*, 27, 19-34.
- Nishenko, S.P. and Jacob, K.H. (1990). Seismic potential of the Queen-Charlotte-Alaska-Aleutian seismic zone. *Journal of Geophysical Research*, 95, 2511-2532.
- Johnson, J.M. (1999): Heterogeneous coupling along Alaska-Aleutians as inferred from tsunami, seismic, and geodetic inversions. *Advances in Geophysics*, 39, 1-116.
- Spaeth, M.G. (1964): The tsunami of March 28, 1964, as recorded at tide stations.
- Suleimani, E.N., Combellick, R.A., Hansen, R.A. and Carver, G.A. (2002). Tsunami hazard mapping of Alaska coastal communities. *Alaska GeoSurvey News*, 6(2), 5p.
- Synolakis, C.E., E.N. Bernard, V.V. Titov, U. Kanoglu and F.I. Gonzalez (2008), Validation and verification of tsunami numerical models, *Pure and Applied Geophysics*, 165(11-12), 2197-2228.
- Tang, L., V. V. Titov, and C. D. Chamberlin (2009), Development, Testing, and Applications of Site-specific Tsunami Inundation Models for Real-time Forecasting, *J. Geophys. Res.*, doi:10.1029/2009JC005476, in press. [PDF version] (accepted 27 August 2009)
- Taylor, L.A., B.W. Eakins, K.S. Carignan, R.R. Warnken, T. Sazonova, D.C. Schoolcraft, and G.F. Sharman, 2008. Digital Elevation Models of Sand Point, Alaska: Procedures, Data Sources and Analysis, *NOAA Technical Memorandum NESDIS NGDC-5*, National Geophysical Data Center, Boulder, CO, 25 pp.
- Titov, V.V. (2008), Tsunami forecasting, in *The Sea*, vol. 15, edited by E. Bernard, and A. Robinson, chap. 12, pp. 367-396, Harvard Univ. Press, Cambridge, Mass.

Titov, V.V., Gonzalez, F.I., Bernard, E.N., Eble, M.C., Mofjeld, H.O., Newman, J.C. and Venturato, A.J. (2005). Real-time tsunami forecasting: challenges and solutions. *Natural Hazards*, 35(1), 41-58.

Titov, V.V., H.O. Mofjeld, F.I. Gonzalez and J.C. Newman (1999): Offshore forecasting of Alaska-Aleutian subduction zone tsunamis in Hawaii. NOAA Technical Memorandum. ERL PMEL-114, January 1999, 22 pp.

Tonioka, Y., Satake, K., Ruff, L., and Gonzalez, F. (1994): Fault parameters and tsunami excitation of the May 13, 1993, Shumagin Islands earthquake. *Geophysical Research Letters*, 21(11), 967-970.

U. S. Coast and Geodetic Survey (1953): The tsunami of November 4, 1952 as recorded at tide stations. U. S. Department of Commerce, 62p.

Wei, Y. (2008). Tsunami impact assessment for Unalaska, Alaska. Proceedings of the Conference on Solutions to Coastal Disasters, American Society of Civil Engineers, Ed. L. Wallendorf, L. Ewing, C. Jones, and B. Jaffe, 118-131, Oahu, Hawaii.

Wei, Y., E. Bernard, L. Tang, R. Weiss, V. Titov, C. Moore, M. Spillane, M. Hopkins, and U. Kânoğlu (2008): Real-time experimental forecast of the Peruvian tsunami of August 2007 for U.S. coastlines. *Geophys. Res. Lett.*, 35, L04609, doi: 10.1029/2007GL032250.

Figures:

Figure 1 Sand Point, Alaska. Upper panel: map of Sand Point and Shumagin Islands; Lower panel: close aerial view of Sand Point.

Figure 2 Significant tsunami events of last century in the Pacific. ● = significant tsunami events used for validation in this study; ● = destructive historical tsunami events used mode testing; ▲ = US tsunameters; ▲ = non-US tsunameters; □ = tsunami unit source.

Figure 3 Shumagin seismic gaps in the Aleutian, Alaska. Red box represents the tsunami source function in the Alaska-Aleutian Subduction Zone.

Figure 4 Observations before and after tsunami arrivals at the tide station of Sand Point, AK. The dash line indicates the timing of tsunami arrival. The time series in blue shows the noise level before tsunami arriving. The time series in red shows the mixed signals of tsunami wave and the noise.

Figure 5 Source and coverage of datasets used to compile the Sand Point, Alaska DEMs, courtesy of Taylor et al., 2008. White areas denote data gaps.

Figure 6. Bathymetry and topography of outmost grid (A grid) of the reference inundation model for Sand Point. The red rectangular represents the computational domain of the intermediate grid.

Figure 7. Bathymetry and topography of outmost grid (A grid) of the tsunami forecast model for Sand Point. The red rectangular represents the computational domain of the intermediate grid.

Figure 8. Bathymetry and topography of intermediate grid (B grid) of the reference inundation model for Sand Point. The red rectangular represents the computational domain of the inmost grid.

Figure 9. Bathymetry and topography of intermediate grid (B grid) of the tsunami forecast model for Sand Point. The red rectangular represents the computational domain of the inmost grid.

Figure 10. Bathymetry and topography of inmost grid (C grid) of the reference inundation model for Sand Point.

Figure 11. Bathymetry and topography of inmost grid (C grid) of the tsunami forecast model for Sand Point.

Figure 12. Sand Point modeling results and comparison with observations for 11 March 2011 Japan tsunami event. (a) maximum wave amplitude computed by the forecast model; (b) maximum flow speed computed by the forecast model; (c) maximum wave amplitude computed by the reference model; (d) maximum flow speed computed by the reference model; (e) comparison between model computation and measurements at the Sand Point tide station.

Figure 13. Sand Point modeling results and comparison with observations for 27 February 2010 Chile tsunami event. (a) maximum wave amplitude computed by the forecast model; (b) maximum flow speed computed by the forecast model; (c) maximum wave amplitude computed by the reference model; (d) maximum flow speed computed by the reference model; (e) comparison between model computation and measurements at the Sand Point tide station.

Figure 14. Sand Point modeling results and comparison with observations for 15 August Peru tsunami event. (a) maximum wave amplitude computed by the forecast model; (b) maximum flow speed computed by the forecast model; (c) maximum wave amplitude computed by the reference model; (d) maximum flow speed computed by the reference model; (e) comparison between model computation and measurements at the Sand Point tide station.

Figure 15. Sand Point modeling results and comparison with observations for 1 April 2007 Kuril tsunami event. (a) maximum wave amplitude computed by the forecast model; (b) maximum flow speed computed by the forecast model; (c) maximum wave amplitude computed by the reference model; (d) maximum flow speed computed by the reference model; (e) comparison between model computation and measurements at the Sand Point tide station.

Figure 16. Sand Point modeling results and comparison with observations for 13 January 2007 Kuril tsunami event. (a) maximum wave amplitude computed by the forecast model; (b) maximum flow speed computed by the forecast model; (c) maximum wave amplitude computed by the reference model; (d) maximum flow speed computed by the reference model; (e) comparison between model computation and measurements at the Sand Point tide station.

Figure 17. Sand Point modeling results and comparison with observations for 15 November 2006 Kuril tsunami event. (a) maximum wave amplitude computed by the forecast model; (b) maximum flow speed computed by the forecast model; (c) maximum wave amplitude computed by the reference model; (d) maximum flow speed computed by the reference model; (e) comparison between model computation and measurements at the Sand Point tide station.

Figure 18. Sand Point modeling results and comparison with observations for 3 May 2006 Tonga tsunami event. (a) maximum wave amplitude computed by the forecast model; (b) maximum flow speed computed by the forecast model; (c) maximum wave amplitude computed by the reference model; (d) maximum flow speed computed by the reference model; (e) comparison between model computation and measurements at the Sand Point tide station.

Figure 19. Sand Point modeling results and comparison with observations for 25 September 2003 Hokkaido tsunami event. (a) maximum wave amplitude computed by the forecast model; (b) maximum flow speed computed by the forecast model; (c) maximum wave amplitude computed by the reference model; (d) maximum flow speed computed by the reference model; (e) comparison between model computation and measurements at the Sand Point tide station.

Figure 20. Sand Point modeling results and comparison with observations for 23 June 2001 Peru tsunami event. (a) maximum wave amplitude computed by the forecast model; (b) maximum flow speed computed by the forecast model; (c) maximum wave amplitude computed by the reference model; (d) maximum flow speed computed by the reference model; (e) comparison between model computation and measurements at the Sand Point tide station.

Figure 21. Sand Point modeling results and comparison with observations for 10 June 1996 Andreanov tsunami event. (a) maximum wave amplitude computed by the forecast model; (b) maximum flow speed computed by the forecast model; (c) maximum wave amplitude computed by the reference model; (d) maximum flow speed computed by the reference model; (e) comparison between model computation and measurements at the Sand Point tide station.

Figure 22. Sand Point modeling results and comparison with observations for 4 October 1994 Kuril tsunami event. (a) maximum wave amplitude computed by the forecast model; (b) maximum flow speed computed by the forecast model; (c) maximum wave amplitude computed by the reference model; (d) maximum flow speed computed by the reference model; (e) comparison between model computation and measurements at the Sand Point tide station.

Figure 23. Sand Point modeling results for 28 May 1964 Alaska Chile tsunami event. (a) maximum wave amplitude computed by the forecast model; (b) maximum flow speed computed by the forecast model; (c) maximum wave amplitude computed by the reference model; (d) maximum flow speed computed by the reference model; (e) computed wave amplitude at the Sand Point tide station.

Figure 24. Sand Point modeling results for 22 May 1960 Chile tsunami event. (a) maximum wave amplitude computed by the forecast model; (b) maximum flow speed computed by the forecast model; (c) maximum wave amplitude computed by the reference model; (d) maximum flow speed computed by the reference model; (e) computed wave amplitude at the Sand Point tide station.

Figure 25. Sand Point modeling results for 1 April 1946 Unimak tsunami event. (a) maximum wave amplitude computed by the forecast model; (b) maximum flow speed computed by the forecast model; (c) maximum wave amplitude computed by the reference model; (d) maximum flow speed computed by the reference model; (e) computed wave amplitude at the Sand Point tide station.

Figure 26. Synthetic tsunami scenarios used for model testing in this study. Each of the box (red or green) indicates the tsunami source area corresponding to a 1000 km × 100 km rupture area of Mw 9.3 earthquake. See Table 4 for the detail of the naming, source zone, source combination and slip coefficient of all synthetic scenarios.

Figure 27. Computed time series of wave amplitude at Sand Point tide station for tsunami waves generated by synthetic scenarios ACSZ 21-30.

Figure 28 Computed maximum wave amplitude and flow speed at Sand Point for synthetic scenario ACSZ 21-30. (a) maximum wave amplitude; (b) maximum flow speed.

Figure 29 Computed time series of wave amplitude at Sand Point tide station for tsunami waves generated by synthetic scenarios.

Figure 30 Computed maximum wave amplitude and flow speed at Sand Point for synthetic scenario ACSZ 56-65. (a) maximum wave amplitude; (b) maximum flow speed.

Figure 31 Computed maximum wave amplitude and flow speed at Sand Point for synthetic scenario CASZ 1-10. (a) maximum wave amplitude; (b) maximum flow speed.

Figure 32 Computed maximum wave amplitude and flow speed at Sand Point for synthetic scenario ECSZ 7-16. (a) maximum wave amplitude; (b) maximum flow speed.

Figure 33 Computed maximum wave amplitude and flow speed at Sand Point for synthetic scenario EPSZ 6-15. (a) maximum wave amplitude; (b) maximum flow speed.

Figure 34 Computed maximum wave amplitude and flow speed at Sand Point for synthetic scenario KISZ 1-10. (a) maximum wave amplitude; (b) maximum flow speed.

Figure 35 Computed maximum wave amplitude and flow speed at Sand Point for synthetic scenario KISZ 30-39. (a) maximum wave amplitude; (b) maximum flow speed.

Figure 36 Computed maximum wave amplitude and flow speed at Sand Point for synthetic scenario MOSZ 1-10. (a) maximum wave amplitude; (b) maximum flow speed.

Figure 37 Computed maximum wave amplitude and flow speed at Sand Point for synthetic scenario NVSZ 28-37. (a) maximum wave amplitude; (b) maximum flow speed.

Figure 38 Computed maximum wave amplitude and flow speed at Sand Point for synthetic scenario NGSZ 2-11. (a) maximum wave amplitude; (b) maximum flow speed.

Figure 39 Computed maximum wave amplitude and flow speed at Sand Point for synthetic scenario NTSZ 30-39. (a) maximum wave amplitude; (b) maximum flow speed.

Figure 40 Computed maximum wave amplitude and flow speed at Sand Point for synthetic scenario RNSZ 1-10. (a) maximum wave amplitude; (b) maximum flow speed.

Figure 41 Computed maximum wave amplitude and flow speed at Sand Point for synthetic scenario SASZ 31-40. (a) maximum wave amplitude; (b) maximum flow speed.

Figure 42 Computed maximum wave amplitude and flow speed at Sand Point for synthetic scenario SCSZ 1-10. (a) maximum wave amplitude; (b) maximum flow speed.

Figure 43 Time series at Sand Point and Unalaska tide stations for tsunami waves generated by synthetic scenarios in the Unalaska seismic gap.

Figure 44 Time series at Sand Point and Unalaska tide stations for tsunami waves generated by synthetic scenarios in the Shumagin seismic gap.

Figure 45 Computed maximum values in Sand Point, AK and Unalaska, AK for hypothetical tsunami scenarios in Unalaska and Shumagin seismic gaps. Yellow and blue bars indicate maximum values at Unalaska and Sand Point respectively. Each group of three bars, from left to right, represents the maximum runup, maximum tsunami height and maximum water elevation at the tide station.

Tables

Tsunami Event	Time	M _w	Source of M _w	Max Amp (cm)
Alaska	1946. 04. 01	8.5	Inversion	Unknown
Chile	1985. 03. 03	8.0	USGS	8
Aleutian	1986. 05. 07	8.0	NGDC	5
Alaska	1989. 09. 04	7.1	NGDC	10
Chile	1995. 07. 30	7.8	Lander, 1996	11
Alutian	1996. 06. 10	7.9	USGS	5
Peru	2001. 06. 23	8.1	Inversion	12
Rat Island	2003. 11. 17	8.0	Inversion	4
Sumatra	2004. 12. 26	9.1	USGS	14
Tonga	2006. 05. 03	8.1	Inversion	5
Kuril	2006. 11. 15	8.1	Inversion	11
Peru	2007. 08. 15	8.0	Inversion	4
Chile	2010.02.27	8.8	Inversion	40
Japan	2011.03.11	9.0	Inversion	61
Haida Gwaii	2012.10.28	7.7	Inversion	8

Table 1. Observed maximum wave amplitude at Sand Point tide station for historical tsunami events.

Earthquake / Seismic				Model		
Event	USGS Date Time (UTC) Epicenter	CMT Date Time (UTC) Centroid	Magnitude Mw	Tsunami Magnitude ¹	Subduction Zone	Tsunami Source
1946 Unimak	01 Apr 12:28:56 52.75°N 163.50°W	01 Apr 12:28:56 53.32°N 163.19°W	² 8.5	8.5	Aleutian-Alaska-Cascadia (ACSZ)	$7.5 \times b23 + 19.7 \times b24 + 3.7 \times b25$
1952 Kamchatka	04 Nov 16:58:26.0 ³ 52.76°N 160.06°E	04 Nov 16:58:26.0 52.75°N 159.50°E	³ 9.0	8.7	Kamchatka-Kuril-Japan-Izu-Mariana-Yap (KISZ)	-
1957 Andreanov	09 Mar 14:22:31 51.56°N 175.39°W	09 Mar 14:22:31.9 51.292°N 175.629°W	³ 8.6	8.7	Aleutian-Alaska-Cascadia (ACSZ)	$31.4 \times a15 + 10.6 \times a16 + 12.2 \times a17$
1960 Chile	22 May 19:11:14 ³ 38.29°S 73.05°W	22 May 19:11:14 38.50°S 74.50°W	⁴ 9.5		Central-South America (CSSZ)	Kanamori & Ciper (1974) /store/c2/data/tang/src_all/1960s1kana/pago_?.nc
1964 Alaska	28 Mar 03:36:00 ³ 61.02°N 147.65°W	28 Mar 03:36:14 61.10°N 147.50°W	³ 9.2	9.0	Aleutian-Alaska-Cascadia (ACSZ)	Tang <i>et al.</i> (2009) /store/c2/data/tang/src_all/1964cs1/samoa1964_cs2_?.nc)
1994 East Kuril	04 Oct 13:22:58 43.73°N 147.321°E	04 Oct 13:23:28.5 43.60°N 147.63°E	⁵ 8.3	8.1	Kamchatka-Kuril-Japan-Izu-Mariana-Yap (KISZ)	$9.0 \times a20$
1996 Andreanov	10 Jun 04:03:35 51.56°N 175.39°W	10 Jun 04:04:03.4 51.10°N 177.410°W	⁵ 7.9	7.8	Aleutian-Alaska-Cascadia (ACSZ)	$2.40 \times a15 + 0.80 \times b16$
2001 Peru	23 Jun 20:33:14 16.265°S 73.641°W	23 Jun 20:34:23.3 17.28°S 72.71°W	⁵ 8.4	8.2	Central-South America (CSSZ)	$5.7 \times a15 + 2.9 \times b16 + 1.98 \times a16$ (old database, pls consult with Diego for new database inversion)
2003 Hokkaido	25 Sep 19:50:06 41.775°N 143.904°E	25 Sep 19:50:38.2 42.21°N 143.84°E	⁵ 8.3	8.0	Kamchatka-Kuril-Japan-Izu-Mariana-Yap (KISZ)	$3.6m \times (100 \times 100\text{km})$ 109#rake, 20#dip, 230#strike, 25 m depth
2003 Rat Island	17 Nov 06:43:07 51.13°N 178.74°E	17 Nov 06:43:31.0 51.14°N 177.86°E	⁵ 7.7	7.8	Aleutian-Alaska-Cascadia (ACSZ)	⁶ 2.81 × b11
2006 Tonga	03 May 15:26:39 20.13°S 174.161°W	03 May 15:27:03.7 20.39°S 173.47°W	⁵ 8.0	8.0	New Zealand-Kermadec-Tonga (NTSZ)	$6.6 \times b29$
2006 Kuril	15 Nov 11:14:16 46.607°N 153.230°E	15 Nov 11:15:08 46.71°N 154.33°E	⁵ 8.3	8.1	Kamchatka-Kuril-Japan-Izu-Mariana-Yap (KISZ)	⁶ 4 × a12 + 0.5 × b12 + 2 × a13 + 1.5 × b13

¹ Preliminary source – derived from source and deep-ocean observations

² López and Okal (2006)

³ United States Geological Survey (USGS)

⁴ Kanamori and Ciper (1974)

⁵ Centroid Moment Tensor

⁶ Tsunami source was obtained in real time and applied to the forecast

2007 Kuril	13 Jan 04:23:20 46.272°N 154.455°E	13 Jan 04:23:48.1 46.17°N 154.80°E	⁵ 8.1	7.9	Kamchatka-Kuril-Japan-Izu-Mariana-Yap (KISZ)	-3.64 × b13
2007 Solomon	01 Apr 20:39:56 8.481°S 156.978°E	01 Apr 20:40:38.9 7.76°S 156.34°E	³ 8.1	8.2	New Britain-Solomons-Vanuatu (NVSZ)	12.0 × b10
2007 Peru	15 Aug 23:40:57 13.354°S 76.509°W	15 Aug 23:41:57.9 13.73°S 77.04°W	⁵ 8.0	8.1	Central-South America (CSSZ)	$0.9 \times a61 + 1.25 \times b61 + 5.6 \times a62 + 6.97 \times b62 + 3.5 \times z62$
2007 Chile	14 Nov 15:40:50 22.204°S 69.869°W	14 Nov 15:41:11.2 22.64°S 70.62°W	³ 7.7	7.6	Central-South America (CSSZ)	$z73 \times 1.65$ (Diego Inversion)
2009 Samoa	29 Sep 17:48:10 15.509°S 172.034°W	29 Sep 17:48:26.8 15.13°S 171.97°W	⁵ 8.1	8.1	New Zealand-Kermadec-Tonga (NTSZ)	⁶ 3.96 × a34+3.96 × b34 (forecast) 4.7xa34+6.5xb34+1.5*c34+0.4*a35+4.5*b35+3.6*c35+0.4*b36+0.6*c36 (revised with outer rise) -4.21 × 34b -1.72 × 34c -10.58 × b35 +2.02 × a35 -5.28 × c35 +3.42 × b36 +4.57 × 36c (source obtained through OT&E of 2009 Samoa event)
2010 Chile	27 Feb 06:34:14 35.909°S 72.733°W	27 Feb 06:35:15.4 35.95°S 73.15°W	⁵ 8.8	8.8	Central-South America (CSSZ)	⁶ a88 × 17.24 + a90 × 8.82 + b88 × 11.86 + b89 × 18.39 + b90 × 16.75 + z88 × 20.78 + z90 × 7.06
2011 Japan	11 Mar 05:46:23 38.322°N 142.369°E		9.1	8.9	Kamchatka-Kuril-Japan-Izu-Mariana-Yap (KISZ)	b24 × 4.66 + b25 × 12.23 +a26 × 26.31+b26 × 21.27 + a27 × 22.75 + b27 × 4.98
2012 Haida Gwaii, Canada	28 Oct 93:04:10 52.7682°N, 131.9273°W		7.7	7.7	Aleutian-Alaska-Cascadia (ACSZ)	b51 × 4.3 + b52 × 0.36

Table 2. Tsunami sources of historical events.

Grid	Region	Reference Model					Forecast Model				
		Coverage Lat. [°N] Lon. [°W]	Cell Size [""]	nx x ny	Time Step [sec]	Coverage Lat. [°N] Lon. [°W]	Cell Size [""]	nx x ny	Time Step [sec]		
A	Alaska Peninsula	52.5-57.0 163-158	36 × 36	501 × 451	2.4	52.5-57.0 163-158	120 × 120	301 × 351	8.0		
B	Shumagin Islands	54.699583 - 55.697917 161 – 160	6 × 6	601 × 600	1.8	- 55.694583 161 – 159.805417	18 × 18	240 × 200	6.0		
C	Sand Point	55.25 – 55.425 160.6 – 160.4	0.5 × 0.381	1441 × 1891	0.2	55.27 – 55.425 160.6 – 160.4	3 × 2	241 × 280	1.0		
Minimum offshore depth [m]		1					1				
Water depth for dry land [m]		0.1					0.1				
Friction coefficient [n^2]		0.001225					0.001225				
CPU time for 4-hr simulation		10.14 hours					10.4 minutes				

Table 3. Model setup and input parameters for tsunami forecast model and reference model of Sand Point, AK.

Scenario	Source Zone	Tsunami Source	Alpha (m)
ACSZ 1-10	Aleutian-Alaska-Cascadia	A1-A10, B1-B10	28.4
ACSZ 11-20	Aleutian-Alaska-Cascadia	A11-A20, B11-B20	28.4
ACSZ 21-30	Aleutian-Alaska-Cascadia	A21-A30, B21-B30	28.4
ACSZ 31-40	Aleutian-Alaska-Cascadia	A31-A40, B31-B40	28.4
ACSZ 41-50	Aleutian-Alaska-Cascadia	A41-A50, B41-B50	28.4
ACSZ 46-55	Aleutian-Alaska-Cascadia	A46-A55, B46-B55	28.4
ACSZ 56-65	Aleutian-Alaska-Cascadia	A56-A65, B56-B65	28.4
CASZ 1-10	Central America	A1-A10, B1-B10	28.4
CASZ 5-14	Central America	A5-A14, B5-B14	28.4
CASZ 15-24	Central America	A15-A24, B15-B24	28.4
CASZ 25-34	Central America	A25-A34, B25-B34	28.4
ECSZ 1-10	Ecuador-Columbia	A1-A10, B1-B10	28.4
ECSZ 7-16	Ecuador-Columbia	A7-A16, B1-B16	28.4
EPSZ 1-10	East-Philippines	A1-A10, B1-B10	28.4
EPSZ 6-15	East-Philippines	A6-A15, B6-B15	28.4
KISZ 1-10	Kamchatka-Yap-Mariana-Izu-Bonin	A1-A10, B1-B10	28.4
KISZ 8-17	Kamchatka-Yap-Mariana-Izu-Bonin	A8-A17, B8-B17	28.4
KISZ 13-22	Kamchatka-Yap-Mariana-Izu-Bonin	A13-A22, B13-B22	28.4
KISZ 22-31	Kamchatka-Yap-Mariana-Izu-Bonin	A22-A31, B22-B31	28.4
MOSZ 1-10	Manus Ocean Convergence Boundary	A1-10, B1-10	28.4
MOSZ 8-17	Manus Ocean Convergence Boundary	A8-10, B8-10	28.4
NGSZ 2-11	North New Guinea	A2-11, B2-11	28.4
NVSZ 1-10	New-Britain-Solomons-Vanuatu	A1-A10, B1-B10	28.4
NVSZ 11-20	New-Britain-Solomons-Vanuatu	A11-A20, B11-20	28.4
NVSZ 23-32	New-Britain-Solomons-Vanuatu	A23-A32, B23-B32	28.4
NVSZ 28-37	New-Britain-Solomons-Vanuatu	A28-A37, B28-37	28.4
NTSZ 4-13	New Zealand-Kermadec-Tonga	A4-13, B4-13	28.4
NTSZ 14-23	New Zealand-Kermadec-Tonga	A14-23, B14-23	28.4
NTSZ 24-33	New Zealand-Kermadec-Tonga	A24-33, B24-33	28.4
NTSZ 30-39	New Zealand-Kermadec-Tonga	A30-39, B30-39	28.4
RNSZ 1-10	Ryukyu-Kyushu-Nankai	A1-A10, B1-B10	28.4
RNSZ 13-22	Ryukyu-Kyushu-Nankai	A13-A22, B13-B22	28.4
SASZ 11-20	South America	A11-A20, B11-B20	28.4
SASZ 21-30	South America	A21-A30, B21-B30	28.4

SASZ 31-40	South America	A31-A40, B31-B40	28.4
SASZ 40-49	South America	A40-A49, B40-B49	28.4
SASZ 71-80	South America	A71-A80, B71-B80	28.4
SCSZ 1-10	South Chile	A1-A10, B1-B10	28.4
SCSZ 6-15	South Chile	A6-A15, B6-B15	28.4
KISZ 30-39	Kamchatka-Yap-Mariana-Izu-Bonin	A30-A39, B30-B39	28.4
KISZ 40-49	Kamchatka-Yap-Mariana-Izu-Bonin	A40-A49, B40-B49	28.4
KISZ 50-59	Kamchatka-Yap-Mariana-Izu-Bonin	A50-A59, B50-B59	28.4
KISZ 57-66	Kamchatka-Yap-Mariana-Izu-Bonin	A57-A66, B57-B66	28.4

Table 4. Tsunami source of 51 artificial scenarios used for stability testing.

Appendix A.

Development of the Sand Point, Alaska, tsunami forecast model occurred prior to parameters changes that were made to reflect modification to the MOST model code. As a results, the input file for running both the optimized tsunami forecast model and the high-resolution reference inundation model in MOST have been updated accordingly. Appendix A1 and A2 provide the updated files for Sand Point, Alaska.

A1. Reference model *.in file for Sand Point, Alaska

```
0.001      Minimum amplitude of input offshore wave (m)
1.0        Input minimum depth for offshore (m)
0.1        Input "dry land" depth for inundation (m)
0.001225   Input friction coefficient (n**2)
1          let a and b run up
300.0      blowup limit
0.2        input time step (sec)
108000    input amount of steps
12         Compute "A" arrays every n-th time step, n=
9          Compute "B" arrays every n-th time step, n=
900        Input number of steps between snapshots
0          ...Starting from
1          ...saving grid every n-th node, n=
```

A2. Forecast model *.in file for Sand Point, Alaska

```
0.0001     Minimum amplitude of input offshore wave (m)
5.0        Input minimum depth for offshore (m)
0.1        Input "dry land" depth for inundation (m)
0.001225   Input friction coefficient (n**2)
1          let a and b run up
300.0      blowup limit
1.0        input time step (sec)
43200     input amount of steps
8          Compute "A" arrays every n-th time step, n=
6          Compute "B" arrays every n-th time step, n=
24         Input number of steps between snapshots
0          ...Starting from
1          ...saving grid every n-th node, n=
```

Appendix B. Propagation database:

Pacific Ocean Unit Sources

These propagation source details reflect the database as of February 2013, and there may have been updates in the earthquake source parameters after this date.

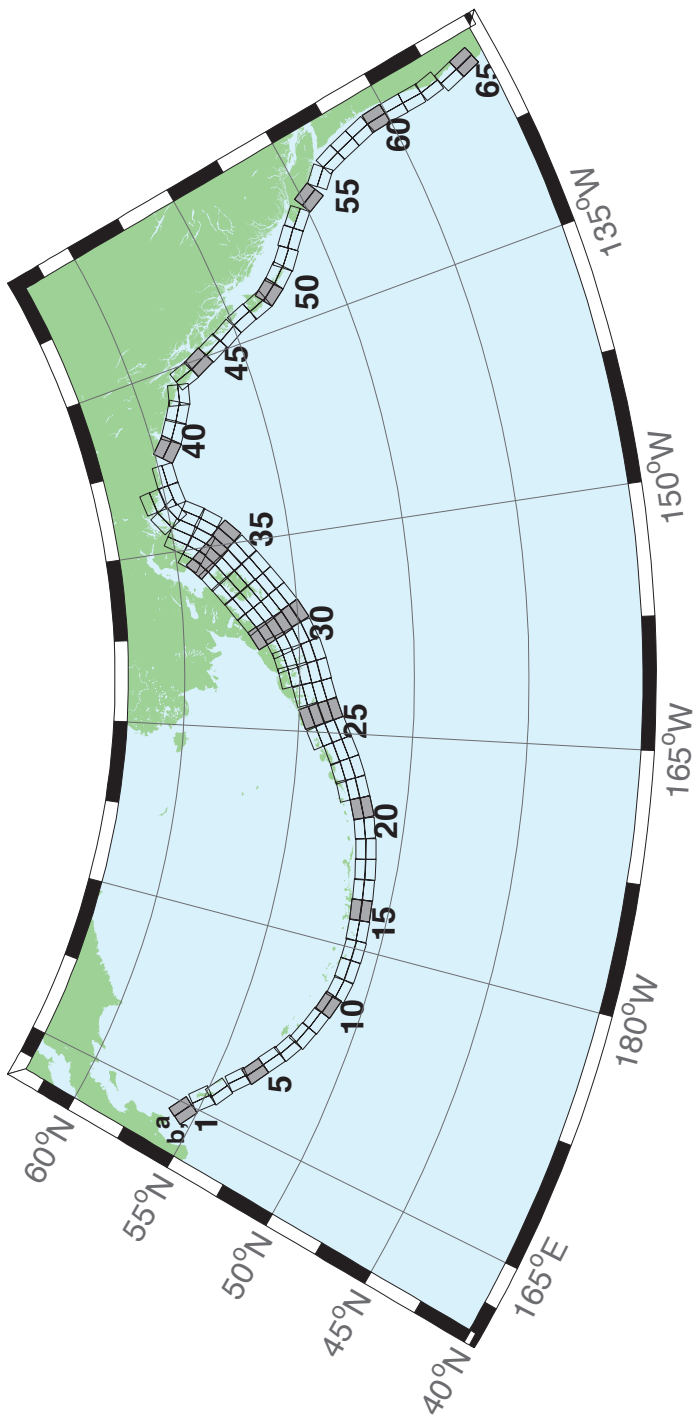


Figure B.1: Aleutian–Alaska–Cascadia Subduction Zone unit sources.

Table B.1: Earthquake parameters for Aleutian–Alaska–Cascadia Subduction Zone unit sources.

Segment	Description	Longitude(°E)	Latitude(°N)	Strike(°)	Dip(°)	Depth (km)
acsz-1a	Aleutian–Alaska–Cascadia	164.7994	55.9606	299	17	19.61
acsz-1b	Aleutian–Alaska–Cascadia	164.4310	55.5849	299	17	5
acsz-2a	Aleutian–Alaska–Cascadia	166.3418	55.4016	310.2	17	19.61
acsz-2b	Aleutian–Alaska–Cascadia	165.8578	55.0734	310.2	17	5
acsz-3a	Aleutian–Alaska–Cascadia	167.2939	54.8919	300.2	23.36	24.82
acsz-3b	Aleutian–Alaska–Cascadia	166.9362	54.5356	300.2	23.36	5
acsz-4a	Aleutian–Alaska–Cascadia	168.7131	54.2852	310.2	38.51	25.33
acsz-4b	Aleutian–Alaska–Cascadia	168.3269	54.0168	310.2	24	5
acsz-5a	Aleutian–Alaska–Cascadia	169.7447	53.7808	302.8	37.02	23.54
acsz-5b	Aleutian–Alaska–Cascadia	169.4185	53.4793	302.8	21.77	5
acsz-6a	Aleutian–Alaska–Cascadia	171.0144	53.3054	303.2	35.31	22.92
acsz-6b	Aleutian–Alaska–Cascadia	170.6813	52.9986	303.2	21	5
acsz-7a	Aleutian–Alaska–Cascadia	172.1500	52.8528	298.2	35.56	20.16
acsz-7b	Aleutian–Alaska–Cascadia	171.8665	52.5307	298.2	17.65	5
acsz-8a	Aleutian–Alaska–Cascadia	173.2726	52.4579	290.8	37.92	20.35
acsz-8b	Aleutian–Alaska–Cascadia	173.0681	52.1266	290.8	17.88	5
acsz-9a	Aleutian–Alaska–Cascadia	174.5866	52.1434	289	39.09	21.05
acsz-9b	Aleutian–Alaska–Cascadia	174.4027	51.8138	289	18.73	5
acsz-10a	Aleutian–Alaska–Cascadia	175.8784	51.8526	286.1	40.51	20.87
acsz-10b	Aleutian–Alaska–Cascadia	175.7265	51.5245	286.1	18.51	5
acsz-11a	Aleutian–Alaska–Cascadia	177.1140	51.6488	280	15	17.94
acsz-11b	Aleutian–Alaska–Cascadia	176.9937	51.2215	280	15	5
acsz-12a	Aleutian–Alaska–Cascadia	178.4500	51.5690	273	15	17.94
acsz-12b	Aleutian–Alaska–Cascadia	178.4130	51.1200	273	15	5
acsz-13a	Aleutian–Alaska–Cascadia	179.8550	51.5340	271	15	17.94
acsz-13b	Aleutian–Alaska–Cascadia	179.8420	51.0850	271	15	5
acsz-14a	Aleutian–Alaska–Cascadia	181.2340	51.5780	267	15	17.94
acsz-14b	Aleutian–Alaska–Cascadia	181.2720	51.1290	267	15	5
acsz-15a	Aleutian–Alaska–Cascadia	182.6380	51.6470	265	15	17.94
acsz-15b	Aleutian–Alaska–Cascadia	182.7000	51.2000	265	15	5
acsz-16a	Aleutian–Alaska–Cascadia	184.0550	51.7250	264	15	17.94
acsz-16b	Aleutian–Alaska–Cascadia	184.1280	51.2780	264	15	5
acsz-17a	Aleutian–Alaska–Cascadia	185.4560	51.8170	262	15	17.94
acsz-17b	Aleutian–Alaska–Cascadia	185.5560	51.3720	262	15	5
acsz-18a	Aleutian–Alaska–Cascadia	186.8680	51.9410	261	15	17.94
acsz-18b	Aleutian–Alaska–Cascadia	186.9810	51.4970	261	15	5
acsz-19a	Aleutian–Alaska–Cascadia	188.2430	52.1280	257	15	17.94
acsz-19b	Aleutian–Alaska–Cascadia	188.4060	51.6900	257	15	5
acsz-20a	Aleutian–Alaska–Cascadia	189.5810	52.3550	251	15	17.94
acsz-20b	Aleutian–Alaska–Cascadia	189.8180	51.9300	251	15	5
acsz-21a	Aleutian–Alaska–Cascadia	190.9570	52.6470	251	15	17.94
acsz-21b	Aleutian–Alaska–Cascadia	191.1960	52.2220	251	15	5
acsz-21z	Aleutian–Alaska–Cascadia	190.7399	53.0443	250.8	15	30.88
acsz-22a	Aleutian–Alaska–Cascadia	192.2940	52.9430	247	15	17.94
acsz-22b	Aleutian–Alaska–Cascadia	192.5820	52.5300	247	15	5
acsz-22z	Aleutian–Alaska–Cascadia	192.0074	53.3347	247.8	15	30.88
acsz-23a	Aleutian–Alaska–Cascadia	193.6270	53.3070	245	15	17.94
acsz-23b	Aleutian–Alaska–Cascadia	193.9410	52.9000	245	15	5
acsz-23z	Aleutian–Alaska–Cascadia	193.2991	53.6768	244.6	15	30.88
acsz-24a	Aleutian–Alaska–Cascadia	194.9740	53.6870	245	15	17.94
acsz-24b	Aleutian–Alaska–Cascadia	195.2910	53.2800	245	15	5
acsz-24y	Aleutian–Alaska–Cascadia	194.3645	54.4604	244.4	15	43.82
acsz-24z	Aleutian–Alaska–Cascadia	194.6793	54.0674	244.6	15	30.88

Continued on next page

Table B.1 – continued

Segment	Description	Longitude(°E)	Latitude(°N)	Strike(°)	Dip(°)	Depth (km)
acsz-25a	Aleutian–Alaska–Cascadia	196.4340	54.0760	250	15	17.94
acsz-25b	Aleutian–Alaska–Cascadia	196.6930	53.6543	250	15	5
acsz-25y	Aleutian–Alaska–Cascadia	195.9009	54.8572	247.9	15	43.82
acsz-25z	Aleutian–Alaska–Cascadia	196.1761	54.4536	248.1	15	30.88
acsz-26a	Aleutian–Alaska–Cascadia	197.8970	54.3600	253	15	17.94
acsz-26b	Aleutian–Alaska–Cascadia	198.1200	53.9300	253	15	5
acsz-26y	Aleutian–Alaska–Cascadia	197.5498	55.1934	253.1	15	43.82
acsz-26z	Aleutian–Alaska–Cascadia	197.7620	54.7770	253.3	15	30.88
acsz-27a	Aleutian–Alaska–Cascadia	199.4340	54.5960	256	15	17.94
acsz-27b	Aleutian–Alaska–Cascadia	199.6200	54.1600	256	15	5
acsz-27x	Aleutian–Alaska–Cascadia	198.9736	55.8631	256.5	15	56.24
acsz-27y	Aleutian–Alaska–Cascadia	199.1454	55.4401	256.6	15	43.82
acsz-27z	Aleutian–Alaska–Cascadia	199.3135	55.0170	256.8	15	30.88
acsz-28a	Aleutian–Alaska–Cascadia	200.8820	54.8300	253	15	17.94
acsz-28b	Aleutian–Alaska–Cascadia	201.1080	54.4000	253	15	5
acsz-28x	Aleutian–Alaska–Cascadia	200.1929	56.0559	252.5	15	56.24
acsz-28y	Aleutian–Alaska–Cascadia	200.4167	55.6406	252.7	15	43.82
acsz-28z	Aleutian–Alaska–Cascadia	200.6360	55.2249	252.9	15	30.88
acsz-29a	Aleutian–Alaska–Cascadia	202.2610	55.1330	247	15	17.94
acsz-29b	Aleutian–Alaska–Cascadia	202.5650	54.7200	247	15	5
acsz-29x	Aleutian–Alaska–Cascadia	201.2606	56.2861	245.7	15	56.24
acsz-29y	Aleutian–Alaska–Cascadia	201.5733	55.8888	246	15	43.82
acsz-29z	Aleutian–Alaska–Cascadia	201.8797	55.4908	246.2	15	30.88
acsz-30a	Aleutian–Alaska–Cascadia	203.6040	55.5090	240	15	17.94
acsz-30b	Aleutian–Alaska–Cascadia	203.9970	55.1200	240	15	5
acsz-30w	Aleutian–Alaska–Cascadia	201.9901	56.9855	239.5	15	69.12
acsz-30x	Aleutian–Alaska–Cascadia	202.3851	56.6094	239.8	15	56.24
acsz-30y	Aleutian–Alaska–Cascadia	202.7724	56.2320	240.2	15	43.82
acsz-30z	Aleutian–Alaska–Cascadia	203.1521	55.8534	240.5	15	30.88
acsz-31a	Aleutian–Alaska–Cascadia	204.8950	55.9700	236	15	17.94
acsz-31b	Aleutian–Alaska–Cascadia	205.3400	55.5980	236	15	5
acsz-31w	Aleutian–Alaska–Cascadia	203.0825	57.3740	234.5	15	69.12
acsz-31x	Aleutian–Alaska–Cascadia	203.5408	57.0182	234.9	15	56.24
acsz-31y	Aleutian–Alaska–Cascadia	203.9904	56.6607	235.3	15	43.82
acsz-31z	Aleutian–Alaska–Cascadia	204.4315	56.3016	235.7	15	30.88
acsz-32a	Aleutian–Alaska–Cascadia	206.2080	56.4730	236	15	17.94
acsz-32b	Aleutian–Alaska–Cascadia	206.6580	56.1000	236	15	5
acsz-32w	Aleutian–Alaska–Cascadia	204.4129	57.8908	234.3	15	69.12
acsz-32x	Aleutian–Alaska–Cascadia	204.8802	57.5358	234.7	15	56.24
acsz-32y	Aleutian–Alaska–Cascadia	205.3385	57.1792	235.1	15	43.82
acsz-32z	Aleutian–Alaska–Cascadia	205.7880	56.8210	235.5	15	30.88
acsz-33a	Aleutian–Alaska–Cascadia	207.5370	56.9750	236	15	17.94
acsz-33b	Aleutian–Alaska–Cascadia	207.9930	56.6030	236	15	5
acsz-33w	Aleutian–Alaska–Cascadia	205.7126	58.3917	234.2	15	69.12
acsz-33x	Aleutian–Alaska–Cascadia	206.1873	58.0371	234.6	15	56.24
acsz-33y	Aleutian–Alaska–Cascadia	206.6527	57.6808	235	15	43.82
acsz-33z	Aleutian–Alaska–Cascadia	207.1091	57.3227	235.4	15	30.88
acsz-34a	Aleutian–Alaska–Cascadia	208.9371	57.5124	236	15	17.94
acsz-34b	Aleutian–Alaska–Cascadia	209.4000	57.1400	236	15	5
acsz-34w	Aleutian–Alaska–Cascadia	206.9772	58.8804	233.5	15	69.12
acsz-34x	Aleutian–Alaska–Cascadia	207.4677	58.5291	233.9	15	56.24
acsz-34y	Aleutian–Alaska–Cascadia	207.9485	58.1760	234.3	15	43.82
acsz-34z	Aleutian–Alaska–Cascadia	208.4198	57.8213	234.7	15	30.88
acsz-35a	Aleutian–Alaska–Cascadia	210.2597	58.0441	230	15	17.94
acsz-35b	Aleutian–Alaska–Cascadia	210.8000	57.7000	230	15	5

Continued on next page

Table B.1 – continued

Segment	Description	Longitude(°E)	Latitude(°N)	Strike(°)	Dip(°)	Depth (km)
acsz-35w	Aleutian–Alaska–Cascadia	208.0204	59.3199	228.8	15	69.12
acsz-35x	Aleutian–Alaska–Cascadia	208.5715	58.9906	229.3	15	56.24
acsz-35y	Aleutian–Alaska–Cascadia	209.1122	58.6590	229.7	15	43.82
acsz-35z	Aleutian–Alaska–Cascadia	209.6425	58.3252	230.2	15	30.88
acsz-36a	Aleutian–Alaska–Cascadia	211.3249	58.6565	218	15	17.94
acsz-36b	Aleutian–Alaska–Cascadia	212.0000	58.3800	218	15	5
acsz-36w	Aleutian–Alaska–Cascadia	208.5003	59.5894	215.6	15	69.12
acsz-36x	Aleutian–Alaska–Cascadia	209.1909	59.3342	216.2	15	56.24
acsz-36y	Aleutian–Alaska–Cascadia	209.8711	59.0753	216.8	15	43.82
acsz-36z	Aleutian–Alaska–Cascadia	210.5412	58.8129	217.3	15	30.88
acsz-37a	Aleutian–Alaska–Cascadia	212.2505	59.2720	213.7	15	17.94
acsz-37b	Aleutian–Alaska–Cascadia	212.9519	59.0312	213.7	15	5
acsz-37x	Aleutian–Alaska–Cascadia	210.1726	60.0644	213	15	56.24
acsz-37y	Aleutian–Alaska–Cascadia	210.8955	59.8251	213.7	15	43.82
acsz-37z	Aleutian–Alaska–Cascadia	211.6079	59.5820	214.3	15	30.88
acsz-38a	Aleutian–Alaska–Cascadia	214.6555	60.1351	260.1	0	15
acsz-38b	Aleutian–Alaska–Cascadia	214.8088	59.6927	260.1	0	15
acsz-38y	Aleutian–Alaska–Cascadia	214.3737	60.9838	259	0	15
acsz-38z	Aleutian–Alaska–Cascadia	214.5362	60.5429	259	0	15
acsz-39a	Aleutian–Alaska–Cascadia	216.5607	60.2480	267	0	15
acsz-39b	Aleutian–Alaska–Cascadia	216.6068	59.7994	267	0	15
acsz-40a	Aleutian–Alaska–Cascadia	219.3069	59.7574	310.9	0	15
acsz-40b	Aleutian–Alaska–Cascadia	218.7288	59.4180	310.9	0	15
acsz-41a	Aleutian–Alaska–Cascadia	220.4832	59.3390	300.7	0	15
acsz-41b	Aleutian–Alaska–Cascadia	220.0382	58.9529	300.7	0	15
acsz-42a	Aleutian–Alaska–Cascadia	221.8835	58.9310	298.9	0	15
acsz-42b	Aleutian–Alaska–Cascadia	221.4671	58.5379	298.9	0	15
acsz-43a	Aleutian–Alaska–Cascadia	222.9711	58.6934	282.3	0	15
acsz-43b	Aleutian–Alaska–Cascadia	222.7887	58.2546	282.3	0	15
acsz-44a	Aleutian–Alaska–Cascadia	224.9379	57.9054	340.9	12	11.09
acsz-44b	Aleutian–Alaska–Cascadia	224.1596	57.7617	340.9	7	5
acsz-45a	Aleutian–Alaska–Cascadia	225.4994	57.1634	334.1	12	11.09
acsz-45b	Aleutian–Alaska–Cascadia	224.7740	56.9718	334.1	7	5
acsz-46a	Aleutian–Alaska–Cascadia	226.1459	56.3552	334.1	12	11.09
acsz-46b	Aleutian–Alaska–Cascadia	225.4358	56.1636	334.1	7	5
acsz-47a	Aleutian–Alaska–Cascadia	226.7731	55.5830	332.3	12	11.09
acsz-47b	Aleutian–Alaska–Cascadia	226.0887	55.3785	332.3	7	5
acsz-48a	Aleutian–Alaska–Cascadia	227.4799	54.6763	339.4	12	11.09
acsz-48b	Aleutian–Alaska–Cascadia	226.7713	54.5217	339.4	7	5
acsz-49a	Aleutian–Alaska–Cascadia	227.9482	53.8155	341.2	12	11.09
acsz-49b	Aleutian–Alaska–Cascadia	227.2462	53.6737	341.2	7	5
acsz-50a	Aleutian–Alaska–Cascadia	228.3970	53.2509	324.5	12	11.09
acsz-50b	Aleutian–Alaska–Cascadia	227.8027	52.9958	324.5	7	5
acsz-51a	Aleutian–Alaska–Cascadia	229.1844	52.6297	318.4	12	11.09
acsz-51b	Aleutian–Alaska–Cascadia	228.6470	52.3378	318.4	7	5
acsz-52a	Aleutian–Alaska–Cascadia	230.0306	52.0768	310.9	12	11.09
acsz-52b	Aleutian–Alaska–Cascadia	229.5665	51.7445	310.9	7	5
acsz-53a	Aleutian–Alaska–Cascadia	231.1735	51.5258	310.9	12	11.09
acsz-53b	Aleutian–Alaska–Cascadia	230.7150	51.1935	310.9	7	5
acsz-54a	Aleutian–Alaska–Cascadia	232.2453	50.8809	314.1	12	11.09
acsz-54b	Aleutian–Alaska–Cascadia	231.7639	50.5655	314.1	7	5
acsz-55a	Aleutian–Alaska–Cascadia	233.3066	49.9032	333.7	12	11.09
acsz-55b	Aleutian–Alaska–Cascadia	232.6975	49.7086	333.7	7	5
acsz-56a	Aleutian–Alaska–Cascadia	234.0588	49.1702	315	11	12.82
acsz-56b	Aleutian–Alaska–Cascadia	233.5849	48.8584	315	9	5

Continued on next page

Table B.1 – continued

Segment	Description	Longitude($^{\circ}$ E)	Latitude($^{\circ}$ N)	Strike($^{\circ}$)	Dip($^{\circ}$)	Depth (km)
acsz-57a	Aleutian–Alaska–Cascadia	234.9041	48.2596	341	11	12.82
acsz-57b	Aleutian–Alaska–Cascadia	234.2797	48.1161	341	9	5
acsz-58a	Aleutian–Alaska–Cascadia	235.3021	47.3812	344	11	12.82
acsz-58b	Aleutian–Alaska–Cascadia	234.6776	47.2597	344	9	5
acsz-59a	Aleutian–Alaska–Cascadia	235.6432	46.5082	345	11	12.82
acsz-59b	Aleutian–Alaska–Cascadia	235.0257	46.3941	345	9	5
acsz-60a	Aleutian–Alaska–Cascadia	235.8640	45.5429	356	11	12.82
acsz-60b	Aleutian–Alaska–Cascadia	235.2363	45.5121	356	9	5
acsz-61a	Aleutian–Alaska–Cascadia	235.9106	44.6227	359	11	12.82
acsz-61b	Aleutian–Alaska–Cascadia	235.2913	44.6150	359	9	5
acsz-62a	Aleutian–Alaska–Cascadia	235.9229	43.7245	359	11	12.82
acsz-62b	Aleutian–Alaska–Cascadia	235.3130	43.7168	359	9	5
acsz-63a	Aleutian–Alaska–Cascadia	236.0220	42.9020	350	11	12.82
acsz-63b	Aleutian–Alaska–Cascadia	235.4300	42.8254	350	9	5
acsz-64a	Aleutian–Alaska–Cascadia	235.9638	41.9818	345	11	12.82
acsz-64b	Aleutian–Alaska–Cascadia	235.3919	41.8677	345	9	5
acsz-65a	Aleutian–Alaska–Cascadia	236.2643	41.1141	345	11	12.82
acsz-65b	Aleutian–Alaska–Cascadia	235.7000	41.0000	345	9	5
acsz-238a	Aleutian–Alaska–Cascadia	213.2878	59.8406	236.8	15	17.94
acsz-238y	Aleutian–Alaska–Cascadia	212.3424	60.5664	236.8	15	43.82
acsz-238z	Aleutian–Alaska–Cascadia	212.8119	60.2035	236.8	15	30.88

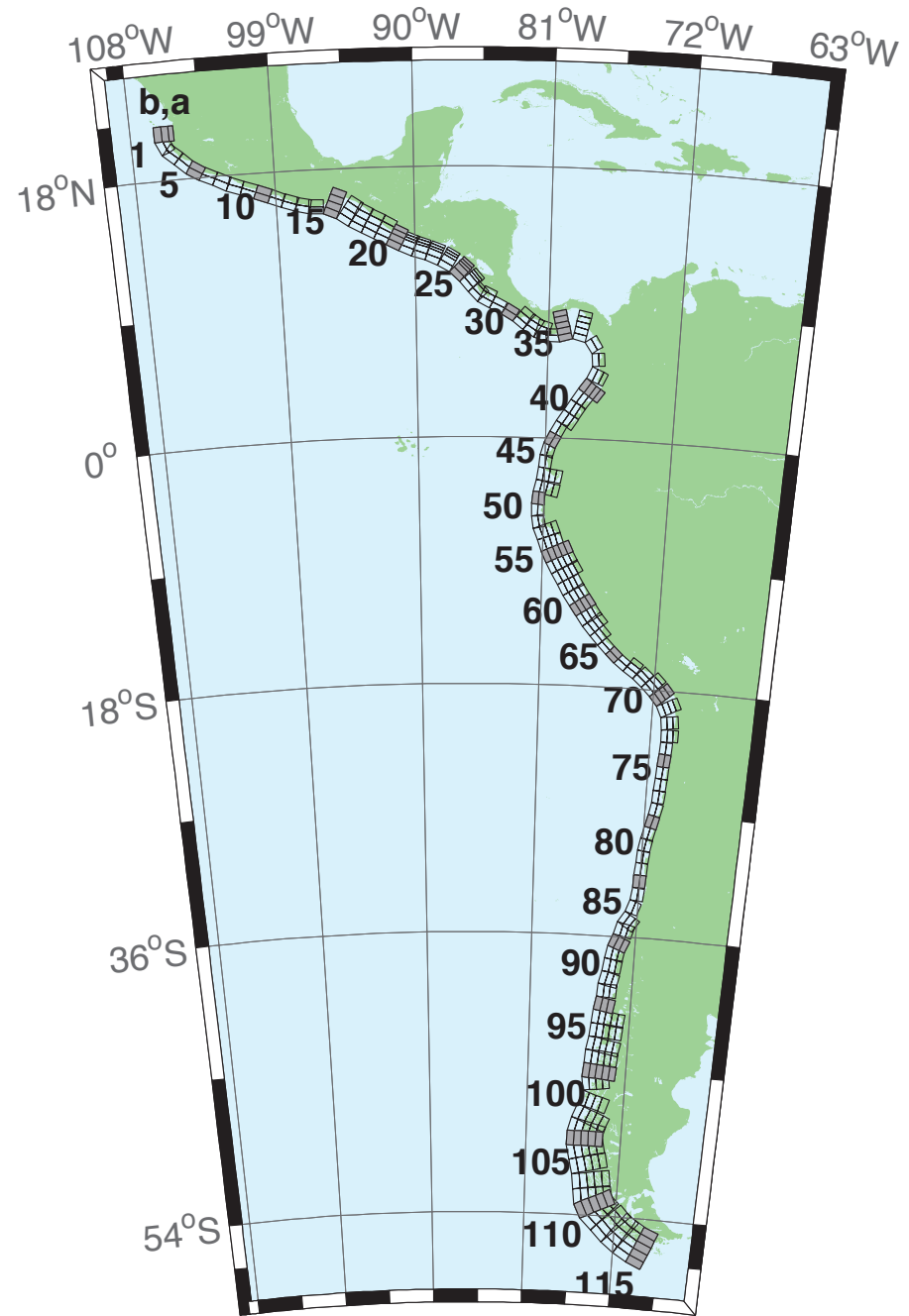


Figure B.2: Central and South America Subduction Zone unit sources.

Table B.2: Earthquake parameters for Central and South America Subduction Zone unit sources.

Segment	Description	Longitude(°E)	Latitude(°N)	Strike(°)	Dip(°)	Depth (km)
cssz-1a	Central and South America	254.4573	20.8170	359	19	15.4
cssz-1b	Central and South America	254.0035	20.8094	359	12	5
cssz-1z	Central and South America	254.7664	20.8222	359	50	31.67
cssz-2a	Central and South America	254.5765	20.2806	336.8	19	15.4
cssz-2b	Central and South America	254.1607	20.1130	336.8	12	5
cssz-3a	Central and South America	254.8789	19.8923	310.6	18.31	15.27
cssz-3b	Central and South America	254.5841	19.5685	310.6	11.85	5
cssz-4a	Central and South America	255.6167	19.2649	313.4	17.62	15.12
cssz-4b	Central and South America	255.3056	18.9537	313.4	11.68	5
cssz-5a	Central and South America	256.2240	18.8148	302.7	16.92	15
cssz-5b	Central and South America	255.9790	18.4532	302.7	11.54	5
cssz-6a	Central and South America	256.9425	18.4383	295.1	16.23	14.87
cssz-6b	Central and South America	256.7495	18.0479	295.1	11.38	5
cssz-7a	Central and South America	257.8137	18.0339	296.9	15.54	14.74
cssz-7b	Central and South America	257.6079	17.6480	296.9	11.23	5
cssz-8a	Central and South America	258.5779	17.7151	290.4	14.85	14.61
cssz-8b	Central and South America	258.4191	17.3082	290.4	11.08	5
cssz-9a	Central and South America	259.4578	17.4024	290.5	14.15	14.47
cssz-9b	Central and South America	259.2983	16.9944	290.5	10.92	5
cssz-10a	Central and South America	260.3385	17.0861	290.8	13.46	14.34
cssz-10b	Central and South America	260.1768	16.6776	290.8	10.77	5
cssz-11a	Central and South America	261.2255	16.7554	291.8	12.77	14.21
cssz-11b	Central and South America	261.0556	16.3487	291.8	10.62	5
cssz-12a	Central and South America	262.0561	16.4603	288.9	12.08	14.08
cssz-12b	Central and South America	261.9082	16.0447	288.9	10.46	5
cssz-13a	Central and South America	262.8638	16.2381	283.2	11.38	13.95
cssz-13b	Central and South America	262.7593	15.8094	283.2	10.31	5
cssz-14a	Central and South America	263.6066	16.1435	272.1	10.69	13.81
cssz-14b	Central and South America	263.5901	15.7024	272.1	10.15	5
cssz-15a	Central and South America	264.8259	15.8829	293	10	13.68
cssz-15b	Central and South America	264.6462	15.4758	293	10	5
cssz-15y	Central and South America	265.1865	16.6971	293	10	31.05
cssz-15z	Central and South America	265.0060	16.2900	293	10	22.36
cssz-16a	Central and South America	265.7928	15.3507	304.9	15	15.82
cssz-16b	Central and South America	265.5353	14.9951	304.9	12.5	5
cssz-16y	Central and South America	266.3092	16.0619	304.9	15	41.7
cssz-16z	Central and South America	266.0508	15.7063	304.9	15	28.76
cssz-17a	Central and South America	266.4947	14.9019	299.5	20	17.94
cssz-17b	Central and South America	266.2797	14.5346	299.5	15	5
cssz-17y	Central and South America	266.9259	15.6365	299.5	20	52.14
cssz-17z	Central and South America	266.7101	15.2692	299.5	20	35.04
cssz-18a	Central and South America	267.2827	14.4768	298	21.5	17.94
cssz-18b	Central and South America	267.0802	14.1078	298	15	5
cssz-18y	Central and South America	267.6888	15.2148	298	21.5	54.59
cssz-18z	Central and South America	267.4856	14.8458	298	21.5	36.27
cssz-19a	Central and South America	268.0919	14.0560	297.6	23	17.94
cssz-19b	Central and South America	267.8943	13.6897	297.6	15	5
cssz-19y	Central and South America	268.4880	14.7886	297.6	23	57.01
cssz-19z	Central and South America	268.2898	14.4223	297.6	23	37.48
cssz-20a	Central and South America	268.8929	13.6558	296.2	24	17.94
cssz-20b	Central and South America	268.7064	13.2877	296.2	15	5
cssz-20y	Central and South America	269.1796	14.2206	296.2	45.5	73.94
cssz-20z	Central and South America	269.0362	13.9382	296.2	45.5	38.28

Continued on next page

Table B.2 – continued

Segment	Description	Longitude($^{\circ}$ E)	Latitude($^{\circ}$ N)	Strike($^{\circ}$)	Dip($^{\circ}$)	Depth (km)
cssz-21a	Central and South America	269.6797	13.3031	292.6	25	17.94
cssz-21b	Central and South America	269.5187	12.9274	292.6	15	5
cssz-21x	Central and South America	269.8797	13.7690	292.6	68	131.8
cssz-21y	Central and South America	269.8130	13.6137	292.6	68	85.43
cssz-21z	Central and South America	269.7463	13.4584	292.6	68	39.07
cssz-22a	Central and South America	270.4823	13.0079	288.6	25	17.94
cssz-22b	Central and South America	270.3492	12.6221	288.6	15	5
cssz-22x	Central and South America	270.6476	13.4864	288.6	68	131.8
cssz-22y	Central and South America	270.5925	13.3269	288.6	68	85.43
cssz-22z	Central and South America	270.5374	13.1674	288.6	68	39.07
cssz-23a	Central and South America	271.3961	12.6734	292.4	25	17.94
cssz-23b	Central and South America	271.2369	12.2972	292.4	15	5
cssz-23x	Central and South America	271.5938	13.1399	292.4	68	131.8
cssz-23y	Central and South America	271.5279	12.9844	292.4	68	85.43
cssz-23z	Central and South America	271.4620	12.8289	292.4	68	39.07
cssz-24a	Central and South America	272.3203	12.2251	300.2	25	17.94
cssz-24b	Central and South America	272.1107	11.8734	300.2	15	5
cssz-24x	Central and South America	272.5917	12.6799	300.2	67	131.1
cssz-24y	Central and South America	272.5012	12.5283	300.2	67	85.1
cssz-24z	Central and South America	272.4107	12.3767	300.2	67	39.07
cssz-25a	Central and South America	273.2075	11.5684	313.8	25	17.94
cssz-25b	Central and South America	272.9200	11.2746	313.8	15	5
cssz-25x	Central and South America	273.5950	11.9641	313.8	66	130.4
cssz-25y	Central and South America	273.4658	11.8322	313.8	66	84.75
cssz-25z	Central and South America	273.3366	11.7003	313.8	66	39.07
cssz-26a	Central and South America	273.8943	10.8402	320.4	25	17.94
cssz-26b	Central and South America	273.5750	10.5808	320.4	15	5
cssz-26x	Central and South America	274.3246	11.1894	320.4	66	130.4
cssz-26y	Central and South America	274.1811	11.0730	320.4	66	84.75
cssz-26z	Central and South America	274.0377	10.9566	320.4	66	39.07
cssz-27a	Central and South America	274.4569	10.2177	316.1	25	17.94
cssz-27b	Central and South America	274.1590	9.9354	316.1	15	5
cssz-27z	Central and South America	274.5907	10.3444	316.1	66	39.07
cssz-28a	Central and South America	274.9586	9.8695	297.1	22	14.54
cssz-28b	Central and South America	274.7661	9.4988	297.1	11	5
cssz-28z	Central and South America	275.1118	10.1643	297.1	42.5	33.27
cssz-29a	Central and South America	275.7686	9.4789	296.6	19	11.09
cssz-29b	Central and South America	275.5759	9.0992	296.6	7	5
cssz-30a	Central and South America	276.6346	8.9973	302.2	19	9.36
cssz-30b	Central and South America	276.4053	8.6381	302.2	5	5
cssz-31a	Central and South America	277.4554	8.4152	309.1	19	7.62
cssz-31b	Central and South America	277.1851	8.0854	309.1	3	5
cssz-31z	Central and South America	277.7260	8.7450	309.1	19	23.9
cssz-32a	Central and South America	278.1112	7.9425	303	18.67	8.49
cssz-32b	Central and South America	277.8775	7.5855	303	4	5
cssz-32z	Central and South America	278.3407	8.2927	303	21.67	24.49
cssz-33a	Central and South America	278.7082	7.6620	287.6	18.33	10.23
cssz-33b	Central and South America	278.5785	7.2555	287.6	6	5
cssz-33z	Central and South America	278.8328	8.0522	287.6	24.33	25.95
cssz-34a	Central and South America	279.3184	7.5592	269.5	18	17.94
cssz-34b	Central and South America	279.3223	7.1320	269.5	15	5
cssz-35a	Central and South America	280.0039	7.6543	255.9	17.67	14.54
cssz-35b	Central and South America	280.1090	7.2392	255.9	11	5
cssz-35x	Central and South America	279.7156	8.7898	255.9	29.67	79.22
cssz-35y	Central and South America	279.8118	8.4113	255.9	29.67	54.47

Continued on next page

Table B.2 – continued

Segment	Description	Longitude(°E)	Latitude(°N)	Strike(°)	Dip(°)	Depth (km)
cssz-35z	Central and South America	279.9079	8.0328	255.9	29.67	29.72
cssz-36a	Central and South America	281.2882	7.6778	282.5	17.33	11.09
cssz-36b	Central and South America	281.1948	7.2592	282.5	7	5
cssz-36x	Central and South America	281.5368	8.7896	282.5	32.33	79.47
cssz-36y	Central and South America	281.4539	8.4190	282.5	32.33	52.73
cssz-36z	Central and South America	281.3710	8.0484	282.5	32.33	25.99
cssz-37a	Central and South America	282.5252	6.8289	326.9	17	10.23
cssz-37b	Central and South America	282.1629	6.5944	326.9	6	5
cssz-38a	Central and South America	282.9469	5.5973	355.4	17	10.23
cssz-38b	Central and South America	282.5167	5.5626	355.4	6	5
cssz-39a	Central and South America	282.7236	4.3108	24.13	17	10.23
cssz-39b	Central and South America	282.3305	4.4864	24.13	6	5
cssz-39z	Central and South America	283.0603	4.1604	24.13	35	24.85
cssz-40a	Central and South America	282.1940	3.3863	35.28	17	10.23
cssz-40b	Central and South America	281.8427	3.6344	35.28	6	5
cssz-40y	Central and South America	282.7956	2.9613	35.28	35	53.52
cssz-40z	Central and South America	282.4948	3.1738	35.28	35	24.85
cssz-41a	Central and South America	281.6890	2.6611	34.27	17	10.23
cssz-41b	Central and South America	281.3336	2.9030	34.27	6	5
cssz-41z	Central and South America	281.9933	2.4539	34.27	35	24.85
cssz-42a	Central and South America	281.2266	1.9444	31.29	17	10.23
cssz-42b	Central and South America	280.8593	2.1675	31.29	6	5
cssz-42z	Central and South America	281.5411	1.7533	31.29	35	24.85
cssz-43a	Central and South America	280.7297	1.1593	33.3	17	10.23
cssz-43b	Central and South America	280.3706	1.3951	33.3	6	5
cssz-43z	Central and South America	281.0373	0.9573	33.3	35	24.85
cssz-44a	Central and South America	280.3018	0.4491	28.8	17	10.23
cssz-44b	Central and South America	279.9254	0.6560	28.8	6	5
cssz-45a	Central and South America	279.9083	-0.3259	26.91	10	8.49
cssz-45b	Central and South America	279.5139	-0.1257	26.91	4	5
cssz-46a	Central and South America	279.6461	-0.9975	15.76	10	8.49
cssz-46b	Central and South America	279.2203	-0.8774	15.76	4	5
cssz-47a	Central and South America	279.4972	-1.7407	6.9	10	8.49
cssz-47b	Central and South America	279.0579	-1.6876	6.9	4	5
cssz-48a	Central and South America	279.3695	-2.6622	8.96	10	8.49
cssz-48b	Central and South America	278.9321	-2.5933	8.96	4	5
cssz-48y	Central and South America	280.2444	-2.8000	8.96	10	25.85
cssz-48z	Central and South America	279.8070	-2.7311	8.96	10	17.17
cssz-49a	Central and South America	279.1852	-3.6070	13.15	10	8.49
cssz-49b	Central and South America	278.7536	-3.5064	13.15	4	5
cssz-49y	Central and South America	280.0486	-3.8082	13.15	10	25.85
cssz-49z	Central and South America	279.6169	-3.7076	13.15	10	17.17
cssz-50a	Central and South America	279.0652	-4.3635	4.78	10.33	9.64
cssz-50b	Central and South America	278.6235	-4.3267	4.78	5.33	5
cssz-51a	Central and South America	279.0349	-5.1773	359.4	10.67	10.81
cssz-51b	Central and South America	278.5915	-5.1817	359.4	6.67	5
cssz-52a	Central and South America	279.1047	-5.9196	349.8	11	11.96
cssz-52b	Central and South America	278.6685	-5.9981	349.8	8	5
cssz-53a	Central and South America	279.3044	-6.6242	339.2	10.25	11.74
cssz-53b	Central and South America	278.8884	-6.7811	339.2	7.75	5
cssz-53y	Central and South America	280.1024	-6.3232	339.2	19.25	37.12
cssz-53z	Central and South America	279.7035	-6.4737	339.2	19.25	20.64
cssz-54a	Central and South America	279.6256	-7.4907	340.8	9.5	11.53
cssz-54b	Central and South America	279.2036	-7.6365	340.8	7.5	5
cssz-54y	Central and South America	280.4267	-7.2137	340.8	20.5	37.29

Continued on next page

Table B.2 – continued

Segment	Description	Longitude(°E)	Latitude(°N)	Strike(°)	Dip(°)	Depth (km)
cssz-54z	Central and South America	280.0262	-7.3522	340.8	20.5	19.78
cssz-55a	Central and South America	279.9348	-8.2452	335.4	8.75	11.74
cssz-55b	Central and South America	279.5269	-8.4301	335.4	7.75	5
cssz-55x	Central and South America	281.0837	-7.7238	335.4	21.75	56.4
cssz-55y	Central and South America	280.7009	-7.8976	335.4	21.75	37.88
cssz-55z	Central and South America	280.3180	-8.0714	335.4	21.75	19.35
cssz-56a	Central and South America	280.3172	-8.9958	331.6	8	11.09
cssz-56b	Central and South America	279.9209	-9.2072	331.6	7	5
cssz-56x	Central and South America	281.4212	-8.4063	331.6	23	57.13
cssz-56y	Central and South America	281.0534	-8.6028	331.6	23	37.59
cssz-56z	Central and South America	280.6854	-8.7993	331.6	23	18.05
cssz-57a	Central and South America	280.7492	-9.7356	328.7	8.6	10.75
cssz-57b	Central and South America	280.3640	-9.9663	328.7	6.6	5
cssz-57x	Central and South America	281.8205	-9.0933	328.7	23.4	57.94
cssz-57y	Central and South America	281.4636	-9.3074	328.7	23.4	38.08
cssz-57z	Central and South America	281.1065	-9.5215	328.7	23.4	18.22
cssz-58a	Central and South America	281.2275	-10.5350	330.5	9.2	10.4
cssz-58b	Central and South America	280.8348	-10.7532	330.5	6.2	5
cssz-58y	Central and South America	281.9548	-10.1306	330.5	23.8	38.57
cssz-58z	Central and South America	281.5913	-10.3328	330.5	23.8	18.39
cssz-59a	Central and South America	281.6735	-11.2430	326.2	9.8	10.05
cssz-59b	Central and South America	281.2982	-11.4890	326.2	5.8	5
cssz-59y	Central and South America	282.3675	-10.7876	326.2	24.2	39.06
cssz-59z	Central and South America	282.0206	-11.0153	326.2	24.2	18.56
cssz-60a	Central and South America	282.1864	-11.9946	326.5	10.4	9.71
cssz-60b	Central and South America	281.8096	-12.2384	326.5	5.4	5
cssz-60y	Central and South America	282.8821	-11.5438	326.5	24.6	39.55
cssz-60z	Central and South America	282.5344	-11.7692	326.5	24.6	18.73
cssz-61a	Central and South America	282.6944	-12.7263	325.5	11	9.36
cssz-61b	Central and South America	282.3218	-12.9762	325.5	5	5
cssz-61y	Central and South America	283.3814	-12.2649	325.5	25	40.03
cssz-61z	Central and South America	283.0381	-12.4956	325.5	25	18.9
cssz-62a	Central and South America	283.1980	-13.3556	319	11	9.79
cssz-62b	Central and South America	282.8560	-13.6451	319	5.5	5
cssz-62y	Central and South America	283.8178	-12.8300	319	27	42.03
cssz-62z	Central and South America	283.5081	-13.0928	319	27	19.33
cssz-63a	Central and South America	283.8032	-14.0147	317.9	11	10.23
cssz-63b	Central and South America	283.4661	-14.3106	317.9	6	5
cssz-63z	Central and South America	284.1032	-13.7511	317.9	29	19.77
cssz-64a	Central and South America	284.4144	-14.6482	315.7	13	11.96
cssz-64b	Central and South America	284.0905	-14.9540	315.7	8	5
cssz-65a	Central and South America	285.0493	-15.2554	313.2	15	13.68
cssz-65b	Central and South America	284.7411	-15.5715	313.2	10	5
cssz-66a	Central and South America	285.6954	-15.7816	307.7	14.5	13.68
cssz-66b	Central and South America	285.4190	-16.1258	307.7	10	5
cssz-67a	Central and South America	286.4127	-16.2781	304.3	14	13.68
cssz-67b	Central and South America	286.1566	-16.6381	304.3	10	5
cssz-67z	Central and South America	286.6552	-15.9365	304.3	23	25.78
cssz-68a	Central and South America	287.2481	-16.9016	311.8	14	13.68
cssz-68b	Central and South America	286.9442	-17.2264	311.8	10	5
cssz-68z	Central and South America	287.5291	-16.6007	311.8	26	25.78
cssz-69a	Central and South America	287.9724	-17.5502	314.9	14	13.68
cssz-69b	Central and South America	287.6496	-17.8590	314.9	10	5
cssz-69y	Central and South America	288.5530	-16.9934	314.9	29	50.02
cssz-69z	Central and South America	288.2629	-17.2718	314.9	29	25.78

Continued on next page

Table B.2 – continued

Segment	Description	Longitude($^{\circ}$ E)	Latitude($^{\circ}$ N)	Strike($^{\circ}$)	Dip($^{\circ}$)	Depth (km)
cssz-70a	Central and South America	288.6731	-18.2747	320.4	14	13.25
cssz-70b	Central and South America	288.3193	-18.5527	320.4	9.5	5
cssz-70y	Central and South America	289.3032	-17.7785	320.4	30	50.35
cssz-70z	Central and South America	288.9884	-18.0266	320.4	30	25.35
cssz-71a	Central and South America	289.3089	-19.1854	333.2	14	12.82
cssz-71b	Central and South America	288.8968	-19.3820	333.2	9	5
cssz-71y	Central and South America	290.0357	-18.8382	333.2	31	50.67
cssz-71z	Central and South America	289.6725	-19.0118	333.2	31	24.92
cssz-72a	Central and South America	289.6857	-20.3117	352.4	14	12.54
cssz-72b	Central and South America	289.2250	-20.3694	352.4	8.67	5
cssz-72z	Central and South America	290.0882	-20.2613	352.4	32	24.63
cssz-73a	Central and South America	289.7731	-21.3061	358.9	14	12.24
cssz-73b	Central and South America	289.3053	-21.3142	358.9	8.33	5
cssz-73z	Central and South America	290.1768	-21.2991	358.9	33	24.34
cssz-74a	Central and South America	289.7610	-22.2671	3.06	14	11.96
cssz-74b	Central and South America	289.2909	-22.2438	3.06	8	5
cssz-75a	Central and South America	289.6982	-23.1903	4.83	14.09	11.96
cssz-75b	Central and South America	289.2261	-23.1536	4.83	8	5
cssz-76a	Central and South America	289.6237	-24.0831	4.67	14.18	11.96
cssz-76b	Central and South America	289.1484	-24.0476	4.67	8	5
cssz-77a	Central and South America	289.5538	-24.9729	4.3	14.27	11.96
cssz-77b	Central and South America	289.0750	-24.9403	4.3	8	5
cssz-78a	Central and South America	289.4904	-25.8621	3.86	14.36	11.96
cssz-78b	Central and South America	289.0081	-25.8328	3.86	8	5
cssz-79a	Central and South America	289.3491	-26.8644	11.34	14.45	11.96
cssz-79b	Central and South America	288.8712	-26.7789	11.34	8	5
cssz-80a	Central and South America	289.1231	-27.7826	14.16	14.54	11.96
cssz-80b	Central and South America	288.6469	-27.6762	14.16	8	5
cssz-81a	Central and South America	288.8943	-28.6409	13.19	14.63	11.96
cssz-81b	Central and South America	288.4124	-28.5417	13.19	8	5
cssz-82a	Central and South America	288.7113	-29.4680	9.68	14.72	11.96
cssz-82b	Central and South America	288.2196	-29.3950	9.68	8	5
cssz-83a	Central and South America	288.5944	-30.2923	5.36	14.81	11.96
cssz-83b	Central and South America	288.0938	-30.2517	5.36	8	5
cssz-84a	Central and South America	288.5223	-31.1639	3.8	14.9	11.96
cssz-84b	Central and South America	288.0163	-31.1351	3.8	8	5
cssz-85a	Central and South America	288.4748	-32.0416	2.55	15	11.96
cssz-85b	Central and South America	287.9635	-32.0223	2.55	8	5
cssz-86a	Central and South America	288.3901	-33.0041	7.01	15	11.96
cssz-86b	Central and South America	287.8768	-32.9512	7.01	8	5
cssz-87a	Central and South America	288.1050	-34.0583	19.4	15	11.96
cssz-87b	Central and South America	287.6115	-33.9142	19.4	8	5
cssz-88a	Central and South America	287.5309	-35.0437	32.81	15	11.96
cssz-88b	Central and South America	287.0862	-34.8086	32.81	8	5
cssz-88z	Central and South America	287.9308	-35.2545	32.81	30	24.9
cssz-89a	Central and South America	287.2380	-35.5993	14.52	16.67	11.96
cssz-89b	Central and South America	286.7261	-35.4914	14.52	8	5
cssz-89z	Central and South America	287.7014	-35.6968	14.52	30	26.3
cssz-90a	Central and South America	286.8442	-36.5645	22.64	18.33	11.96
cssz-90b	Central and South America	286.3548	-36.4004	22.64	8	5
cssz-90z	Central and South America	287.2916	-36.7142	22.64	30	27.68
cssz-91a	Central and South America	286.5925	-37.2488	10.9	20	11.96
cssz-91b	Central and South America	286.0721	-37.1690	10.9	8	5
cssz-91z	Central and South America	287.0726	-37.3224	10.9	30	29.06
cssz-92a	Central and South America	286.4254	-38.0945	8.23	20	11.96

Continued on next page

Table B.2 – continued

Segment	Description	Longitude(°E)	Latitude(°N)	Strike(°)	Dip(°)	Depth (km)
cssz-92b	Central and South America	285.8948	-38.0341	8.23	8	5
cssz-92z	Central and South America	286.9303	-38.1520	8.23	26.67	29.06
cssz-93a	Central and South America	286.2047	-39.0535	13.46	20	11.96
cssz-93b	Central and South America	285.6765	-38.9553	13.46	8	5
cssz-93z	Central and South America	286.7216	-39.1495	13.46	23.33	29.06
cssz-94a	Central and South America	286.0772	-39.7883	3.4	20	11.96
cssz-94b	Central and South America	285.5290	-39.7633	3.4	8	5
cssz-94z	Central and South America	286.6255	-39.8133	3.4	20	29.06
cssz-95a	Central and South America	285.9426	-40.7760	9.84	20	11.96
cssz-95b	Central and South America	285.3937	-40.7039	9.84	8	5
cssz-95z	Central and South America	286.4921	-40.8481	9.84	20	29.06
cssz-96a	Central and South America	285.7839	-41.6303	7.6	20	11.96
cssz-96b	Central and South America	285.2245	-41.5745	7.6	8	5
cssz-96x	Central and South America	287.4652	-41.7977	7.6	20	63.26
cssz-96y	Central and South America	286.9043	-41.7419	7.6	20	46.16
cssz-96z	Central and South America	286.3439	-41.6861	7.6	20	29.06
cssz-97a	Central and South America	285.6695	-42.4882	5.3	20	11.96
cssz-97b	Central and South America	285.0998	-42.4492	5.3	8	5
cssz-97x	Central and South America	287.3809	-42.6052	5.3	20	63.26
cssz-97y	Central and South America	286.8101	-42.5662	5.3	20	46.16
cssz-97z	Central and South America	286.2396	-42.5272	5.3	20	29.06
cssz-98a	Central and South America	285.5035	-43.4553	10.53	20	11.96
cssz-98b	Central and South America	284.9322	-43.3782	10.53	8	5
cssz-98x	Central and South America	287.2218	-43.6866	10.53	20	63.26
cssz-98y	Central and South America	286.6483	-43.6095	10.53	20	46.16
cssz-98z	Central and South America	286.0755	-43.5324	10.53	20	29.06
cssz-99a	Central and South America	285.3700	-44.2595	4.86	20	11.96
cssz-99b	Central and South America	284.7830	-44.2237	4.86	8	5
cssz-99x	Central and South America	287.1332	-44.3669	4.86	20	63.26
cssz-99y	Central and South America	286.5451	-44.3311	4.86	20	46.16
cssz-99z	Central and South America	285.9574	-44.2953	4.86	20	29.06
cssz-100a	Central and South America	285.2713	-45.1664	5.68	20	11.96
cssz-100b	Central and South America	284.6758	-45.1246	5.68	8	5
cssz-100x	Central and South America	287.0603	-45.2918	5.68	20	63.26
cssz-100y	Central and South America	286.4635	-45.2500	5.68	20	46.16
cssz-100z	Central and South America	285.8672	-45.2082	5.68	20	29.06
cssz-101a	Central and South America	285.3080	-45.8607	352.6	20	9.36
cssz-101b	Central and South America	284.7067	-45.9152	352.6	5	5
cssz-101y	Central and South America	286.5089	-45.7517	352.6	20	43.56
cssz-101z	Central and South America	285.9088	-45.8062	352.6	20	26.46
cssz-102a	Central and South America	285.2028	-47.1185	17.72	5	9.36
cssz-102b	Central and South America	284.5772	-46.9823	17.72	5	5
cssz-102y	Central and South America	286.4588	-47.3909	17.72	5	18.07
cssz-102z	Central and South America	285.8300	-47.2547	17.72	5	13.72
cssz-103a	Central and South America	284.7075	-48.0396	23.37	7.5	11.53
cssz-103b	Central and South America	284.0972	-47.8630	23.37	7.5	5
cssz-103x	Central and South America	286.5511	-48.5694	23.37	7.5	31.11
cssz-103y	Central and South America	285.9344	-48.3928	23.37	7.5	24.58
cssz-103z	Central and South America	285.3199	-48.2162	23.37	7.5	18.05
cssz-104a	Central and South America	284.3440	-48.7597	14.87	10	13.68
cssz-104b	Central and South America	283.6962	-48.6462	14.87	10	5
cssz-104x	Central and South America	286.2962	-49.1002	14.87	10	39.73
cssz-104y	Central and South America	285.6440	-48.9867	14.87	10	31.05
cssz-104z	Central and South America	284.9933	-48.8732	14.87	10	22.36
cssz-105a	Central and South America	284.2312	-49.4198	0.25	9.67	13.4

Continued on next page

Table B.2 – continued

Segment	Description	Longitude(°E)	Latitude(°N)	Strike(°)	Dip(°)	Depth (km)
cssz-105b	Central and South America	283.5518	-49.4179	0.25	9.67	5
cssz-105x	Central and South America	286.2718	-49.4255	0.25	9.67	38.59
cssz-105y	Central and South America	285.5908	-49.4236	0.25	9.67	30.2
cssz-105z	Central and South America	284.9114	-49.4217	0.25	9.67	21.8
cssz-106a	Central and South America	284.3730	-50.1117	347.5	9.25	13.04
cssz-106b	Central and South America	283.6974	-50.2077	347.5	9.25	5
cssz-106x	Central and South America	286.3916	-49.8238	347.5	9.25	37.15
cssz-106y	Central and South America	285.7201	-49.9198	347.5	9.25	29.11
cssz-106z	Central and South America	285.0472	-50.0157	347.5	9.25	21.07
cssz-107a	Central and South America	284.7130	-50.9714	346.5	9	12.82
cssz-107b	Central and South America	284.0273	-51.0751	346.5	9	5
cssz-107x	Central and South America	286.7611	-50.6603	346.5	9	36.29
cssz-107y	Central and South America	286.0799	-50.7640	346.5	9	28.47
cssz-107z	Central and South America	285.3972	-50.8677	346.5	9	20.64
cssz-108a	Central and South America	285.0378	-51.9370	352	8.67	12.54
cssz-108b	Central and South America	284.3241	-51.9987	352	8.67	5
cssz-108x	Central and South America	287.1729	-51.7519	352	8.67	35.15
cssz-108y	Central and South America	286.4622	-51.8136	352	8.67	27.61
cssz-108z	Central and South America	285.7505	-51.8753	352	8.67	20.07
cssz-109a	Central and South America	285.2635	-52.8439	353.1	8.33	12.24
cssz-109b	Central and South America	284.5326	-52.8974	353.1	8.33	5
cssz-109x	Central and South America	287.4508	-52.6834	353.1	8.33	33.97
cssz-109y	Central and South America	286.7226	-52.7369	353.1	8.33	26.73
cssz-109z	Central and South America	285.9935	-52.7904	353.1	8.33	19.49
cssz-110a	Central and South America	285.5705	-53.4139	334.2	8	11.96
cssz-110b	Central and South America	284.8972	-53.6076	334.2	8	5
cssz-110x	Central and South America	287.5724	-52.8328	334.2	8	32.83
cssz-110y	Central and South America	286.9081	-53.0265	334.2	8	25.88
cssz-110z	Central and South America	286.2408	-53.2202	334.2	8	18.92
cssz-111a	Central and South America	286.1627	-53.8749	313.8	8	11.96
cssz-111b	Central and South America	285.6382	-54.1958	313.8	8	5
cssz-111x	Central and South America	287.7124	-52.9122	313.8	8	32.83
cssz-111y	Central and South America	287.1997	-53.2331	313.8	8	25.88
cssz-111z	Central and South America	286.6832	-53.5540	313.8	8	18.92
cssz-112a	Central and South America	287.3287	-54.5394	316.4	8	11.96
cssz-112b	Central and South America	286.7715	-54.8462	316.4	8	5
cssz-112x	Central and South America	288.9756	-53.6190	316.4	8	32.83
cssz-112y	Central and South America	288.4307	-53.9258	316.4	8	25.88
cssz-112z	Central and South America	287.8817	-54.2326	316.4	8	18.92
cssz-113a	Central and South America	288.3409	-55.0480	307.6	8	11.96
cssz-113b	Central and South America	287.8647	-55.4002	307.6	8	5
cssz-113x	Central and South America	289.7450	-53.9914	307.6	8	32.83
cssz-113y	Central and South America	289.2810	-54.3436	307.6	8	25.88
cssz-113z	Central and South America	288.8130	-54.6958	307.6	8	18.92
cssz-114a	Central and South America	289.5342	-55.5026	301.5	8	11.96
cssz-114b	Central and South America	289.1221	-55.8819	301.5	8	5
cssz-114x	Central and South America	290.7472	-54.3647	301.5	8	32.83
cssz-114y	Central and South America	290.3467	-54.7440	301.5	8	25.88
cssz-114z	Central and South America	289.9424	-55.1233	301.5	8	18.92
cssz-115a	Central and South America	290.7682	-55.8485	292.7	8	11.96
cssz-115b	Central and South America	290.4608	-56.2588	292.7	8	5
cssz-115x	Central and South America	291.6714	-54.6176	292.7	8	32.83
cssz-115y	Central and South America	291.3734	-55.0279	292.7	8	25.88
cssz-115z	Central and South America	291.0724	-55.4382	292.7	8	18.92

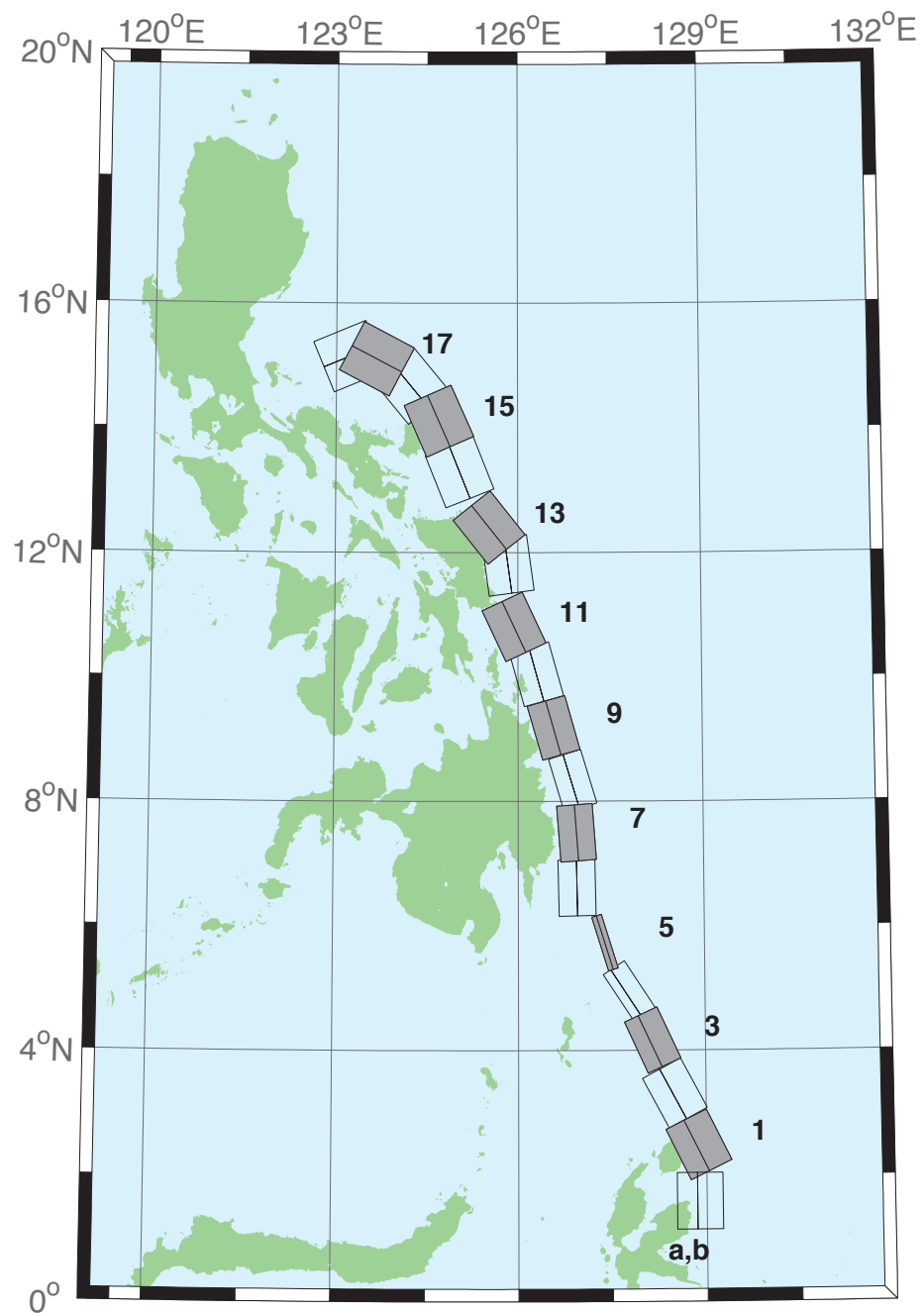


Figure B.3: Eastern Philippines Subduction Zone unit sources.

Table B.3: Earthquake parameters for Eastern Philippines Subduction Zone unit sources.

Segment	Description	Longitude($^{\circ}$ E)	Latitude($^{\circ}$ N)	Strike($^{\circ}$)	Dip($^{\circ}$)	Depth (km)
epsz-1a	Eastern Philippines	128.5521	2.3289	153.6	44.2	27.62
epsz-1b	Eastern Philippines	128.8408	2.4720	153.6	26.9	5
epsz-2a	Eastern Philippines	128.1943	3.1508	151.9	45.9	32.44
epsz-2b	Eastern Philippines	128.4706	3.2979	151.9	32.8	5.35
epsz-3a	Eastern Philippines	127.8899	4.0428	155.2	57.3	40.22
epsz-3b	Eastern Philippines	128.1108	4.1445	155.2	42.7	6.31
epsz-4a	Eastern Philippines	127.6120	4.8371	146.8	71.4	48.25
epsz-4b	Eastern Philippines	127.7324	4.9155	146.8	54.8	7.39
epsz-5a	Eastern Philippines	127.3173	5.7040	162.9	79.9	57.4
epsz-5b	Eastern Philippines	127.3930	5.7272	162.9	79.4	8.25
epsz-6a	Eastern Philippines	126.6488	6.6027	178.9	48.6	45.09
epsz-6b	Eastern Philippines	126.9478	6.6085	178.9	48.6	7.58
epsz-7a	Eastern Philippines	126.6578	7.4711	175.8	50.7	45.52
epsz-7b	Eastern Philippines	126.9439	7.4921	175.8	50.7	6.83
epsz-8a	Eastern Philippines	126.6227	8.2456	163.3	56.7	45.6
epsz-8b	Eastern Philippines	126.8614	8.3164	163.3	48.9	7.92
epsz-9a	Eastern Philippines	126.2751	9.0961	164.1	47	43.59
epsz-9b	Eastern Philippines	126.5735	9.1801	164.1	44.9	8.3
epsz-10a	Eastern Philippines	125.9798	9.9559	164.5	43.1	42.25
epsz-10b	Eastern Philippines	126.3007	10.0438	164.5	43.1	8.09
epsz-11a	Eastern Philippines	125.6079	10.6557	155	37.8	38.29
epsz-11b	Eastern Philippines	125.9353	10.8059	155	37.8	7.64
epsz-12a	Eastern Philippines	125.4697	11.7452	172.1	36	37.01
epsz-12b	Eastern Philippines	125.8374	11.7949	172.1	36	7.62
epsz-13a	Eastern Philippines	125.2238	12.1670	141.5	32.4	33.87
epsz-13b	Eastern Philippines	125.5278	12.4029	141.5	32.4	7.08
epsz-14a	Eastern Philippines	124.6476	13.1365	158.2	23	25.92
epsz-14b	Eastern Philippines	125.0421	13.2898	158.2	23	6.38
epsz-15a	Eastern Philippines	124.3107	13.9453	156.1	24.1	26.51
epsz-15b	Eastern Philippines	124.6973	14.1113	156.1	24.1	6.09
epsz-16a	Eastern Philippines	123.8998	14.4025	140.3	19.5	21.69
epsz-16b	Eastern Philippines	124.2366	14.6728	140.3	19.5	5
epsz-17a	Eastern Philippines	123.4604	14.7222	117.6	15.3	18.19
epsz-17b	Eastern Philippines	123.6682	15.1062	117.6	15.3	5
epsz-18a	Eastern Philippines	123.3946	14.7462	67.4	15	17.94
epsz-18b	Eastern Philippines	123.2219	15.1467	67.4	15	5
epsz-19a	Eastern Philippines	121.3638	15.7400	189.6	15	17.94
epsz-19b	Eastern Philippines	121.8082	15.6674	189.6	15	5
epsz-20a	Eastern Philippines	121.6833	16.7930	203.3	15	17.94
epsz-20b	Eastern Philippines	122.0994	16.6216	203.3	15	5
epsz-21a	Eastern Philippines	121.8279	17.3742	184.2	15	17.94
epsz-21b	Eastern Philippines	122.2814	17.3425	184.2	15	5

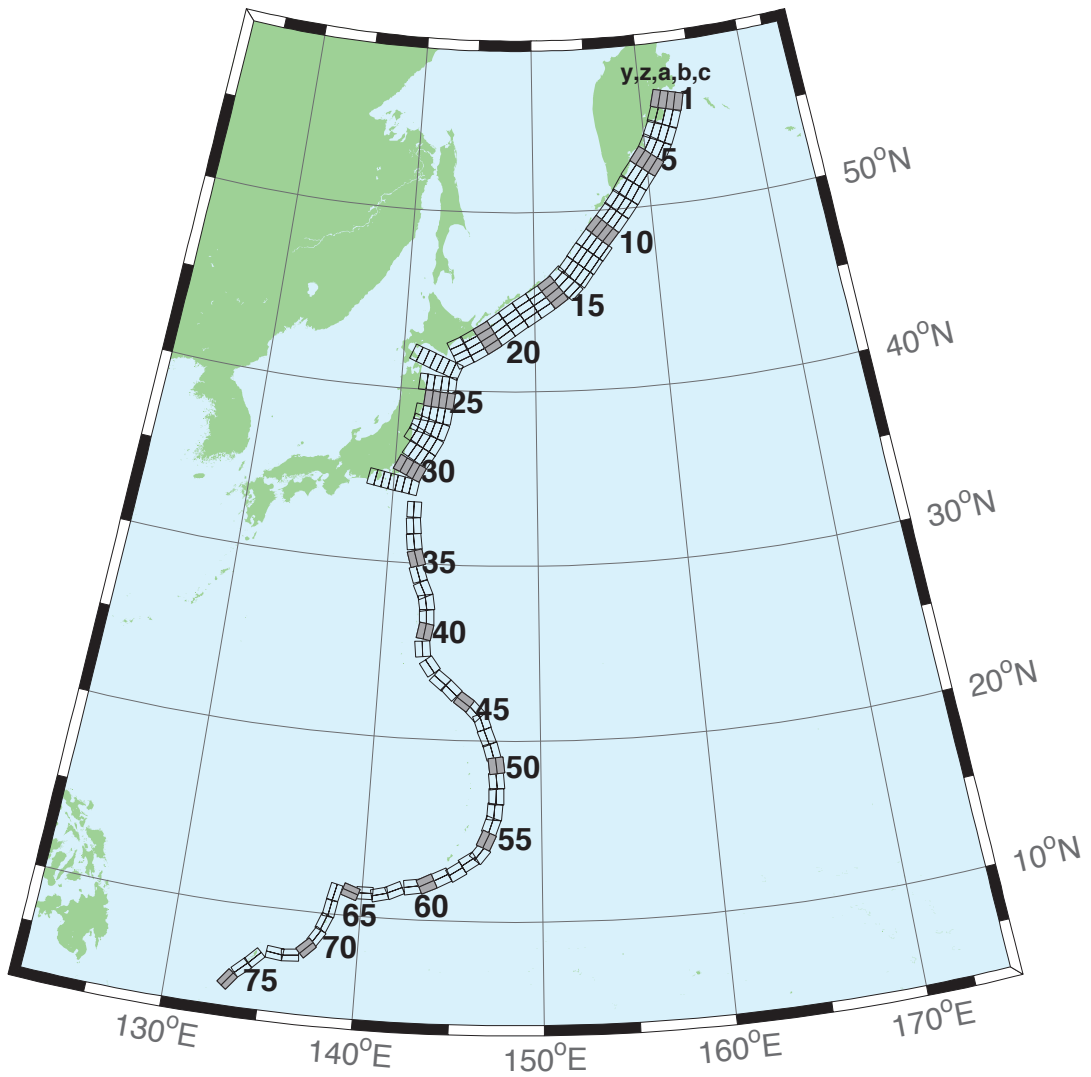


Figure B.4: Kamchatka-Kuril-Japan-Izu-Mariana-Yap Subduction Zone unit sources.

Table B.4: Earthquake parameters for Kamchatka-Kuril-Japan-Izu-Mariana-Yap Subduction Zone unit sources.

Segment	Description	Longitude(°E)	Latitude(°N)	Strike(°)	Dip(°)	Depth (km)
kisz-1a	Kamchatka-Kuril-Japan-Izu-Mariana-Yap	162.4318	55.5017	195	29	26.13
kisz-1b	Kamchatka-Kuril-Japan-Izu-Mariana-Yap	163.1000	55.4000	195	25	5
kisz-1y	Kamchatka-Kuril-Japan-Izu-Mariana-Yap	161.0884	55.7050	195	29	74.61
kisz-1z	Kamchatka-Kuril-Japan-Izu-Mariana-Yap	161.7610	55.6033	195	29	50.37
kisz-2a	Kamchatka-Kuril-Japan-Izu-Mariana-Yap	161.9883	54.6784	200	29	26.13
kisz-2b	Kamchatka-Kuril-Japan-Izu-Mariana-Yap	162.6247	54.5440	200	25	5
kisz-2y	Kamchatka-Kuril-Japan-Izu-Mariana-Yap	160.7072	54.9471	200	29	74.61
kisz-2z	Kamchatka-Kuril-Japan-Izu-Mariana-Yap	161.3488	54.8127	200	29	50.37
kisz-3a	Kamchatka-Kuril-Japan-Izu-Mariana-Yap	161.4385	53.8714	204	29	26.13
kisz-3b	Kamchatka-Kuril-Japan-Izu-Mariana-Yap	162.0449	53.7116	204	25	5
kisz-3y	Kamchatka-Kuril-Japan-Izu-Mariana-Yap	160.2164	54.1910	204	29	74.61
kisz-3z	Kamchatka-Kuril-Japan-Izu-Mariana-Yap	160.8286	54.0312	204	29	50.37
kisz-4a	Kamchatka-Kuril-Japan-Izu-Mariana-Yap	160.7926	53.1087	210	29	26.13
kisz-4b	Kamchatka-Kuril-Japan-Izu-Mariana-Yap	161.3568	52.9123	210	25	5
kisz-4y	Kamchatka-Kuril-Japan-Izu-Mariana-Yap	159.6539	53.5015	210	29	74.61
kisz-4z	Kamchatka-Kuril-Japan-Izu-Mariana-Yap	160.2246	53.3051	210	29	50.37
kisz-5a	Kamchatka-Kuril-Japan-Izu-Mariana-Yap	160.0211	52.4113	218	29	26.13
kisz-5b	Kamchatka-Kuril-Japan-Izu-Mariana-Yap	160.5258	52.1694	218	25	5
kisz-5y	Kamchatka-Kuril-Japan-Izu-Mariana-Yap	159.0005	52.8950	218	29	74.61
kisz-5z	Kamchatka-Kuril-Japan-Izu-Mariana-Yap	159.5122	52.6531	218	29	50.37
kisz-6a	Kamchatka-Kuril-Japan-Izu-Mariana-Yap	159.1272	51.7034	218	29	26.13
kisz-6b	Kamchatka-Kuril-Japan-Izu-Mariana-Yap	159.6241	51.4615	218	25	5
kisz-6y	Kamchatka-Kuril-Japan-Izu-Mariana-Yap	158.1228	52.1871	218	29	74.61
kisz-6z	Kamchatka-Kuril-Japan-Izu-Mariana-Yap	158.6263	51.9452	218	29	50.37
kisz-7a	Kamchatka-Kuril-Japan-Izu-Mariana-Yap	158.2625	50.9549	214	29	26.13
kisz-7b	Kamchatka-Kuril-Japan-Izu-Mariana-Yap	158.7771	50.7352	214	25	5
kisz-7y	Kamchatka-Kuril-Japan-Izu-Mariana-Yap	157.2236	51.3942	214	29	74.61
kisz-7z	Kamchatka-Kuril-Japan-Izu-Mariana-Yap	157.7443	51.1745	214	29	50.37
kisz-8a	Kamchatka-Kuril-Japan-Izu-Mariana-Yap	157.4712	50.2459	218	31	27.7
kisz-8b	Kamchatka-Kuril-Japan-Izu-Mariana-Yap	157.9433	50.0089	218	27	5
kisz-8y	Kamchatka-Kuril-Japan-Izu-Mariana-Yap	156.5176	50.7199	218	31	79.2
kisz-8z	Kamchatka-Kuril-Japan-Izu-Mariana-Yap	156.9956	50.4829	218	31	53.45
kisz-9a	Kamchatka-Kuril-Japan-Izu-Mariana-Yap	156.6114	49.5583	220	31	27.7
kisz-9b	Kamchatka-Kuril-Japan-Izu-Mariana-Yap	157.0638	49.3109	220	27	5
kisz-9y	Kamchatka-Kuril-Japan-Izu-Mariana-Yap	155.6974	50.0533	220	31	79.2
kisz-9z	Kamchatka-Kuril-Japan-Izu-Mariana-Yap	156.1556	49.8058	220	31	53.45
kisz-10a	Kamchatka-Kuril-Japan-Izu-Mariana-Yap	155.7294	48.8804	221	31	27.7
kisz-10b	Kamchatka-Kuril-Japan-Izu-Mariana-Yap	156.1690	48.6278	221	27	5
kisz-10y	Kamchatka-Kuril-Japan-Izu-Mariana-Yap	154.8413	49.3856	221	31	79.2
kisz-10z	Kamchatka-Kuril-Japan-Izu-Mariana-Yap	155.2865	49.1330	221	31	53.45
kisz-11a	Kamchatka-Kuril-Japan-Izu-Mariana-Yap	154.8489	48.1821	219	31	27.7
kisz-11b	Kamchatka-Kuril-Japan-Izu-Mariana-Yap	155.2955	47.9398	219	27	5
kisz-11y	Kamchatka-Kuril-Japan-Izu-Mariana-Yap	153.9472	48.6667	219	31	79.2
kisz-11z	Kamchatka-Kuril-Japan-Izu-Mariana-Yap	154.3991	48.4244	219	31	53.45
kisz-11c	Kamchatka-Kuril-Japan-Izu-Mariana-Yap	156.0358	47.5374	39	57.89	4.602
kisz-12a	Kamchatka-Kuril-Japan-Izu-Mariana-Yap	153.9994	47.4729	217	31	27.7
kisz-12b	Kamchatka-Kuril-Japan-Izu-Mariana-Yap	154.4701	47.2320	217	27	5
kisz-12y	Kamchatka-Kuril-Japan-Izu-Mariana-Yap	153.0856	47.9363	217	31	79.2
kisz-12z	Kamchatka-Kuril-Japan-Izu-Mariana-Yap	153.5435	47.7046	217	31	53.45
kisz-12c	Kamchatka-Kuril-Japan-Izu-Mariana-Yap	155.2208	46.8473	37	57.89	4.602
kisz-13a	Kamchatka-Kuril-Japan-Izu-Mariana-Yap	153.2239	46.7564	218	31	27.7
kisz-13b	Kamchatka-Kuril-Japan-Izu-Mariana-Yap	153.6648	46.5194	218	27	5

Continued on next page

Table B.4 – continued

Segment	Description	Longitude($^{\circ}$ E)	Latitude($^{\circ}$ N)	Strike($^{\circ}$)	Dip($^{\circ}$)	Depth (km)
kisz-13y	Kamchatka-Kuril-Japan-Izu-Mariana-Yap	152.3343	47.2304	218	31	79.2
kisz-13z	Kamchatka-Kuril-Japan-Izu-Mariana-Yap	152.7801	46.9934	218	31	53.45
kisz-13c	Kamchatka-Kuril-Japan-Izu-Mariana-Yap	154.3957	46.1257	38	57.89	4.602
kisz-14a	Kamchatka-Kuril-Japan-Izu-Mariana-Yap	152.3657	46.1514	225	23	24.54
kisz-14b	Kamchatka-Kuril-Japan-Izu-Mariana-Yap	152.7855	45.8591	225	23	5
kisz-14y	Kamchatka-Kuril-Japan-Izu-Mariana-Yap	151.5172	46.7362	225	23	63.62
kisz-14z	Kamchatka-Kuril-Japan-Izu-Mariana-Yap	151.9426	46.4438	225	23	44.08
kisz-14c	Kamchatka-Kuril-Japan-Izu-Mariana-Yap	153.4468	45.3976	45	57.89	4.602
kisz-15a	Kamchatka-Kuril-Japan-Izu-Mariana-Yap	151.4663	45.5963	233	25	23.73
kisz-15b	Kamchatka-Kuril-Japan-Izu-Mariana-Yap	151.8144	45.2712	233	22	5
kisz-15y	Kamchatka-Kuril-Japan-Izu-Mariana-Yap	150.7619	46.2465	233	25	65.99
kisz-15z	Kamchatka-Kuril-Japan-Izu-Mariana-Yap	151.1151	45.9214	233	25	44.86
kisz-16a	Kamchatka-Kuril-Japan-Izu-Mariana-Yap	150.4572	45.0977	237	25	23.73
kisz-16b	Kamchatka-Kuril-Japan-Izu-Mariana-Yap	150.7694	44.7563	237	22	5
kisz-16y	Kamchatka-Kuril-Japan-Izu-Mariana-Yap	149.8253	45.7804	237	25	65.99
kisz-16z	Kamchatka-Kuril-Japan-Izu-Mariana-Yap	150.1422	45.4390	237	25	44.86
kisz-17a	Kamchatka-Kuril-Japan-Izu-Mariana-Yap	149.3989	44.6084	237	25	23.73
kisz-17b	Kamchatka-Kuril-Japan-Izu-Mariana-Yap	149.7085	44.2670	237	22	5
kisz-17y	Kamchatka-Kuril-Japan-Izu-Mariana-Yap	148.7723	45.2912	237	25	65.99
kisz-17z	Kamchatka-Kuril-Japan-Izu-Mariana-Yap	149.0865	44.9498	237	25	44.86
kisz-18a	Kamchatka-Kuril-Japan-Izu-Mariana-Yap	148.3454	44.0982	235	25	23.73
kisz-18b	Kamchatka-Kuril-Japan-Izu-Mariana-Yap	148.6687	43.7647	235	22	5
kisz-18y	Kamchatka-Kuril-Japan-Izu-Mariana-Yap	147.6915	44.7651	235	25	65.99
kisz-18z	Kamchatka-Kuril-Japan-Izu-Mariana-Yap	148.0194	44.4316	235	25	44.86
kisz-19a	Kamchatka-Kuril-Japan-Izu-Mariana-Yap	147.3262	43.5619	233	25	23.73
kisz-19b	Kamchatka-Kuril-Japan-Izu-Mariana-Yap	147.6625	43.2368	233	22	5
kisz-19y	Kamchatka-Kuril-Japan-Izu-Mariana-Yap	146.6463	44.2121	233	25	65.99
kisz-19z	Kamchatka-Kuril-Japan-Izu-Mariana-Yap	146.9872	43.8870	233	25	44.86
kisz-20a	Kamchatka-Kuril-Japan-Izu-Mariana-Yap	146.3513	43.0633	237	25	23.73
kisz-20b	Kamchatka-Kuril-Japan-Izu-Mariana-Yap	146.6531	42.7219	237	22	5
kisz-20y	Kamchatka-Kuril-Japan-Izu-Mariana-Yap	145.7410	43.7461	237	25	65.99
kisz-20z	Kamchatka-Kuril-Japan-Izu-Mariana-Yap	146.0470	43.4047	237	25	44.86
kisz-21a	Kamchatka-Kuril-Japan-Izu-Mariana-Yap	145.3331	42.5948	239	25	23.73
kisz-21b	Kamchatka-Kuril-Japan-Izu-Mariana-Yap	145.6163	42.2459	239	22	5
kisz-21y	Kamchatka-Kuril-Japan-Izu-Mariana-Yap	144.7603	43.2927	239	25	65.99
kisz-21z	Kamchatka-Kuril-Japan-Izu-Mariana-Yap	145.0475	42.9438	239	25	44.86
kisz-22a	Kamchatka-Kuril-Japan-Izu-Mariana-Yap	144.3041	42.1631	242	25	23.73
kisz-22b	Kamchatka-Kuril-Japan-Izu-Mariana-Yap	144.5605	41.8037	242	22	5
kisz-22y	Kamchatka-Kuril-Japan-Izu-Mariana-Yap	143.7854	42.8819	242	25	65.99
kisz-22z	Kamchatka-Kuril-Japan-Izu-Mariana-Yap	144.0455	42.5225	242	25	44.86
kisz-23a	Kamchatka-Kuril-Japan-Izu-Mariana-Yap	143.2863	41.3335	202	21	21.28
kisz-23b	Kamchatka-Kuril-Japan-Izu-Mariana-Yap	143.8028	41.1764	202	19	5
kisz-23v	Kamchatka-Kuril-Japan-Izu-Mariana-Yap	140.6816	42.1189	202	21	110.9
kisz-23w	Kamchatka-Kuril-Japan-Izu-Mariana-Yap	141.2050	41.9618	202	21	92.95
kisz-23x	Kamchatka-Kuril-Japan-Izu-Mariana-Yap	141.7273	41.8047	202	21	75.04
kisz-23y	Kamchatka-Kuril-Japan-Izu-Mariana-Yap	142.2482	41.6476	202	21	57.12
kisz-23z	Kamchatka-Kuril-Japan-Izu-Mariana-Yap	142.7679	41.4905	202	21	39.2
kisz-24a	Kamchatka-Kuril-Japan-Izu-Mariana-Yap	142.9795	40.3490	185	21	21.28
kisz-24b	Kamchatka-Kuril-Japan-Izu-Mariana-Yap	143.5273	40.3125	185	19	5
kisz-24x	Kamchatka-Kuril-Japan-Izu-Mariana-Yap	141.3339	40.4587	185	21	75.04
kisz-24y	Kamchatka-Kuril-Japan-Izu-Mariana-Yap	141.8827	40.4221	185	21	57.12
kisz-24z	Kamchatka-Kuril-Japan-Izu-Mariana-Yap	142.4312	40.3856	185	21	39.2
kisz-25a	Kamchatka-Kuril-Japan-Izu-Mariana-Yap	142.8839	39.4541	185	21	21.28
kisz-25b	Kamchatka-Kuril-Japan-Izu-Mariana-Yap	143.4246	39.4176	185	19	5
kisz-25y	Kamchatka-Kuril-Japan-Izu-Mariana-Yap	141.8012	39.5272	185	21	57.12

Continued on next page

Table B.4 – continued

Segment	Description	Longitude(°E)	Latitude(°N)	Strike(°)	Dip(°)	Depth (km)
kisz-25z	Kamchatka-Kuril-Japan-Izu-Mariana-Yap	142.3426	39.4907	185	21	39.2
kisz-26a	Kamchatka-Kuril-Japan-Izu-Mariana-Yap	142.7622	38.5837	188	21	21.28
kisz-26b	Kamchatka-Kuril-Japan-Izu-Mariana-Yap	143.2930	38.5254	188	19	5
kisz-26x	Kamchatka-Kuril-Japan-Izu-Mariana-Yap	141.1667	38.7588	188	21	75.04
kisz-26y	Kamchatka-Kuril-Japan-Izu-Mariana-Yap	141.6990	38.7004	188	21	57.12
kisz-26z	Kamchatka-Kuril-Japan-Izu-Mariana-Yap	142.2308	38.6421	188	21	39.2
kisz-27a	Kamchatka-Kuril-Japan-Izu-Mariana-Yap	142.5320	37.7830	198	21	21.28
kisz-27b	Kamchatka-Kuril-Japan-Izu-Mariana-Yap	143.0357	37.6534	198	19	5
kisz-27x	Kamchatka-Kuril-Japan-Izu-Mariana-Yap	141.0142	38.1717	198	21	75.04
kisz-27y	Kamchatka-Kuril-Japan-Izu-Mariana-Yap	141.5210	38.0421	198	21	57.12
kisz-27z	Kamchatka-Kuril-Japan-Izu-Mariana-Yap	142.0269	37.9126	198	21	39.2
kisz-28a	Kamchatka-Kuril-Japan-Izu-Mariana-Yap	142.1315	37.0265	208	21	21.28
kisz-28b	Kamchatka-Kuril-Japan-Izu-Mariana-Yap	142.5941	36.8297	208	19	5
kisz-28x	Kamchatka-Kuril-Japan-Izu-Mariana-Yap	140.7348	37.6171	208	21	75.04
kisz-28y	Kamchatka-Kuril-Japan-Izu-Mariana-Yap	141.2016	37.4202	208	21	57.12
kisz-28z	Kamchatka-Kuril-Japan-Izu-Mariana-Yap	141.6671	37.2234	208	21	39.2
kisz-29a	Kamchatka-Kuril-Japan-Izu-Mariana-Yap	141.5970	36.2640	211	21	21.28
kisz-29b	Kamchatka-Kuril-Japan-Izu-Mariana-Yap	142.0416	36.0481	211	19	5
kisz-29y	Kamchatka-Kuril-Japan-Izu-Mariana-Yap	140.7029	36.6960	211	21	57.12
kisz-29z	Kamchatka-Kuril-Japan-Izu-Mariana-Yap	141.1506	36.4800	211	21	39.2
kisz-30a	Kamchatka-Kuril-Japan-Izu-Mariana-Yap	141.0553	35.4332	205	21	21.28
kisz-30b	Kamchatka-Kuril-Japan-Izu-Mariana-Yap	141.5207	35.2560	205	19	5
kisz-30y	Kamchatka-Kuril-Japan-Izu-Mariana-Yap	140.1204	35.7876	205	21	57.12
kisz-30z	Kamchatka-Kuril-Japan-Izu-Mariana-Yap	140.5883	35.6104	205	21	39.2
kisz-31a	Kamchatka-Kuril-Japan-Izu-Mariana-Yap	140.6956	34.4789	190	22	22.1
kisz-31b	Kamchatka-Kuril-Japan-Izu-Mariana-Yap	141.1927	34.4066	190	20	5
kisz-31v	Kamchatka-Kuril-Japan-Izu-Mariana-Yap	138.2025	34.8405	190	22	115.8
kisz-31w	Kamchatka-Kuril-Japan-Izu-Mariana-Yap	138.7021	34.7682	190	22	97.02
kisz-31x	Kamchatka-Kuril-Japan-Izu-Mariana-Yap	139.2012	34.6958	190	22	78.29
kisz-31y	Kamchatka-Kuril-Japan-Izu-Mariana-Yap	139.6997	34.6235	190	22	59.56
kisz-31z	Kamchatka-Kuril-Japan-Izu-Mariana-Yap	140.1979	34.5512	190	22	40.83
kisz-32a	Kamchatka-Kuril-Japan-Izu-Mariana-Yap	141.0551	33.0921	180	32	23.48
kisz-32b	Kamchatka-Kuril-Japan-Izu-Mariana-Yap	141.5098	33.0921	180	21.69	5
kisz-33a	Kamchatka-Kuril-Japan-Izu-Mariana-Yap	141.0924	32.1047	173.8	27.65	20.67
kisz-33b	Kamchatka-Kuril-Japan-Izu-Mariana-Yap	141.5596	32.1473	173.8	18.27	5
kisz-34a	Kamchatka-Kuril-Japan-Izu-Mariana-Yap	141.1869	31.1851	172.1	25	18.26
kisz-34b	Kamchatka-Kuril-Japan-Izu-Mariana-Yap	141.6585	31.2408	172.1	15.38	5
kisz-35a	Kamchatka-Kuril-Japan-Izu-Mariana-Yap	141.4154	30.1707	163	25	17.12
kisz-35b	Kamchatka-Kuril-Japan-Izu-Mariana-Yap	141.8662	30.2899	163	14.03	5
kisz-36a	Kamchatka-Kuril-Japan-Izu-Mariana-Yap	141.6261	29.2740	161.7	25.73	18.71
kisz-36b	Kamchatka-Kuril-Japan-Izu-Mariana-Yap	142.0670	29.4012	161.7	15.91	5
kisz-37a	Kamchatka-Kuril-Japan-Izu-Mariana-Yap	142.0120	28.3322	154.7	20	14.54
kisz-37b	Kamchatka-Kuril-Japan-Izu-Mariana-Yap	142.4463	28.5124	154.7	11	5
kisz-38a	Kamchatka-Kuril-Japan-Izu-Mariana-Yap	142.2254	27.6946	170.3	20	14.54
kisz-38b	Kamchatka-Kuril-Japan-Izu-Mariana-Yap	142.6955	27.7659	170.3	11	5
kisz-39a	Kamchatka-Kuril-Japan-Izu-Mariana-Yap	142.3085	26.9127	177.2	24.23	17.42
kisz-39b	Kamchatka-Kuril-Japan-Izu-Mariana-Yap	142.7674	26.9325	177.2	14.38	5
kisz-40a	Kamchatka-Kuril-Japan-Izu-Mariana-Yap	142.2673	26.1923	189.4	26.49	22.26
kisz-40b	Kamchatka-Kuril-Japan-Izu-Mariana-Yap	142.7090	26.1264	189.4	20.2	5
kisz-41a	Kamchatka-Kuril-Japan-Izu-Mariana-Yap	142.1595	25.0729	173.7	22.07	19.08
kisz-41b	Kamchatka-Kuril-Japan-Izu-Mariana-Yap	142.6165	25.1184	173.7	16.36	5
kisz-42a	Kamchatka-Kuril-Japan-Izu-Mariana-Yap	142.7641	23.8947	143.5	21.54	18.4
kisz-42b	Kamchatka-Kuril-Japan-Izu-Mariana-Yap	143.1321	24.1432	143.5	15.54	5
kisz-43a	Kamchatka-Kuril-Japan-Izu-Mariana-Yap	143.5281	23.0423	129.2	23.02	18.77
kisz-43b	Kamchatka-Kuril-Japan-Izu-Mariana-Yap	143.8128	23.3626	129.2	15.99	5

Continued on next page

Table B.4 – continued

Segment	Description	Longitude(°E)	Latitude(°N)	Strike(°)	Dip(°)	Depth (km)
kisz-44a	Kamchatka-Kuril-Japan-Izu-Mariana-Yap	144.2230	22.5240	134.6	28.24	18.56
kisz-44b	Kamchatka-Kuril-Japan-Izu-Mariana-Yap	144.5246	22.8056	134.6	15.74	5
kisz-45a	Kamchatka-Kuril-Japan-Izu-Mariana-Yap	145.0895	21.8866	125.8	36.73	22.79
kisz-45b	Kamchatka-Kuril-Japan-Izu-Mariana-Yap	145.3171	22.1785	125.8	20.84	5
kisz-46a	Kamchatka-Kuril-Japan-Izu-Mariana-Yap	145.6972	21.3783	135.9	30.75	20.63
kisz-46b	Kamchatka-Kuril-Japan-Izu-Mariana-Yap	145.9954	21.6469	135.9	18.22	5
kisz-47a	Kamchatka-Kuril-Japan-Izu-Mariana-Yap	146.0406	20.9341	160.1	29.87	19.62
kisz-47b	Kamchatka-Kuril-Japan-Izu-Mariana-Yap	146.4330	21.0669	160.1	17	5
kisz-48a	Kamchatka-Kuril-Japan-Izu-Mariana-Yap	146.3836	20.0690	158	32.75	19.68
kisz-48b	Kamchatka-Kuril-Japan-Izu-Mariana-Yap	146.7567	20.2108	158	17.07	5
kisz-49a	Kamchatka-Kuril-Japan-Izu-Mariana-Yap	146.6689	19.3123	164.5	25.07	21.41
kisz-49b	Kamchatka-Kuril-Japan-Izu-Mariana-Yap	147.0846	19.4212	164.5	19.16	5
kisz-50a	Kamchatka-Kuril-Japan-Izu-Mariana-Yap	146.9297	18.5663	172.1	22	22.1
kisz-50b	Kamchatka-Kuril-Japan-Izu-Mariana-Yap	147.3650	18.6238	172.1	20	5
kisz-51a	Kamchatka-Kuril-Japan-Izu-Mariana-Yap	146.9495	17.7148	175.1	22.06	22.04
kisz-51b	Kamchatka-Kuril-Japan-Izu-Mariana-Yap	147.3850	17.7503	175.1	19.93	5
kisz-52a	Kamchatka-Kuril-Japan-Izu-Mariana-Yap	146.9447	16.8869	180	25.51	18.61
kisz-52b	Kamchatka-Kuril-Japan-Izu-Mariana-Yap	147.3683	16.8869	180	15.79	5
kisz-53a	Kamchatka-Kuril-Japan-Izu-Mariana-Yap	146.8626	16.0669	185.2	27.39	18.41
kisz-53b	Kamchatka-Kuril-Japan-Izu-Mariana-Yap	147.2758	16.0309	185.2	15.56	5
kisz-54a	Kamchatka-Kuril-Japan-Izu-Mariana-Yap	146.7068	15.3883	199.1	28.12	20.91
kisz-54b	Kamchatka-Kuril-Japan-Izu-Mariana-Yap	147.0949	15.2590	199.1	18.56	5
kisz-55a	Kamchatka-Kuril-Japan-Izu-Mariana-Yap	146.4717	14.6025	204.3	29.6	26.27
kisz-55b	Kamchatka-Kuril-Japan-Izu-Mariana-Yap	146.8391	14.4415	204.3	25.18	5
kisz-56a	Kamchatka-Kuril-Japan-Izu-Mariana-Yap	146.1678	13.9485	217.4	32.04	26.79
kisz-56b	Kamchatka-Kuril-Japan-Izu-Mariana-Yap	146.4789	13.7170	217.4	25.84	5
kisz-57a	Kamchatka-Kuril-Japan-Izu-Mariana-Yap	145.6515	13.5576	235.8	37	24.54
kisz-57b	Kamchatka-Kuril-Japan-Izu-Mariana-Yap	145.8586	13.2609	235.8	23	5
kisz-58a	Kamchatka-Kuril-Japan-Izu-Mariana-Yap	144.9648	12.9990	237.8	37.72	24.54
kisz-58b	Kamchatka-Kuril-Japan-Izu-Mariana-Yap	145.1589	12.6984	237.8	23	5
kisz-59a	Kamchatka-Kuril-Japan-Izu-Mariana-Yap	144.1799	12.6914	242.9	34.33	22.31
kisz-59b	Kamchatka-Kuril-Japan-Izu-Mariana-Yap	144.3531	12.3613	242.9	20.25	5
kisz-60a	Kamchatka-Kuril-Japan-Izu-Mariana-Yap	143.3687	12.3280	244.9	30.9	20.62
kisz-60b	Kamchatka-Kuril-Japan-Izu-Mariana-Yap	143.5355	11.9788	244.9	18.2	5
kisz-61a	Kamchatka-Kuril-Japan-Izu-Mariana-Yap	142.7051	12.1507	261.8	35.41	25.51
kisz-61b	Kamchatka-Kuril-Japan-Izu-Mariana-Yap	142.7582	11.7883	261.8	24.22	5
kisz-62a	Kamchatka-Kuril-Japan-Izu-Mariana-Yap	141.6301	11.8447	245.7	39.86	34.35
kisz-62b	Kamchatka-Kuril-Japan-Izu-Mariana-Yap	141.7750	11.5305	245.7	35.94	5
kisz-63a	Kamchatka-Kuril-Japan-Izu-Mariana-Yap	140.8923	11.5740	256.2	42	38.46
kisz-63b	Kamchatka-Kuril-Japan-Izu-Mariana-Yap	140.9735	11.2498	256.2	42	5
kisz-64a	Kamchatka-Kuril-Japan-Izu-Mariana-Yap	140.1387	11.6028	269.6	42.48	38.77
kisz-64b	Kamchatka-Kuril-Japan-Izu-Mariana-Yap	140.1410	11.2716	269.6	42.48	5
kisz-65a	Kamchatka-Kuril-Japan-Izu-Mariana-Yap	139.4595	11.5883	288.7	44.16	39.83
kisz-65b	Kamchatka-Kuril-Japan-Izu-Mariana-Yap	139.3541	11.2831	288.7	44.16	5
kisz-66a	Kamchatka-Kuril-Japan-Izu-Mariana-Yap	138.1823	11.2648	193.1	45	40.36
kisz-66b	Kamchatka-Kuril-Japan-Izu-Mariana-Yap	138.4977	11.1929	193.1	45	5
kisz-67a	Kamchatka-Kuril-Japan-Izu-Mariana-Yap	137.9923	10.3398	189.8	45	40.36
kisz-67b	Kamchatka-Kuril-Japan-Izu-Mariana-Yap	138.3104	10.2856	189.8	45	5
kisz-68a	Kamchatka-Kuril-Japan-Izu-Mariana-Yap	137.7607	9.6136	201.7	45	40.36
kisz-68b	Kamchatka-Kuril-Japan-Izu-Mariana-Yap	138.0599	9.4963	201.7	45	5
kisz-69a	Kamchatka-Kuril-Japan-Izu-Mariana-Yap	137.4537	8.8996	213.5	45	40.36
kisz-69b	Kamchatka-Kuril-Japan-Izu-Mariana-Yap	137.7215	8.7241	213.5	45	5
kisz-70a	Kamchatka-Kuril-Japan-Izu-Mariana-Yap	137.0191	8.2872	226.5	45	40.36
kisz-70b	Kamchatka-Kuril-Japan-Izu-Mariana-Yap	137.2400	8.0569	226.5	45	5
kisz-71a	Kamchatka-Kuril-Japan-Izu-Mariana-Yap	136.3863	7.9078	263.9	45	40.36

Continued on next page

Table B.4 – continued

Segment	Description	Longitude($^{\circ}$ E)	Latitude($^{\circ}$ N)	Strike($^{\circ}$)	Dip($^{\circ}$)	Depth (km)
kisz-71b	Kamchatka-Kuril-Japan-Izu-Mariana-Yap	136.4202	7.5920	263.9	45	5
kisz-72a	Kamchatka-Kuril-Japan-Izu-Mariana-Yap	135.6310	7.9130	276.9	45	40.36
kisz-72b	Kamchatka-Kuril-Japan-Izu-Mariana-Yap	135.5926	7.5977	276.9	45	5
kisz-73a	Kamchatka-Kuril-Japan-Izu-Mariana-Yap	134.3296	7.4541	224	45	40.36
kisz-73b	Kamchatka-Kuril-Japan-Izu-Mariana-Yap	134.5600	7.2335	224	45	5
kisz-74a	Kamchatka-Kuril-Japan-Izu-Mariana-Yap	133.7125	6.8621	228.1	45	40.36
kisz-74b	Kamchatka-Kuril-Japan-Izu-Mariana-Yap	133.9263	6.6258	228.1	45	5
kisz-75a	Kamchatka-Kuril-Japan-Izu-Mariana-Yap	133.0224	6.1221	217.7	45	40.36
kisz-75b	Kamchatka-Kuril-Japan-Izu-Mariana-Yap	133.2751	5.9280	217.7	45	5

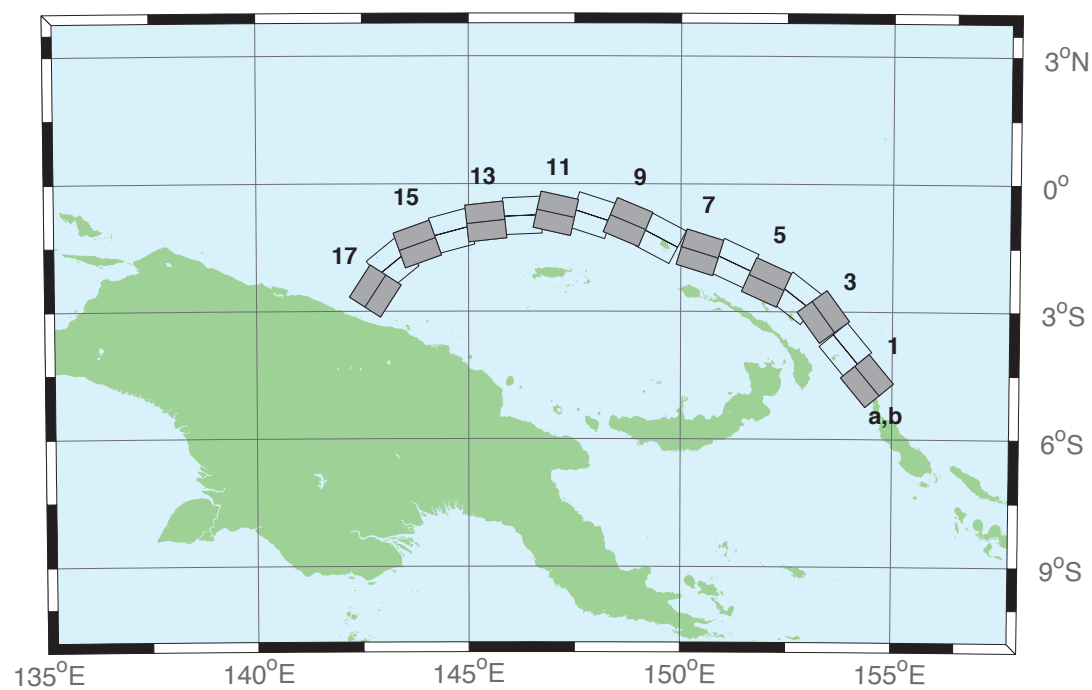


Figure B.5: Manus–Oceanic Convergent Boundary Subduction Zone unit sources.

Table B.5: Earthquake parameters for Manus–Oceanic Convergent Boundary Subduction Zone unit sources.

Segment	Description	Longitude(°E)	Latitude(°N)	Strike(°)	Dip(°)	Depth (km)
mosz-1a	Manus	154.0737	-4.8960	140.2	15	15.88
mosz-1b	Manus	154.4082	-4.6185	140.2	15	2.94
mosz-2a	Manus	153.5589	-4.1575	140.2	15	15.91
mosz-2b	Manus	153.8931	-3.8800	140.2	15	2.97
mosz-3a	Manus	153.0151	-3.3716	143.9	15	16.64
mosz-3b	Manus	153.3662	-3.1160	143.9	15	3.7
mosz-4a	Manus	152.4667	-3.0241	127.7	15	17.32
mosz-4b	Manus	152.7321	-2.6806	127.7	15	4.38
mosz-5a	Manus	151.8447	-2.7066	114.3	15	17.57
mosz-5b	Manus	152.0235	-2.3112	114.3	15	4.63
mosz-6a	Manus	151.0679	-2.2550	115	15	17.66
mosz-6b	Manus	151.2513	-1.8618	115	15	4.72
mosz-7a	Manus	150.3210	-2.0236	107.2	15	17.73
mosz-7b	Manus	150.4493	-1.6092	107.2	15	4.79
mosz-8a	Manus	149.3226	-1.6666	117.8	15	17.83
mosz-8b	Manus	149.5251	-1.2829	117.8	15	4.89
mosz-9a	Manus	148.5865	-1.3017	112.7	15	17.84
mosz-9b	Manus	148.7540	-0.9015	112.7	15	4.9
mosz-10a	Manus	147.7760	-1.1560	108	15	17.78
mosz-10b	Manus	147.9102	-0.7434	108	15	4.84
mosz-11a	Manus	146.9596	-1.1226	102.5	15	17.54
mosz-11b	Manus	147.0531	-0.6990	102.5	15	4.6
mosz-12a	Manus	146.2858	-1.1820	87.48	15	17.29
mosz-12b	Manus	146.2667	-0.7486	87.48	15	4.35
mosz-13a	Manus	145.4540	-1.3214	83.75	15	17.34
mosz-13b	Manus	145.4068	-0.8901	83.75	15	4.4
mosz-14a	Manus	144.7151	-1.5346	75.09	15	17.21
mosz-14b	Manus	144.6035	-1.1154	75.09	15	4.27
mosz-15a	Manus	143.9394	-1.8278	70.43	15	16.52
mosz-15b	Manus	143.7940	-1.4190	70.43	15	3.58
mosz-16a	Manus	143.4850	-2.2118	50.79	15	15.86
mosz-16b	Manus	143.2106	-1.8756	50.79	15	2.92
mosz-17a	Manus	143.1655	-2.7580	33	15	16.64
mosz-17b	Manus	142.8013	-2.5217	33	15	3.7

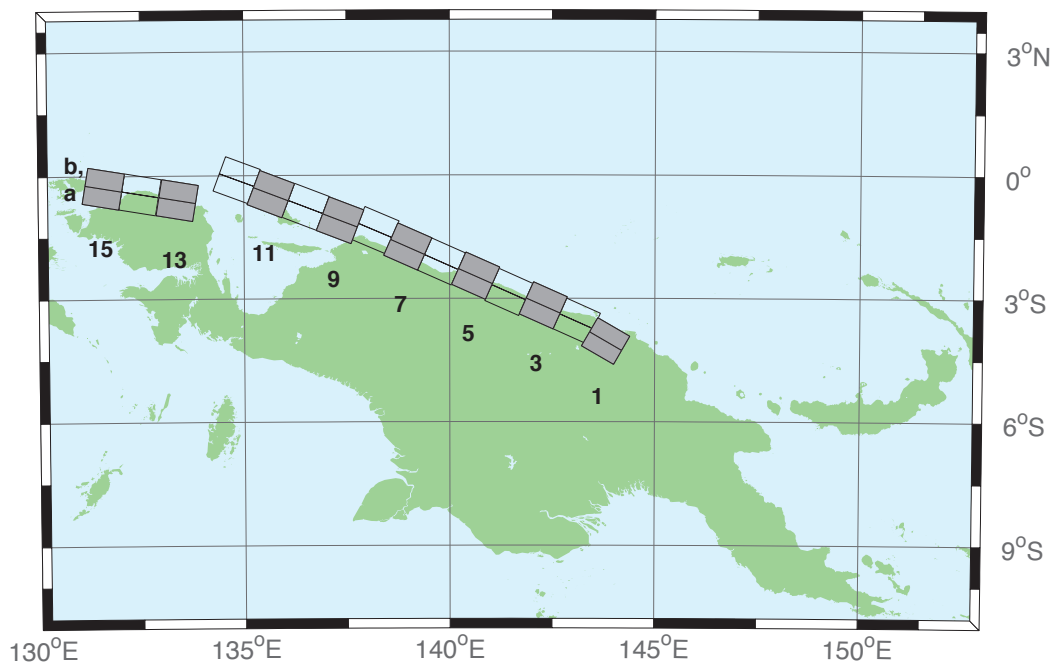


Figure B.6: New Guinea Subduction Zone unit sources.

Table B.6: Earthquake parameters for New Guinea Subduction Zone unit sources.

Segment	Description	Longitude($^{\circ}$ E)	Latitude($^{\circ}$ N)	Strike($^{\circ}$)	Dip($^{\circ}$)	Depth (km)
ngsz-1a	New Guinea	143.6063	-4.3804	120	29	25.64
ngsz-1b	New Guinea	143.8032	-4.0402	120	29	1.4
ngsz-2a	New Guinea	142.9310	-3.9263	114	27.63	20.1
ngsz-2b	New Guinea	143.0932	-3.5628	114	21.72	1.6
ngsz-3a	New Guinea	142.1076	-3.5632	114	20.06	18.73
ngsz-3b	New Guinea	142.2795	-3.1778	114	15.94	5
ngsz-4a	New Guinea	141.2681	-3.2376	114	21	17.76
ngsz-4b	New Guinea	141.4389	-2.8545	114	14.79	5
ngsz-5a	New Guinea	140.4592	-2.8429	114	21.26	16.14
ngsz-5b	New Guinea	140.6296	-2.4605	114	12.87	5
ngsz-6a	New Guinea	139.6288	-2.4960	114	22.72	15.4
ngsz-6b	New Guinea	139.7974	-2.1175	114	12	5
ngsz-7a	New Guinea	138.8074	-2.1312	114	21.39	15.4
ngsz-7b	New Guinea	138.9776	-1.7491	114	12	5
ngsz-8a	New Guinea	138.0185	-1.7353	113.1	18.79	15.14
ngsz-8b	New Guinea	138.1853	-1.3441	113.1	11.7	5
ngsz-9a	New Guinea	137.1805	-1.5037	111	15.24	13.23
ngsz-9b	New Guinea	137.3358	-1.0991	111	9.47	5
ngsz-10a	New Guinea	136.3418	-1.1774	111	13.51	11.09
ngsz-10b	New Guinea	136.4983	-0.7697	111	7	5
ngsz-11a	New Guinea	135.4984	-0.8641	111	11.38	12.49
ngsz-11b	New Guinea	135.6562	-0.4530	111	8.62	5
ngsz-12a	New Guinea	134.6759	-0.5216	110.5	10	13.68
ngsz-12b	New Guinea	134.8307	-0.1072	110.5	10	5
ngsz-13a	New Guinea	133.3065	-1.0298	99.5	10	13.68
ngsz-13b	New Guinea	133.3795	-0.5935	99.5	10	5
ngsz-14a	New Guinea	132.4048	-0.8816	99.5	10	13.68
ngsz-14b	New Guinea	132.4778	-0.4453	99.5	10	5
ngsz-15a	New Guinea	131.5141	-0.7353	99.5	10	13.68
ngsz-15b	New Guinea	131.5871	-0.2990	99.5	10	5

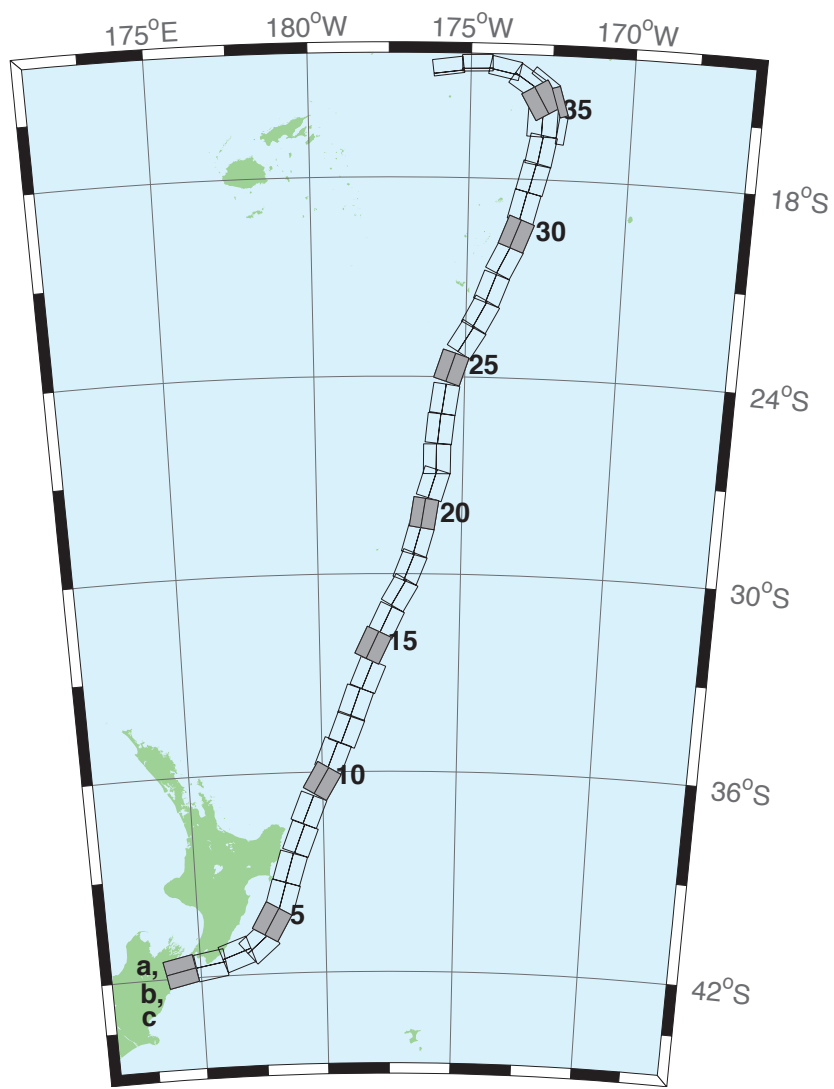


Figure B.7: New Zealand–Kermadec–Tonga Subduction Zone unit sources.

Table B.7: Earthquake parameters for New Zealand–Kermadec–Tonga Subduction Zone unit sources.

Segment	Description	Longitude($^{\circ}$ E)	Latitude($^{\circ}$ N)	Strike($^{\circ}$)	Dip($^{\circ}$)	Depth (km)
ntsz-1a	New Zealand–Tonga	174.0985	-41.3951	258.6	24	25.34
ntsz-1b	New Zealand–Tonga	174.2076	-41.7973	258.6	24	5
ntsz-2a	New Zealand–Tonga	175.3289	-41.2592	260.6	29.38	23.17
ntsz-2b	New Zealand–Tonga	175.4142	-41.6454	260.6	21.31	5
ntsz-3a	New Zealand–Tonga	176.2855	-40.9950	250.7	29.54	21.74
ntsz-3b	New Zealand–Tonga	176.4580	-41.3637	250.7	19.56	5
ntsz-4a	New Zealand–Tonga	177.0023	-40.7679	229.4	24.43	18.87
ntsz-4b	New Zealand–Tonga	177.3552	-41.0785	229.4	16.1	5
ntsz-5a	New Zealand–Tonga	177.4114	-40.2396	210	18.8	19.29
ntsz-5b	New Zealand–Tonga	177.8951	-40.4525	210	16.61	5
ntsz-6a	New Zealand–Tonga	177.8036	-39.6085	196.7	18.17	15.8
ntsz-6b	New Zealand–Tonga	178.3352	-39.7310	196.7	12.48	5
ntsz-7a	New Zealand–Tonga	178.1676	-38.7480	197	28.1	17.85
ntsz-7b	New Zealand–Tonga	178.6541	-38.8640	197	14.89	5
ntsz-8a	New Zealand–Tonga	178.6263	-37.8501	201.4	31.47	18.78
ntsz-8b	New Zealand–Tonga	179.0788	-37.9899	201.4	16	5
ntsz-9a	New Zealand–Tonga	178.9833	-36.9770	202.2	29.58	20.02
ntsz-9b	New Zealand–Tonga	179.4369	-37.1245	202.2	17.48	5
ntsz-10a	New Zealand–Tonga	179.5534	-36.0655	210.6	32.1	20.72
ntsz-10b	New Zealand–Tonga	179.9595	-36.2593	210.6	18.32	5
ntsz-11a	New Zealand–Tonga	179.9267	-35.3538	201.7	25	16.09
ntsz-11b	New Zealand–Tonga	180.3915	-35.5040	201.7	12.81	5
ntsz-12a	New Zealand–Tonga	180.4433	-34.5759	201.2	25	15.46
ntsz-12b	New Zealand–Tonga	180.9051	-34.7230	201.2	12.08	5
ntsz-13a	New Zealand–Tonga	180.7990	-33.7707	199.8	25.87	19.06
ntsz-13b	New Zealand–Tonga	181.2573	-33.9073	199.8	16.33	5
ntsz-14a	New Zealand–Tonga	181.2828	-32.9288	202.4	31.28	22.73
ntsz-14b	New Zealand–Tonga	181.7063	-33.0751	202.4	20.77	5
ntsz-15a	New Zealand–Tonga	181.4918	-32.0035	205.4	32.33	22.64
ntsz-15b	New Zealand–Tonga	181.8967	-32.1665	205.4	20.66	5
ntsz-16a	New Zealand–Tonga	181.9781	-31.2535	205.5	34.29	23.59
ntsz-16b	New Zealand–Tonga	182.3706	-31.4131	205.5	21.83	5
ntsz-17a	New Zealand–Tonga	182.4819	-30.3859	210.3	37.6	25.58
ntsz-17b	New Zealand–Tonga	182.8387	-30.5655	210.3	24.3	5
ntsz-18a	New Zealand–Tonga	182.8176	-29.6545	201.6	37.65	26.13
ntsz-18b	New Zealand–Tonga	183.1985	-29.7856	201.6	25	5
ntsz-19a	New Zealand–Tonga	183.0622	-28.8739	195.7	34.41	26.13
ntsz-19b	New Zealand–Tonga	183.4700	-28.9742	195.7	25	5
ntsz-20a	New Zealand–Tonga	183.2724	-28.0967	188.8	38	26.13
ntsz-20b	New Zealand–Tonga	183.6691	-28.1508	188.8	25	5
ntsz-21a	New Zealand–Tonga	183.5747	-27.1402	197.1	32.29	24.83
ntsz-21b	New Zealand–Tonga	183.9829	-27.2518	197.1	23.37	5
ntsz-22a	New Zealand–Tonga	183.6608	-26.4975	180	29.56	18.63
ntsz-22b	New Zealand–Tonga	184.0974	-26.4975	180	15.82	5
ntsz-23a	New Zealand–Tonga	183.7599	-25.5371	185.8	32.42	20.56
ntsz-23b	New Zealand–Tonga	184.1781	-25.5752	185.8	18.13	5
ntsz-24a	New Zealand–Tonga	183.9139	-24.6201	188.2	33.31	23.73
ntsz-24b	New Zealand–Tonga	184.3228	-24.6734	188.2	22	5
ntsz-25a	New Zealand–Tonga	184.1266	-23.5922	198.5	29.34	19.64
ntsz-25b	New Zealand–Tonga	184.5322	-23.7163	198.5	17.03	5
ntsz-26a	New Zealand–Tonga	184.6613	-22.6460	211.7	30.26	19.43
ntsz-26b	New Zealand–Tonga	185.0196	-22.8497	211.7	16.78	5
ntsz-27a	New Zealand–Tonga	185.0879	-21.9139	207.9	31.73	20.67

Continued on next page

Table B.7 – continued

Segment	Description	Longitude($^{\circ}$ E)	Latitude($^{\circ}$ N)	Strike($^{\circ}$)	Dip($^{\circ}$)	Depth (km)
ntszz-27b	New Zealand–Tonga	185.4522	-22.0928	207.9	18.27	5
ntszz-28a	New Zealand–Tonga	185.4037	-21.1758	200.5	32.44	21.76
ntszz-28b	New Zealand–Tonga	185.7849	-21.3084	200.5	19.58	5
ntszz-29a	New Zealand–Tonga	185.8087	-20.2629	206.4	32.47	20.4
ntszz-29b	New Zealand–Tonga	186.1710	-20.4312	206.4	17.94	5
ntszz-30a	New Zealand–Tonga	186.1499	-19.5087	200.9	32.98	22.46
ntszz-30b	New Zealand–Tonga	186.5236	-19.6432	200.9	20.44	5
ntszz-31a	New Zealand–Tonga	186.3538	-18.7332	193.9	34.41	21.19
ntszz-31b	New Zealand–Tonga	186.7339	-18.8221	193.9	18.89	5
ntszz-32a	New Zealand–Tonga	186.5949	-17.8587	194.1	30	19.12
ntszz-32b	New Zealand–Tonga	186.9914	-17.9536	194.1	16.4	5
ntszz-33a	New Zealand–Tonga	186.8172	-17.0581	190	33.15	23.34
ntszz-33b	New Zealand–Tonga	187.2047	-17.1237	190	21.52	5
ntszz-34a	New Zealand–Tonga	186.7814	-16.2598	182.1	15	13.41
ntszz-34b	New Zealand–Tonga	187.2330	-16.2759	182.1	9.68	5
ntszz-34c	New Zealand–Tonga	187.9697	-16.4956	7.62	57.06	6.571
ntszz-35a	New Zealand–Tonga	186.8000	-15.8563	149.8	15	12.17
ntszz-35b	New Zealand–Tonga	187.1896	-15.6384	149.8	8.24	5
ntszz-35c	New Zealand–Tonga	187.8776	-15.6325	342.4	57.06	6.571
ntszz-36a	New Zealand–Tonga	186.5406	-15.3862	123.9	40.44	36.72
ntszz-36b	New Zealand–Tonga	186.7381	-15.1025	123.9	39.38	5
ntszz-36c	New Zealand–Tonga	187.3791	-14.9234	307	57.06	6.571
ntszz-37a	New Zealand–Tonga	185.9883	-14.9861	102	68.94	30.99
ntszz-37b	New Zealand–Tonga	186.0229	-14.8282	102	31.32	5
ntszz-38a	New Zealand–Tonga	185.2067	-14.8259	88.4	80	26.13
ntszz-38b	New Zealand–Tonga	185.2044	-14.7479	88.4	25	5
ntszz-39a	New Zealand–Tonga	184.3412	-14.9409	82.55	80	26.13
ntszz-39b	New Zealand–Tonga	184.3307	-14.8636	82.55	25	5

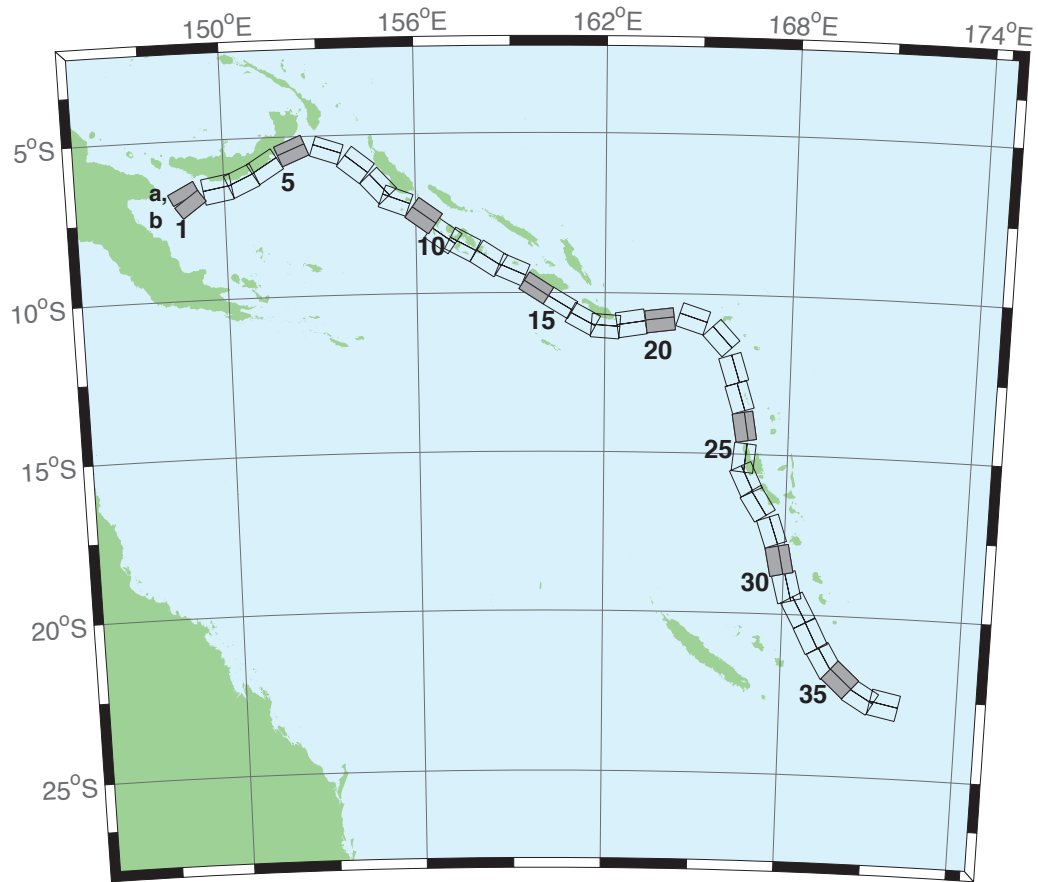


Figure B.8: New Britain–Solomons–Vanuatu Zone unit sources.

Table B.8: Earthquake parameters for New Britain–Solomons–Vanuatu Subduction Zone unit sources.

Segment	Description	Longitude($^{\circ}$ E)	Latitude($^{\circ}$ N)	Strike($^{\circ}$)	Dip($^{\circ}$)	Depth (km)
nvsz-1a	New Britain–Vanuatu	148.6217	-6.4616	243.2	32.34	15.69
nvsz-1b	New Britain–Vanuatu	148.7943	-6.8002	234.2	12.34	5
nvsz-2a	New Britain–Vanuatu	149.7218	-6.1459	260.1	35.1	16.36
nvsz-2b	New Britain–Vanuatu	149.7856	-6.5079	260.1	13.13	5
nvsz-3a	New Britain–Vanuatu	150.4075	-5.9659	245.7	42.35	18.59
nvsz-3b	New Britain–Vanuatu	150.5450	-6.2684	245.7	15.77	5
nvsz-4a	New Britain–Vanuatu	151.1095	-5.5820	238.2	42.41	23.63
nvsz-4b	New Britain–Vanuatu	151.2851	-5.8639	238.2	21.88	5
nvsz-5a	New Britain–Vanuatu	152.0205	-5.1305	247.7	49.22	32.39
nvsz-5b	New Britain–Vanuatu	152.1322	-5.4020	247.7	33.22	5
nvsz-6a	New Britain–Vanuatu	153.3450	-5.1558	288.6	53.53	33.59
nvsz-6b	New Britain–Vanuatu	153.2595	-5.4089	288.6	34.87	5
nvsz-7a	New Britain–Vanuatu	154.3814	-5.6308	308.3	39.72	19.18
nvsz-7b	New Britain–Vanuatu	154.1658	-5.9017	308.3	16.48	5
nvsz-8a	New Britain–Vanuatu	155.1097	-6.3511	317.2	45.33	22.92
nvsz-8b	New Britain–Vanuatu	154.8764	-6.5656	317.2	21	5
nvsz-9a	New Britain–Vanuatu	155.5027	-6.7430	290.5	48.75	22.92
nvsz-9b	New Britain–Vanuatu	155.3981	-7.0204	290.5	21	5
nvsz-10a	New Britain–Vanuatu	156.4742	-7.2515	305.9	36.88	27.62
nvsz-10b	New Britain–Vanuatu	156.2619	-7.5427	305.9	26.9	5
nvsz-11a	New Britain–Vanuatu	157.0830	-7.8830	305.4	32.97	29.72
nvsz-11b	New Britain–Vanuatu	156.8627	-8.1903	305.4	29.63	5
nvsz-12a	New Britain–Vanuatu	157.6537	-8.1483	297.9	37.53	28.57
nvsz-12b	New Britain–Vanuatu	157.4850	-8.4630	297.9	28.13	5
nvsz-13a	New Britain–Vanuatu	158.5089	-8.5953	302.7	33.62	23.02
nvsz-13b	New Britain–Vanuatu	158.3042	-8.9099	302.7	21.12	5
nvsz-14a	New Britain–Vanuatu	159.1872	-8.9516	293.3	38.44	34.06
nvsz-14b	New Britain–Vanuatu	159.0461	-9.2747	293.3	35.54	5
nvsz-15a	New Britain–Vanuatu	159.9736	-9.5993	302.8	46.69	41.38
nvsz-15b	New Britain–Vanuatu	159.8044	-9.8584	302.8	46.69	5
nvsz-16a	New Britain–Vanuatu	160.7343	-10.0574	301	46.05	41
nvsz-16b	New Britain–Vanuatu	160.5712	-10.3246	301	46.05	5
nvsz-17a	New Britain–Vanuatu	161.4562	-10.5241	298.4	40.12	37.22
nvsz-17b	New Britain–Vanuatu	161.2900	-10.8263	298.4	40.12	5
nvsz-18a	New Britain–Vanuatu	162.0467	-10.6823	274.1	40.33	29.03
nvsz-18b	New Britain–Vanuatu	162.0219	-11.0238	274.1	28.72	5
nvsz-19a	New Britain–Vanuatu	162.7818	-10.5645	261.3	34.25	24.14
nvsz-19b	New Britain–Vanuatu	162.8392	-10.9315	261.3	22.51	5
nvsz-20a	New Britain–Vanuatu	163.7222	-10.5014	262.9	50.35	26.3
nvsz-20b	New Britain–Vanuatu	163.7581	-10.7858	262.9	25.22	5
nvsz-21a	New Britain–Vanuatu	164.9445	-10.4183	287.9	40.31	23.3
nvsz-21b	New Britain–Vanuatu	164.8374	-10.7442	287.9	21.47	5
nvsz-22a	New Britain–Vanuatu	166.0261	-11.1069	317.1	42.39	20.78
nvsz-22b	New Britain–Vanuatu	165.7783	-11.3328	317.1	18.4	5
nvsz-23a	New Britain–Vanuatu	166.5179	-12.2260	342.4	47.95	22.43
nvsz-23b	New Britain–Vanuatu	166.2244	-12.3171	342.4	20.4	5
nvsz-24a	New Britain–Vanuatu	166.7236	-13.1065	342.6	47.13	28.52
nvsz-24b	New Britain–Vanuatu	166.4241	-13.1979	342.6	28.06	5
nvsz-25a	New Britain–Vanuatu	166.8914	-14.0785	350.3	54.1	31.16
nvsz-25b	New Britain–Vanuatu	166.6237	-14.1230	350.3	31.55	5
nvsz-26a	New Britain–Vanuatu	166.9200	-15.1450	365.6	50.46	29.05
nvsz-26b	New Britain–Vanuatu	166.6252	-15.1170	365.6	28.75	5
nvsz-27a	New Britain–Vanuatu	167.0053	-15.6308	334.2	44.74	25.46

Continued on next page

Table B.8 – continued

Segment	Description	Longitude($^{\circ}$ E)	Latitude($^{\circ}$ N)	Strike($^{\circ}$)	Dip($^{\circ}$)	Depth (km)
nvsz-27b	New Britain–Vanuatu	166.7068	-15.7695	334.2	24.15	5
nvsz-28a	New Britain–Vanuatu	167.4074	-16.3455	327.5	41.53	22.44
nvsz-28b	New Britain–Vanuatu	167.1117	-16.5264	327.5	20.42	5
nvsz-29a	New Britain–Vanuatu	167.9145	-17.2807	341.2	49.1	24.12
nvsz-29b	New Britain–Vanuatu	167.6229	-17.3757	341.2	22.48	5
nvsz-30a	New Britain–Vanuatu	168.2220	-18.2353	348.6	44.19	23.99
nvsz-30b	New Britain–Vanuatu	167.8895	-18.2991	348.6	22.32	5
nvsz-31a	New Britain–Vanuatu	168.5022	-19.0510	345.6	42.2	22.26
nvsz-31b	New Britain–Vanuatu	168.1611	-19.1338	345.6	20.2	5
nvsz-32a	New Britain–Vanuatu	168.8775	-19.6724	331.1	42.03	21.68
nvsz-32b	New Britain–Vanuatu	168.5671	-19.8338	331.1	19.49	5
nvsz-33a	New Britain–Vanuatu	169.3422	-20.4892	332.9	40.25	22.4
nvsz-33b	New Britain–Vanuatu	169.0161	-20.6453	332.9	20.37	5
nvsz-34a	New Britain–Vanuatu	169.8304	-21.2121	329.1	39	22.73
nvsz-34b	New Britain–Vanuatu	169.5086	-21.3911	329.1	20.77	5
nvsz-35a	New Britain–Vanuatu	170.3119	-21.6945	311.9	39	22.13
nvsz-35b	New Britain–Vanuatu	170.0606	-21.9543	311.9	20.03	5
nvsz-36a	New Britain–Vanuatu	170.9487	-22.1585	300.4	39.42	23.5
nvsz-36b	New Britain–Vanuatu	170.7585	-22.4577	300.4	21.71	5
nvsz-37a	New Britain–Vanuatu	171.6335	-22.3087	281.3	30	22.1
nvsz-37b	New Britain–Vanuatu	171.5512	-22.6902	281.3	20	5

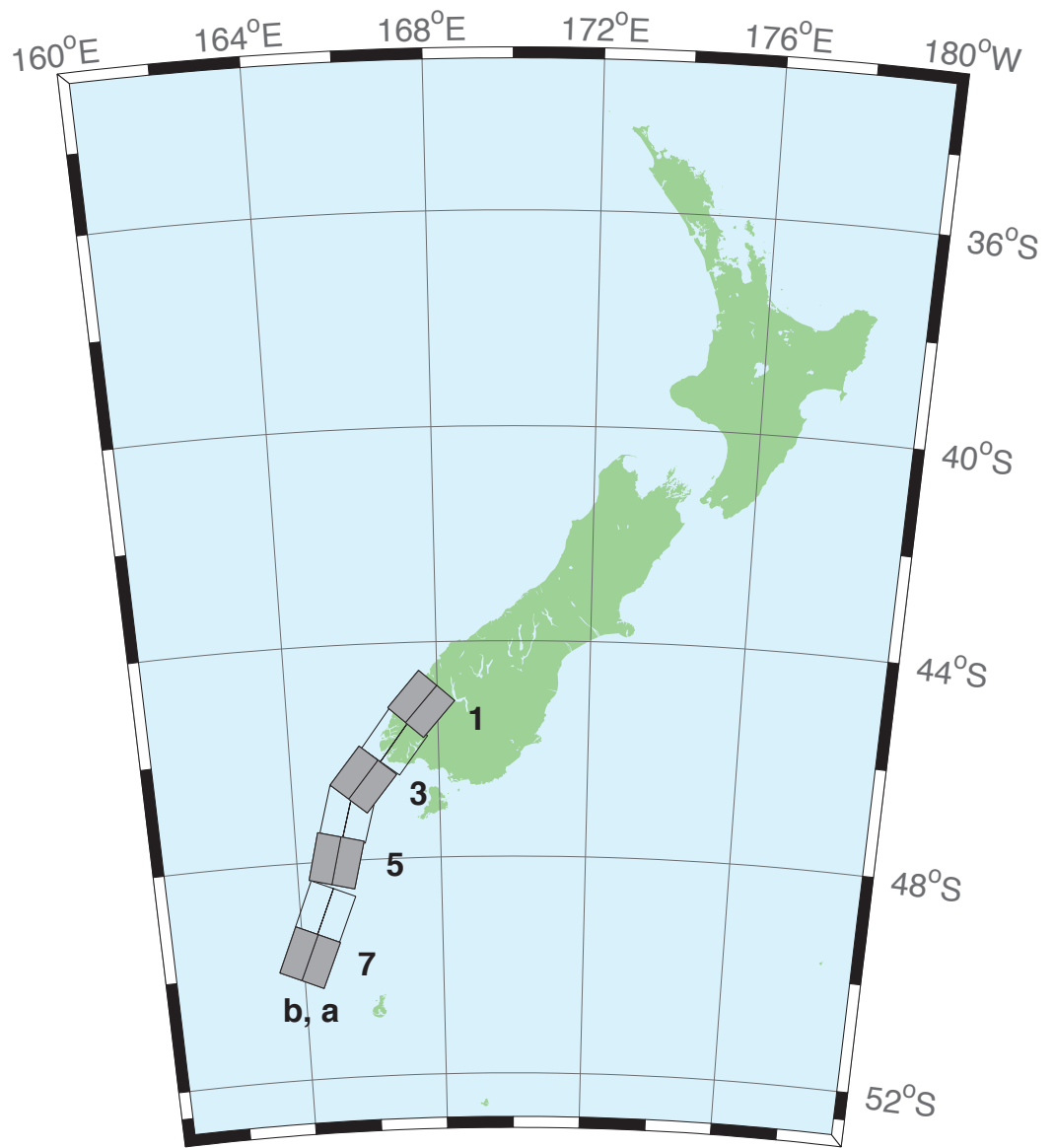


Figure B.9: New Zealand–Puysegur Zone unit sources.

Table B.9: Earthquake parameters for New Zealand–Puysegur Subduction Zone unit sources.

Segment	Description	Longitude($^{\circ}$ E)	Latitude($^{\circ}$ N)	Strike($^{\circ}$)	Dip($^{\circ}$)	Depth (km)
nzs–1a	New Zealand–Puysegur	168.0294	-45.4368	41.5	15	17.94
nzs–1b	New Zealand–Puysegur	167.5675	-45.1493	41.5	15	5
nzs–2a	New Zealand–Puysegur	167.3256	-46.0984	37.14	15	17.94
nzs–2b	New Zealand–Puysegur	166.8280	-45.8365	37.14	15	5
nzs–3a	New Zealand–Puysegur	166.4351	-46.7897	39.53	15	17.94
nzs–3b	New Zealand–Puysegur	165.9476	-46.5136	39.53	15	5
nzs–4a	New Zealand–Puysegur	166.0968	-47.2583	15.38	15	17.94
nzs–4b	New Zealand–Puysegur	165.4810	-47.1432	15.38	15	5
nzs–5a	New Zealand–Puysegur	165.7270	-48.0951	13.94	15	17.94
nzs–5b	New Zealand–Puysegur	165.0971	-47.9906	13.94	15	5
nzs–6a	New Zealand–Puysegur	165.3168	-49.0829	22.71	15	17.94
nzs–6b	New Zealand–Puysegur	164.7067	-48.9154	22.71	15	5
nzs–7a	New Zealand–Puysegur	164.8017	-49.9193	23.25	15	17.94
nzs–7b	New Zealand–Puysegur	164.1836	-49.7480	23.25	15	5

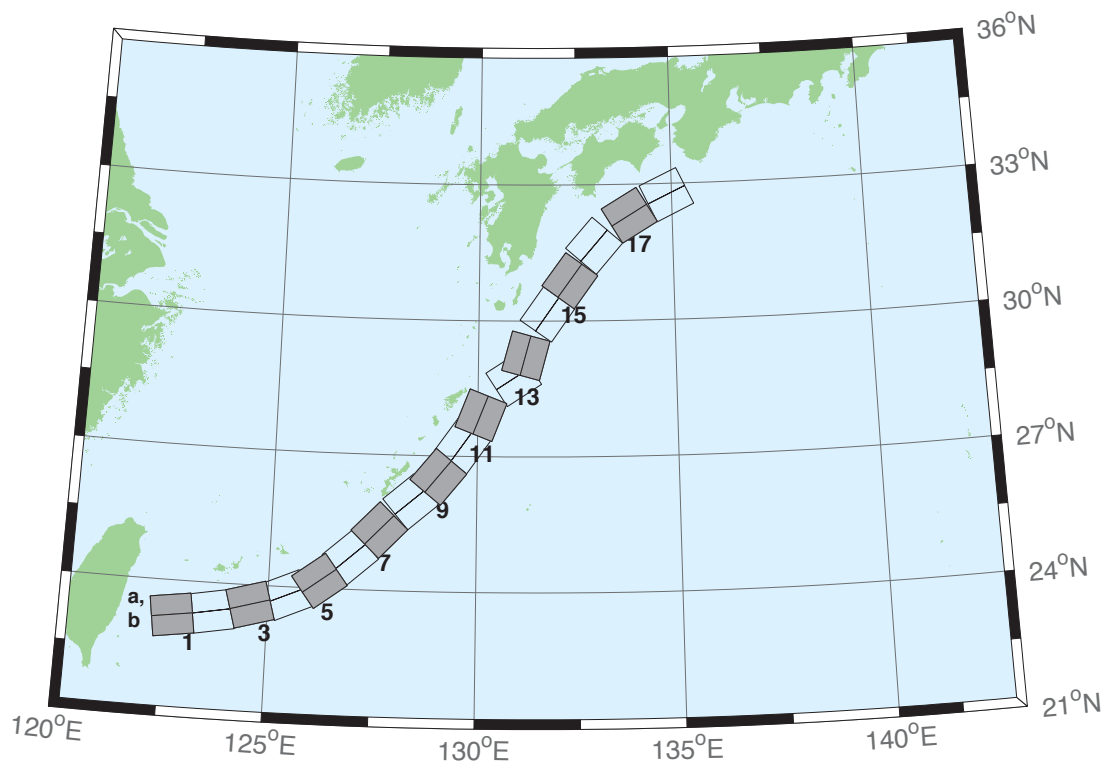


Figure B.10: Ryukyu–Kyushu–Nankai Zone unit sources.

Table B.10: Earthquake parameters for Ryukyu–Kyushu–Nankai Subduction Zone unit sources.

Segment	Description	Longitude($^{\circ}$ E)	Latitude($^{\circ}$ N)	Strike($^{\circ}$)	Dip($^{\circ}$)	Depth (km)
rnsz–1a	Ryukyu–Nankai	122.6672	23.6696	262	14	11.88
rnsz–1b	Ryukyu–Nankai	122.7332	23.2380	262	10	3.2
rnsz–2a	Ryukyu–Nankai	123.5939	23.7929	259.9	18.11	12.28
rnsz–2b	Ryukyu–Nankai	123.6751	23.3725	259.9	10	3.6
rnsz–3a	Ryukyu–Nankai	124.4604	23.9777	254.6	19.27	14.65
rnsz–3b	Ryukyu–Nankai	124.5830	23.5689	254.6	12.18	4.1
rnsz–4a	Ryukyu–Nankai	125.2720	24.2102	246.8	18	20.38
rnsz–4b	Ryukyu–Nankai	125.4563	23.8177	246.8	16	6.6
rnsz–5a	Ryukyu–Nankai	125.9465	24.5085	233.6	18	20.21
rnsz–5b	Ryukyu–Nankai	126.2241	24.1645	233.6	16	6.43
rnsz–6a	Ryukyu–Nankai	126.6349	25.0402	228.7	17.16	19.55
rnsz–6b	Ryukyu–Nankai	126.9465	24.7176	228.7	15.16	6.47
rnsz–7a	Ryukyu–Nankai	127.2867	25.6343	224	15.85	17.98
rnsz–7b	Ryukyu–Nankai	127.6303	25.3339	224	13.56	6.26
rnsz–8a	Ryukyu–Nankai	128.0725	26.3146	229.7	14.55	14.31
rnsz–8b	Ryukyu–Nankai	128.3854	25.9831	229.7	9.64	5.94
rnsz–9a	Ryukyu–Nankai	128.6642	26.8177	219.2	15.4	12.62
rnsz–9b	Ryukyu–Nankai	129.0391	26.5438	219.2	8	5.66
rnsz–10a	Ryukyu–Nankai	129.2286	27.4879	215.2	17	12.55
rnsz–10b	Ryukyu–Nankai	129.6233	27.2402	215.2	8.16	5.45
rnsz–11a	Ryukyu–Nankai	129.6169	28.0741	201.3	17	12.91
rnsz–11b	Ryukyu–Nankai	130.0698	27.9181	201.3	8.8	5.26
rnsz–12a	Ryukyu–Nankai	130.6175	29.0900	236.7	16.42	13.05
rnsz–12b	Ryukyu–Nankai	130.8873	28.7299	236.7	9.57	4.74
rnsz–13a	Ryukyu–Nankai	130.7223	29.3465	195.2	20.25	15.89
rnsz–13b	Ryukyu–Nankai	131.1884	29.2362	195.2	12.98	4.66
rnsz–14a	Ryukyu–Nankai	131.3467	30.3899	215.1	22.16	19.73
rnsz–14b	Ryukyu–Nankai	131.7402	30.1507	215.1	17.48	4.71
rnsz–15a	Ryukyu–Nankai	131.9149	31.1450	216	15.11	16.12
rnsz–15b	Ryukyu–Nankai	132.3235	30.8899	216	13.46	4.48
rnsz–16a	Ryukyu–Nankai	132.5628	31.9468	220.9	10.81	10.88
rnsz–16b	Ryukyu–Nankai	132.9546	31.6579	220.9	7.19	4.62
rnsz–17a	Ryukyu–Nankai	133.6125	32.6956	239	10.14	12.01
rnsz–17b	Ryukyu–Nankai	133.8823	32.3168	239	8.41	4.7
rnsz–18a	Ryukyu–Nankai	134.6416	33.1488	244.7	10.99	14.21
rnsz–18b	Ryukyu–Nankai	134.8656	32.7502	244.5	10.97	4.7
rnsz–19a	Ryukyu–Nankai	135.6450	33.5008	246.5	14.49	14.72
rnsz–19b	Ryukyu–Nankai	135.8523	33.1021	246.5	11.87	4.44
rnsz–20a	Ryukyu–Nankai	136.5962	33.8506	244.8	15	14.38
rnsz–20b	Ryukyu–Nankai	136.8179	33.4581	244.8	12	3.98
rnsz–21a	Ryukyu–Nankai	137.2252	34.3094	231.9	15	15.4
rnsz–21b	Ryukyu–Nankai	137.5480	33.9680	231.9	12	5
rnsz–22a	Ryukyu–Nankai	137.4161	34.5249	192.3	15	15.4
rnsz–22b	Ryukyu–Nankai	137.9301	34.4327	192.3	12	5

Appendix C. SIFT testing results

Authors: Lindsey Wright, Yong Wei

1.0 PURPOSE

Forecast models are tested with synthetic tsunami events covering a range of tsunami source locations. Testing is also done with selected historical tsunami events when available.

The purpose of forecast model testing is three-fold. The first objective is to assure that the results obtained with NOAA's tsunami forecast system, which has been released to the Tsunami Warning Centers for operational use, are consistent with those obtained by the researcher during the development of the forecast model. The second objective is to test the forecast model for consistency, accuracy, time efficiency, and quality of results over a range of possible tsunami locations and magnitudes. The third objective is to identify bugs and issues in need of resolution by the researcher who developed the Forecast Model or by the forecast software development team before the next version release to NOAA's two Tsunami Warning Centers.

Local hardware and software applications, and tools familiar to the researcher(s), are used to run the Method of Splitting Tsunamis (MOST) model during the forecast model development. The test results presented in this report lend confidence that the model performs as developed and produces the same results when initiated within the forecast application in an operational setting as those produced by the researcher during the forecast model development. The test results assure those who rely on the Sand Point tsunami forecast model that consistent results are produced irrespective of system.

2.0 TESTING PROCEDURE

The general procedure for forecast model testing is to run a set of synthetic tsunami scenarios and a selected set of historical tsunami events through the forecast system application and compare the results with those obtained by the researcher during the forecast model development and presented in the Tsunami Forecast Model Report. Specific steps taken to test the model include:

1. Identification of testing scenarios, including the standard set of synthetic events, appropriate historical events, and customized synthetic scenarios that may have been used by the researcher(s) in developing the forecast model.
 2. Creation of new events to represent customized synthetic scenarios used by the researcher(s) in developing the forecast model, if any.
 3. Submission of test model runs with the forecast system, and export of the results from A, B, and C grids, along with time series.
 4. Recording applicable metadata, including the specific version of the forecast system used for testing.
 5. Examination of forecast model results from the forecast system for instabilities in both time series and plot results.
 6. Comparison of forecast model results obtained through the forecast system with those obtained during the forecast model development.
 7. Summarization of results with specific mention of quality, consistency, and time efficiency.
 8. Reporting of issues identified to modeler and forecast software development team.
9. Retesting the forecast models in the forecast system when reported issues have been addressed or explained.

Synthetic model runs were tested on a DELL PowerEdge R510 computer equipped with two Xeon E5670 processors at 2.93 Ghz, each with 12 MBytes of cache and 32GB memory. The processors are hex core and support hyperthreading, resulting in the computer performing as a 24 processor core machine. Additionally, the testing computer supports 10 Gigabit Ethernet for fast network connections. This computer configuration is similar or the same as the configurations of the computers installed at the Tsunami Warning Centers so the compute times should only vary slightly.

Results

The Sand Point forecast model was tested with NOAA's tsunami forecast system version 3.2.

The Sand Point forecast model was tested with four synthetic scenarios and one historical tsunami event. Test results from the forecast system and comparisons with the results obtained during the forecast model development are shown numerically in Table 1 and graphically in Figures 1 to 5. The results show that the forecast model is stable and robust, with consistent and high quality results across geographically distributed tsunami sources and mega-event tsunami magnitudes. The model run time (wall clock time) was 20.47 minutes for 12 hours of simulation time, and 6.80 minutes for 4 hours. This run time is well within the 10 minute run time for 4 hours of simulation time and satisfies time efficiency requirements.

Four synthetic events were run on the Sand Point forecast model. A slip of 28.4 m was used rather than the standard 25m for direct comparison purposes. Because the Sand Point model was developed prior to a shift in location for the Central and South America sources, a direct comparison between model development results and the forecast system output cannot be made for the Central and South America (CSSZ) 89-91 case. The modeled scenarios were stable for all cases tested, with no instabilities or ringing. Results show that the largest modeled height was 144 centimeters (cm) and originated in the New Zealand-Kermadec-Tonga (NTSZ) 30-39 source. This result appears visually larger than that obtained during development. Amplitudes greater than 100 cm were recorded for 3 of the 4 test sources and the smallest signal of 77 cm was recorded at the Kamchatka-Yap-Mariana-Izu-Bonin (KISZ) 22-31 source. These discrepancies are mainly attributed to the update of the propagation database in the past years, especially the expansion of the initial deformation being implemented to the entire computational domain. This issue is currently being investigated, and may be addressed in a revised report of the Sand Point forecast model. The forecast system recorded maximum amplitudes arriving beyond the timescales provided in the development images for the KISZ 22-31 and NTSZ 30-39 cases. The unit source parameters in CSSZ have been updated since the model was developed. This does not allow a direct comparison between SIFT results and the results at the time of model development, and therefore CSSZ 89-98 was left blank in the columns of "Development Max" and "Development Min". The Kuril 2006 historical event was also stable and the wave pattern output from the forecast system appears similar in shape and amplitude when compared to development results (red curve in Figure 16 of forecast model report).

Source Zone	Tsunami Source	α [m]	SIFT Max (cm)	Development Max (cm)	SIFT Min (cm)	Development Min (cm)
Mega-tsunami scenarios						
KISZ	A22-A31, B22-B31	28.4	59.1 (6-hour run) 77.4 (10-hour run)	29.9 (6-hour run)	-65.5 (6-hour run) -80.9 (10-hour run)	-53.5 (6-hour run)
ACSZ	A56-A65, B56-B65	28.4	81.0 (6-hour run) 101.8 (10-hour run)	68.7 (6-hour run)	-105.6 (6-hour run) -111.5 (10-hour run)	-80.4 (6-hour run)
CSSZ	A89-A98, B89-B98	28.4	112.7	-	-116.4	-
NTSZ	A30-39, B30-39	28.4	144.2	111.3 (6-hour run)	-186.8	-119.7 (6-hour run)
Historical events						
Kuril 2006			2.3	2.3	-2.4	-2.2

Table 1. Table of maximum and minimum amplitudes (cm) at the Sand Point, Alaska warning point for synthetic and historical events tested using SIFT 3.2 and obtained during development.

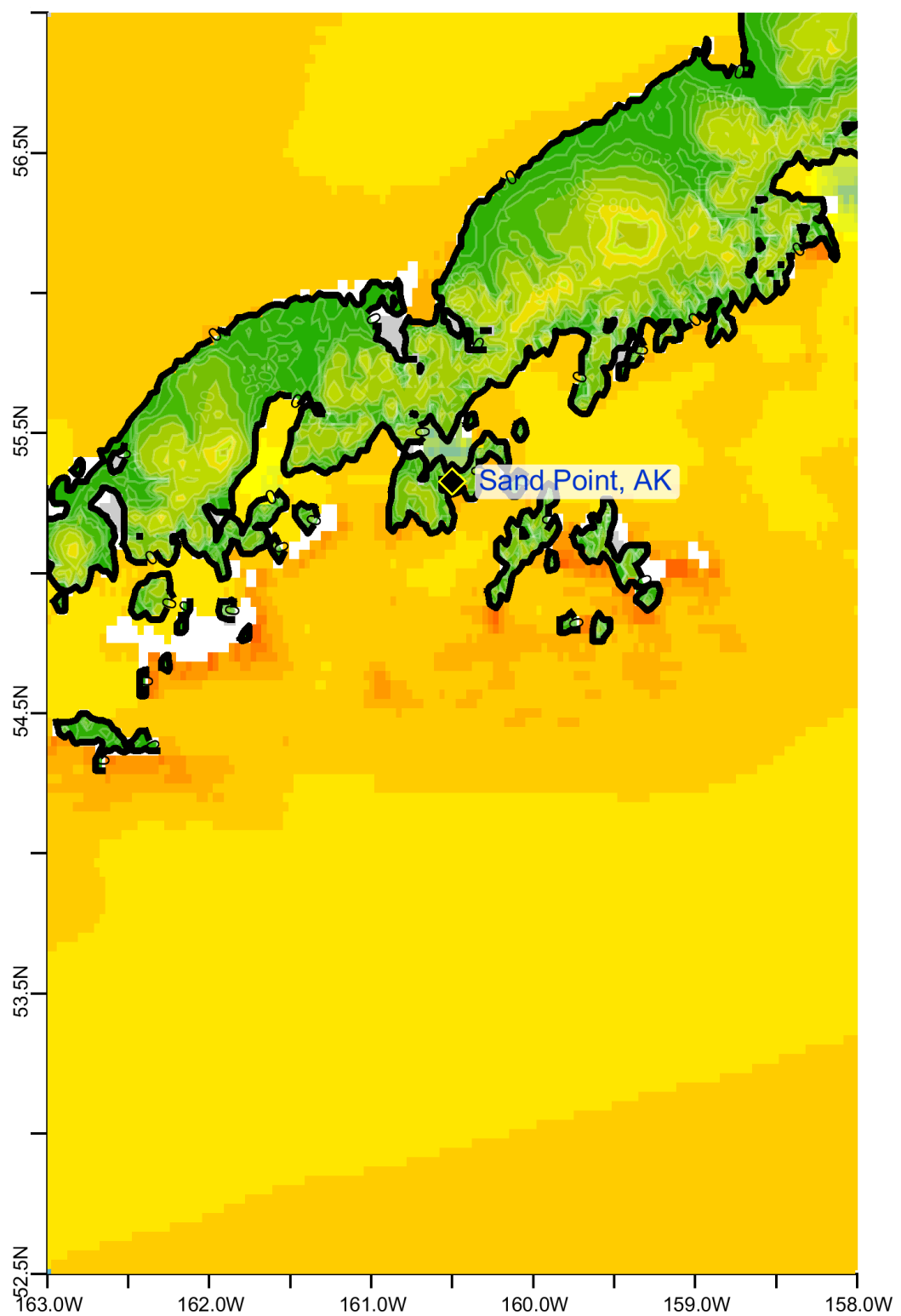


Figure 1. Max computed wave amplitude of A grid, Sand Point, Alaska, for synthetic event KISZ 22-31.

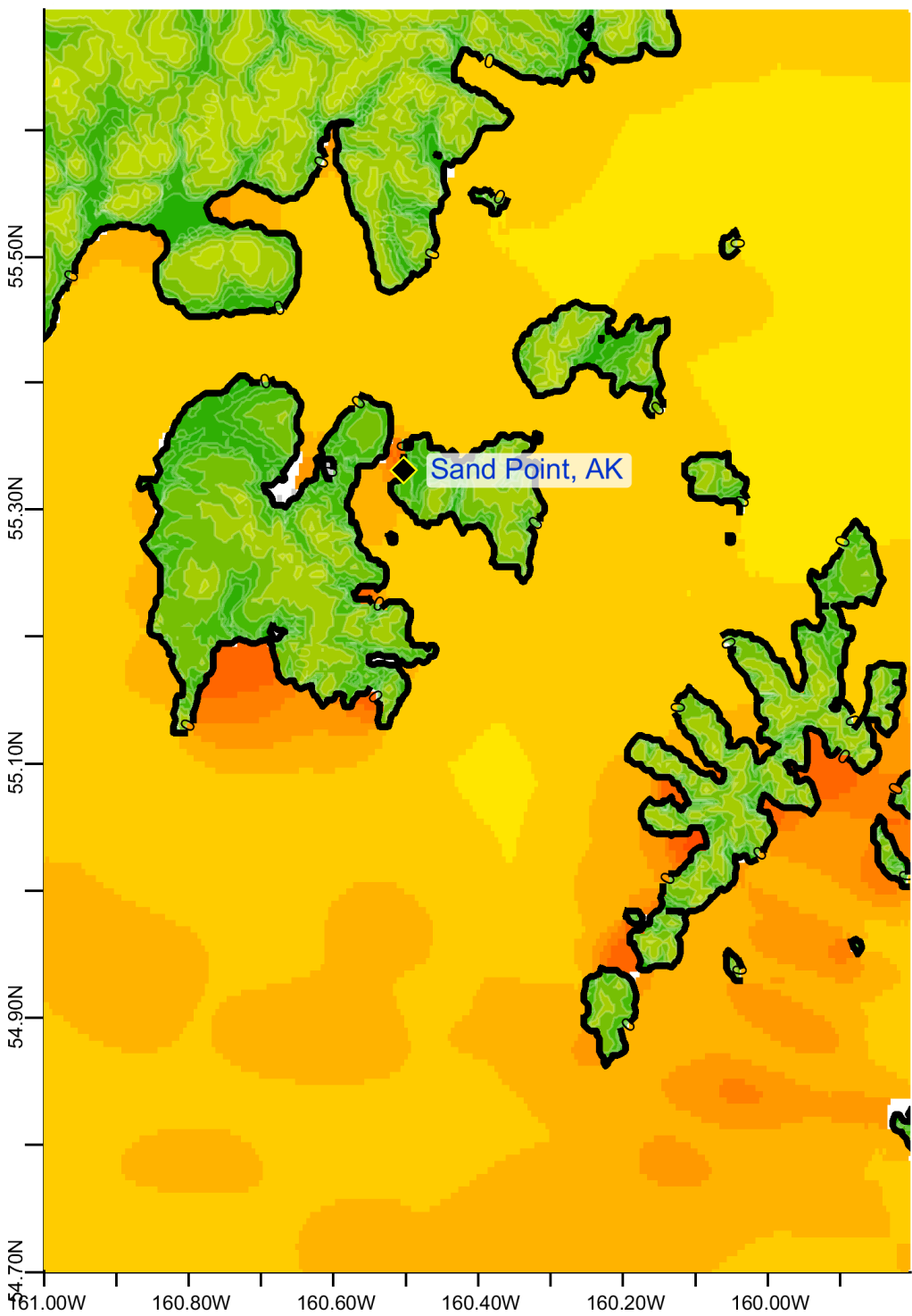


Figure 2. Max computed wave amplitude of B grid, Sand Point, Alaska, for synthetic event KISZ 22-31.

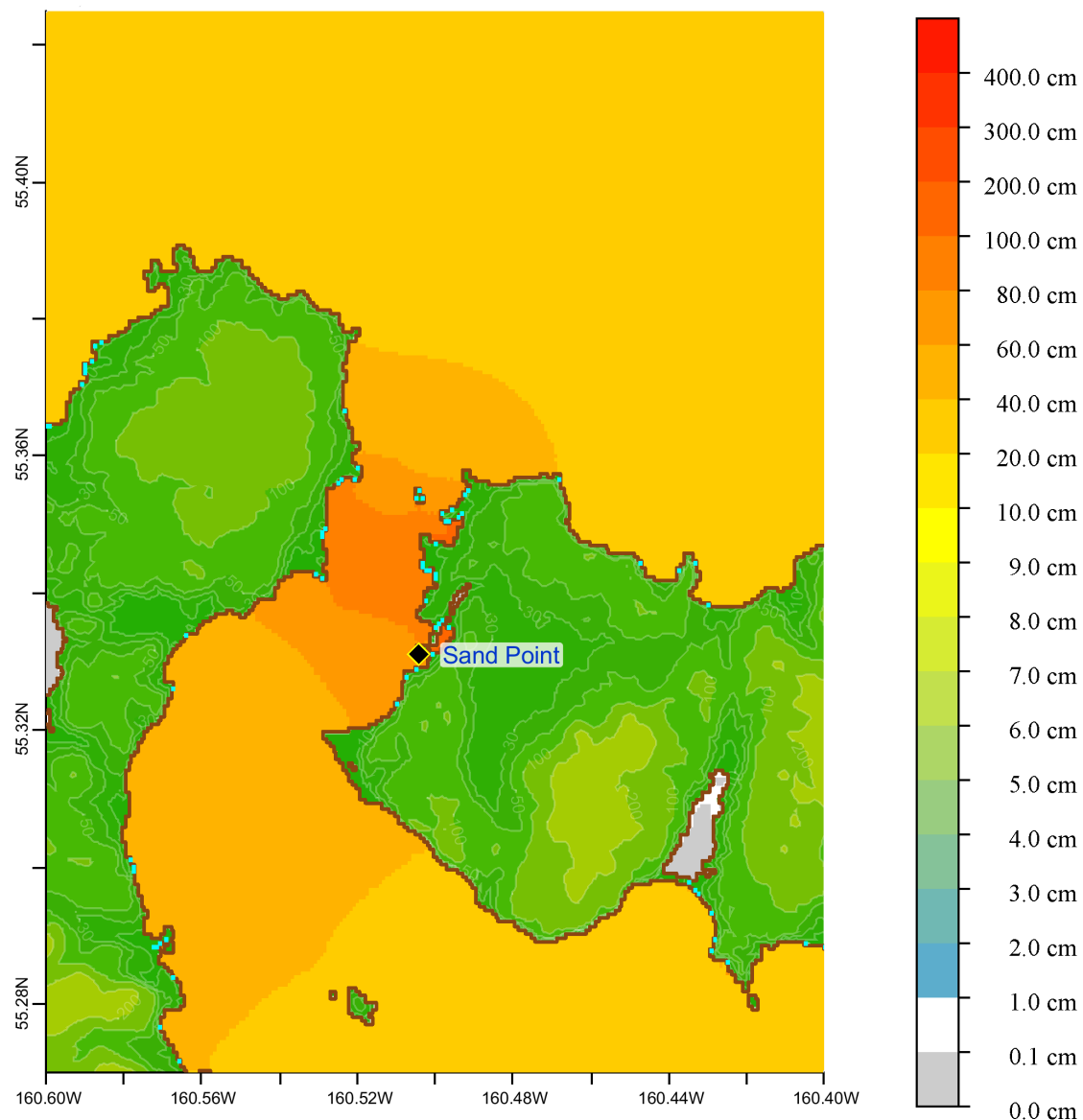


Figure 3. Max computed wave amplitude of C grid, Sand Point, Alaska, for synthetic event KISZ 22-31.

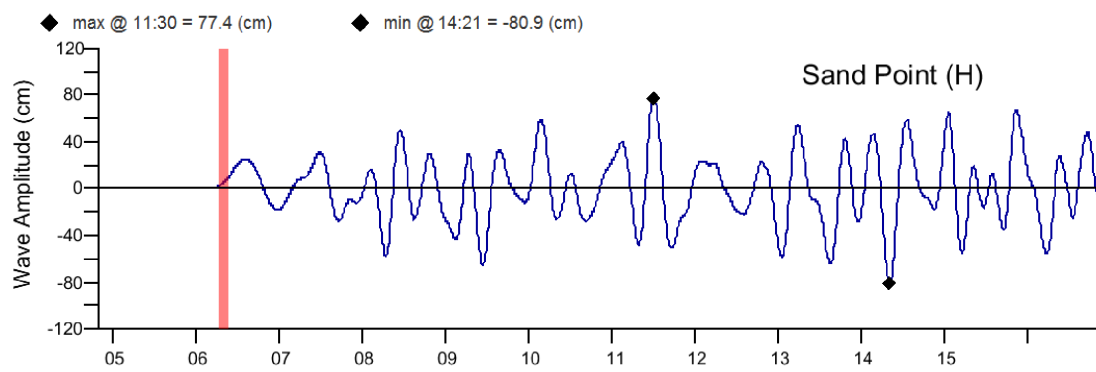


Figure 4. SIFT computed time series at Sand Point tide gage, for synthetic event KISZ 22-31. The computed time series at the time of model development for the same event is shown in Figure 29.

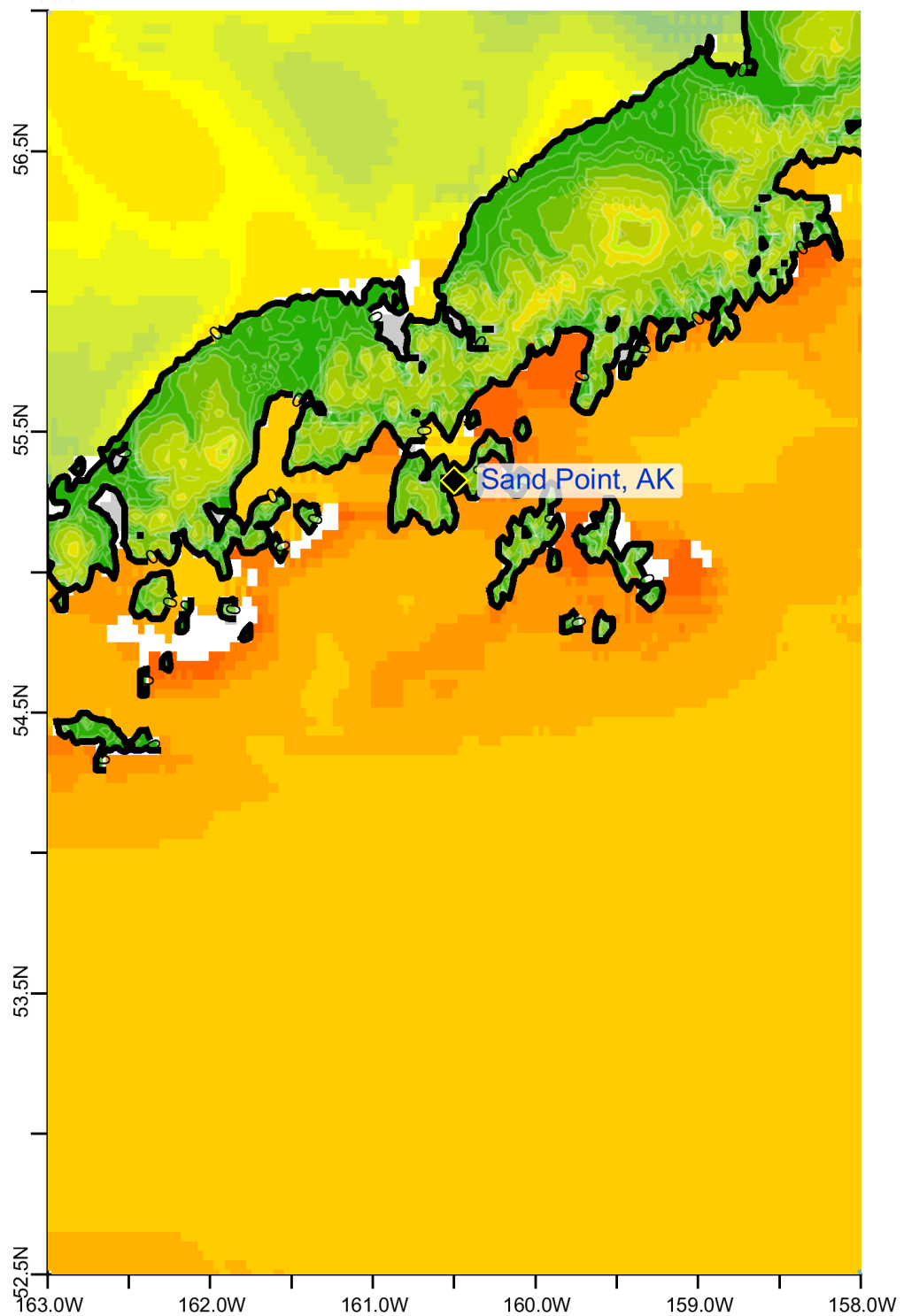


Figure 5. Max computed wave amplitude of A grid, Sand Point, Alaska, for synthetic event ACSZ 56-65.

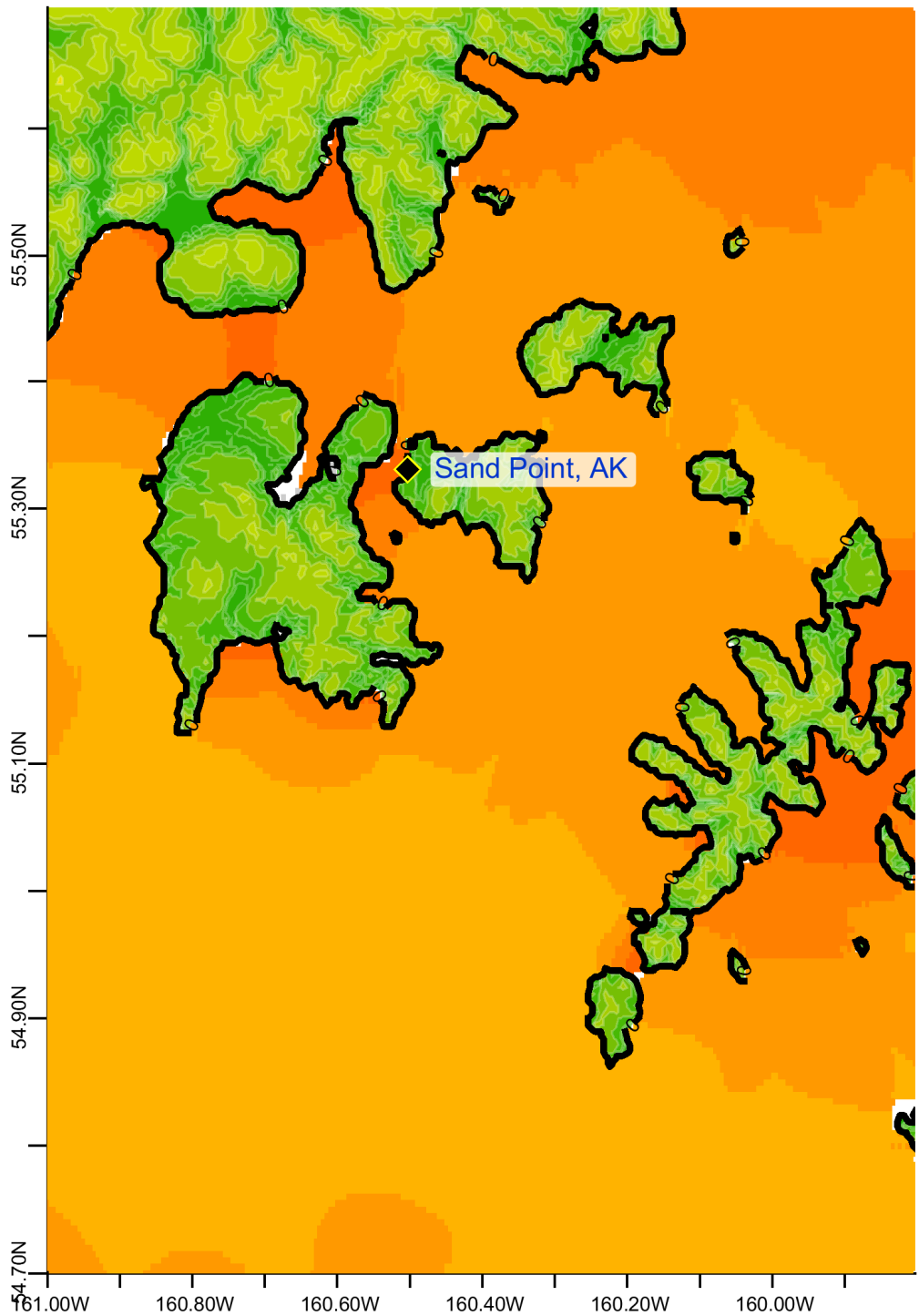


Figure 6. Max computed wave amplitude of B grid, Sand Point, Alaska, for synthetic event ACSZ 56-65.

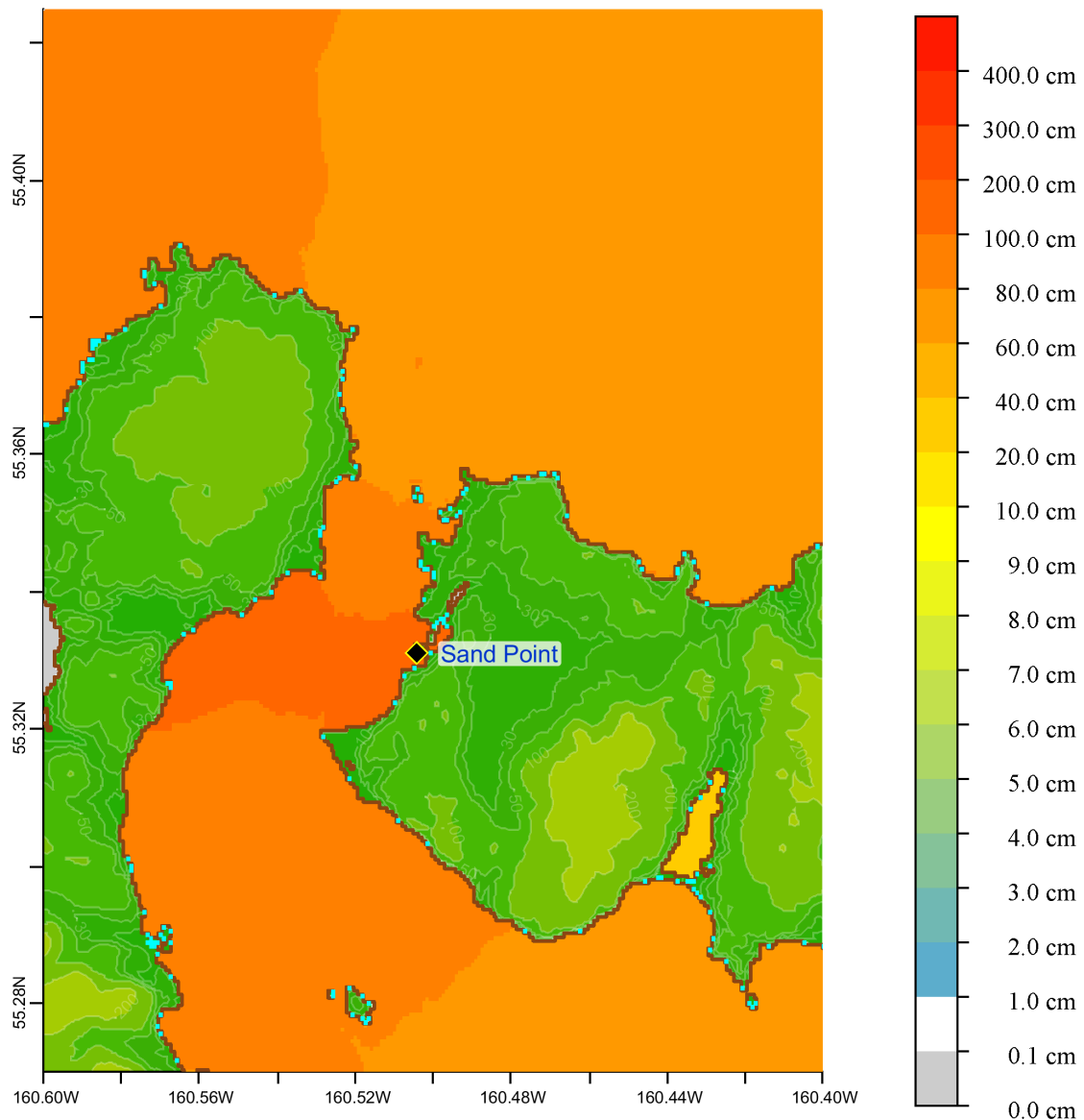


Figure 7. Max computed wave amplitude of C grid, Sand Point, Alaska, for synthetic event ACSZ 56-65.

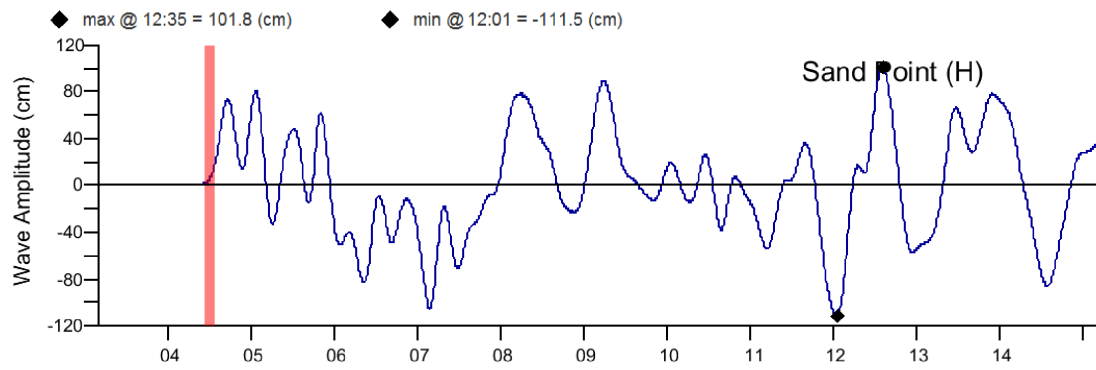


Figure 8. SIFT computed time series at Sand Point tide gage, for synthetic event ACSZ 56-65. The computed time series at the time of model development for the same event is shown in Figure 29.

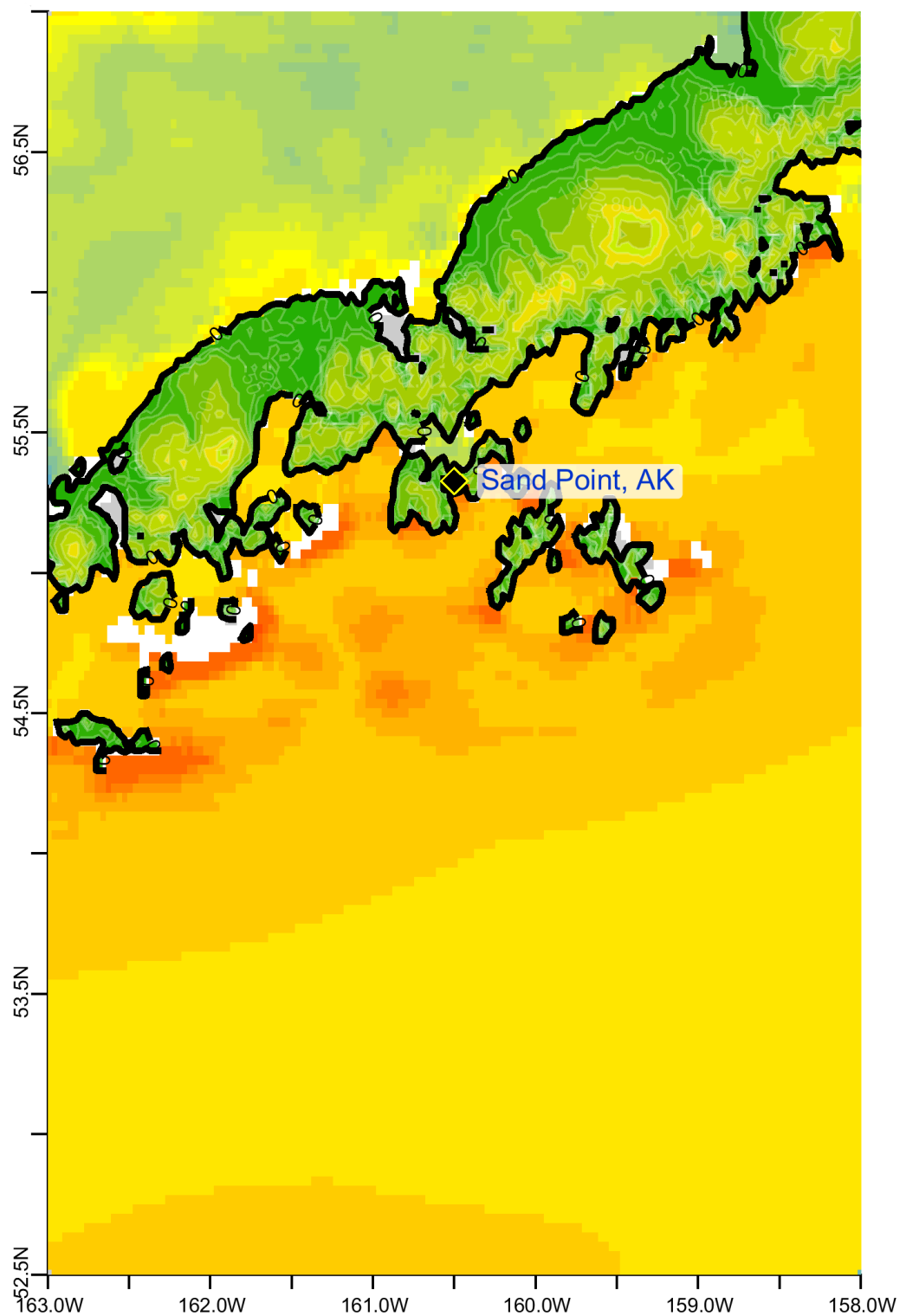


Figure 9. Max computed wave amplitude of A grid, Sand Point, Alaska, for synthetic event CSSZ 89-98.

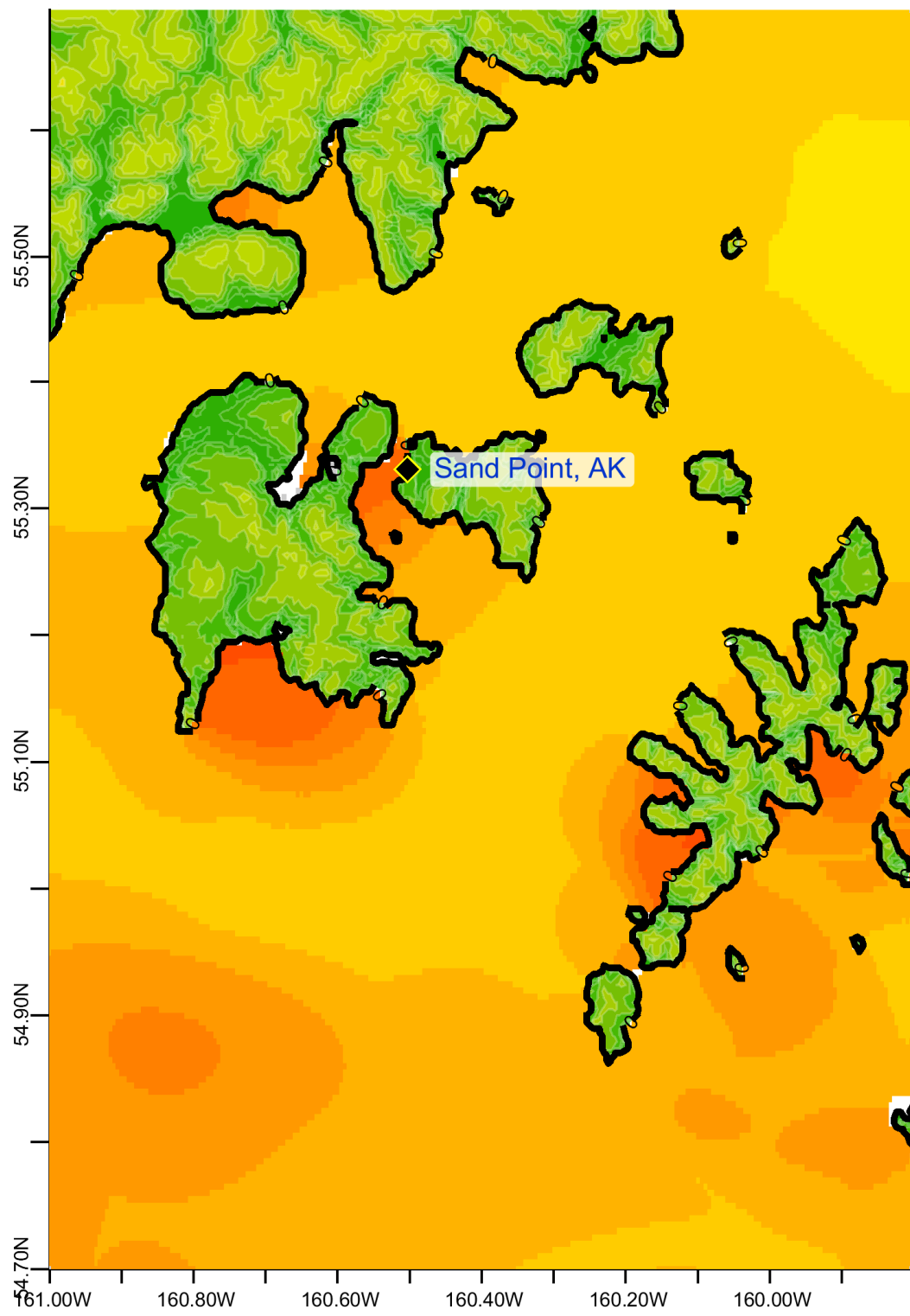


Figure 10. Max computed wave amplitude of B grid, Sand Point, Alaska, for synthetic event CSSZ 89-98.

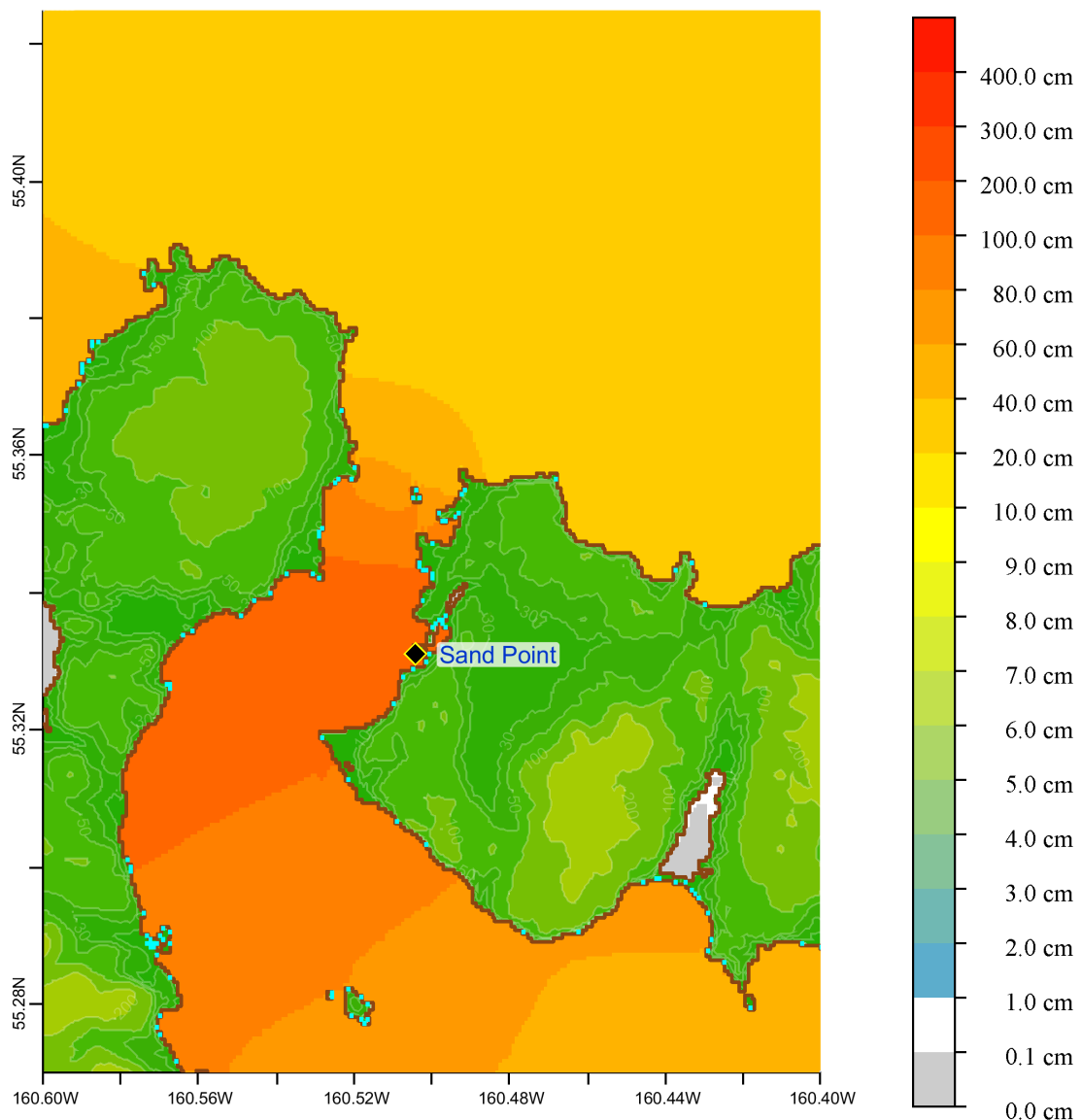


Figure 11. Max computed wave amplitude of C grid, Sand Point, Alaska, for synthetic event CSSZ 89-98.

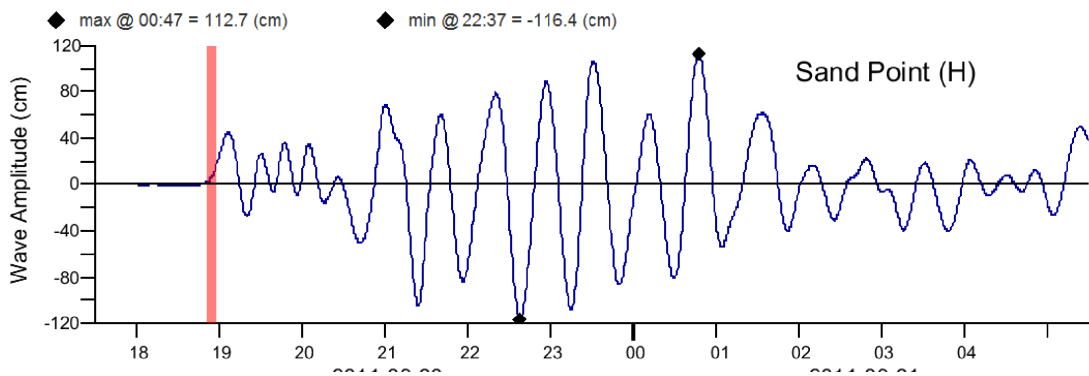


Figure 12. SIFT computed time series at Sand Point tide gage, for synthetic event CSSZ 89-98.

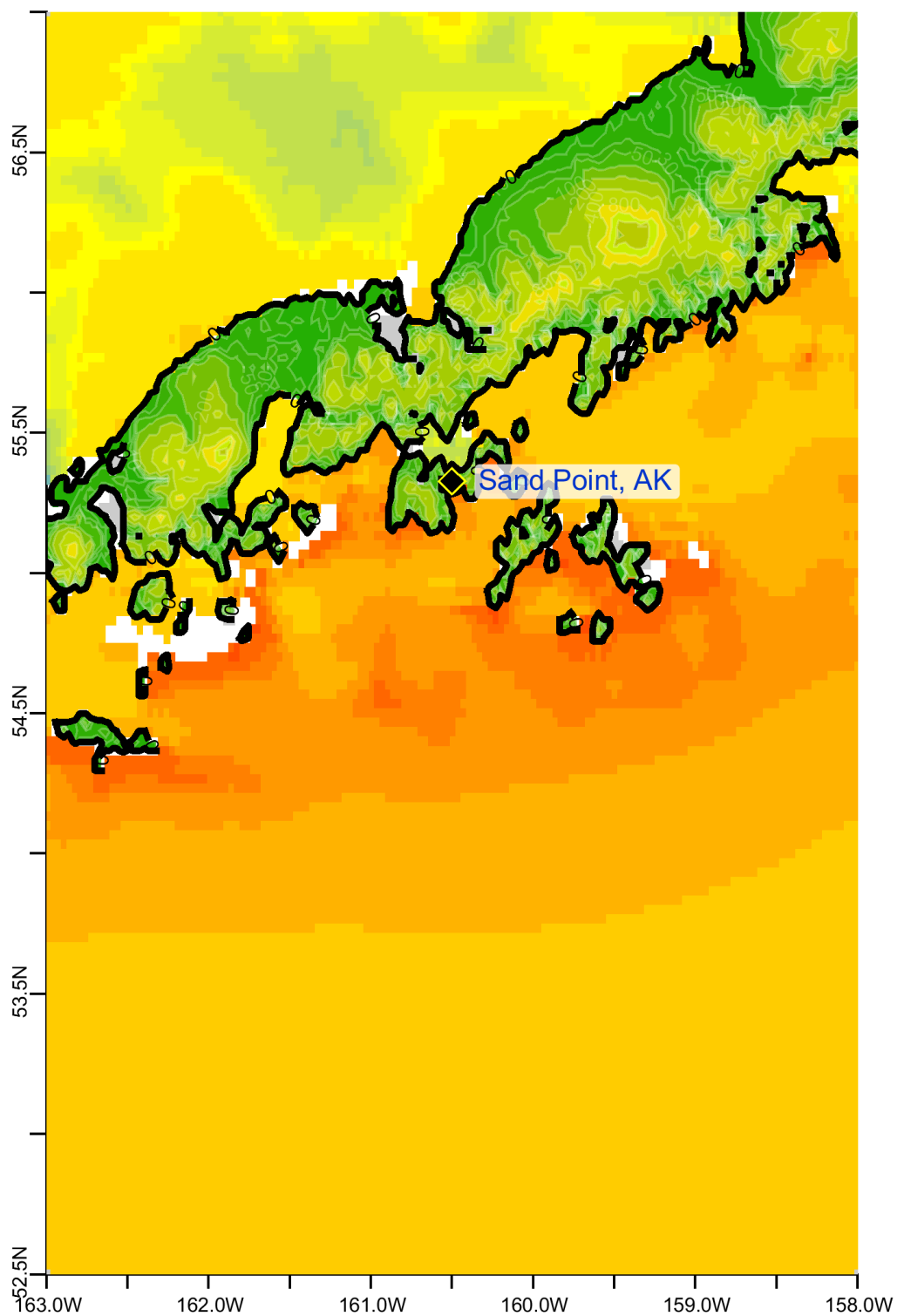


Figure 13. Max computed wave amplitude of A grid, Sand Point, Alaska, for synthetic event NTSZ 30-39.

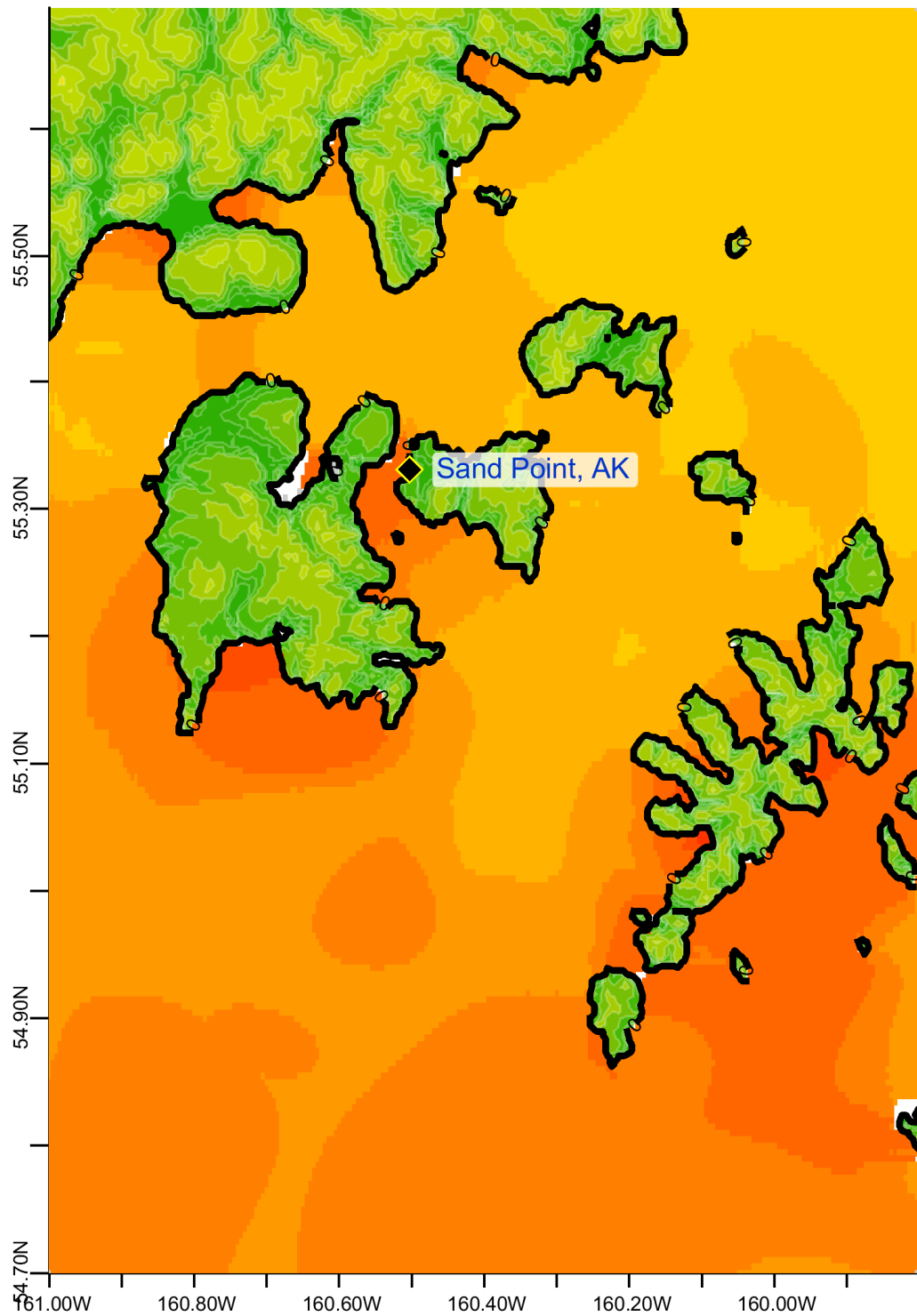


Figure 14. Max computed wave amplitude of B grid, Sand Point, Alaska, for synthetic event NTSZ 30-39.

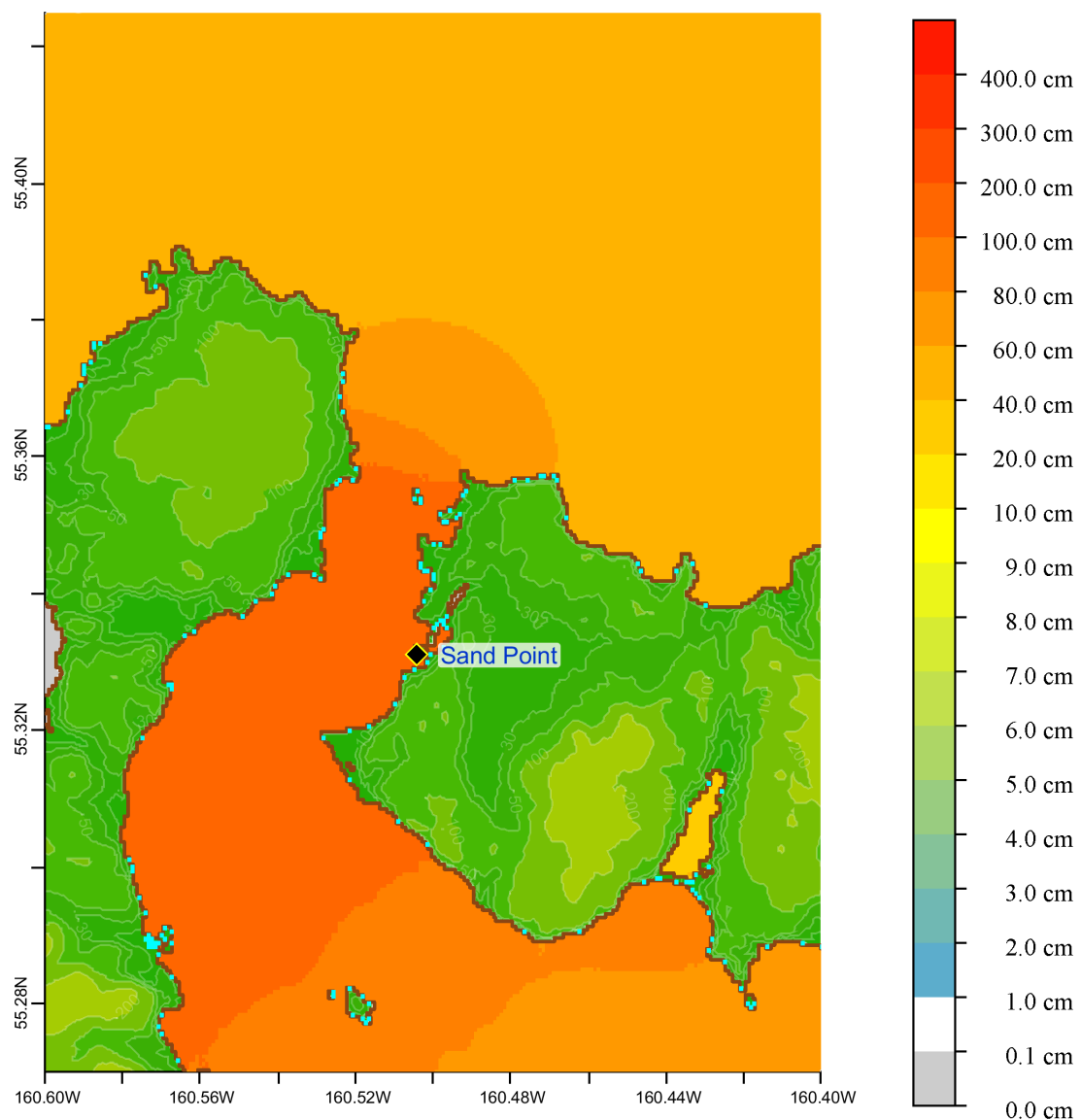


Figure 15. Max computed wave amplitude of C grid, Sand Point, Alaska, for synthetic event NTSZ 30-39.

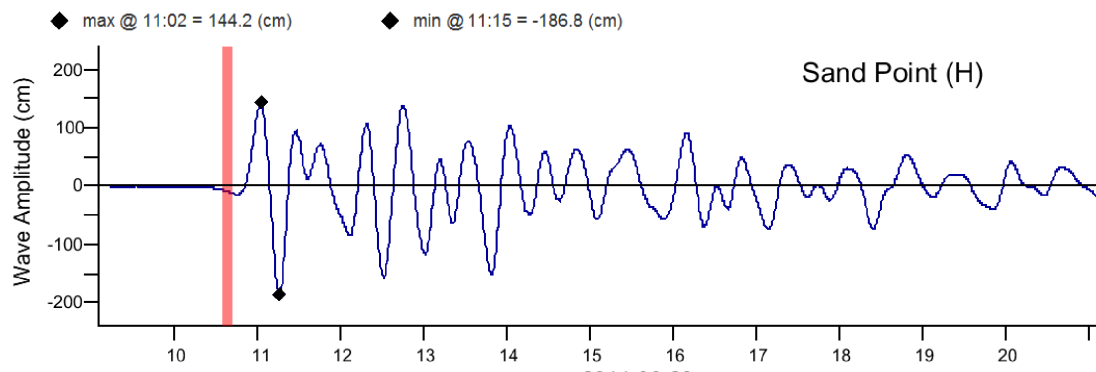


Figure 16. SIFT computed time series at Sand Point tide gage, for synthetic event NTSZ 30-39. The computed time series at the time of model development for the same event is shown in Figure 29.

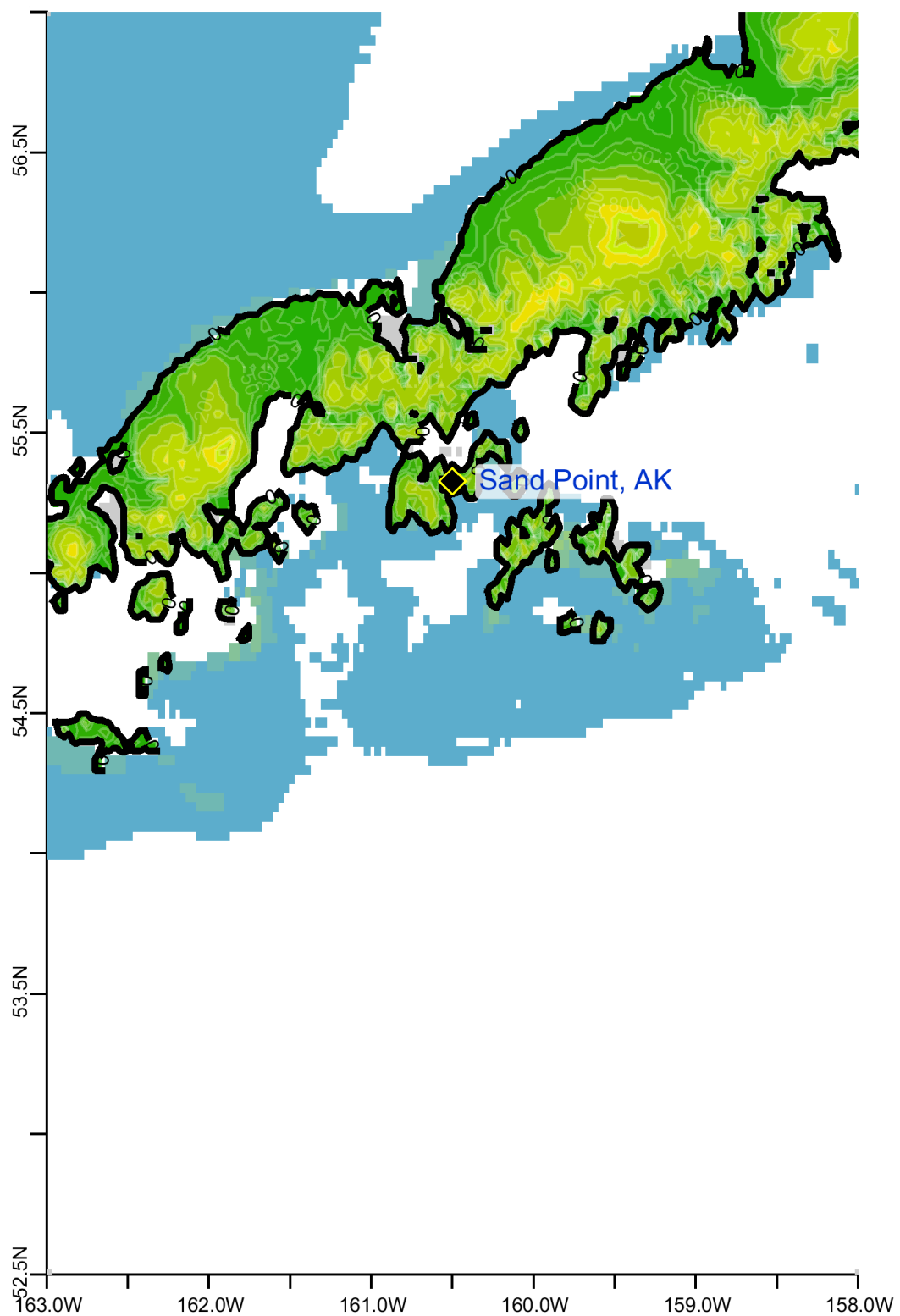


Figure 17. Max computed wave amplitude of A grid, Sand Point Alaska, for 15 November 2006 Kuril tsunami.

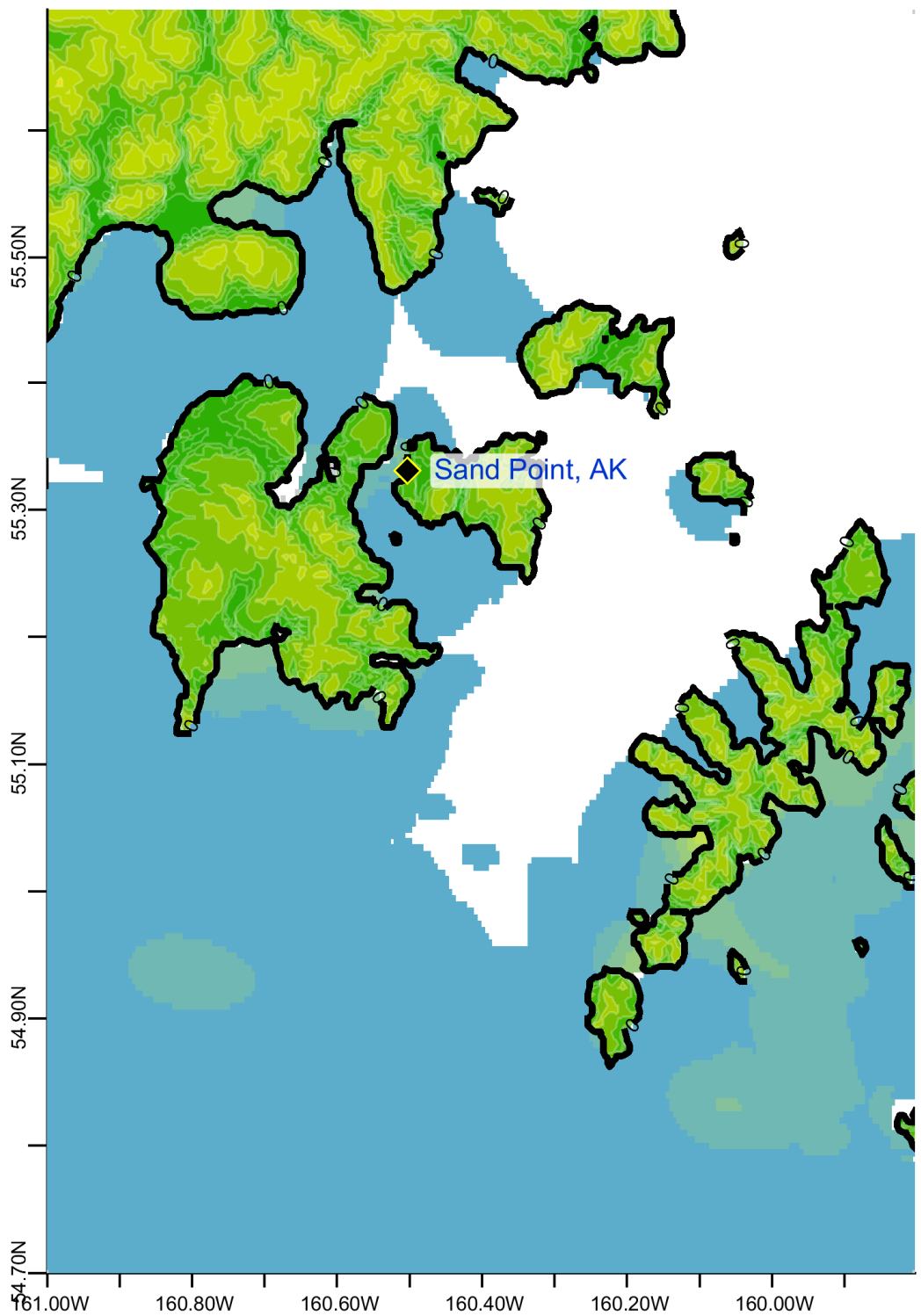


Figure 18. Max computed wave amplitude of B grid, Sand Point Alaska, for 15 November 2006 Kuril tsunami.

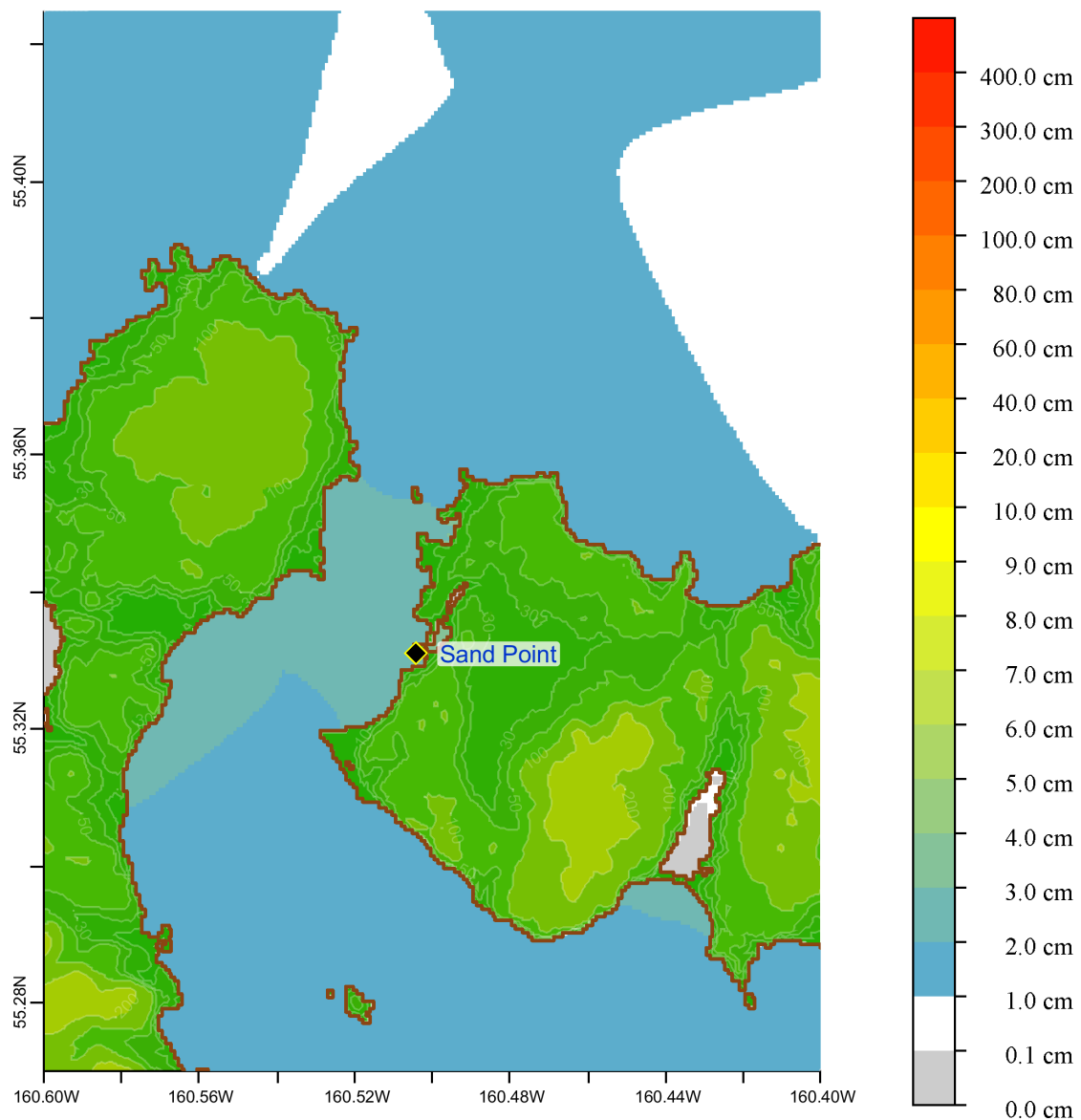


Figure 19. Max computed wave amplitude of C grid, Sand Point Alaska, for 15 November 2006 Kuril tsunami.

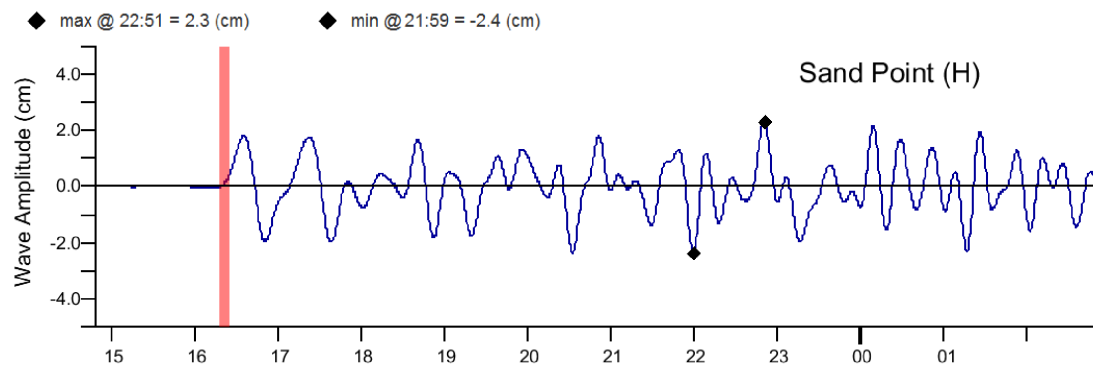


Figure 16. SIFT computed time series at Sand Point tide gage, for 15 November 2006 Kuril tsunami. The computed time series at the time of model development for the same event is shown in Figure 17.

Figure 1a

Alaska Peninsula



Image © 2007 DigitalGlobe
Image © 2007 TerraMetrics

Google™

Unga Island

Figure 1b

Popof
Strait

NOS
Tide Station

City of Sand Point

Humbolt Hr.

Popof Island

Image © 2007 DigitalGlobe

©2006 Google™



Pointer lat 55.328374° lon -160.508789°

Streaming ||||| 100%

Eye alt 4.79 km

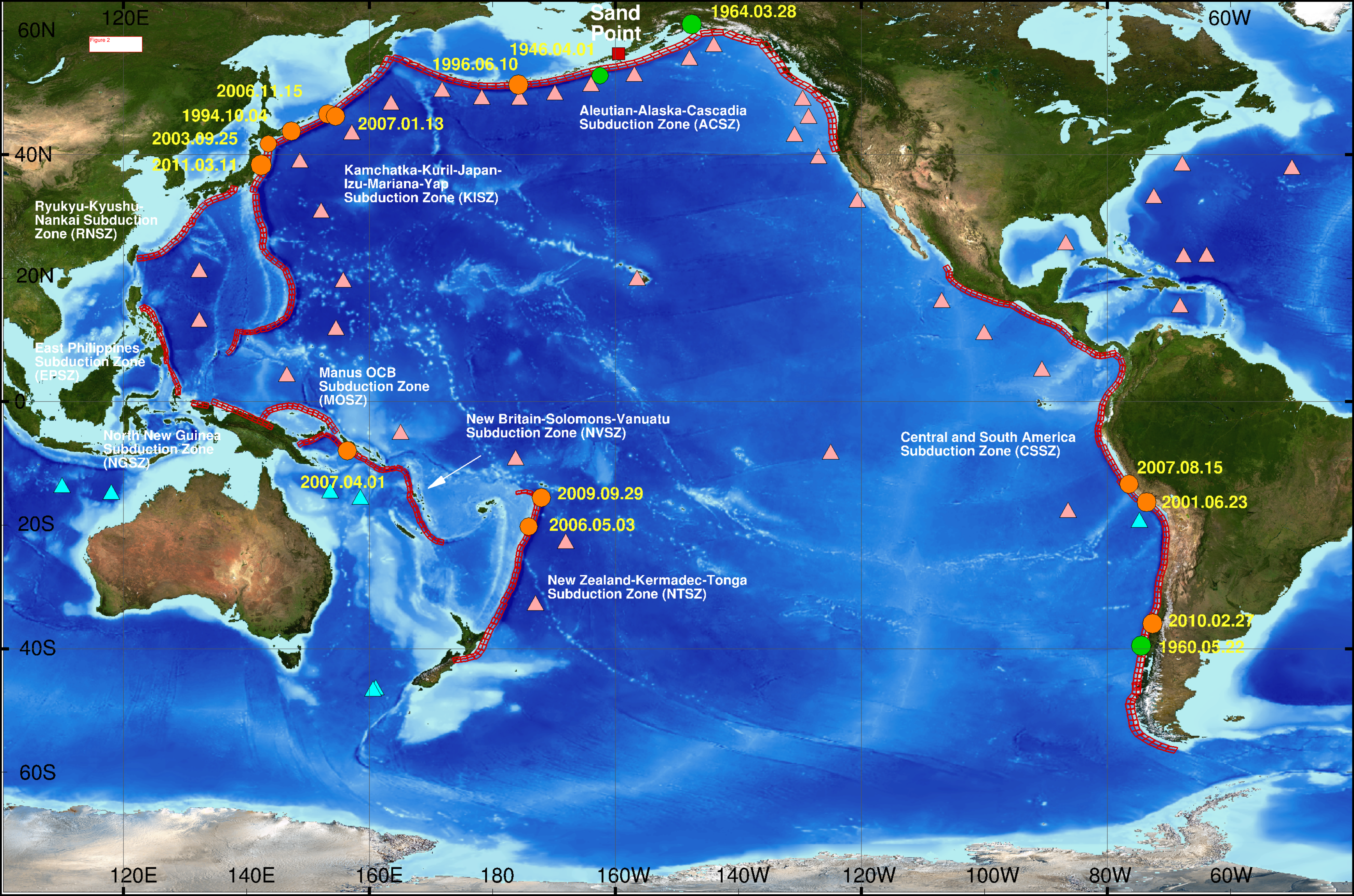
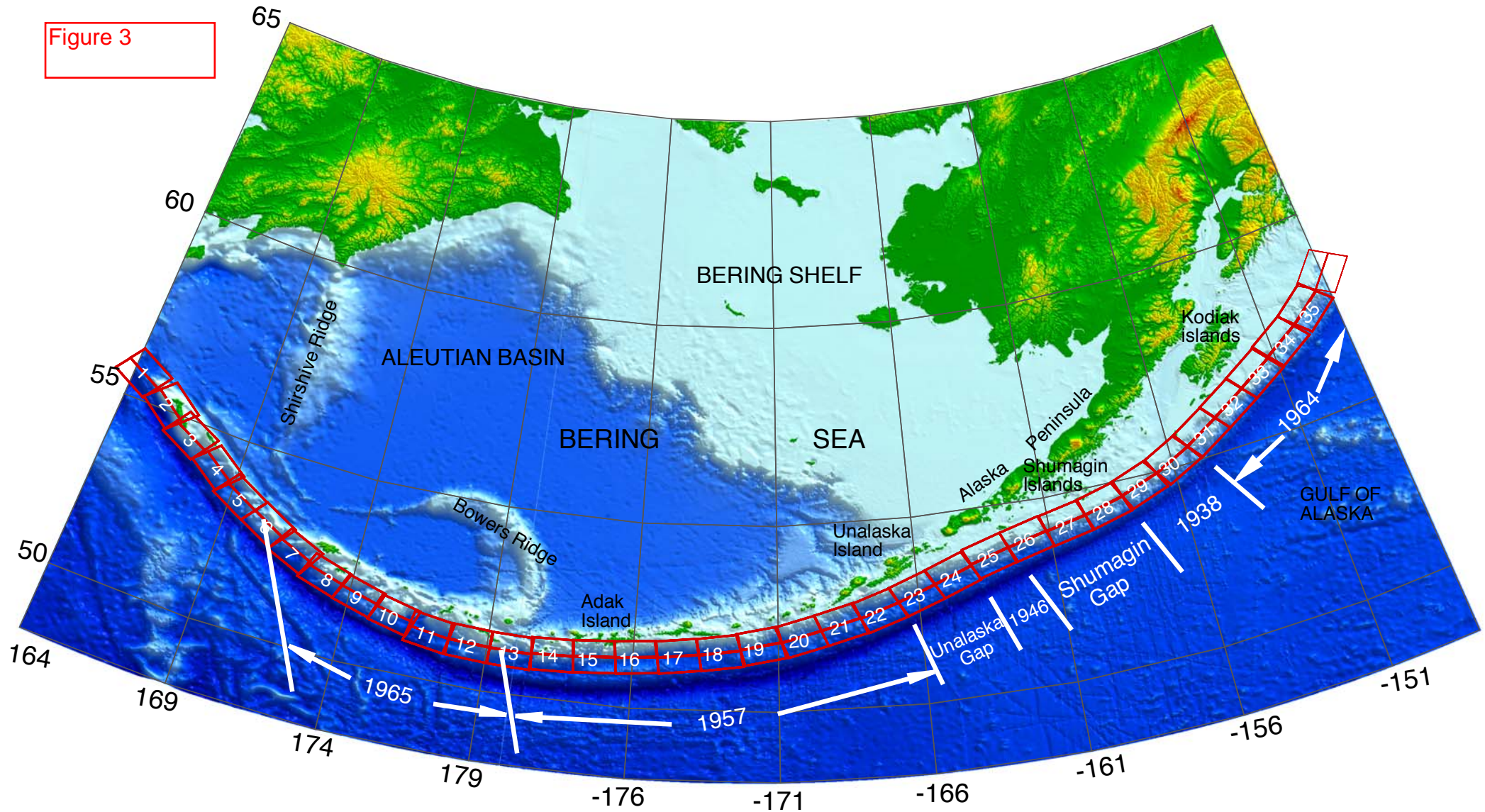


Figure 3



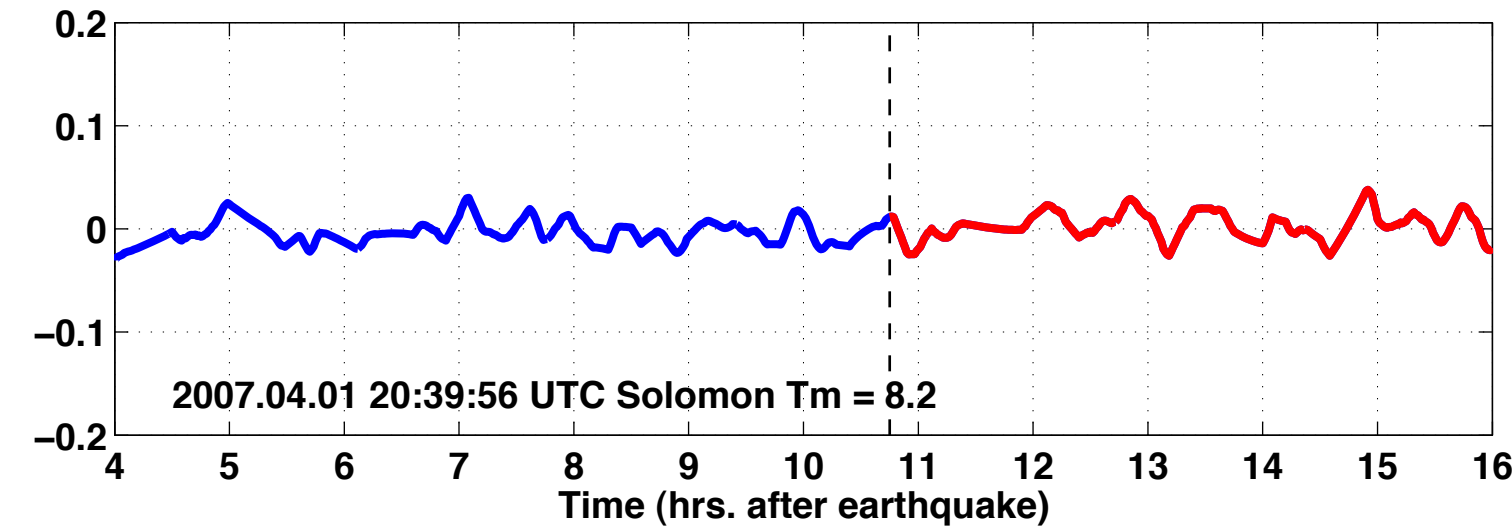
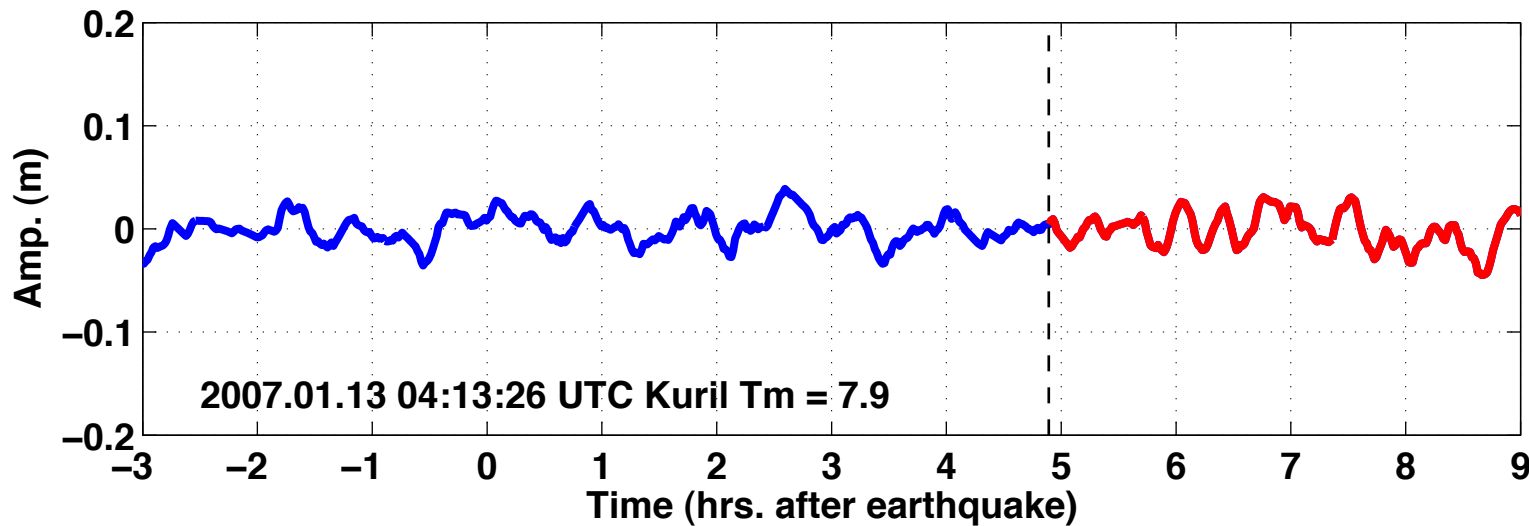
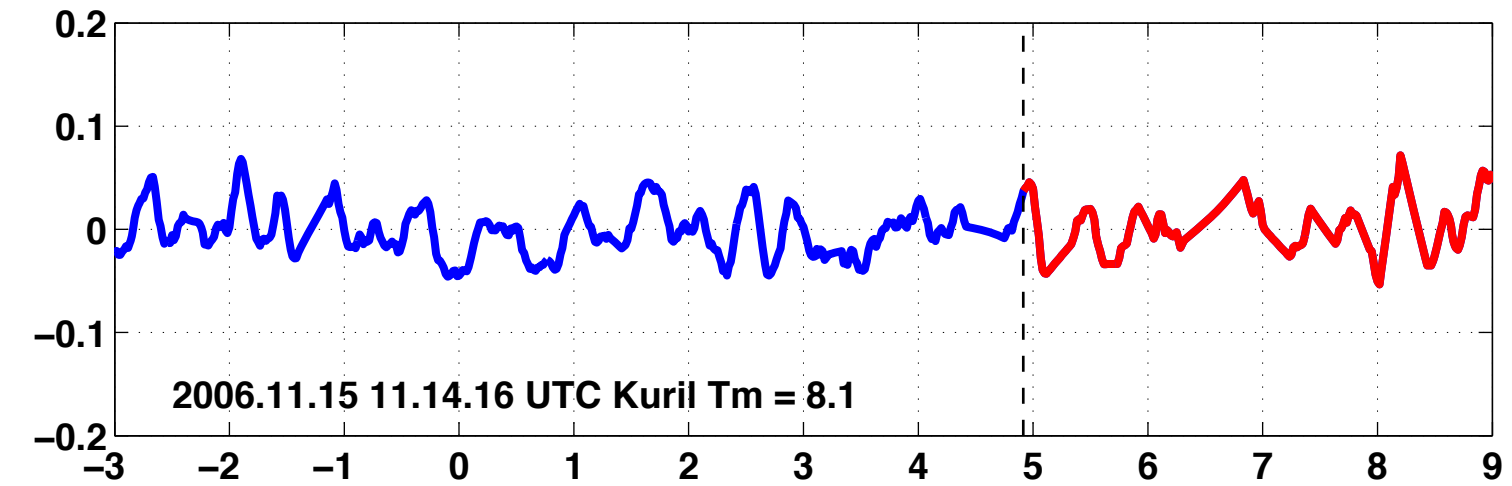
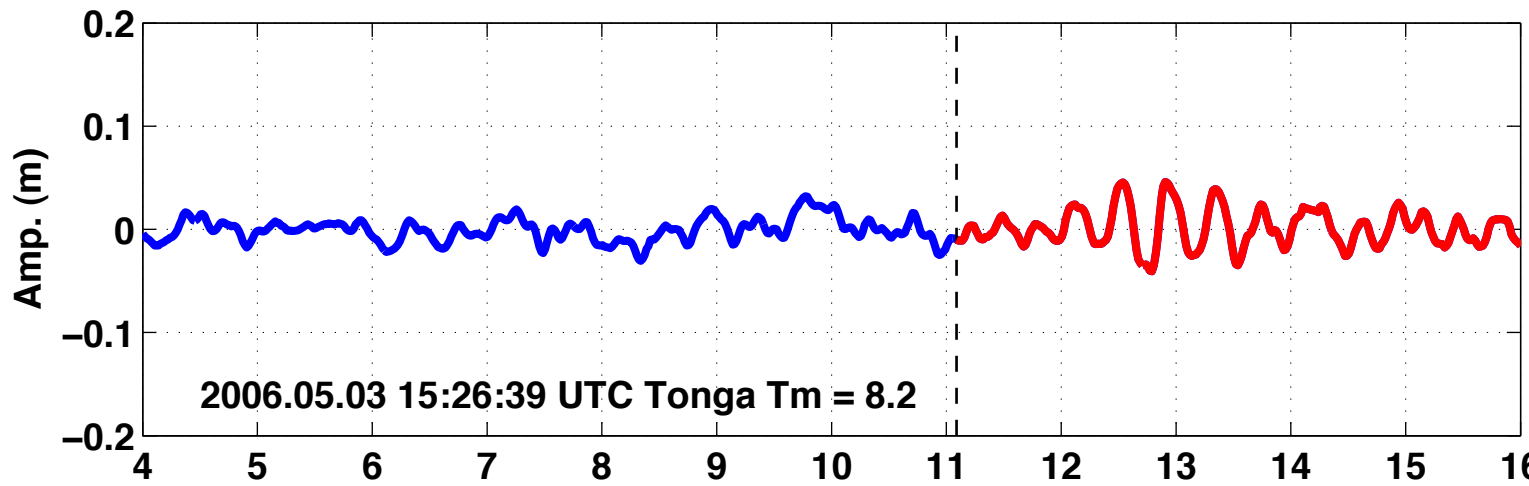
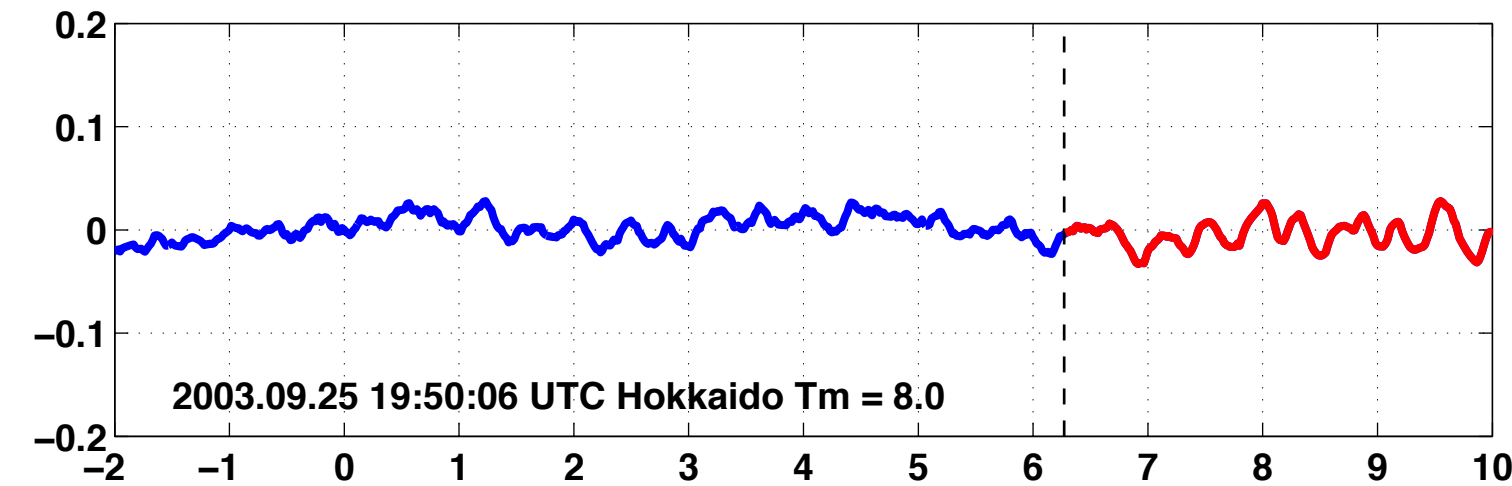
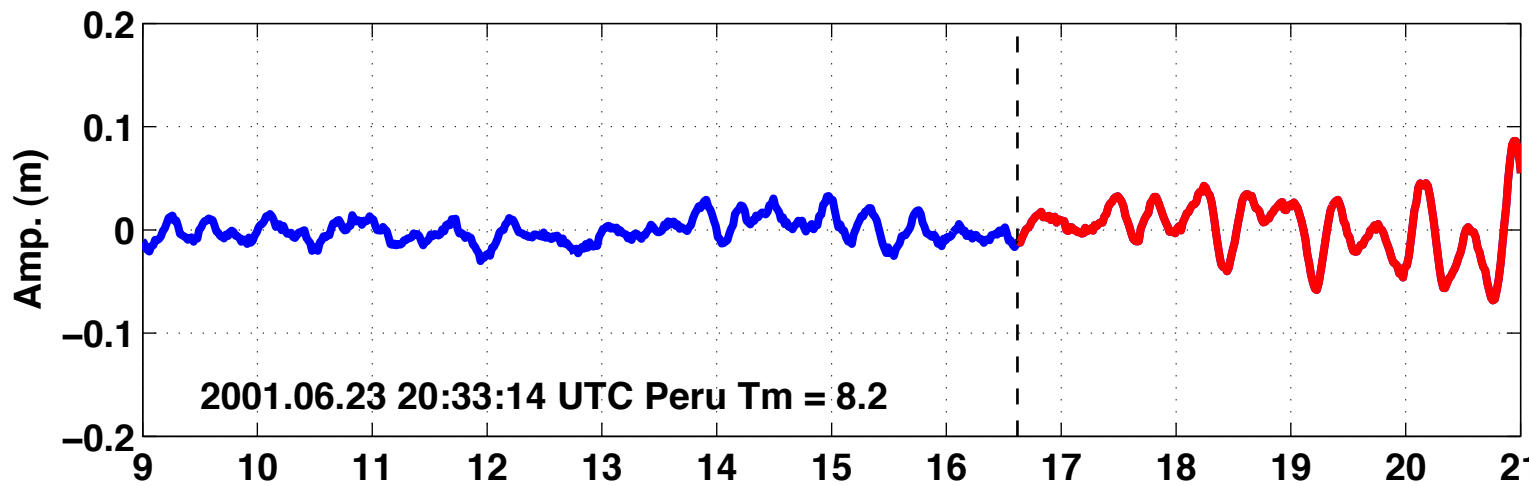
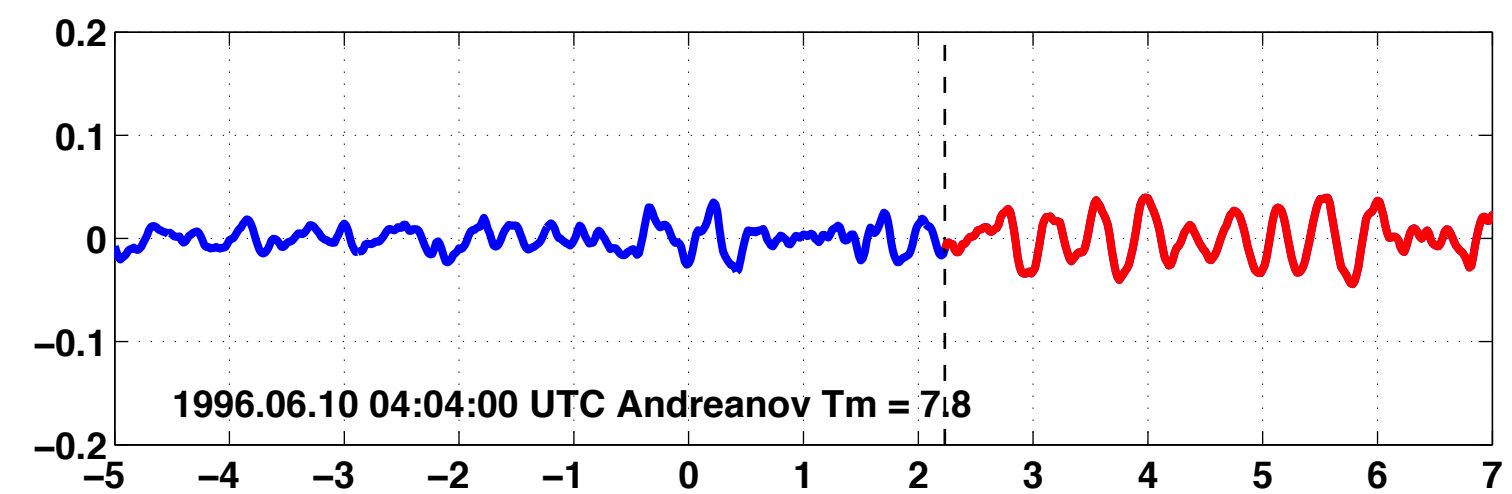
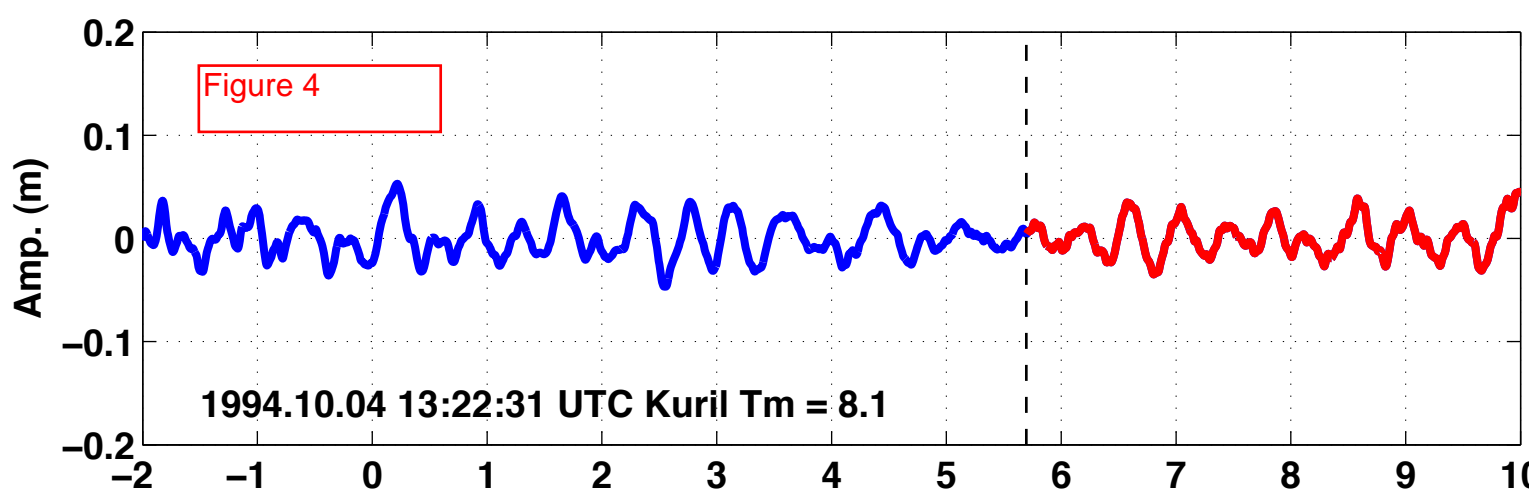
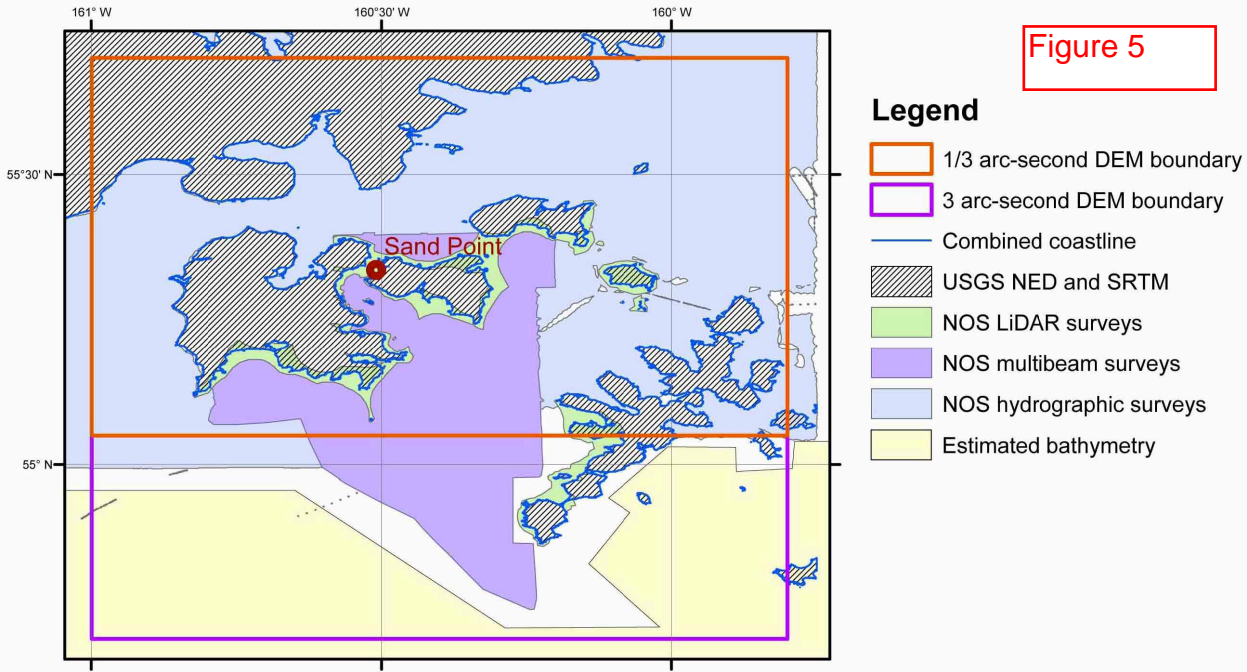
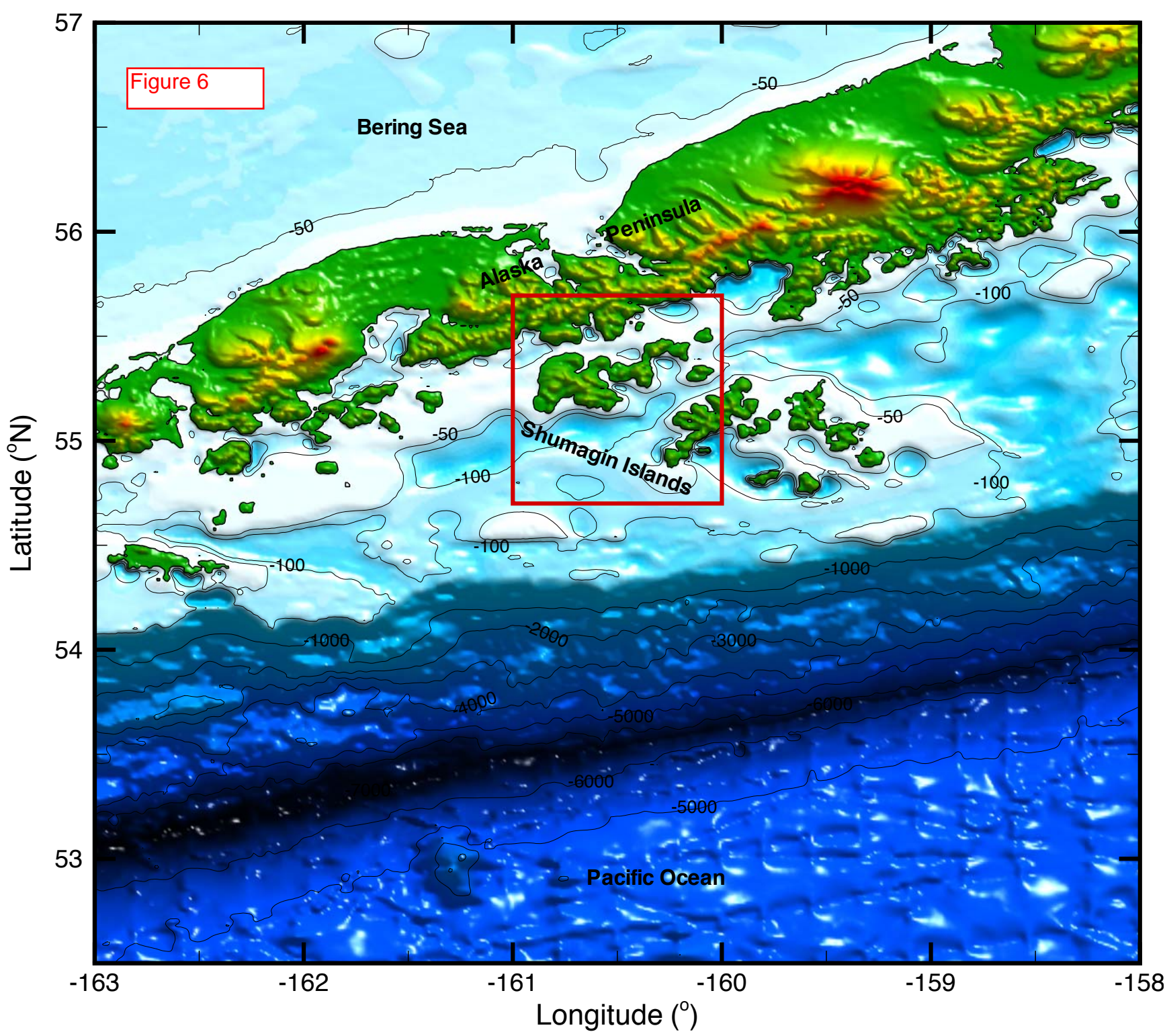
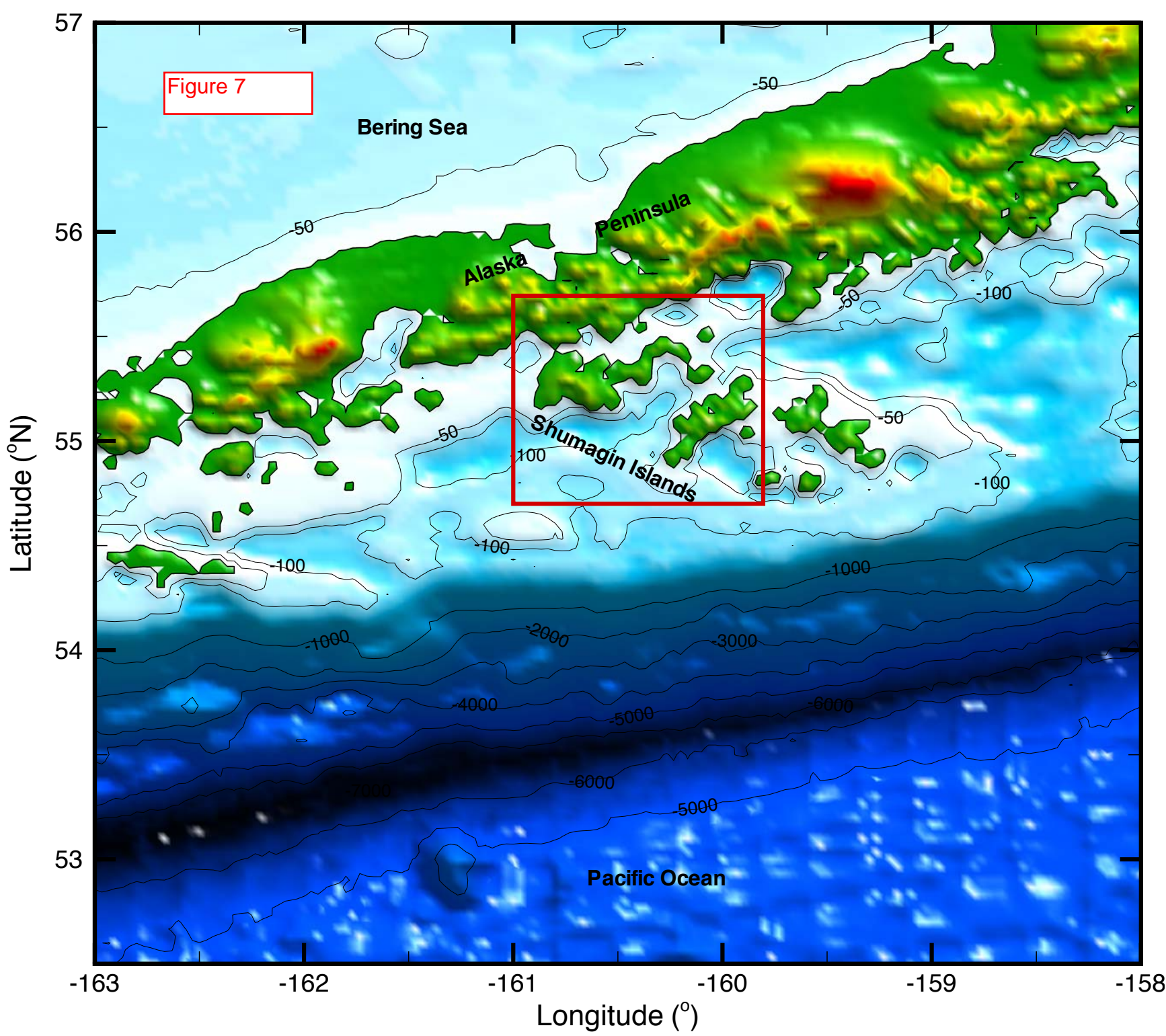


Figure 5







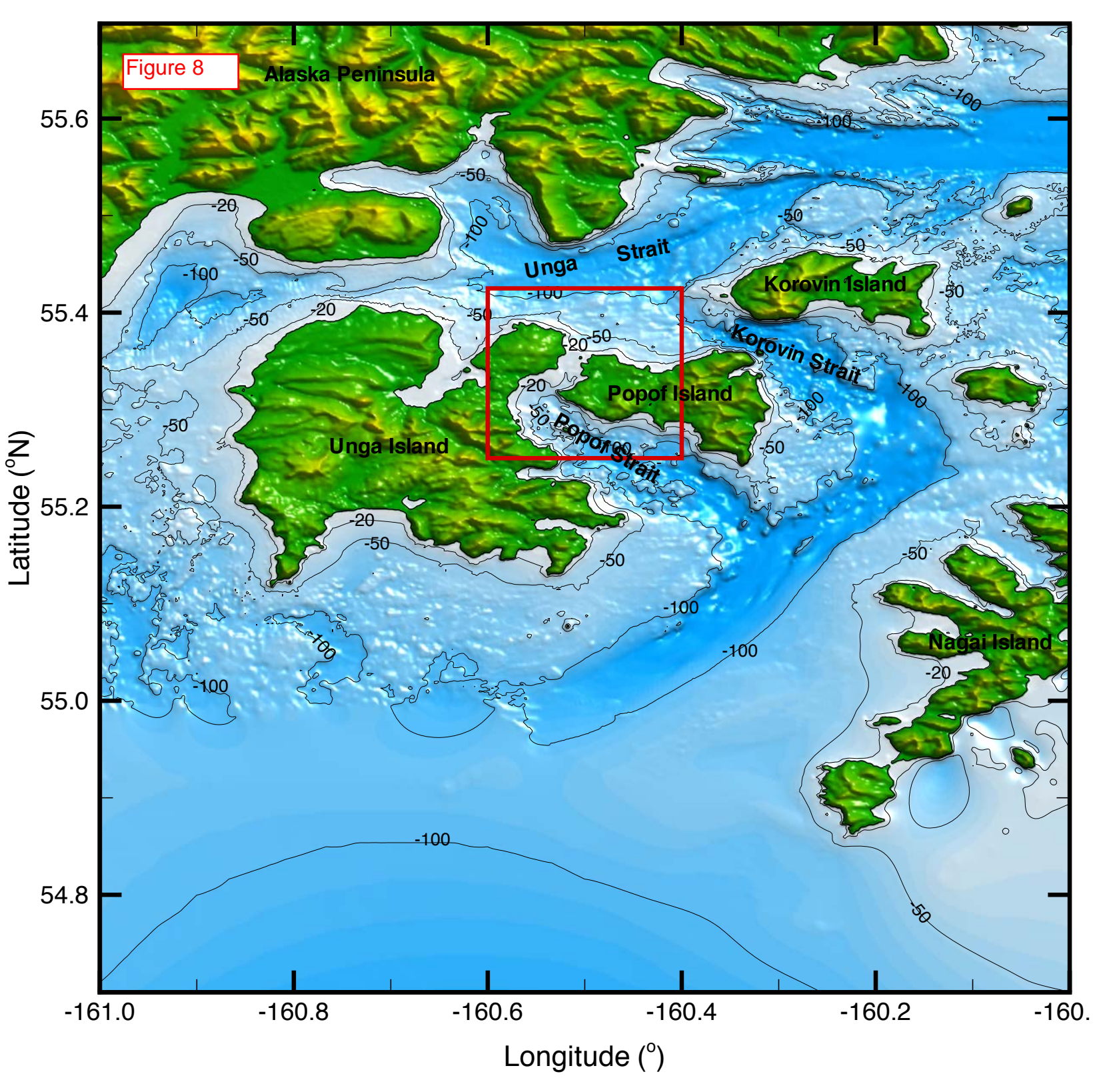


Figure 9

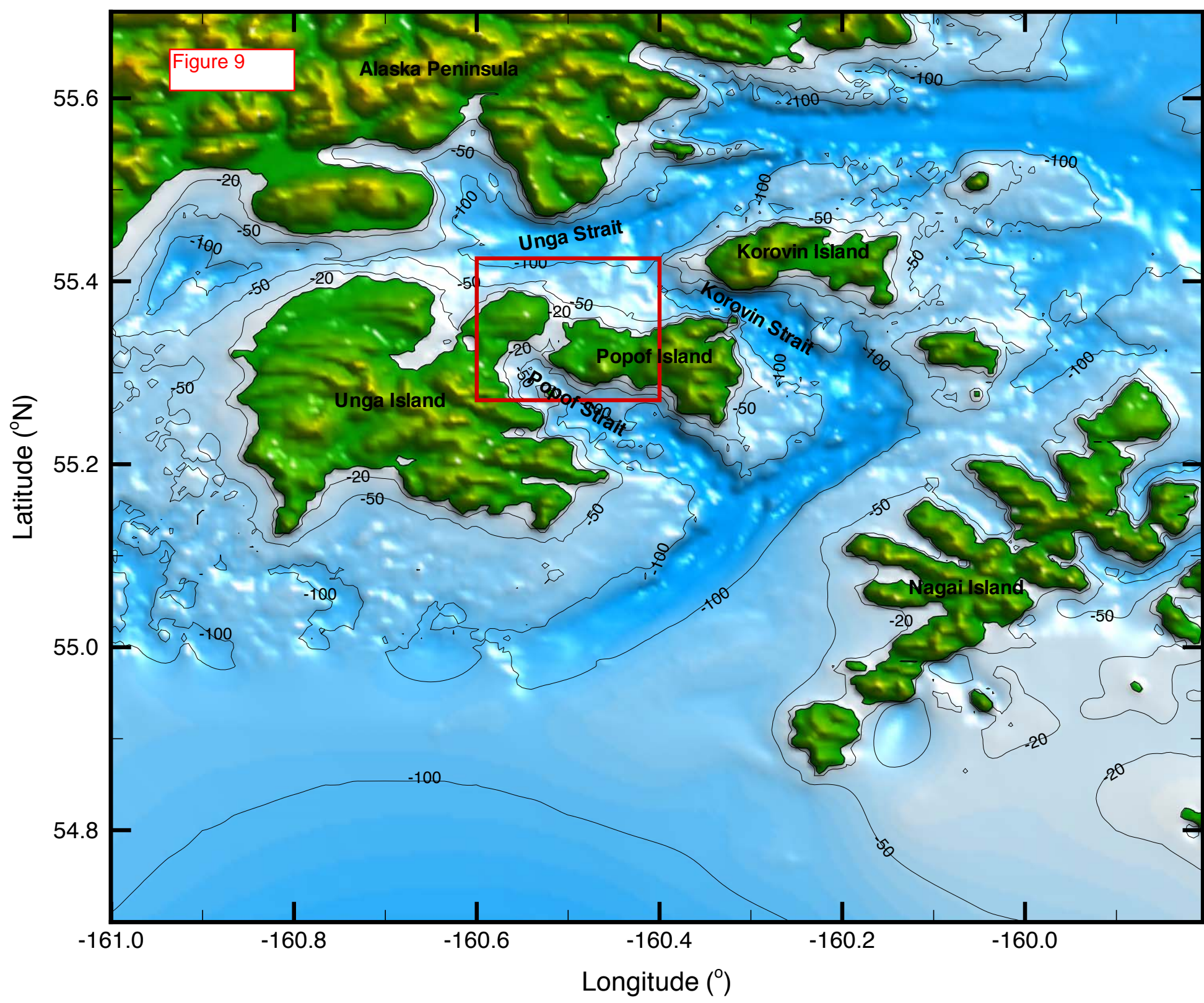
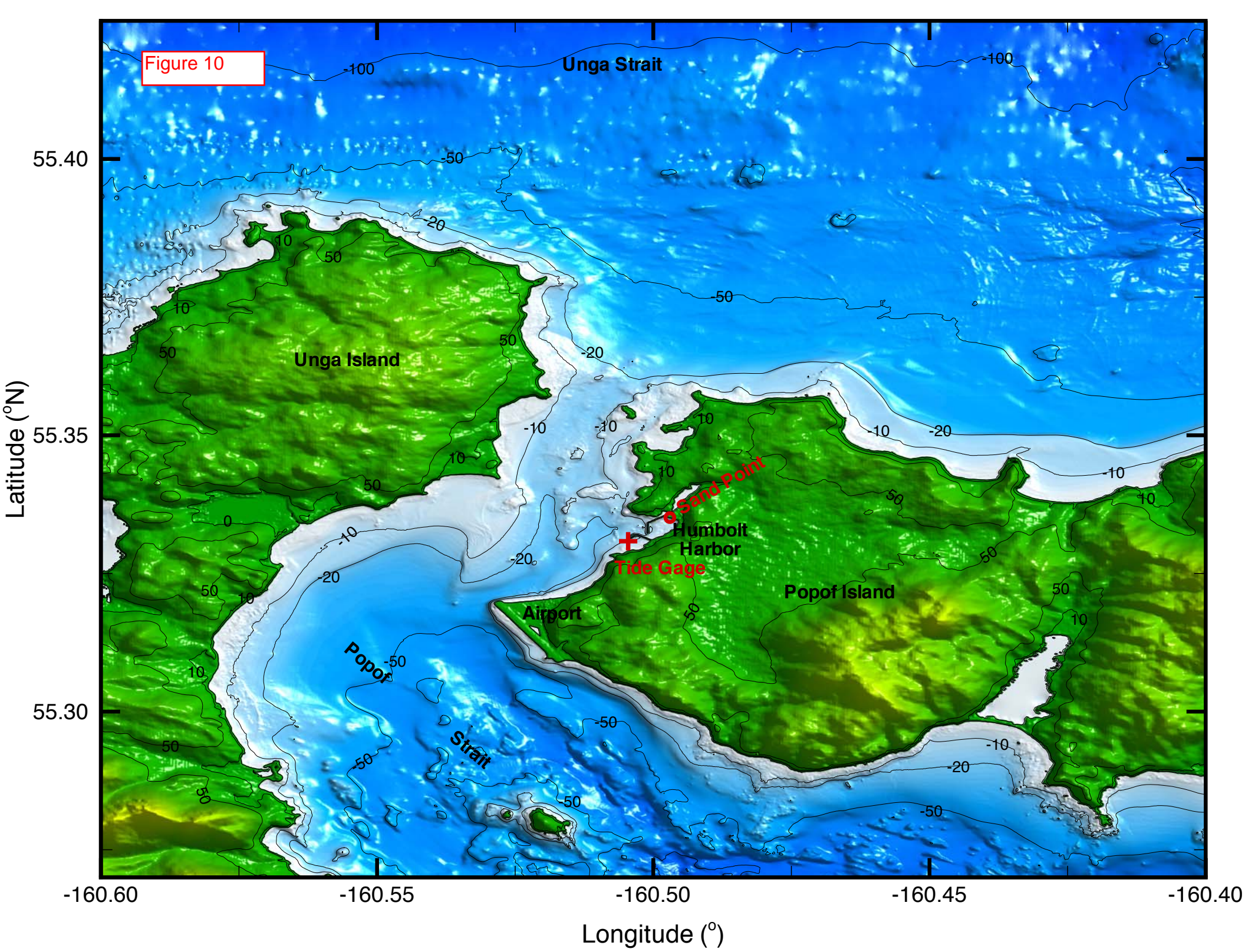
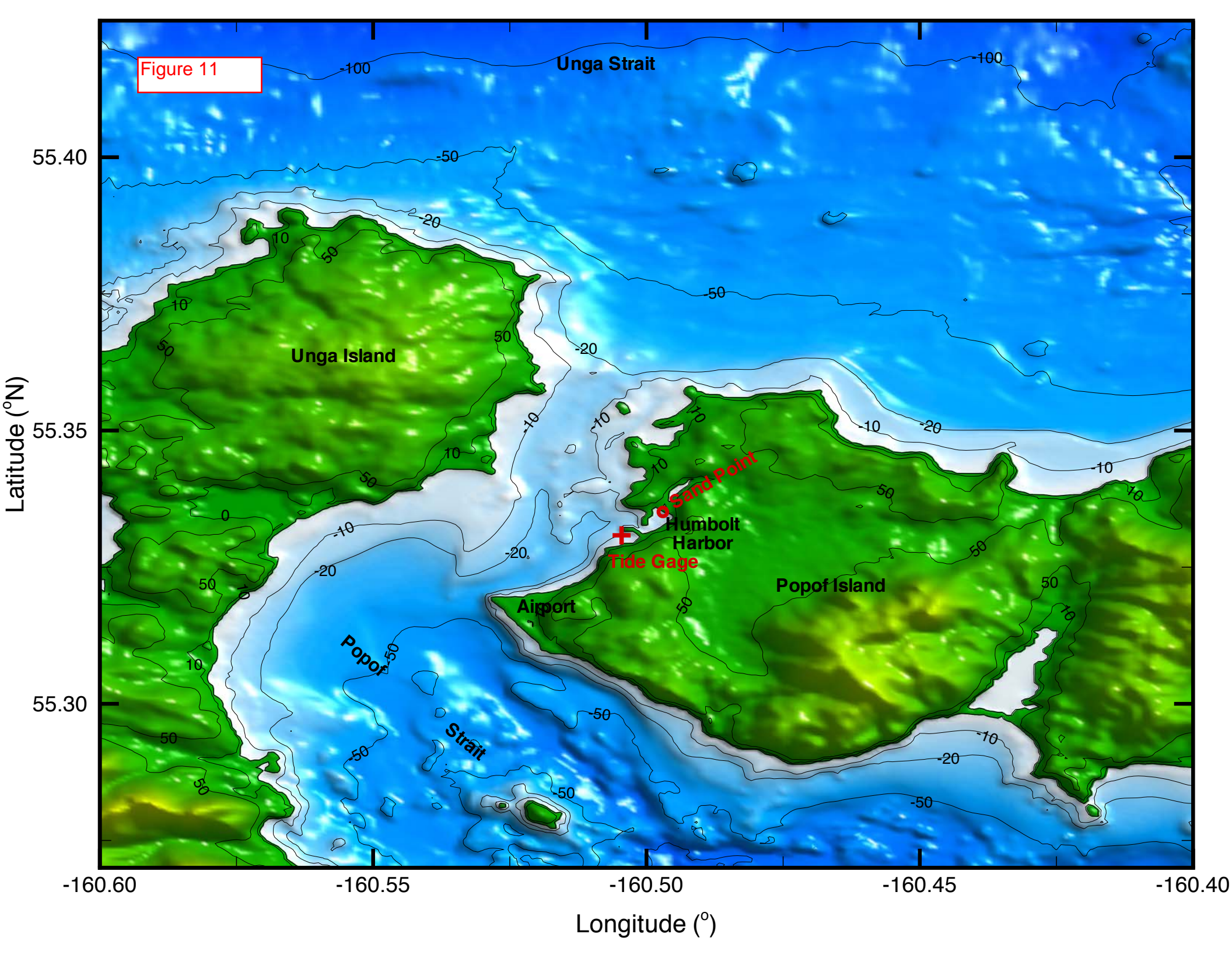
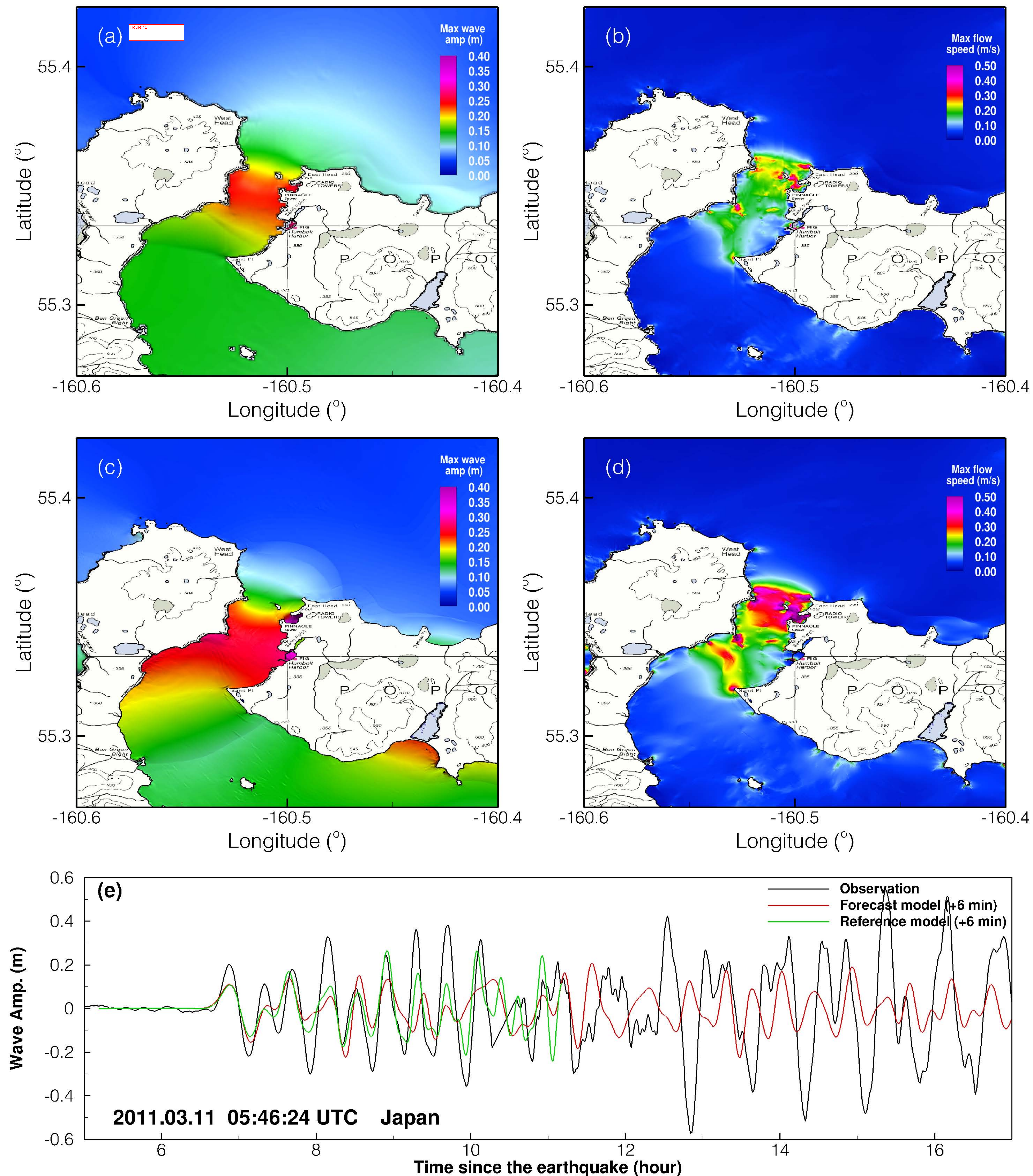
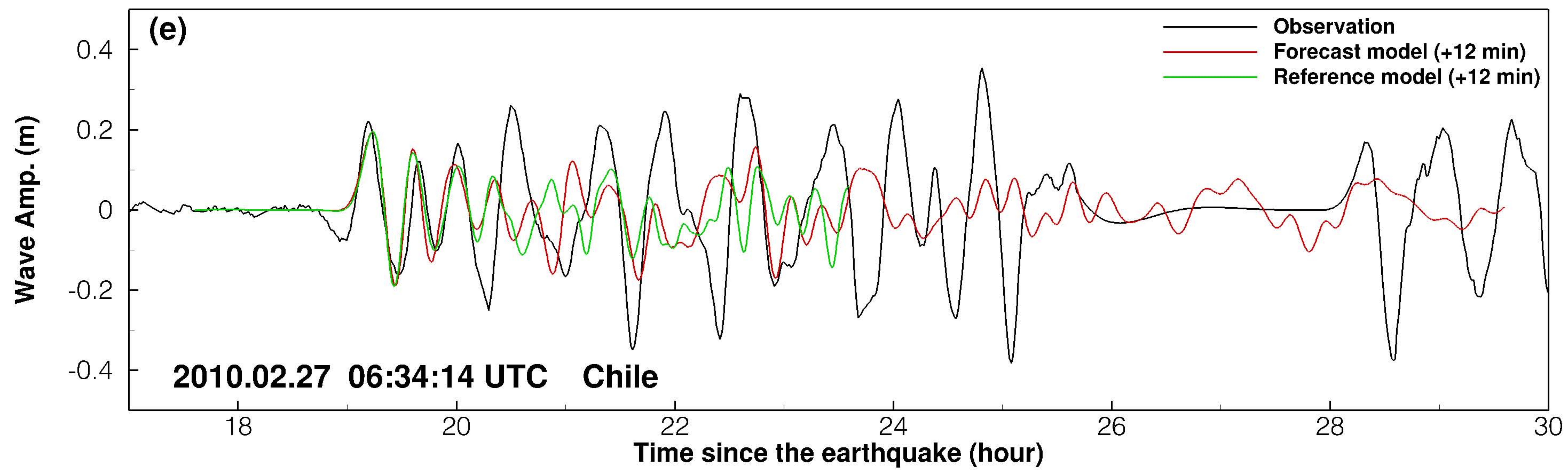
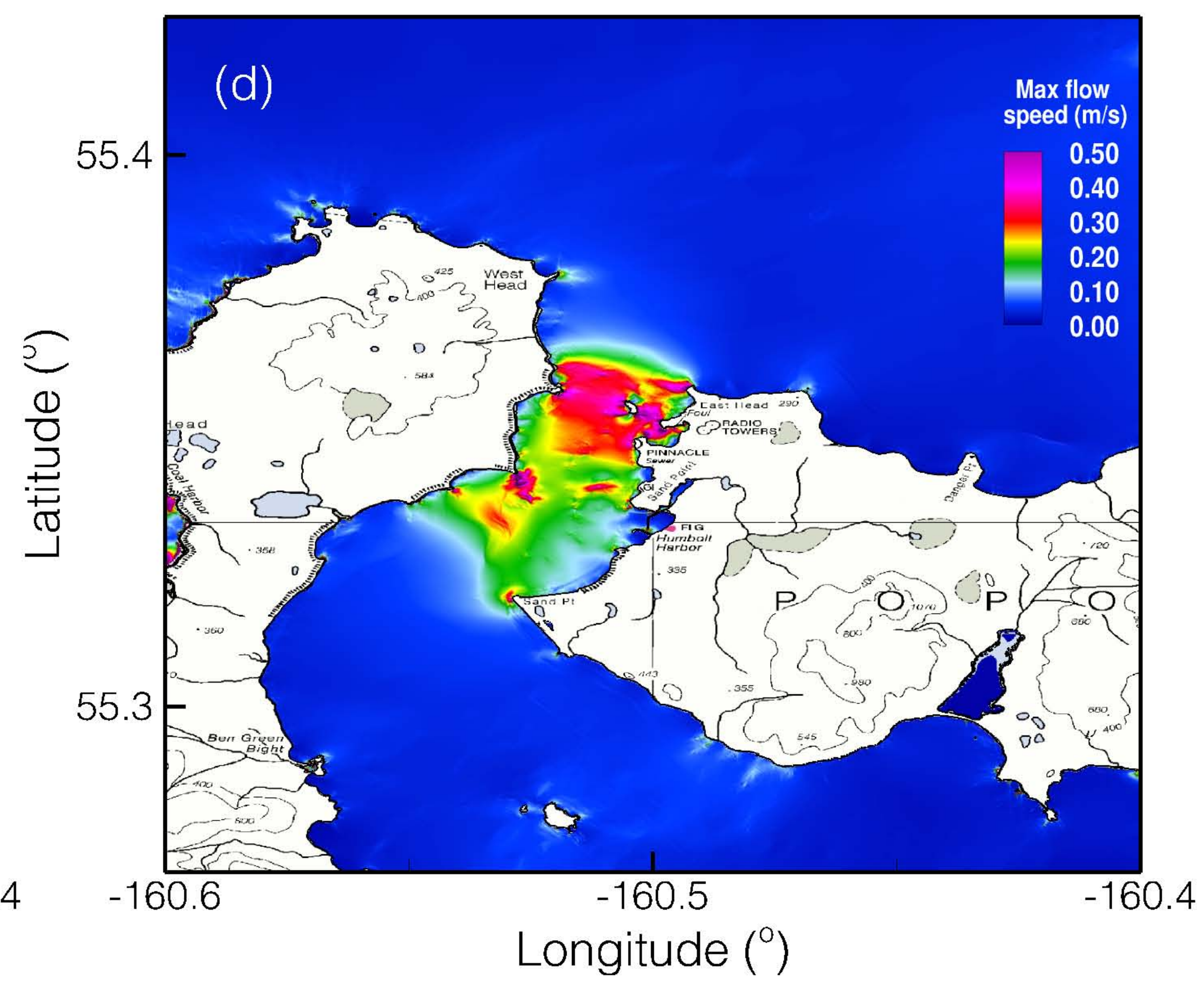
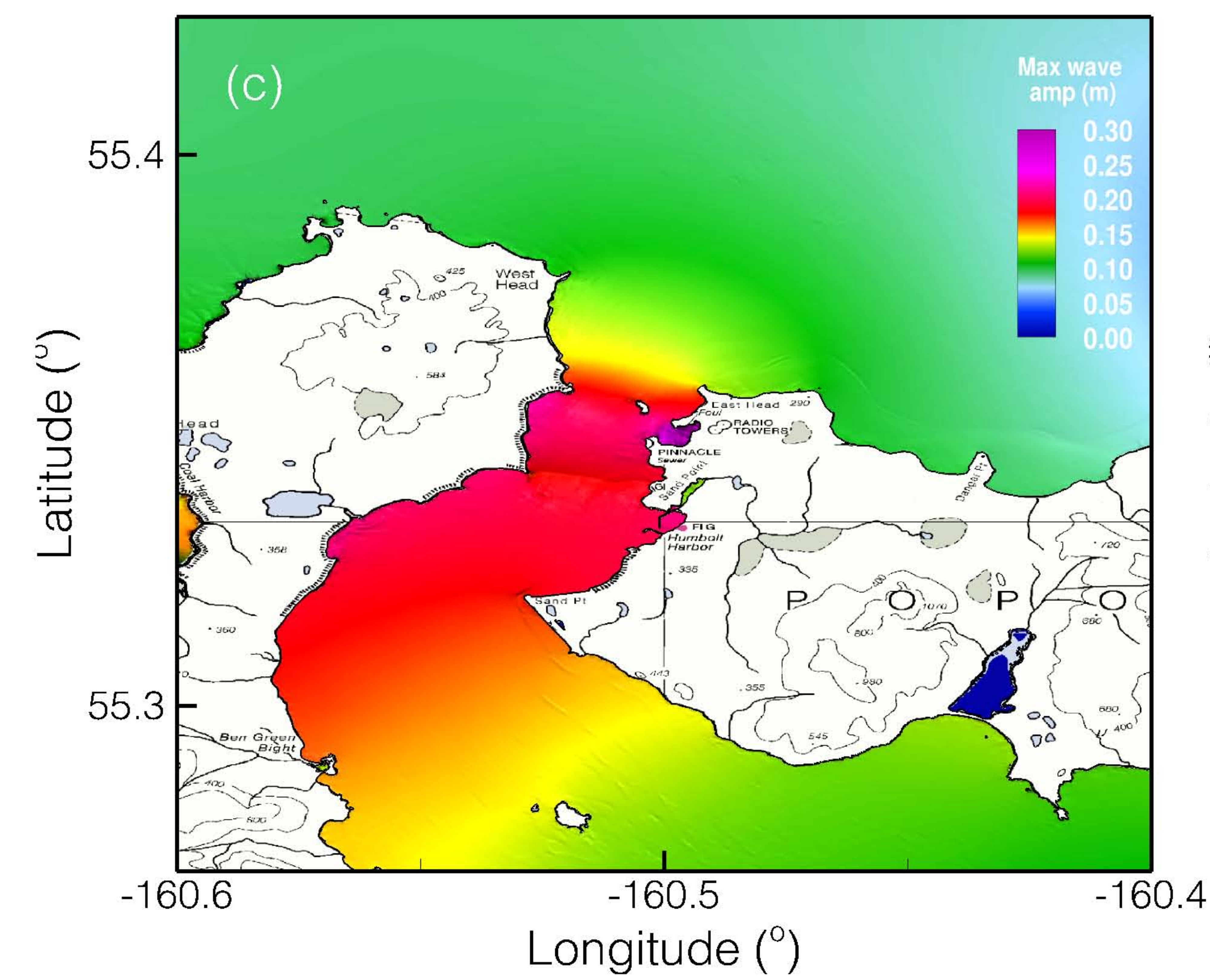
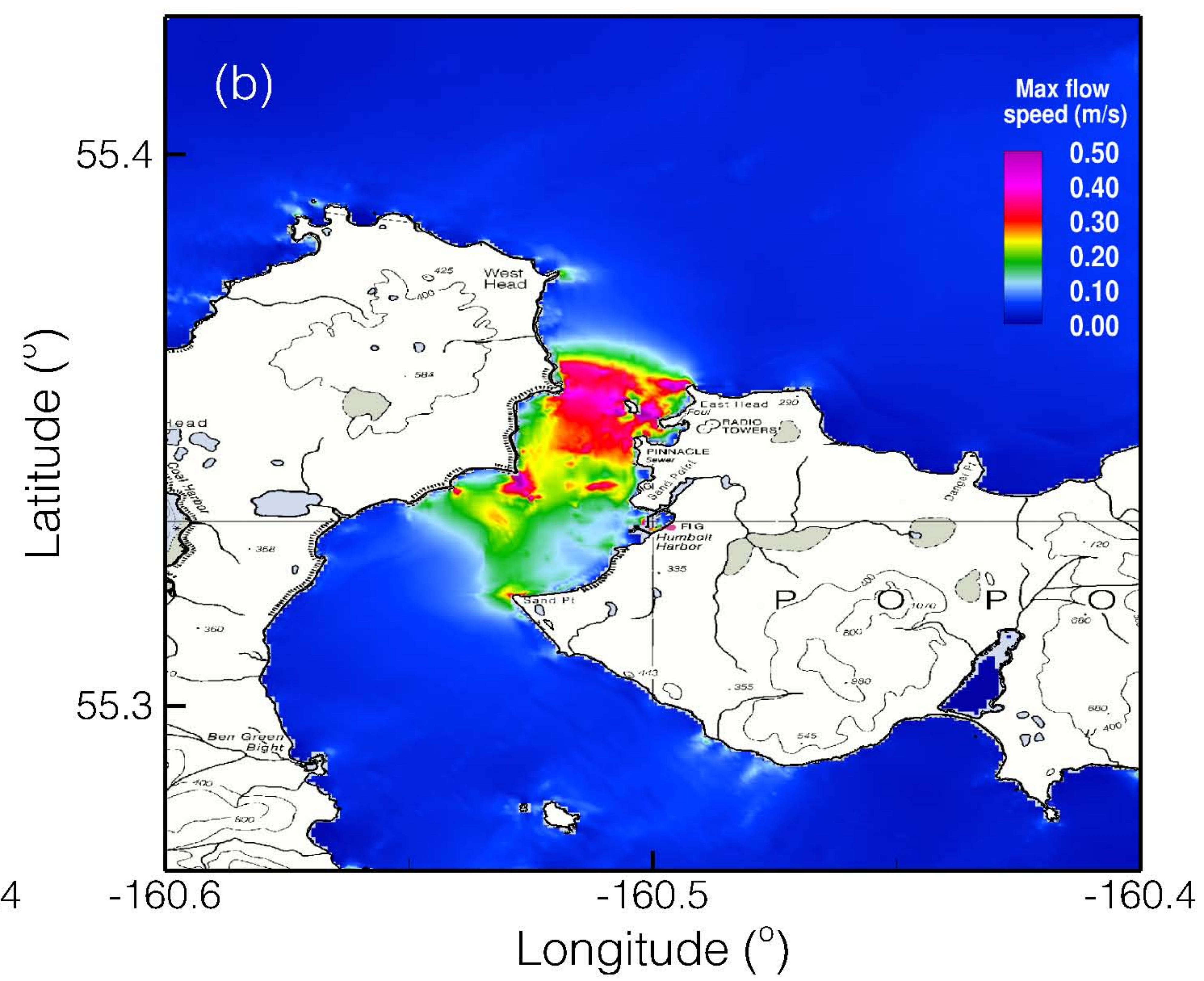
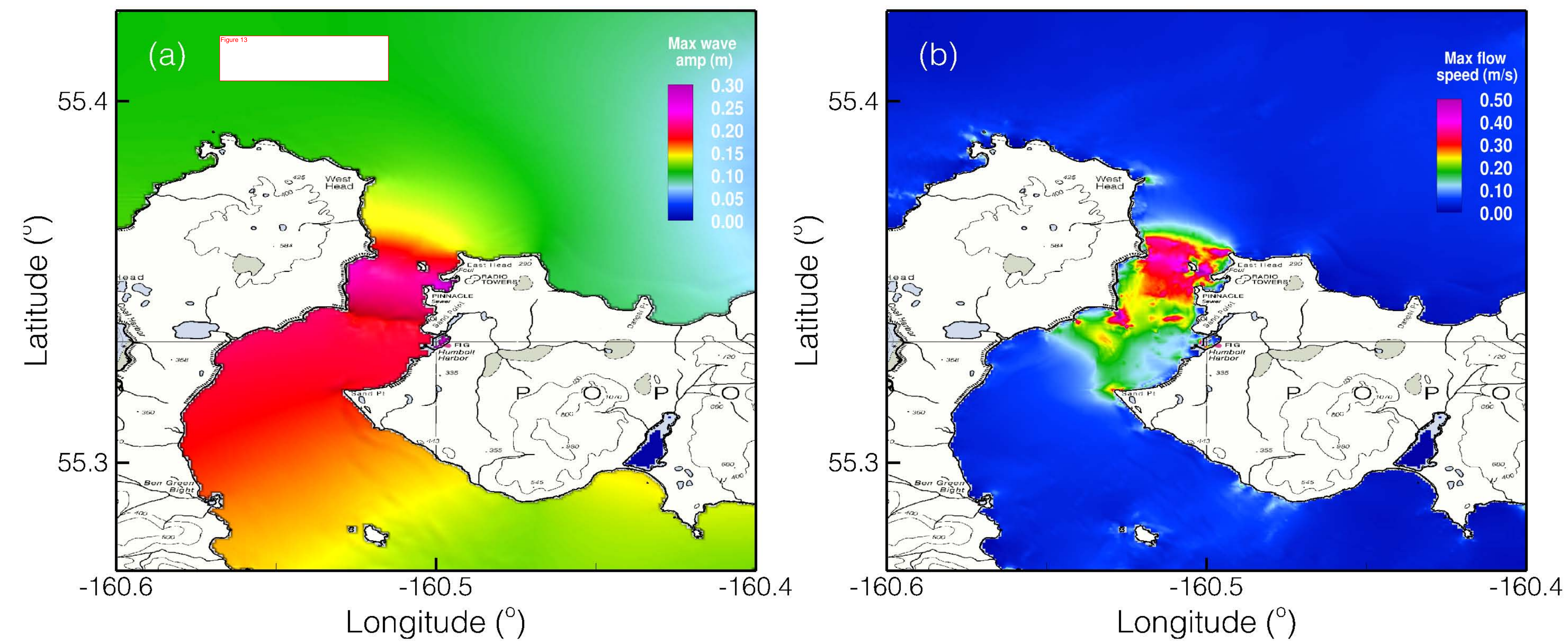


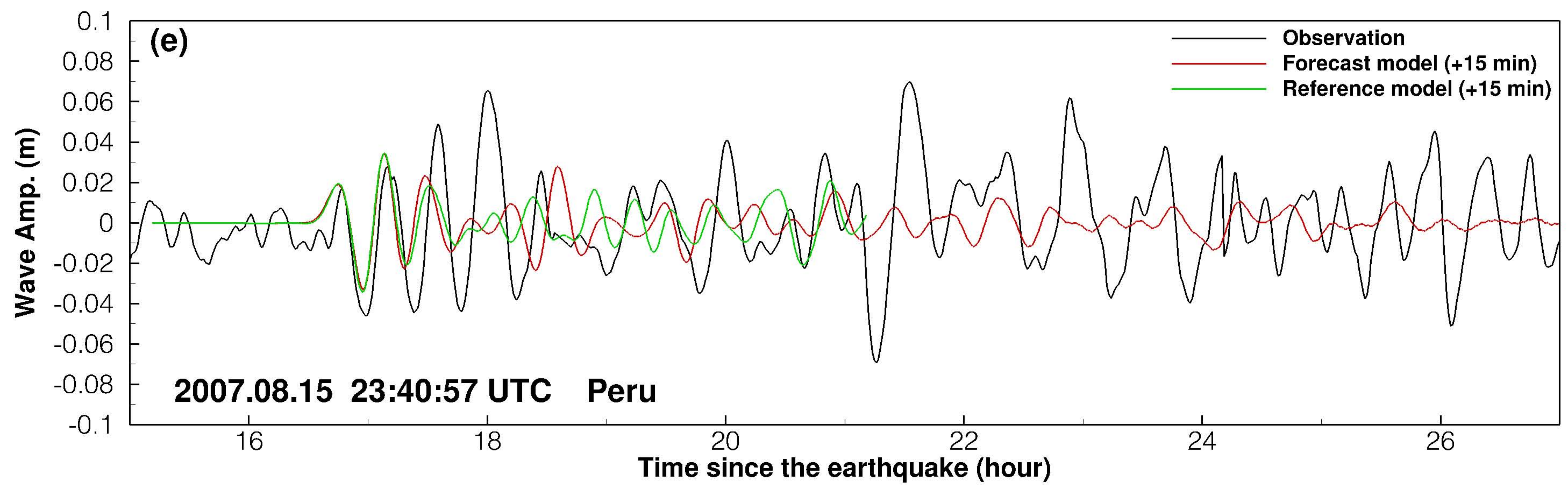
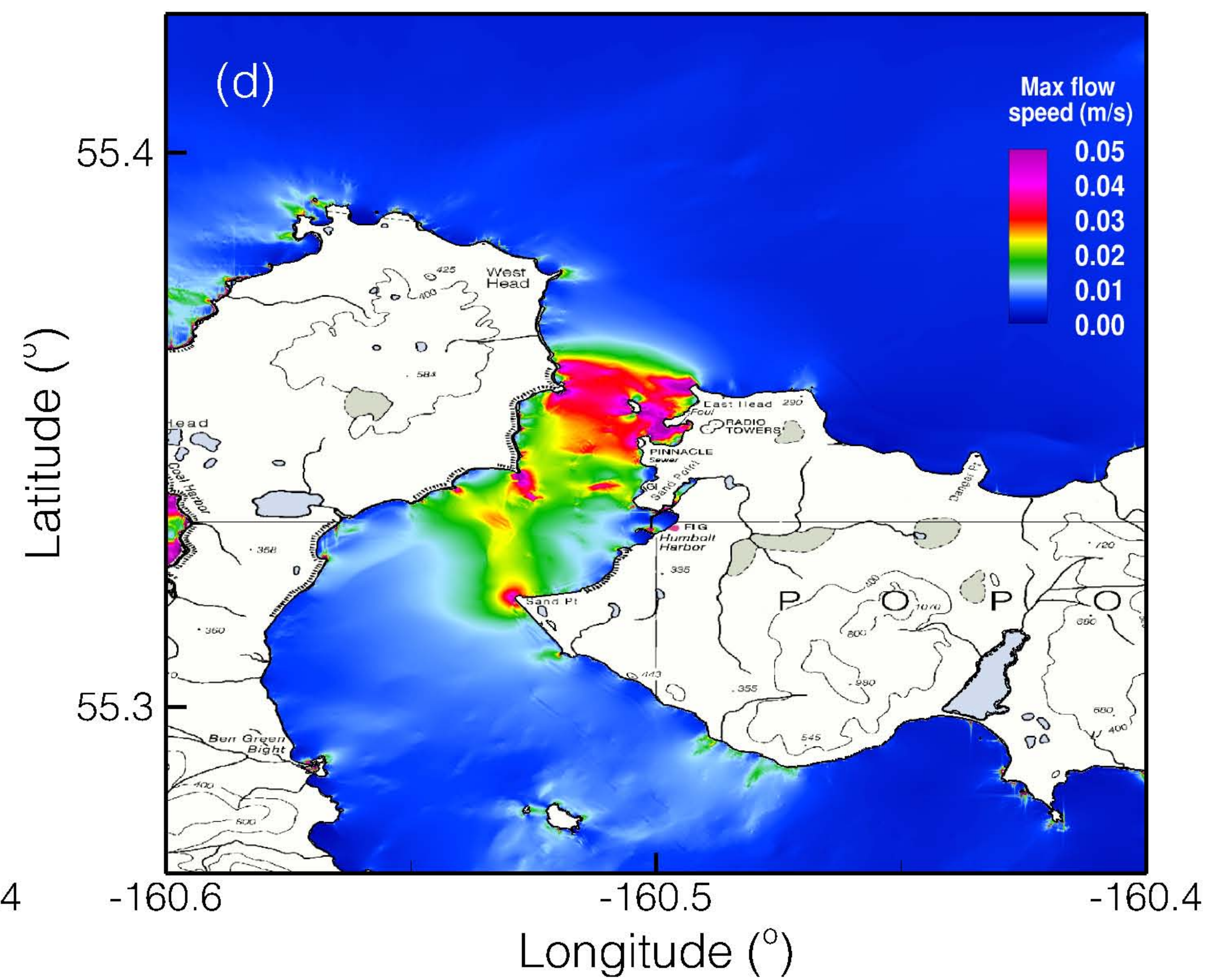
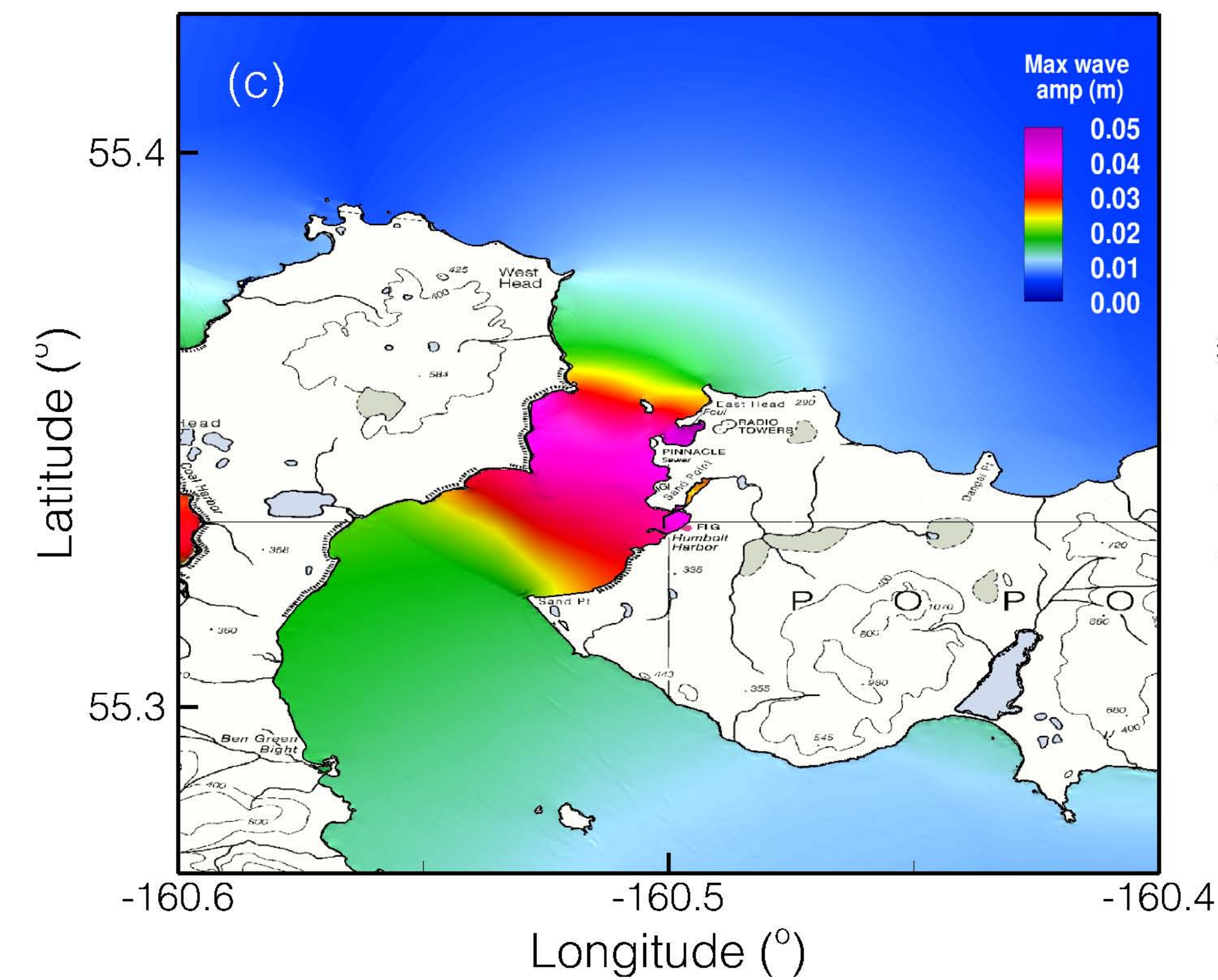
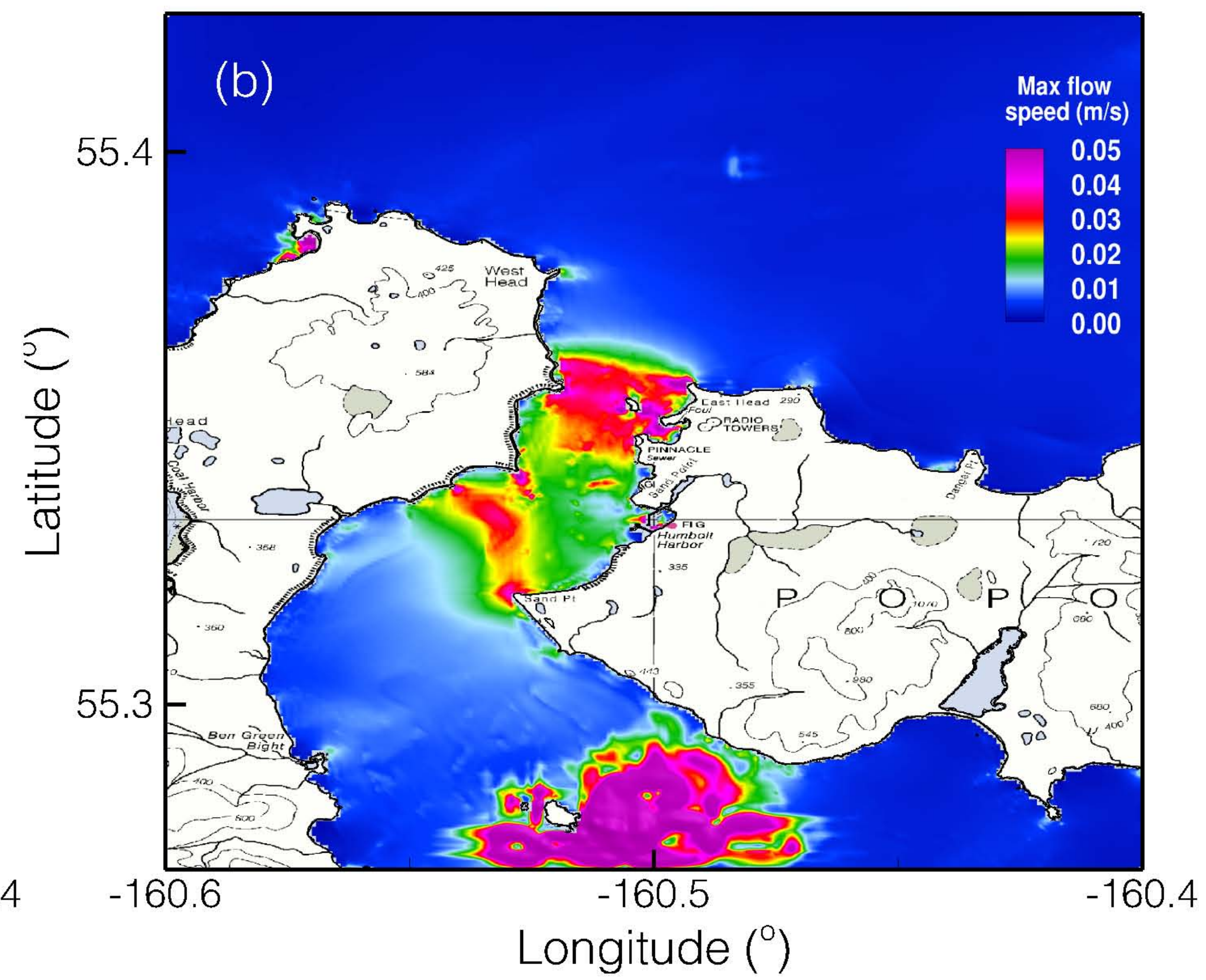
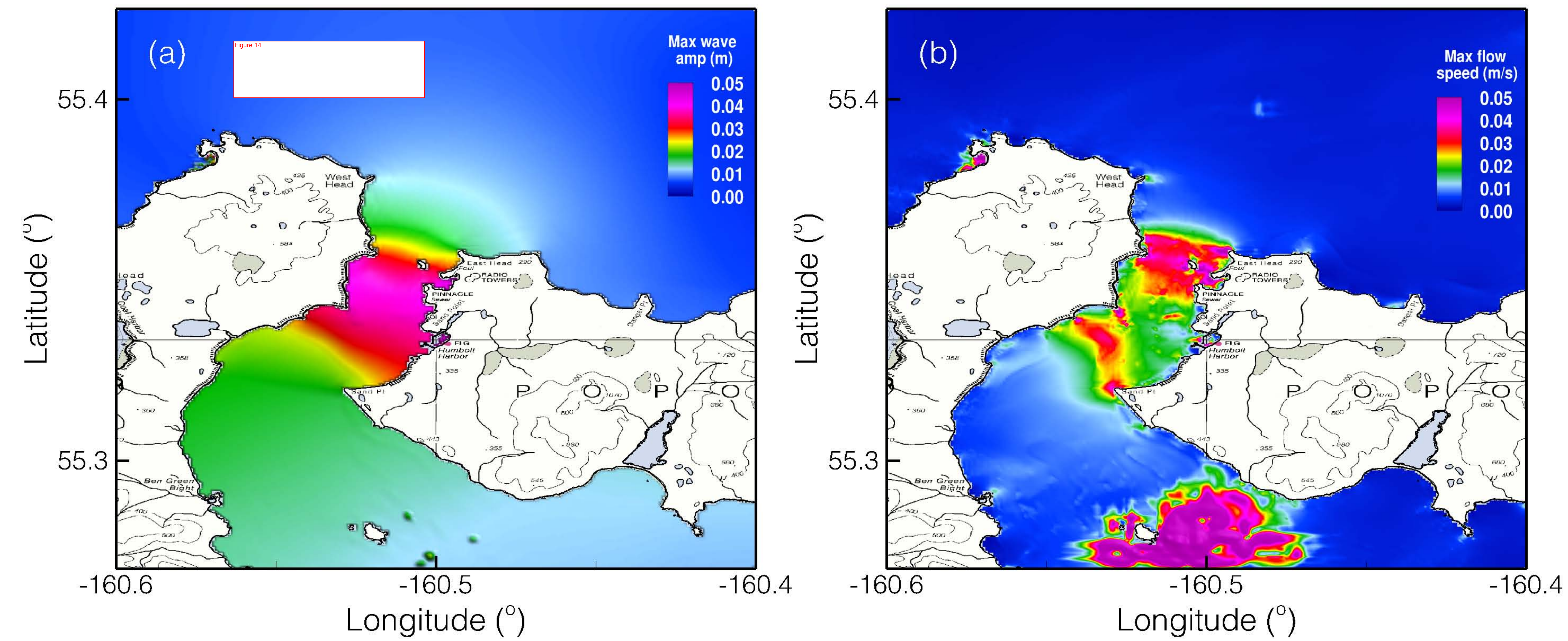
Figure 10

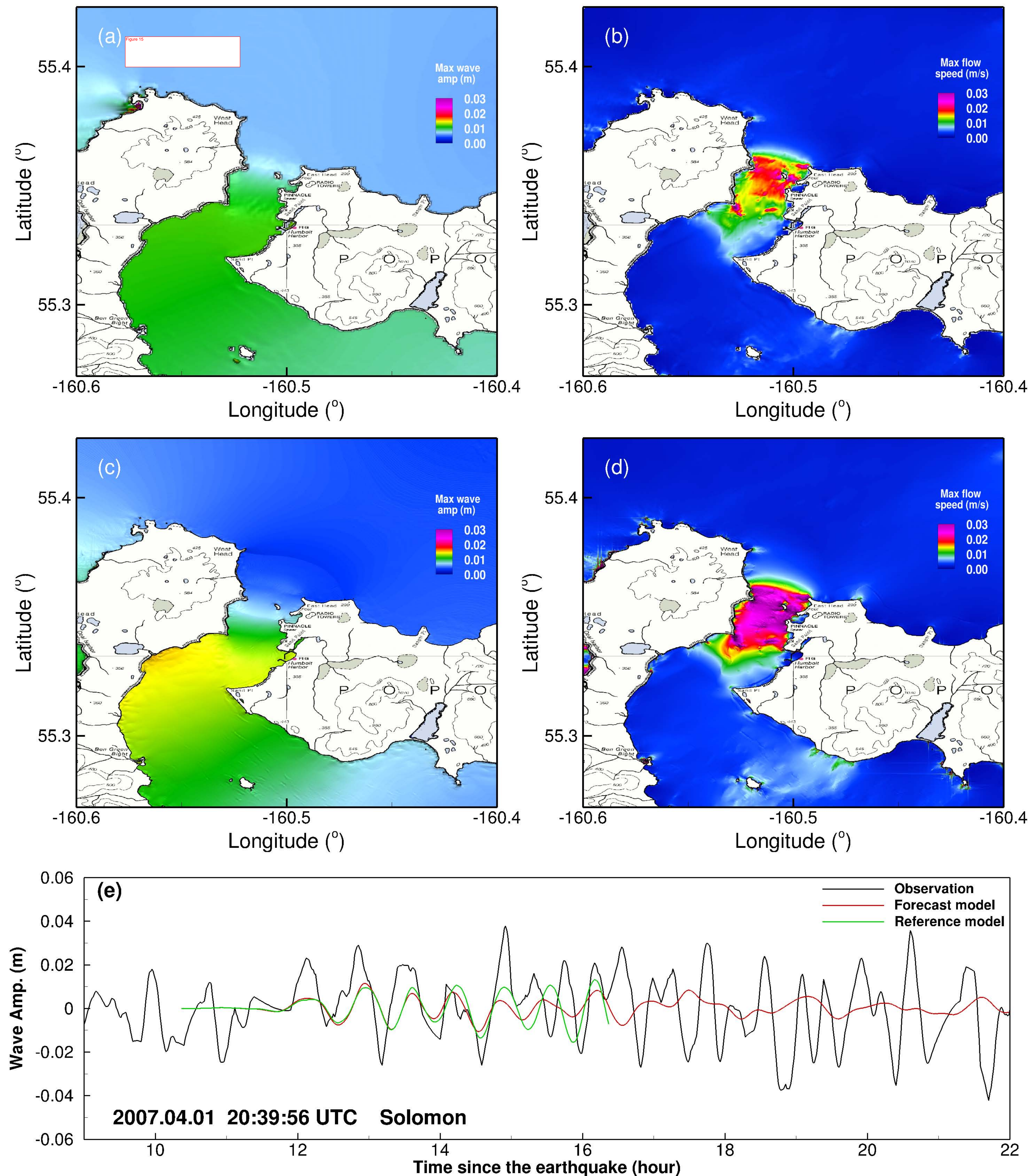


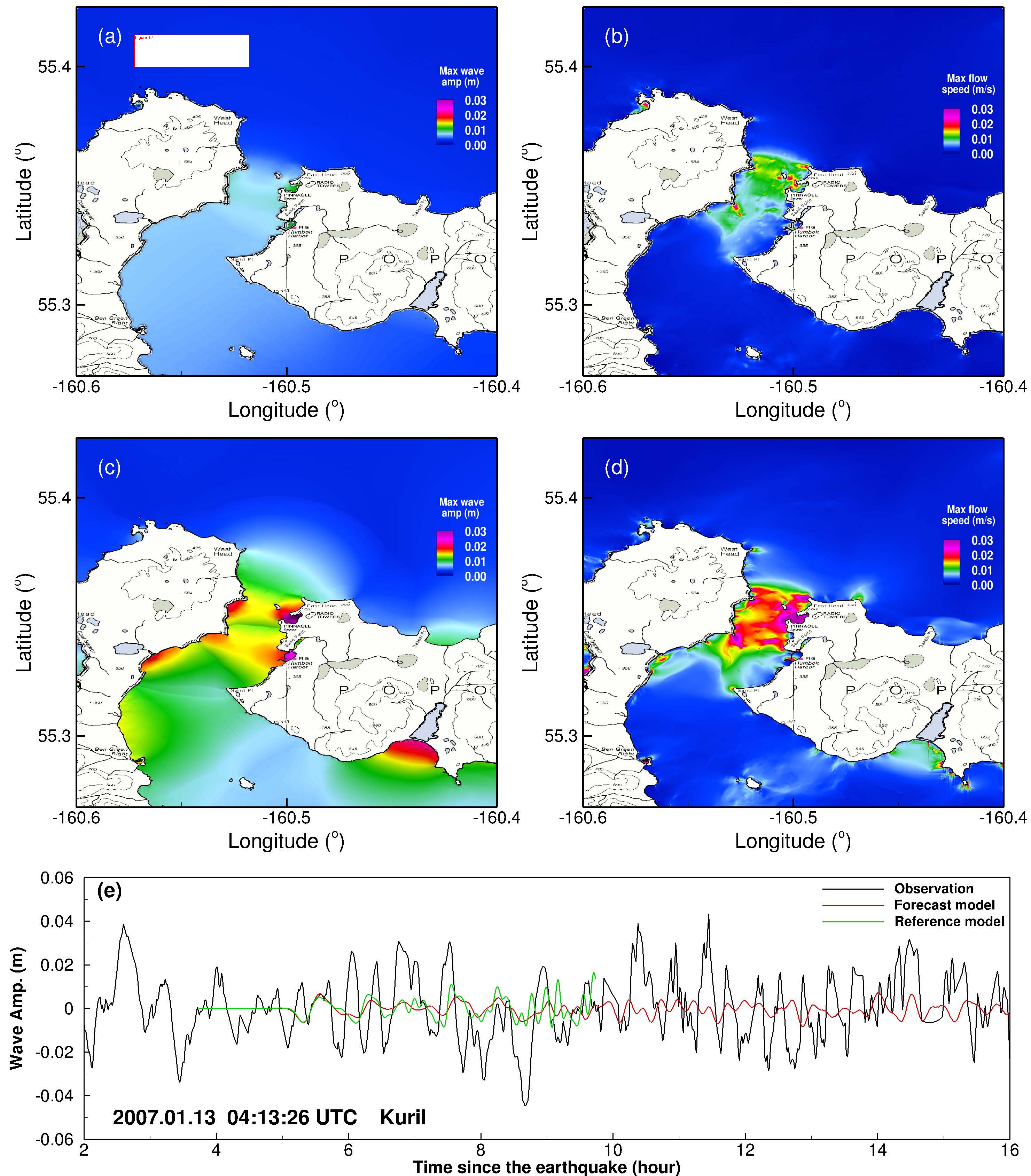


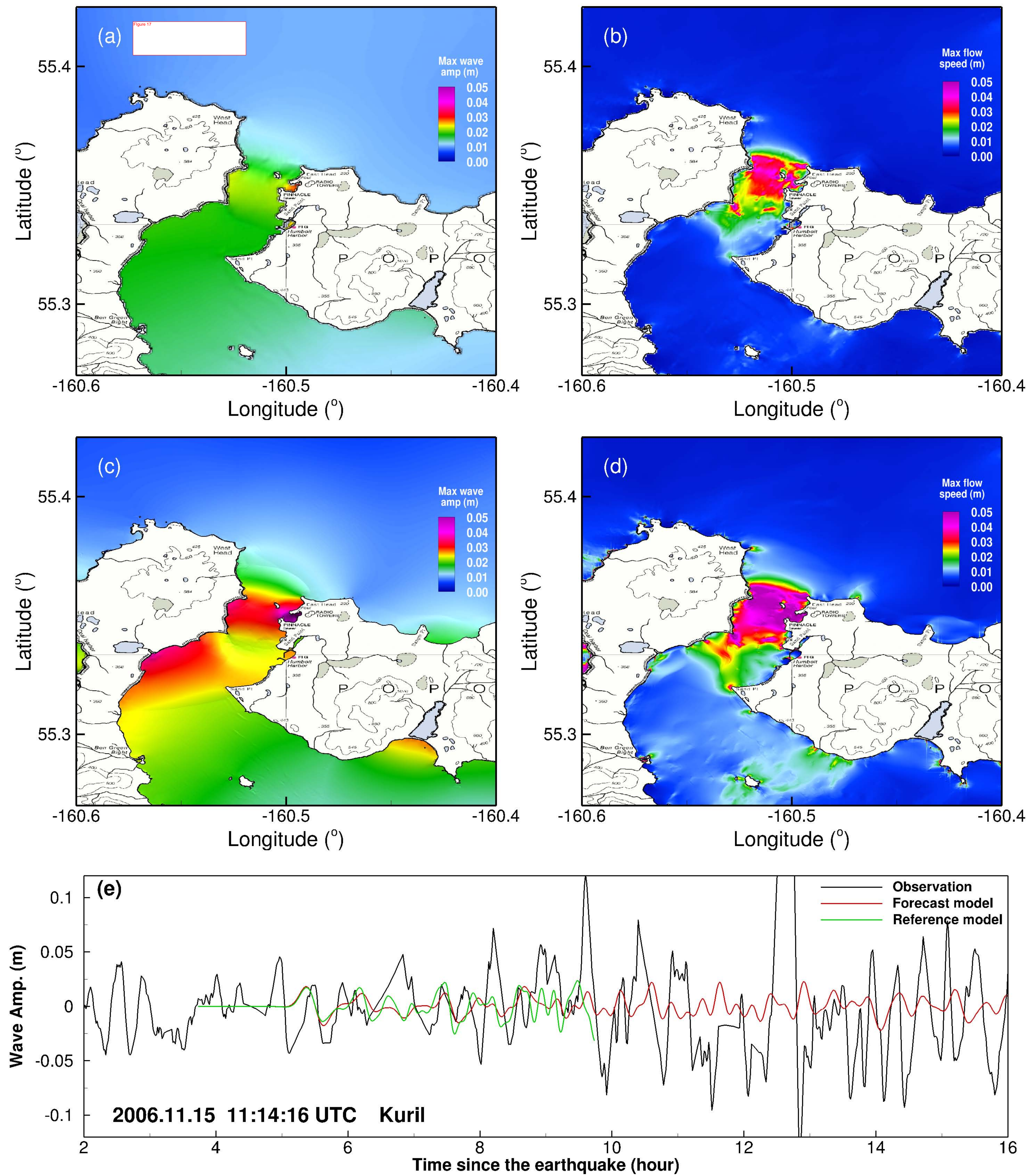


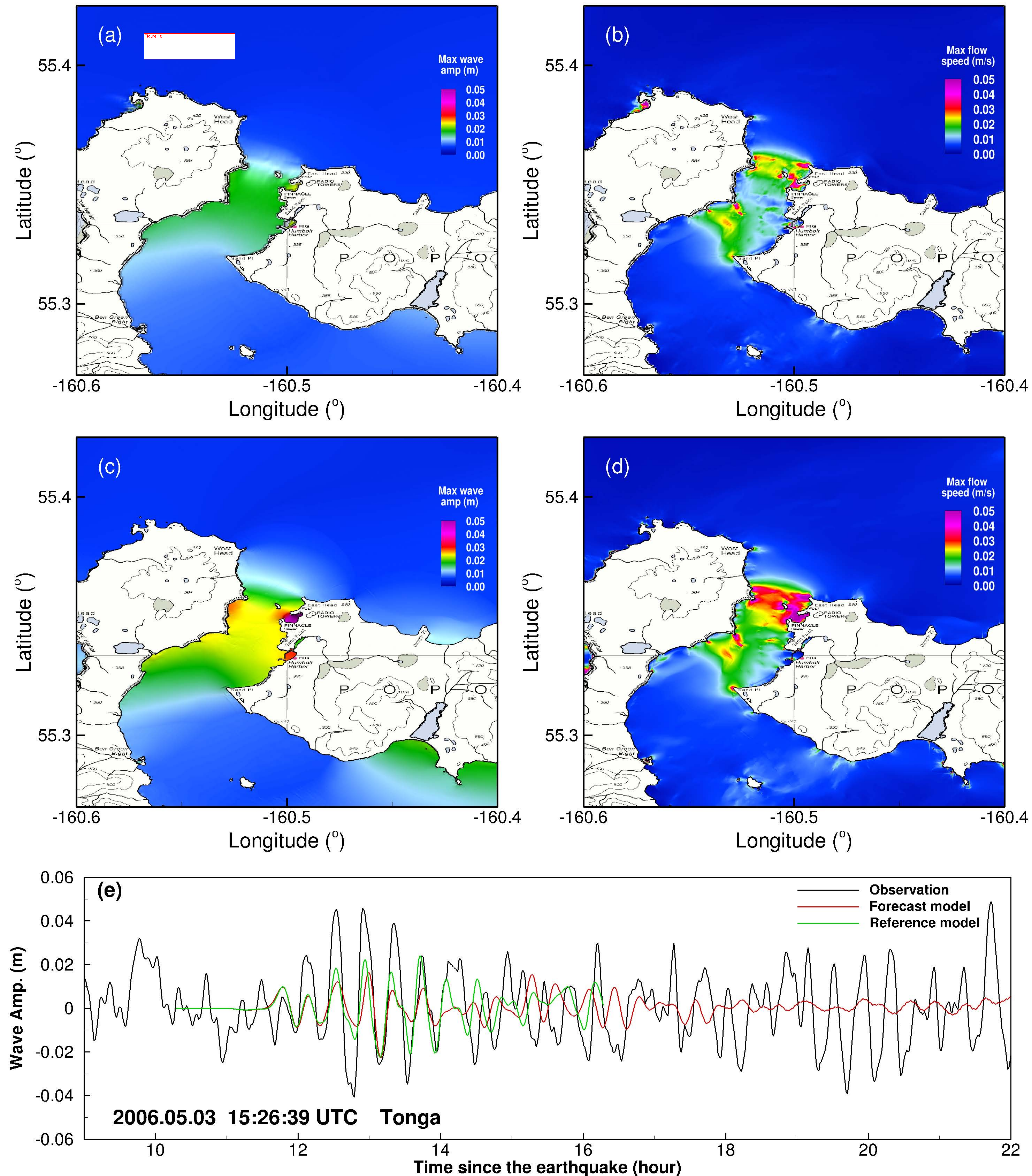


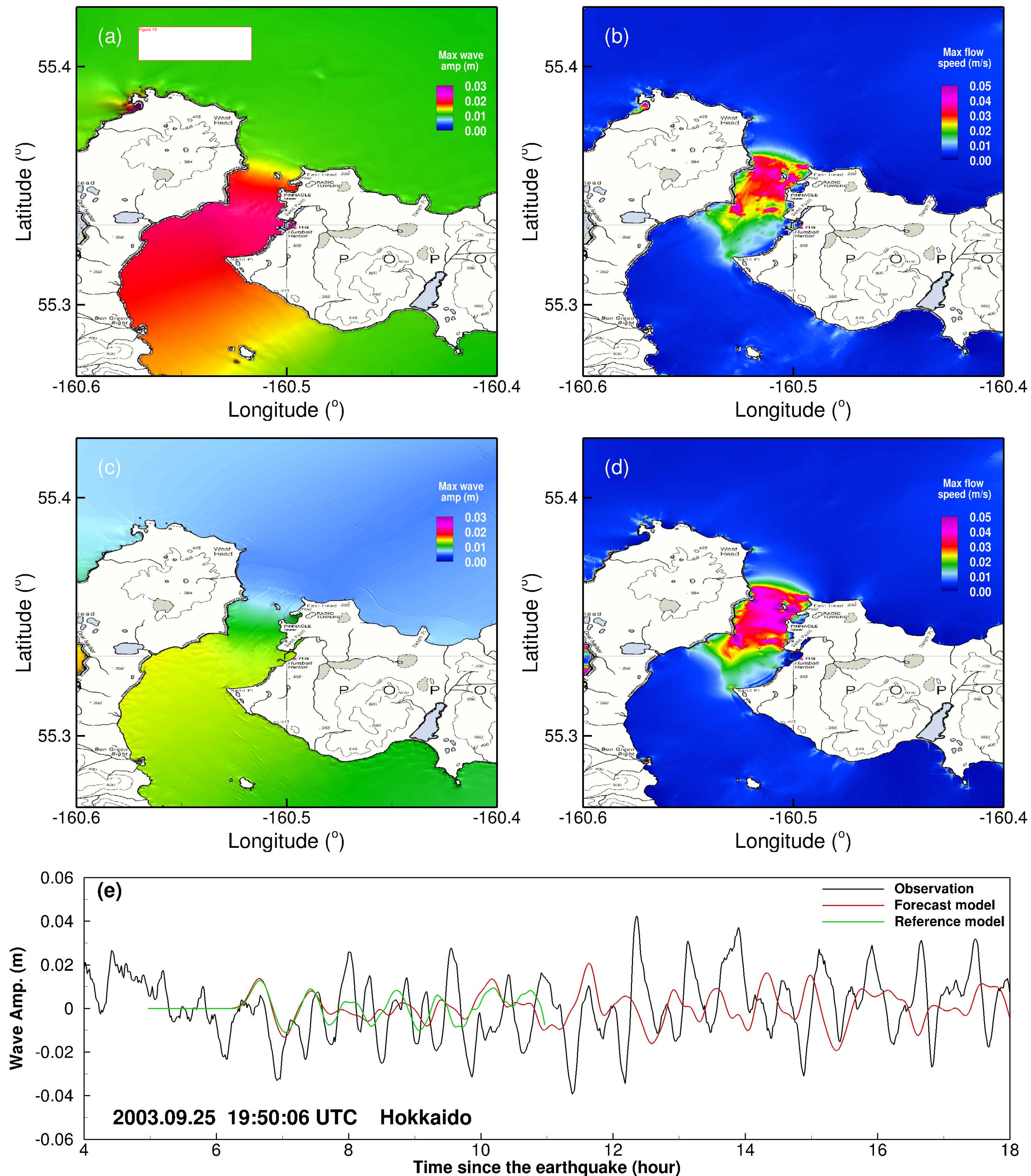


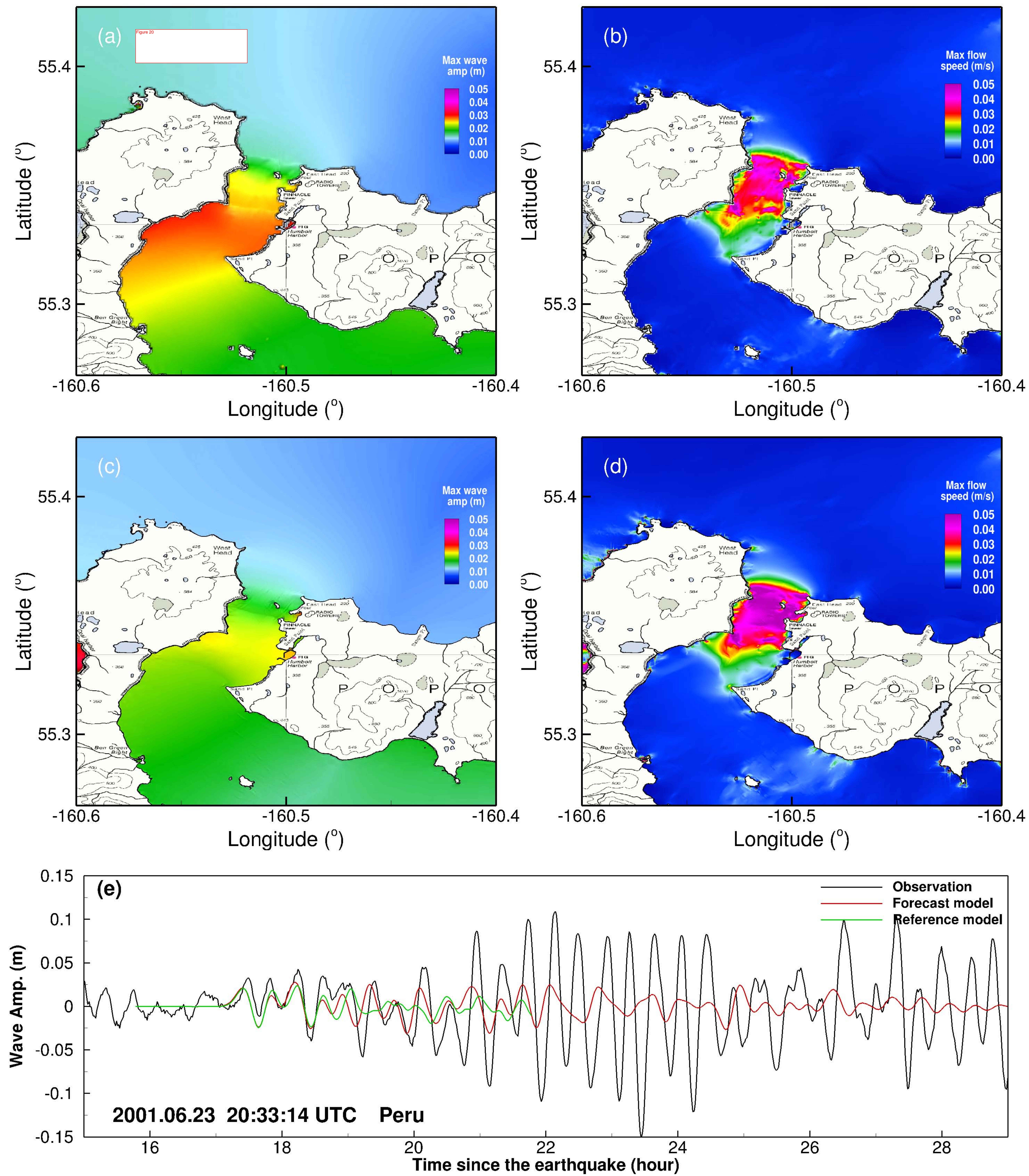


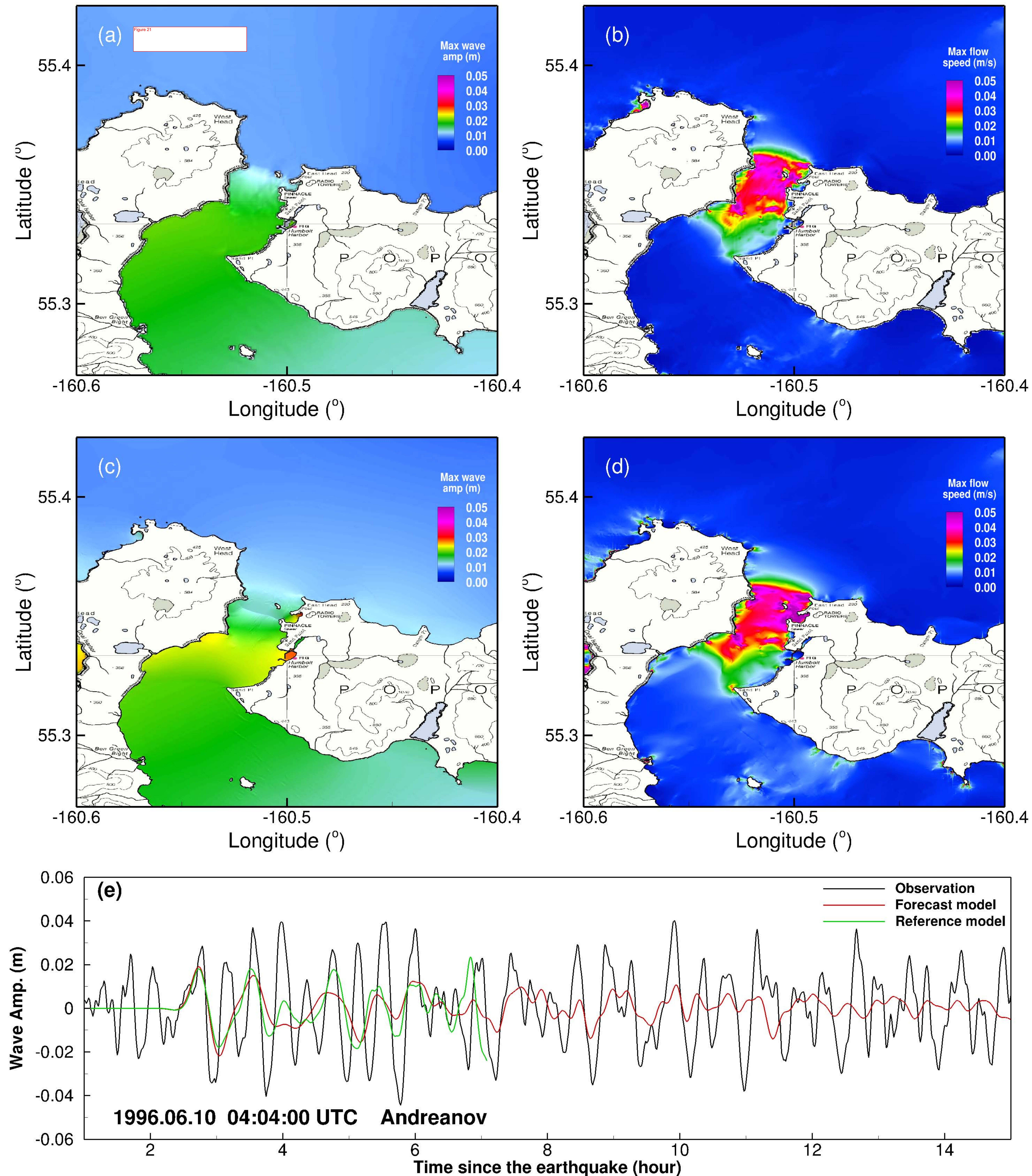


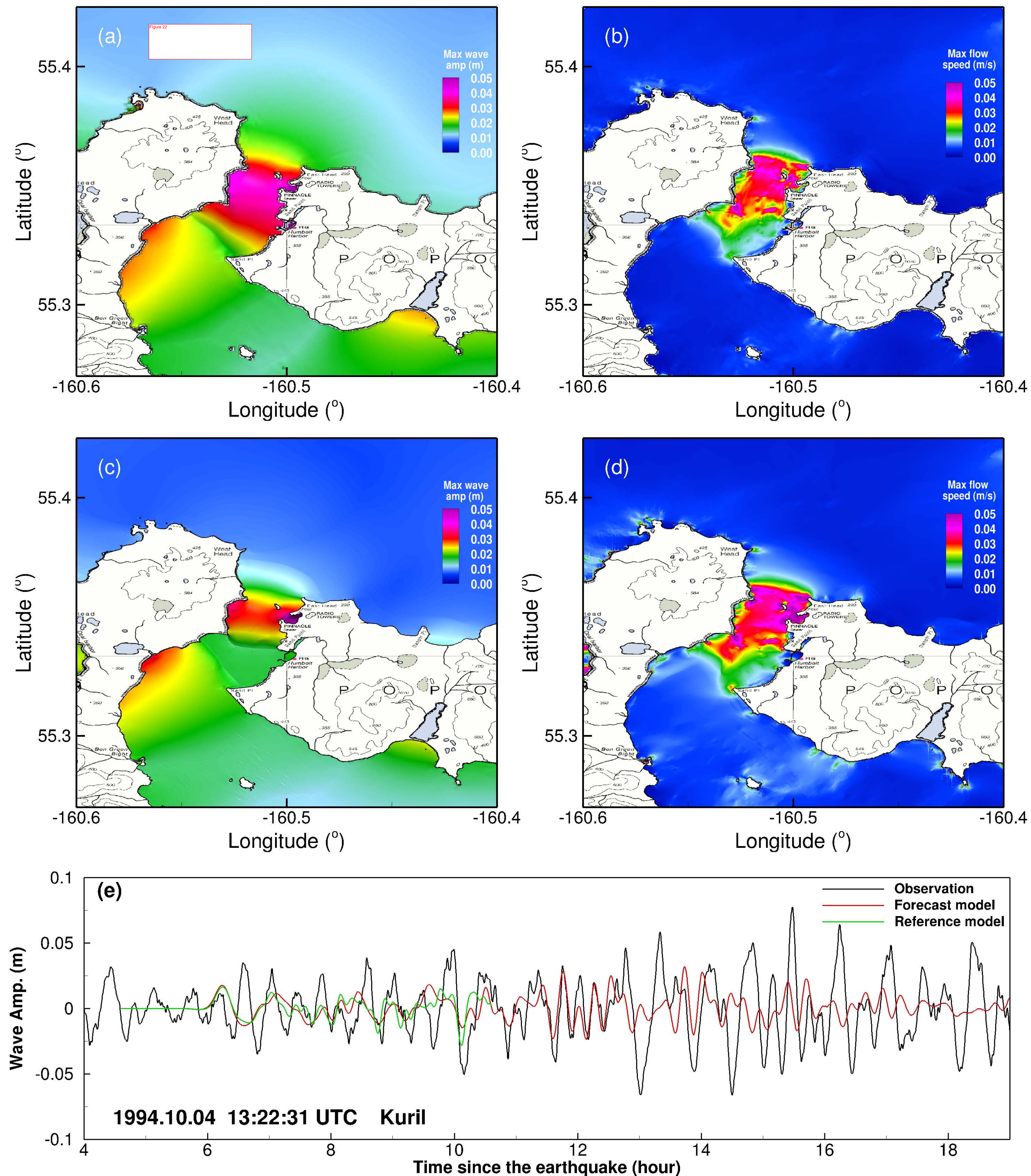


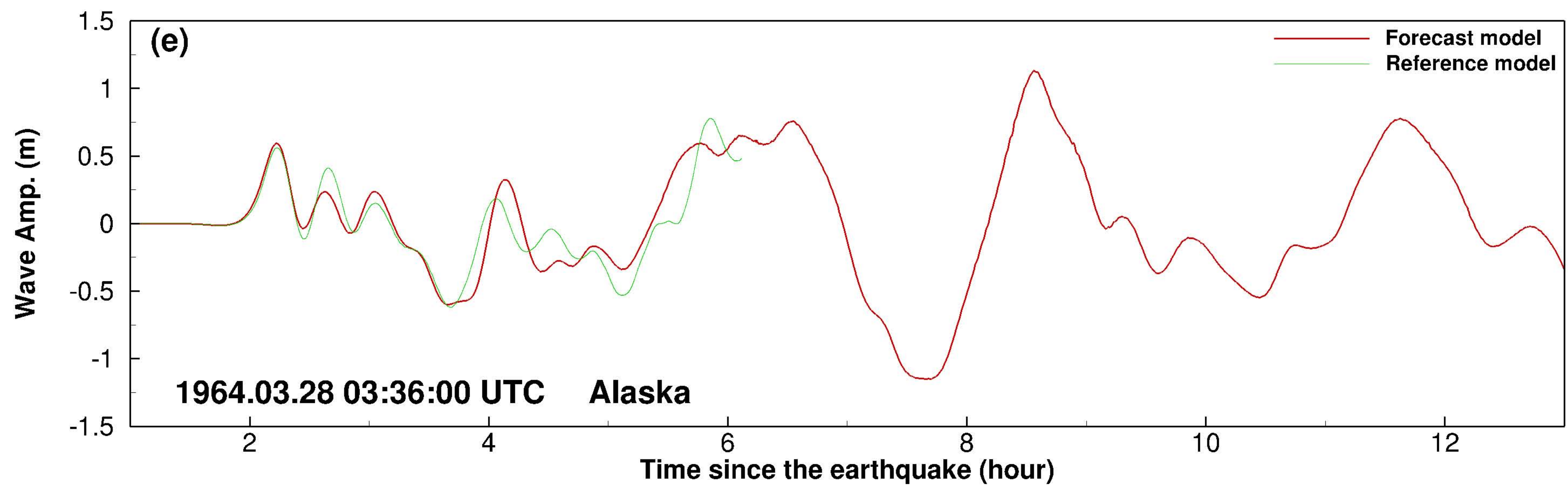
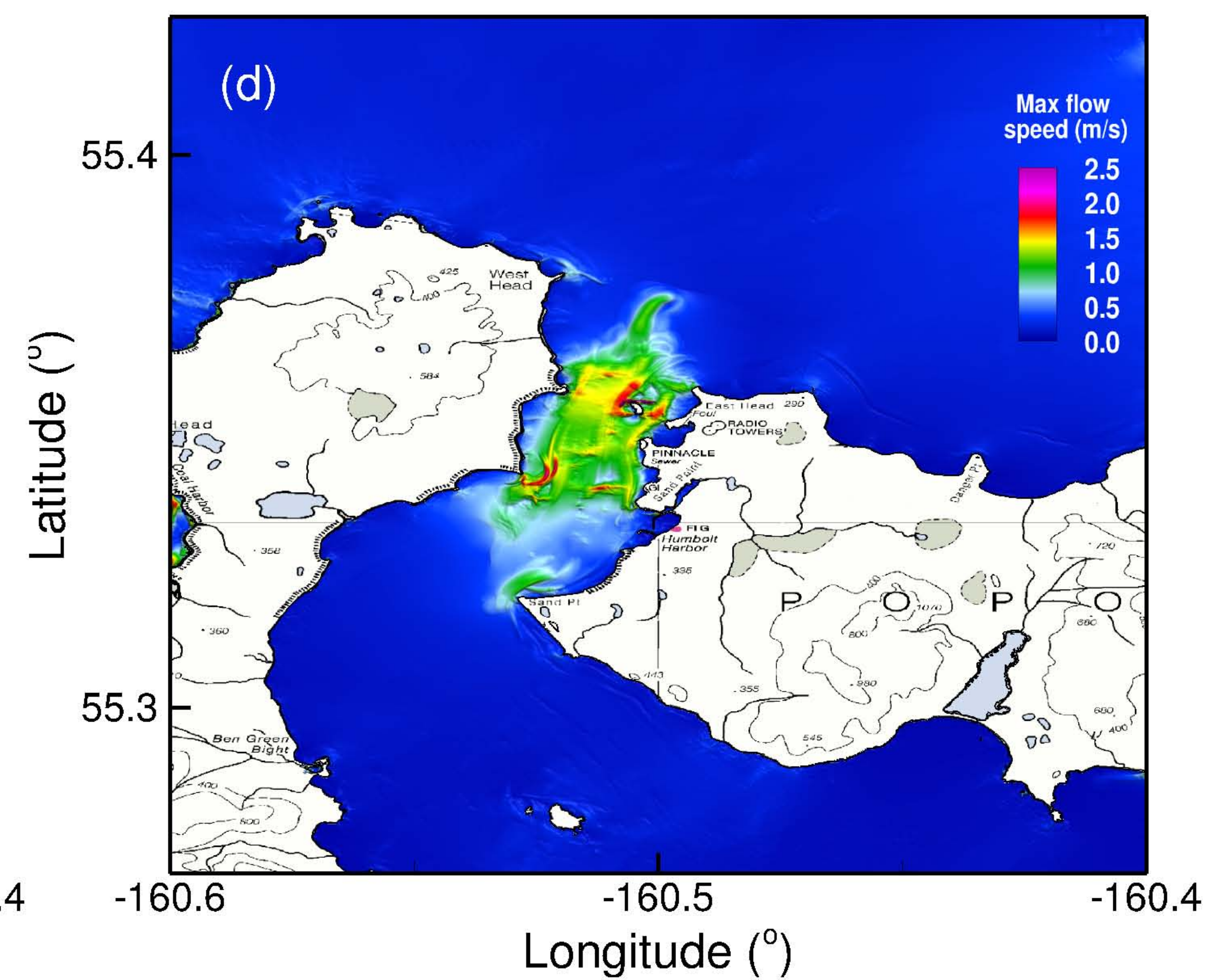
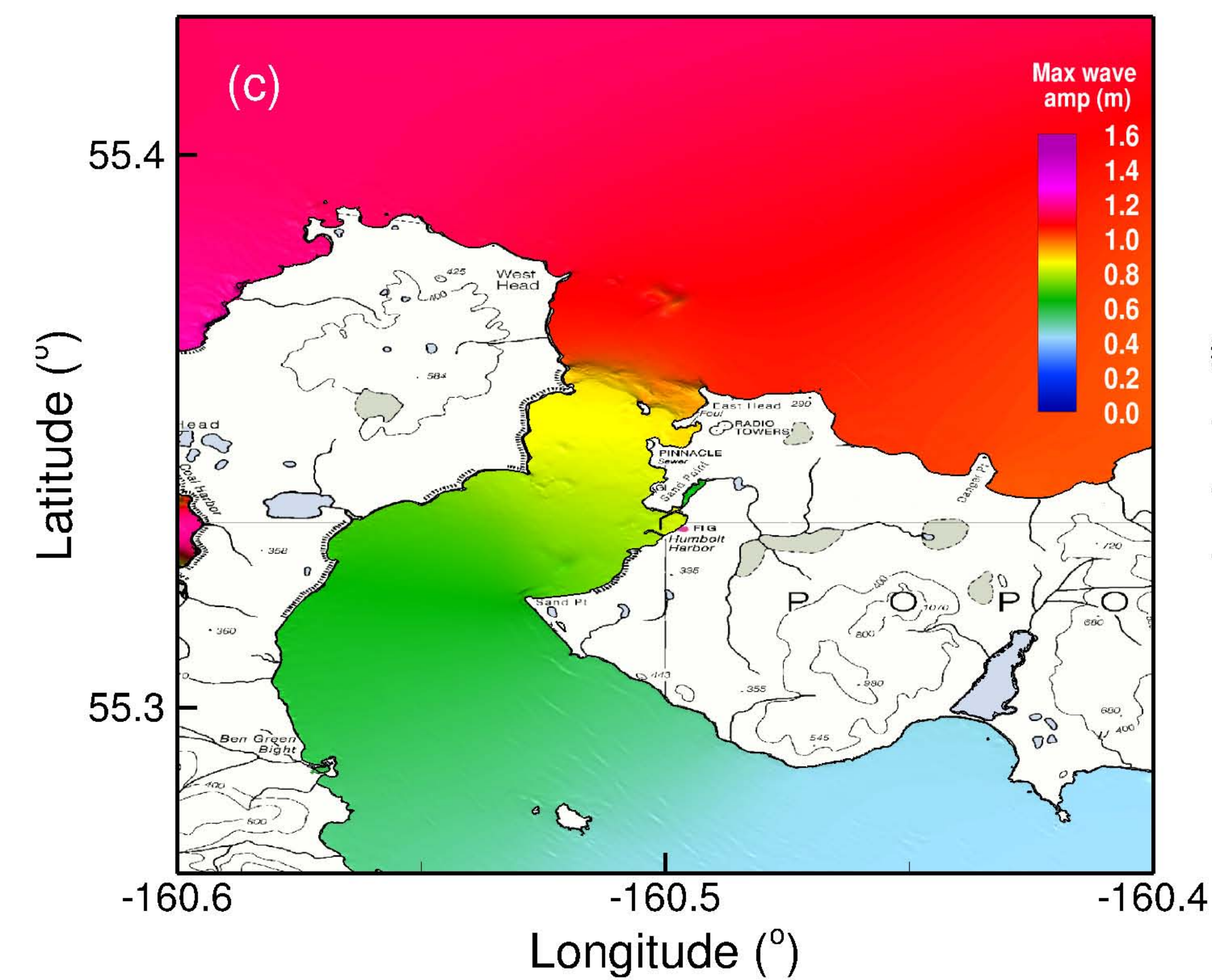
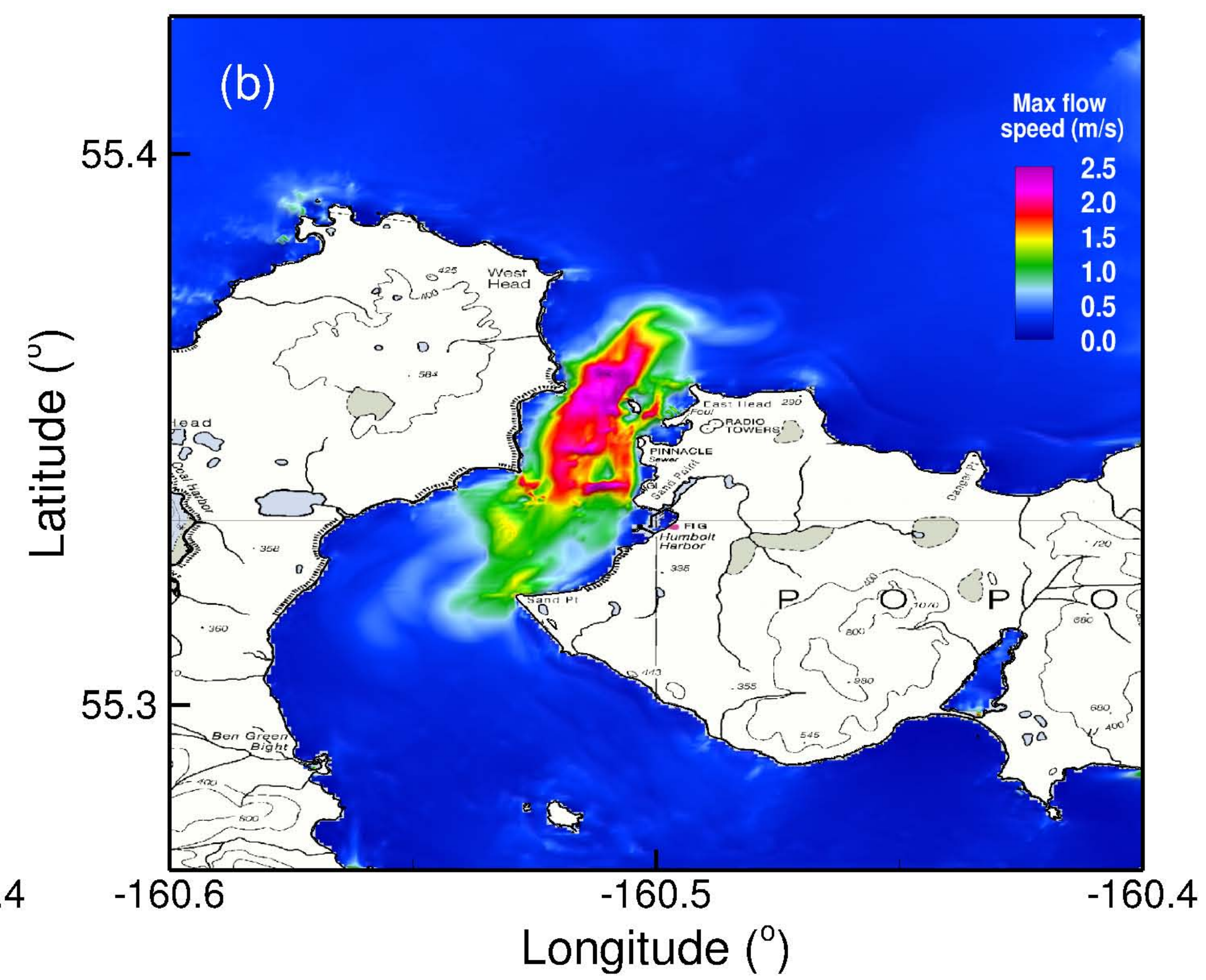
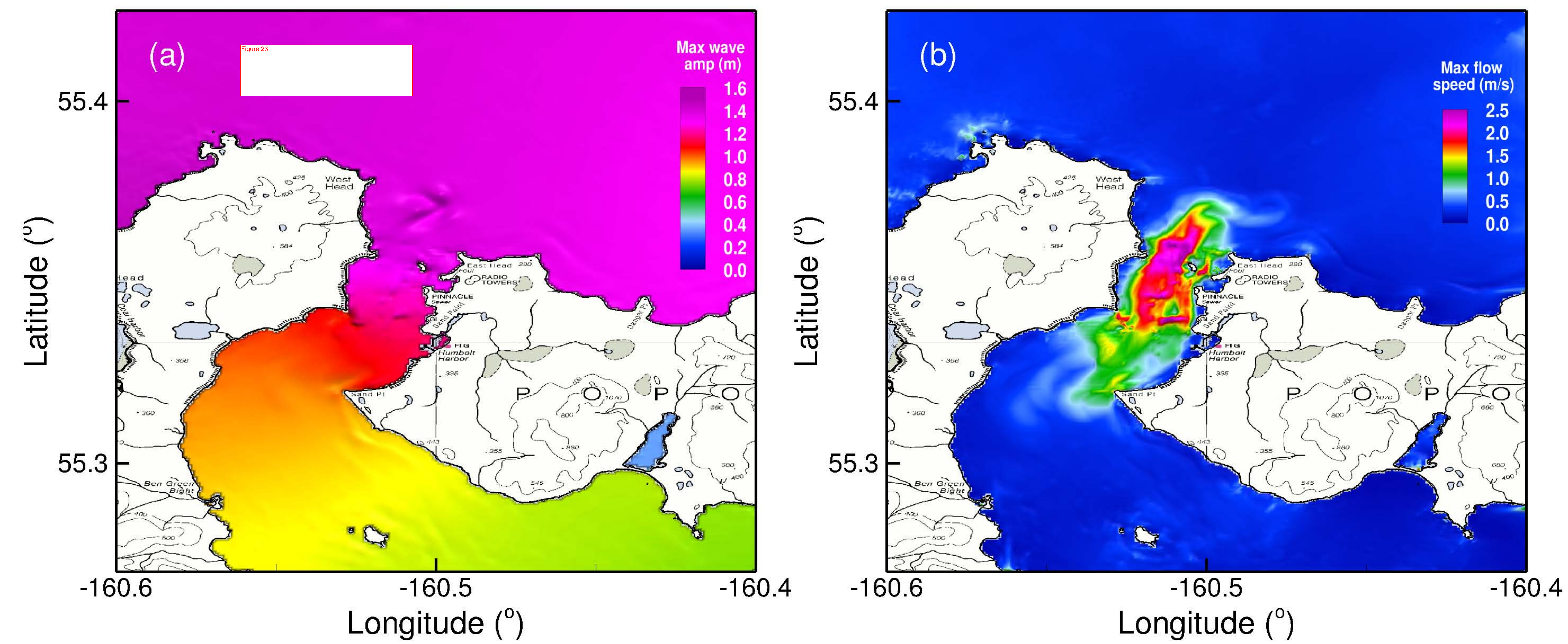


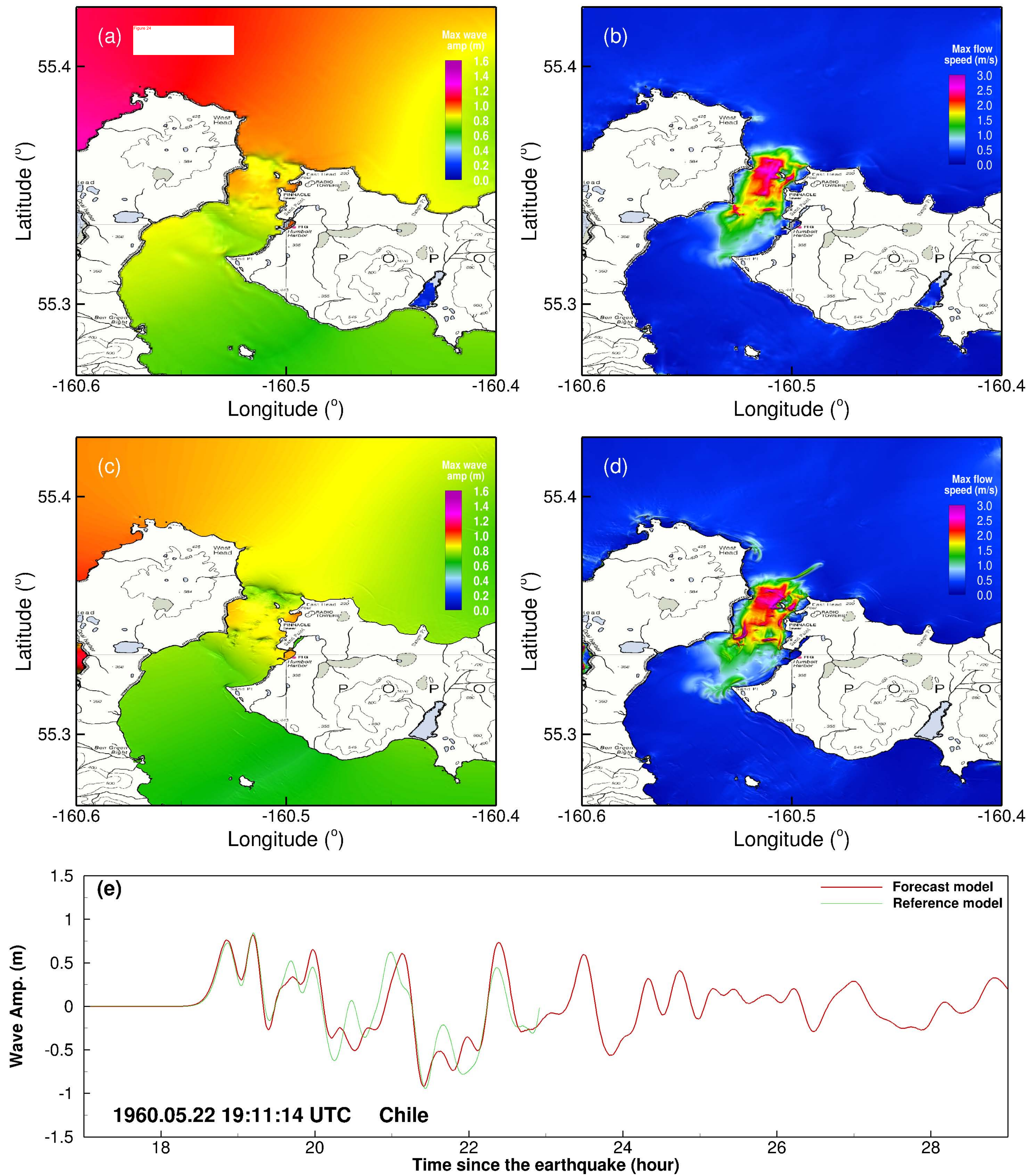


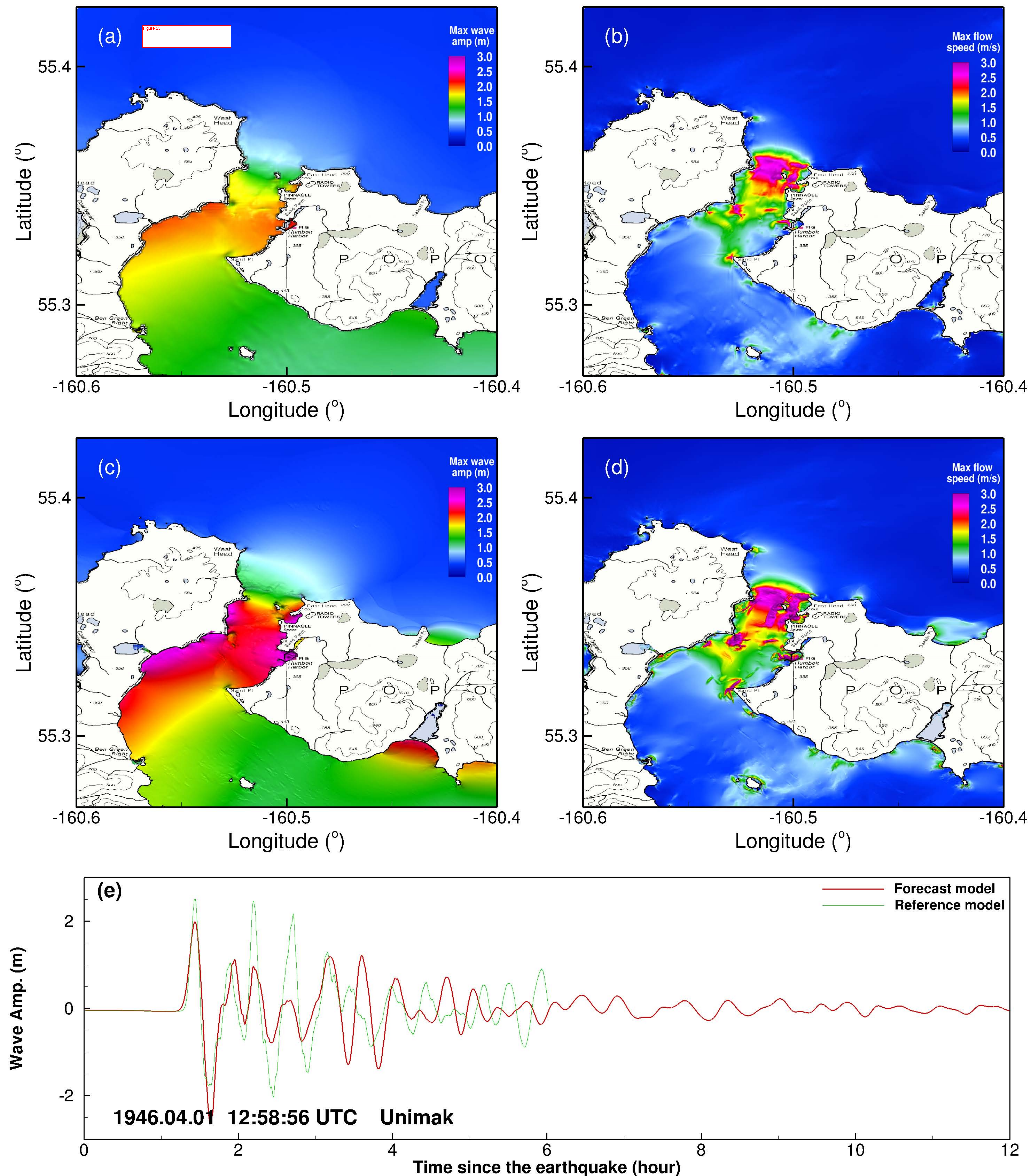


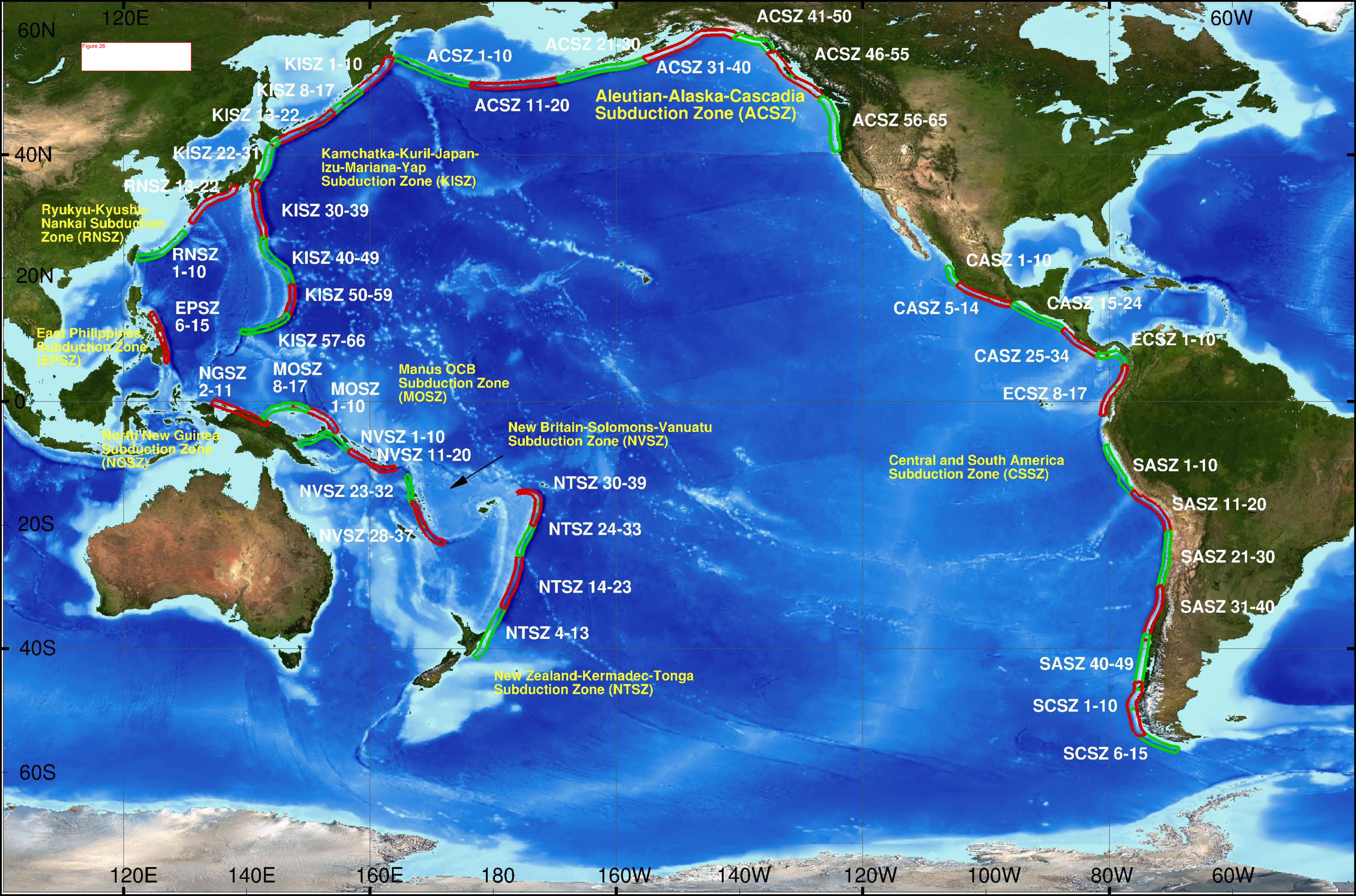


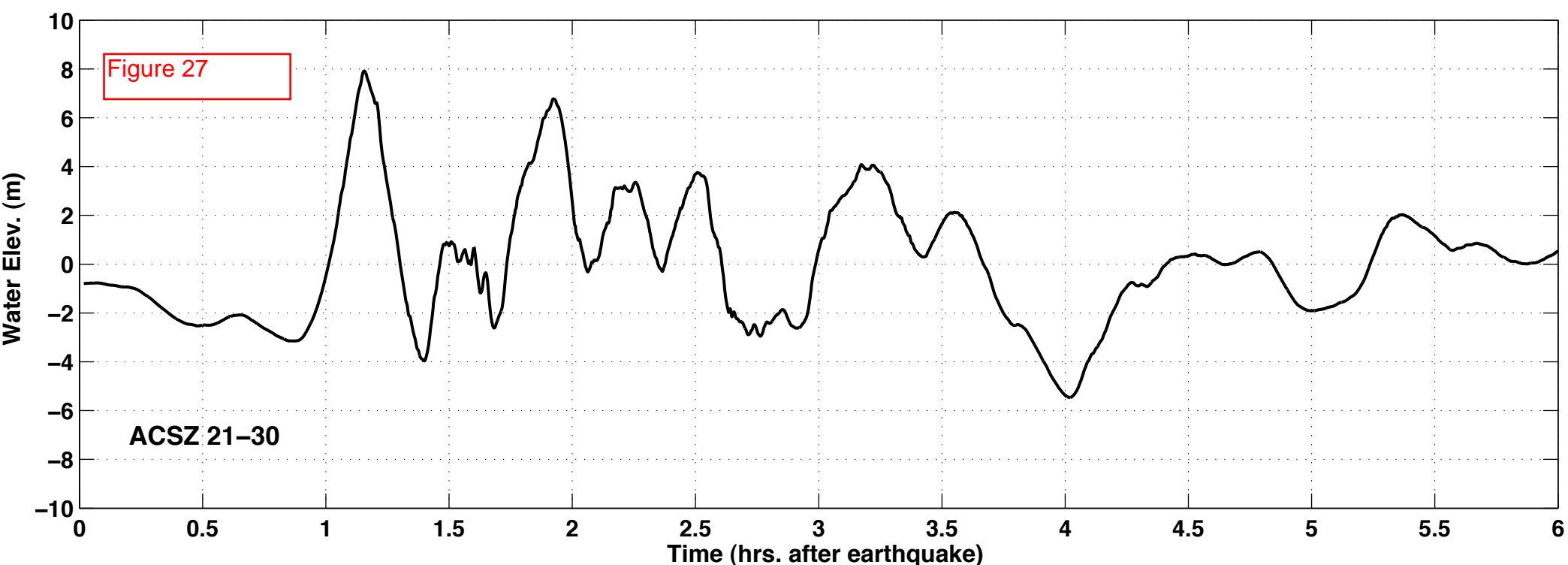


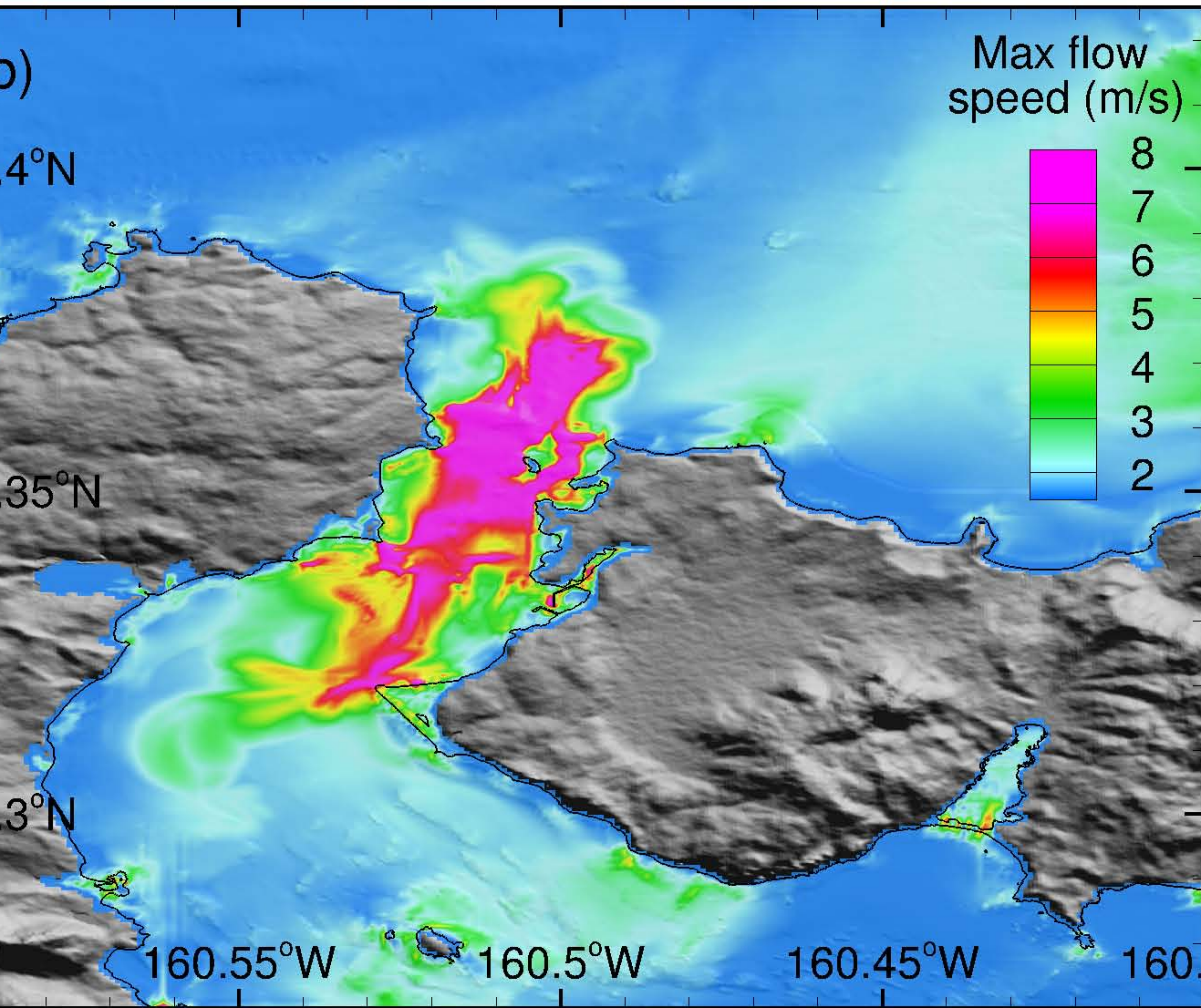
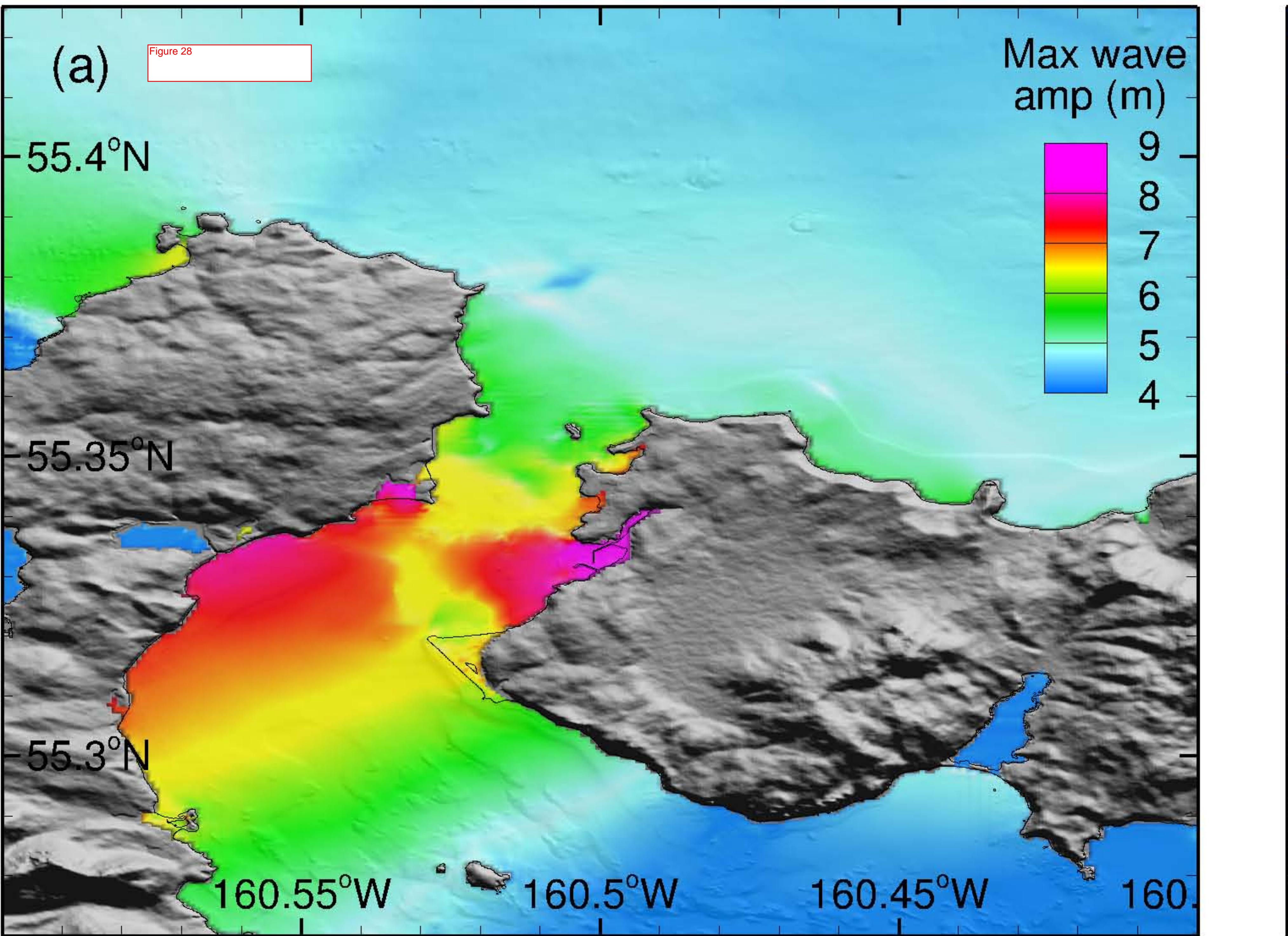












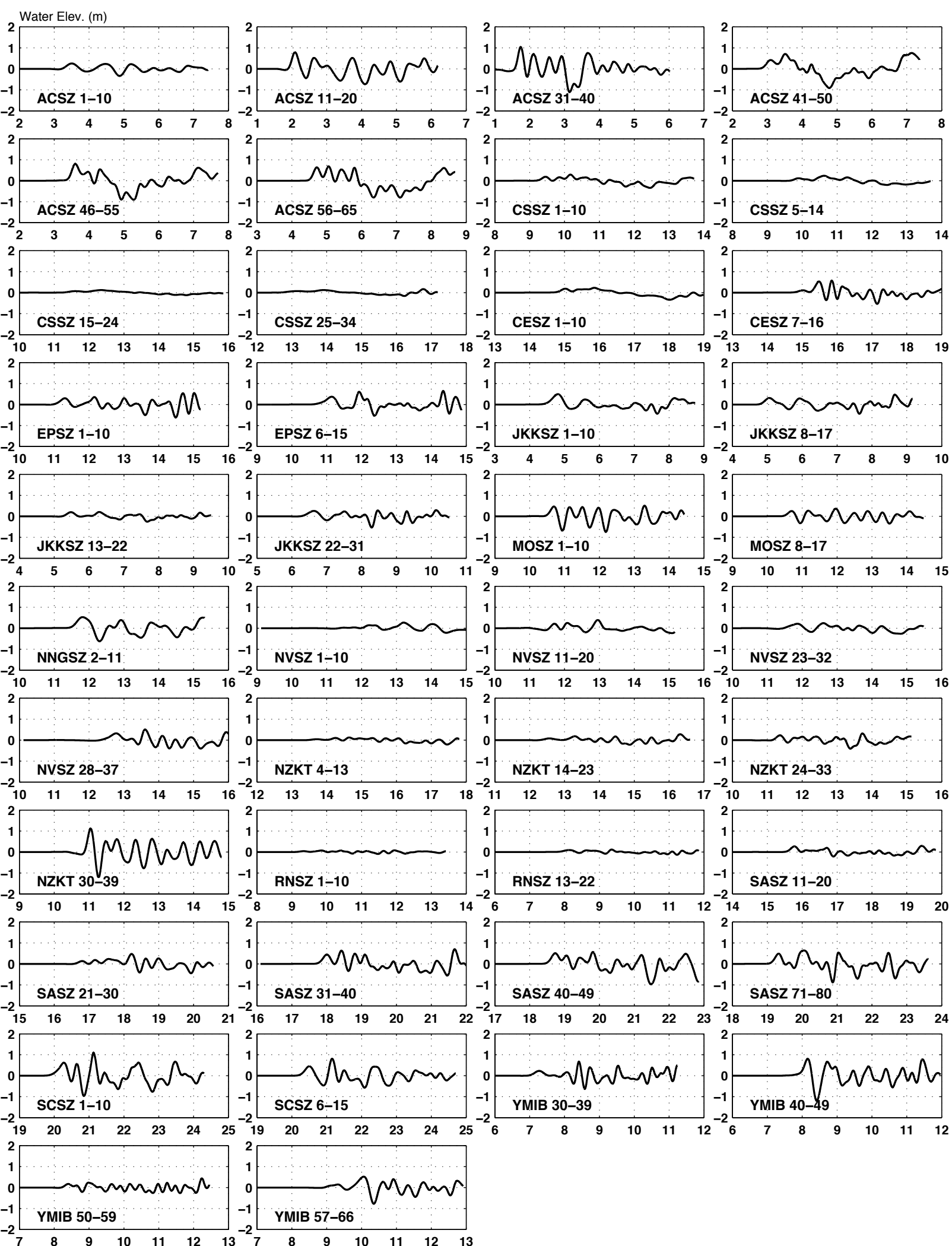


Figure 30

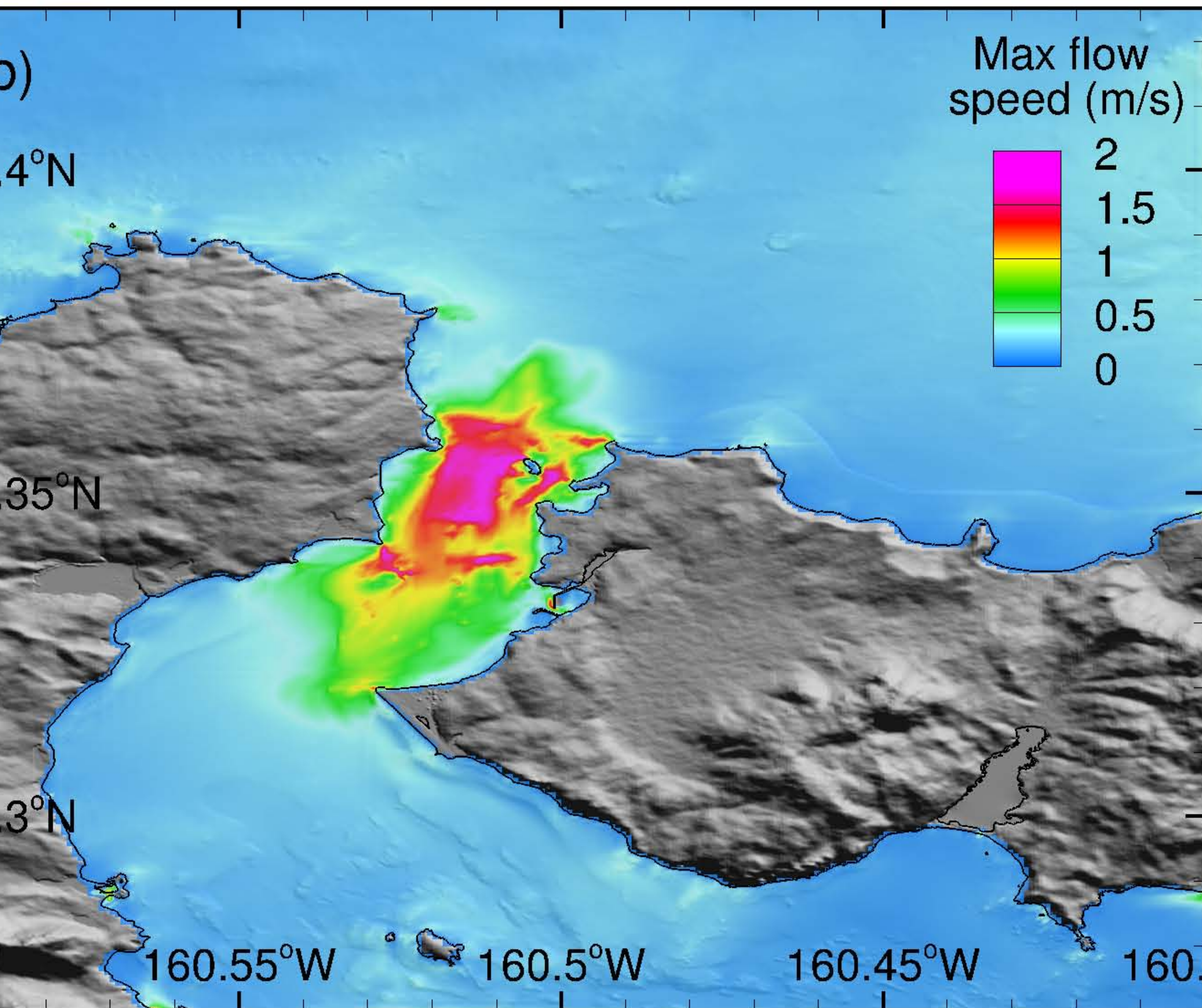
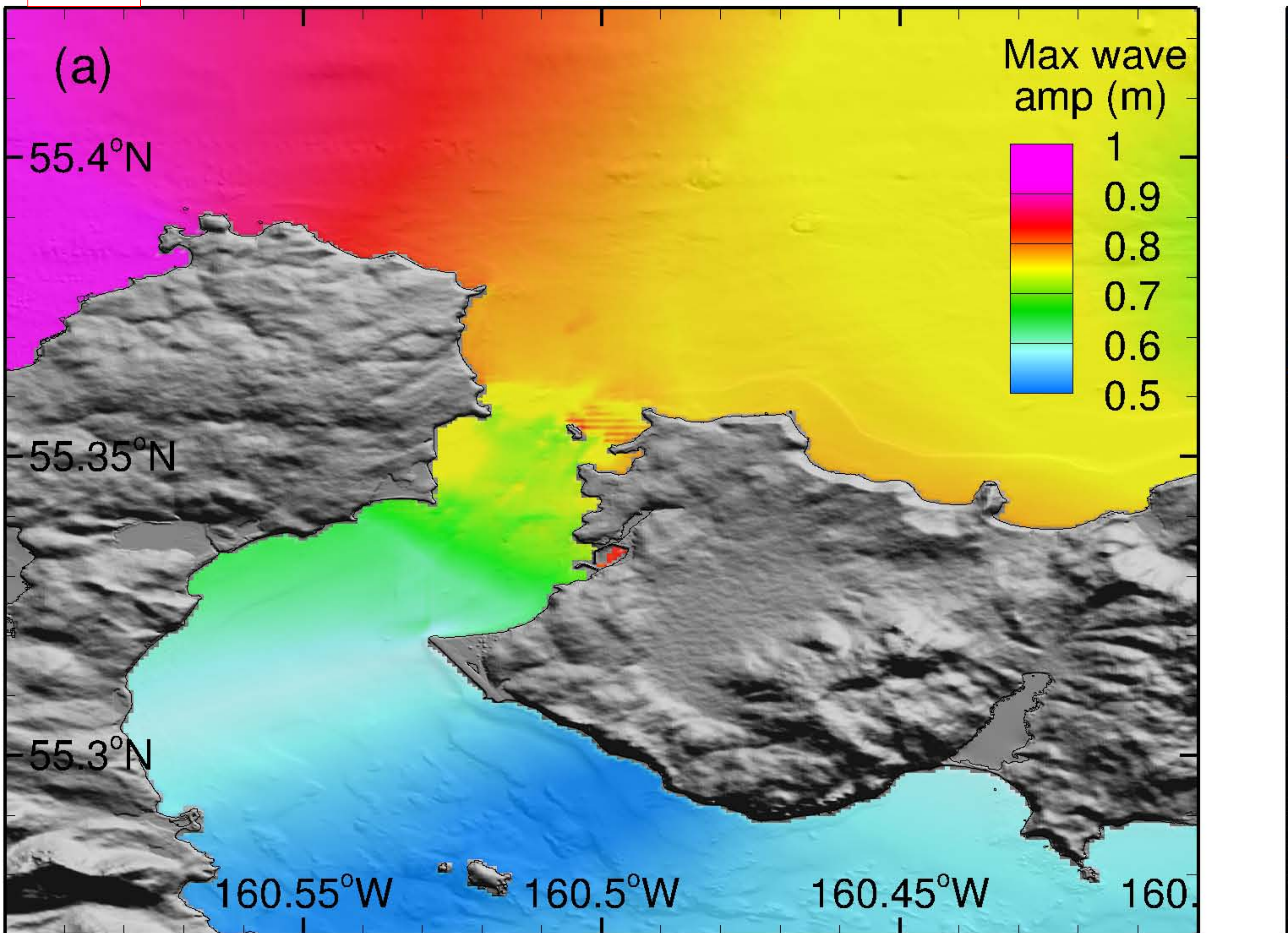


Figure 31

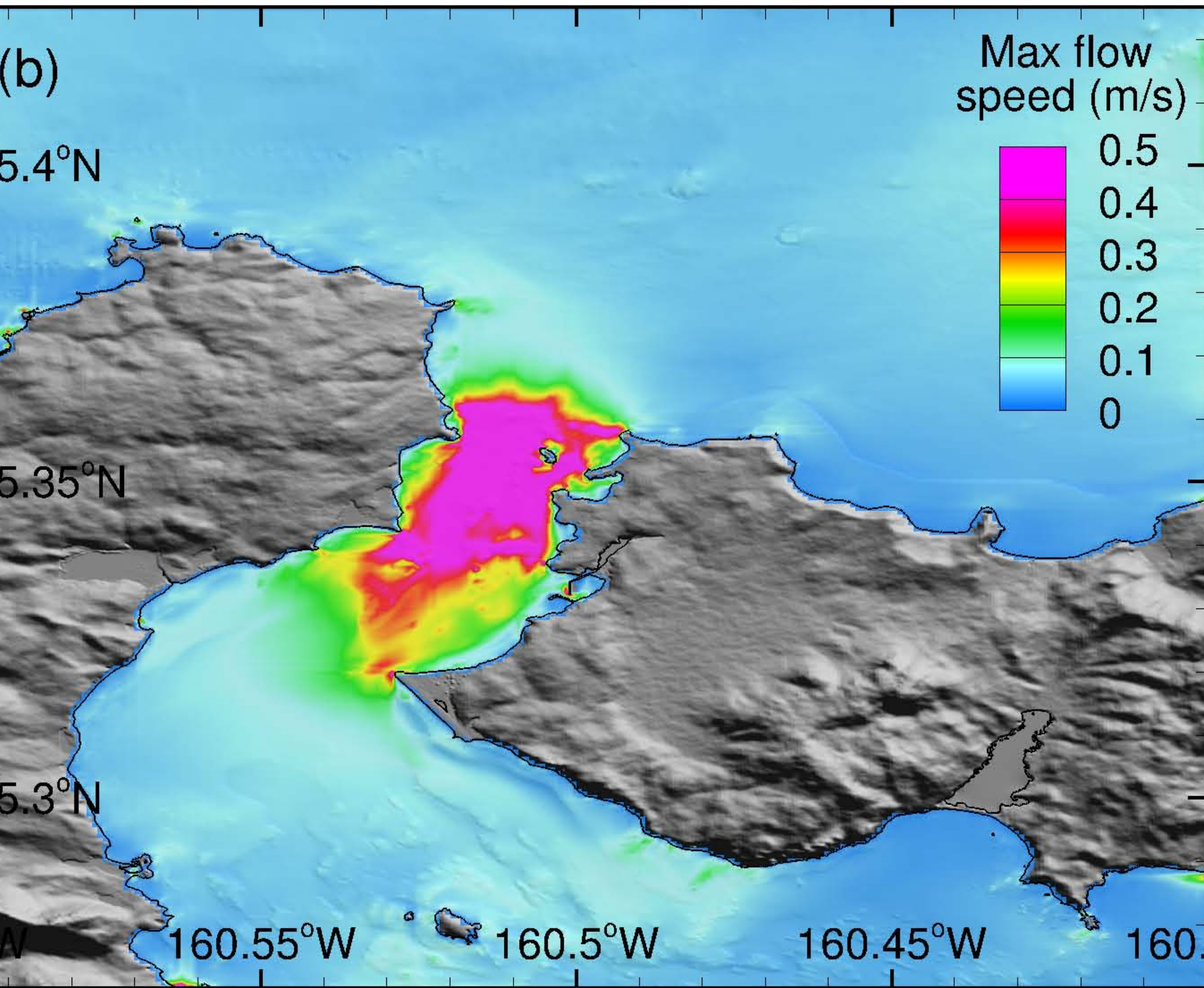
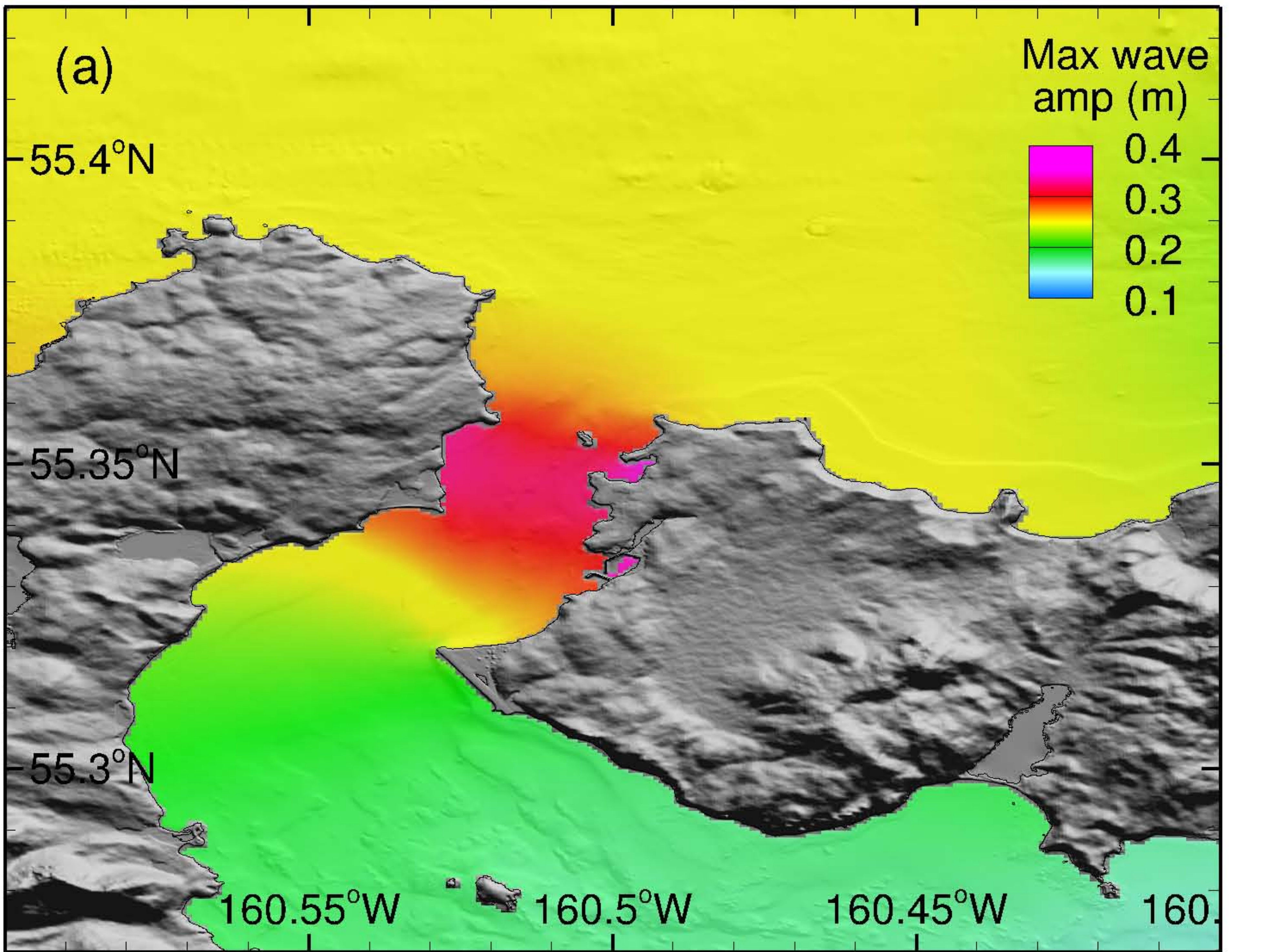


Figure 32

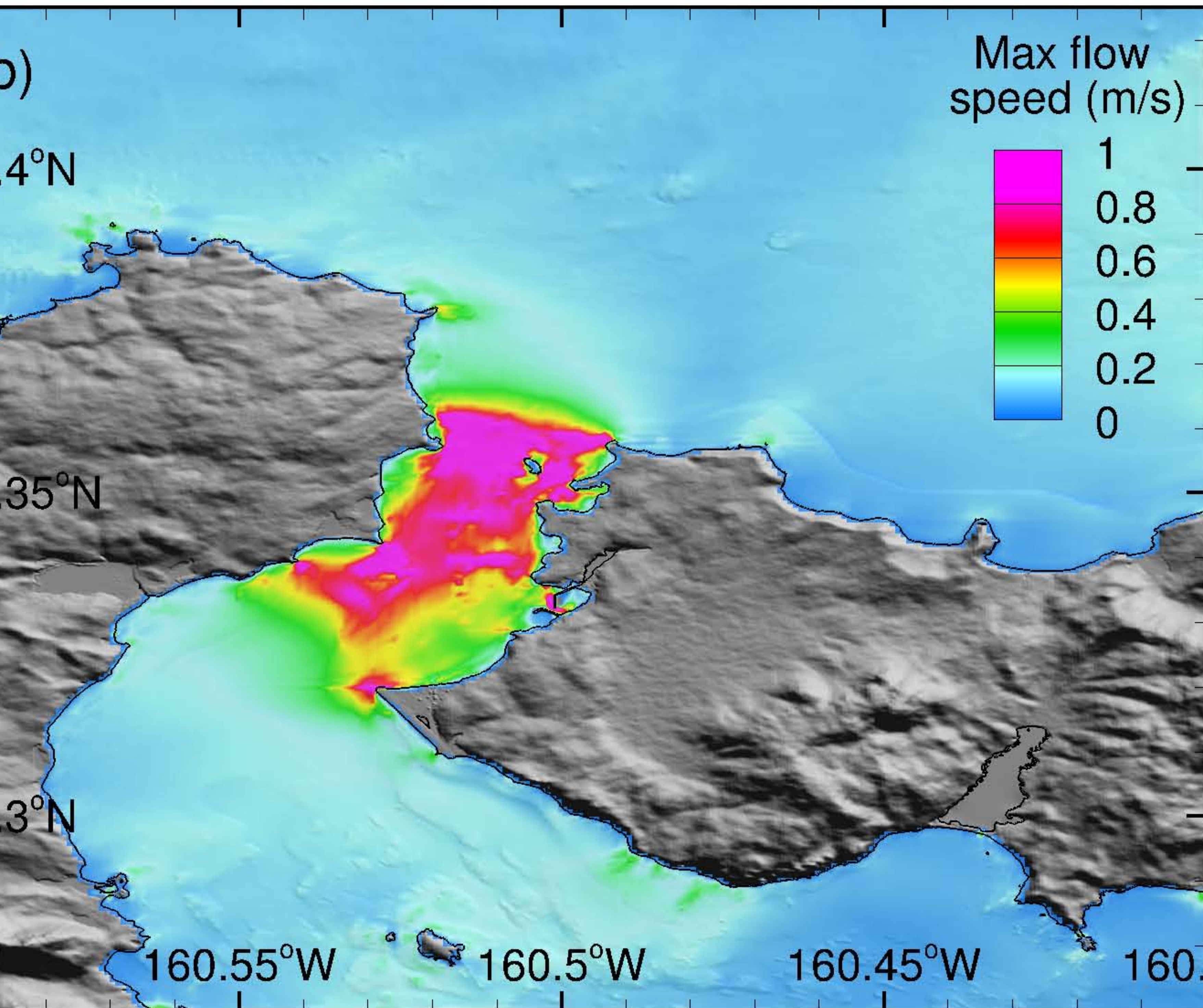
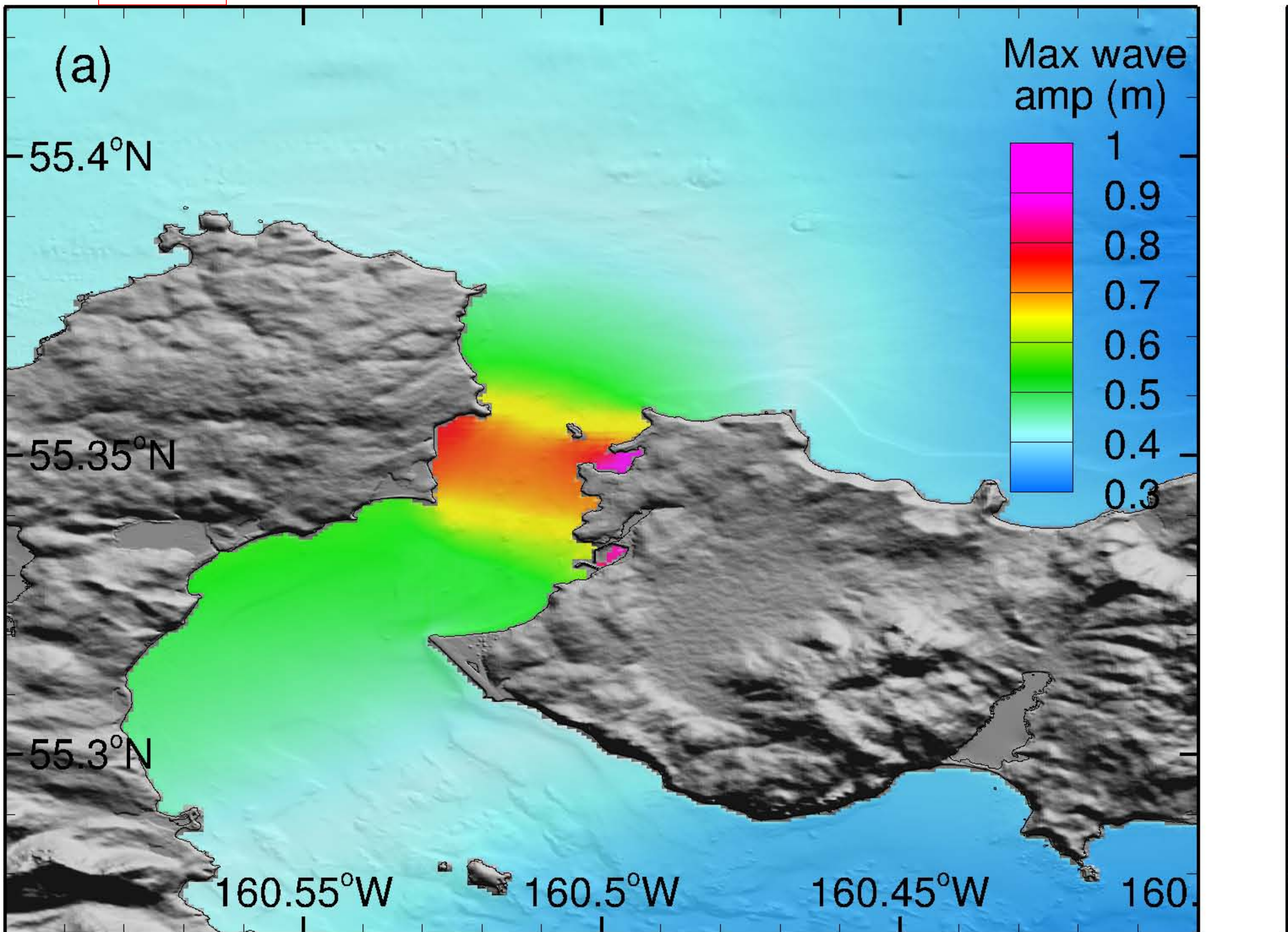


Figure 33

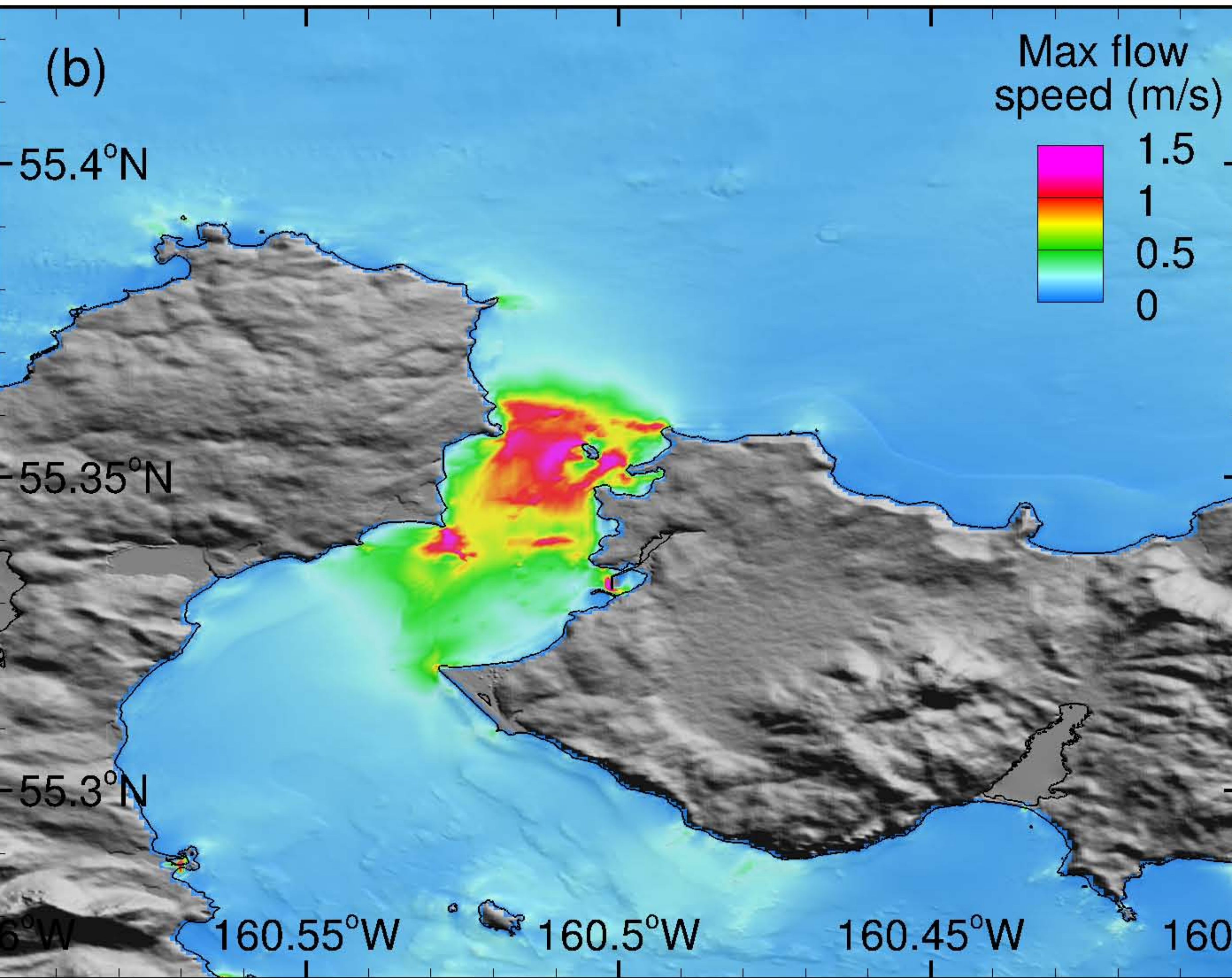
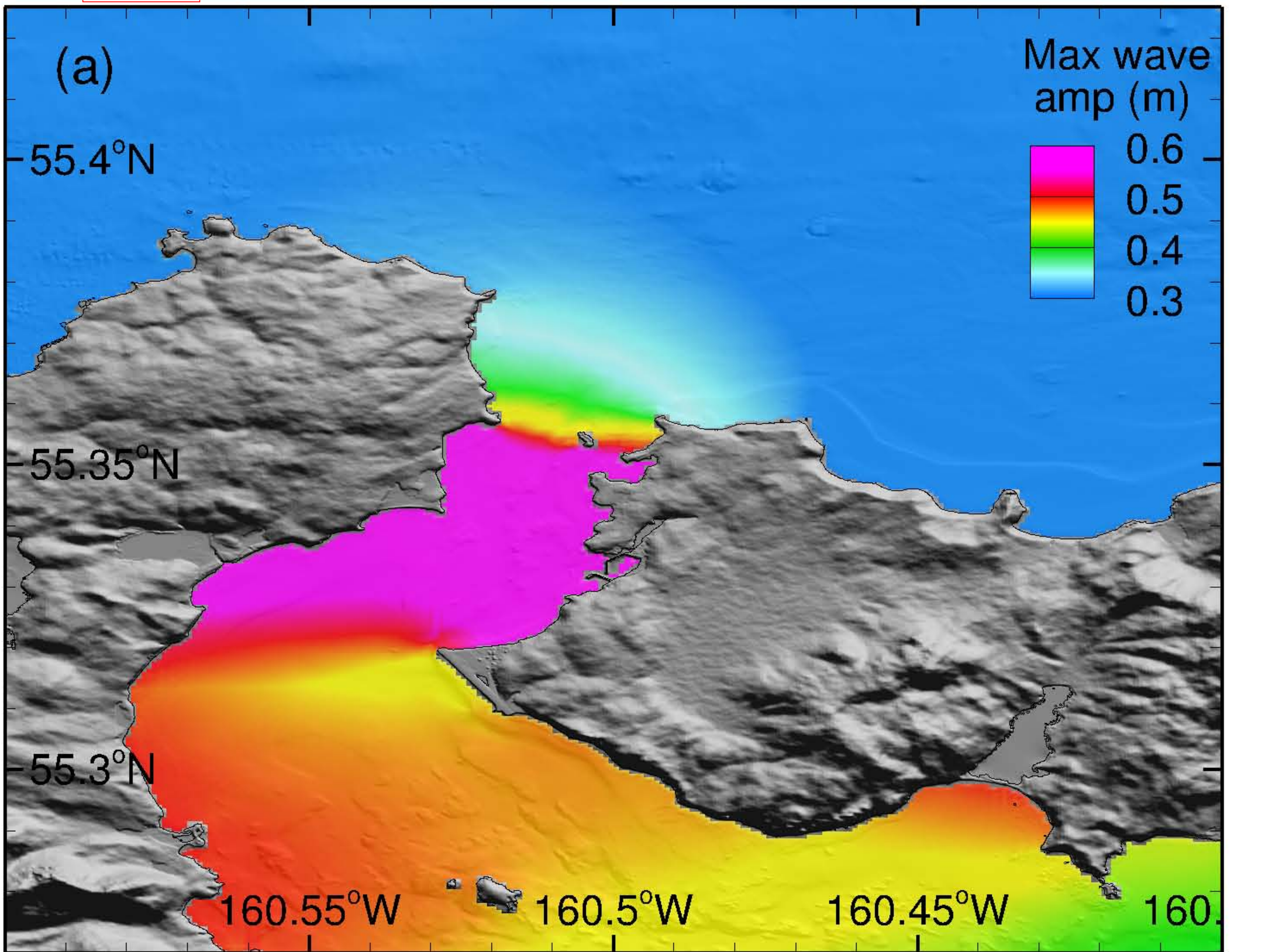


Figure 34

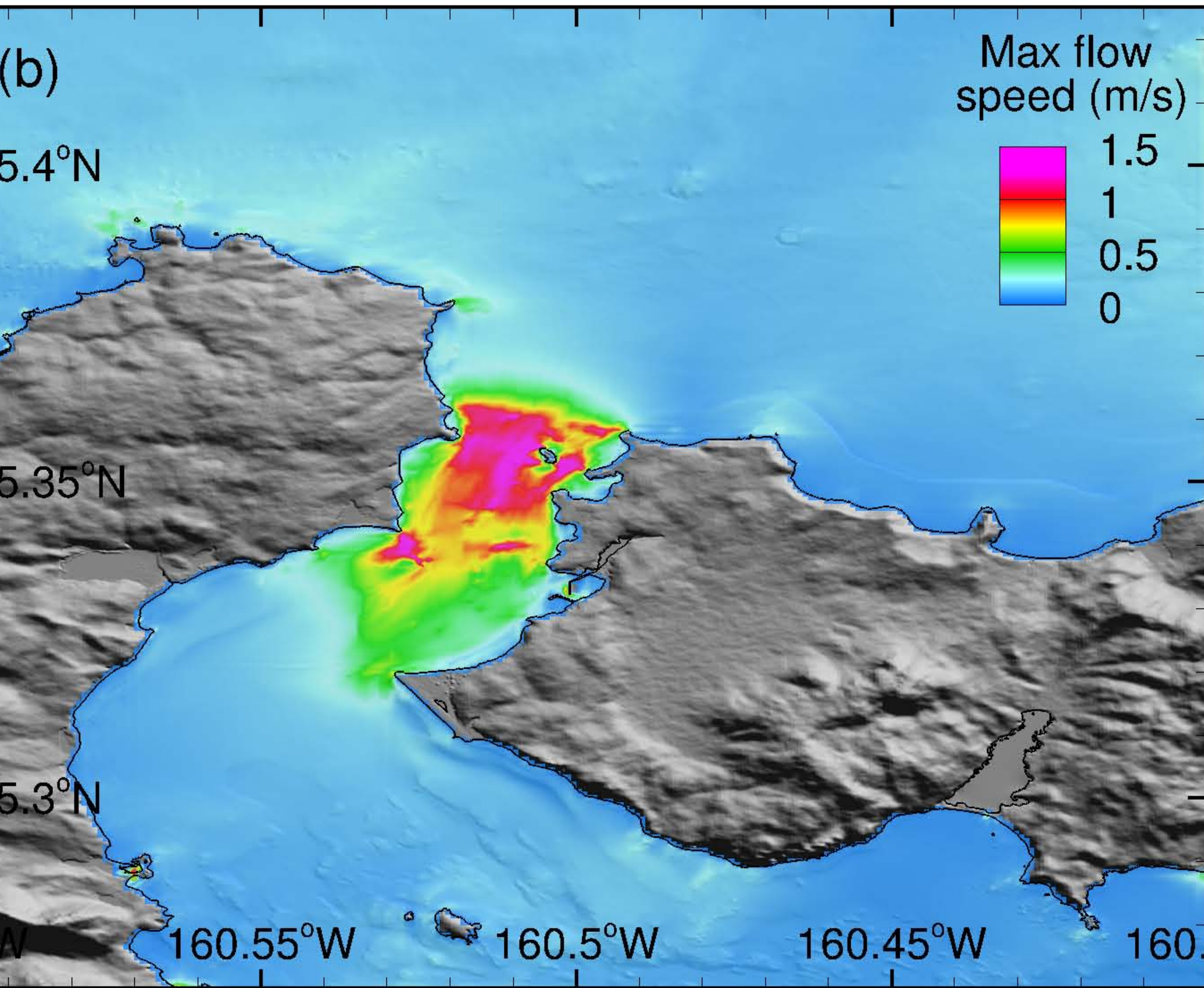
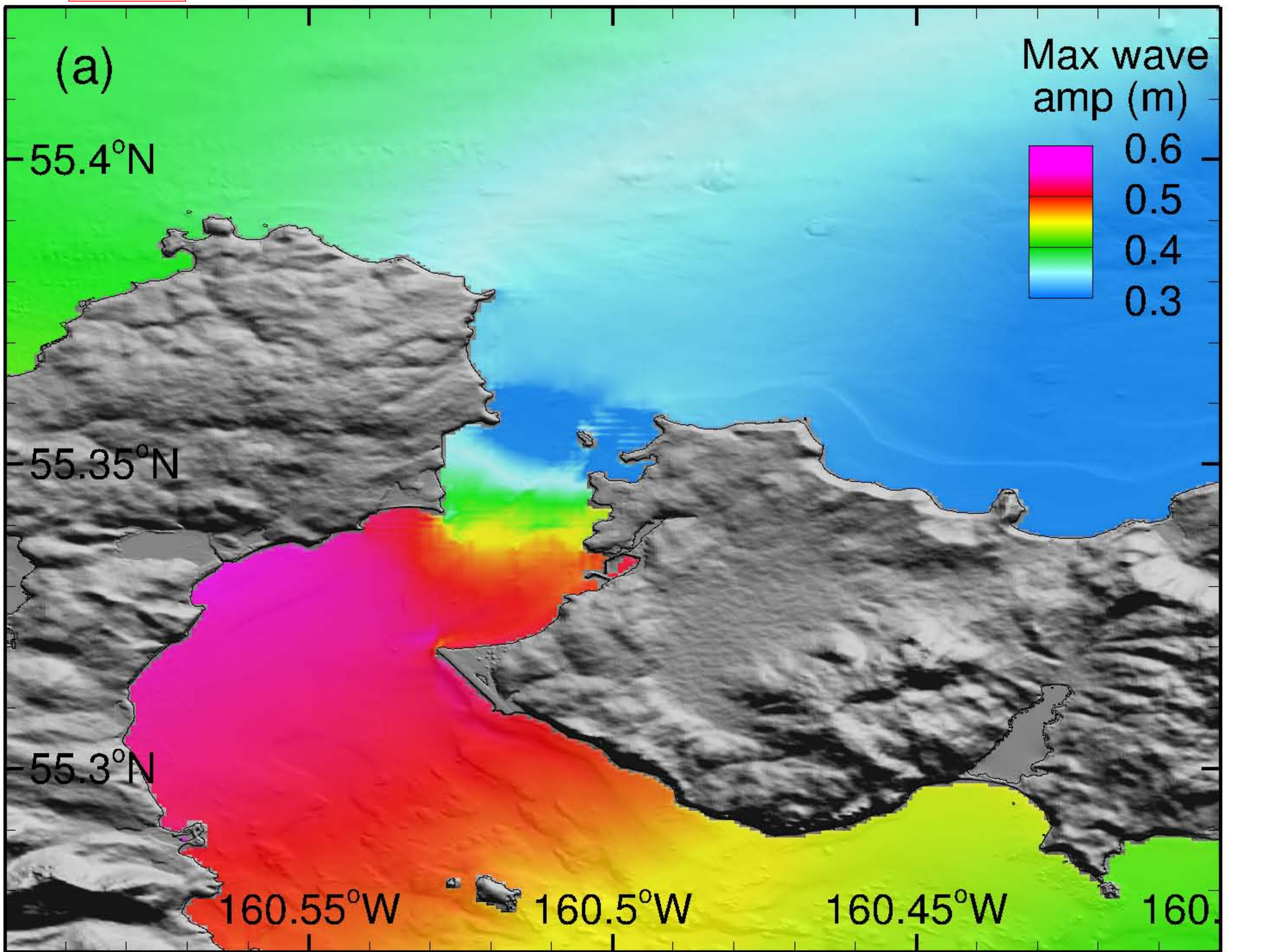


Figure 35

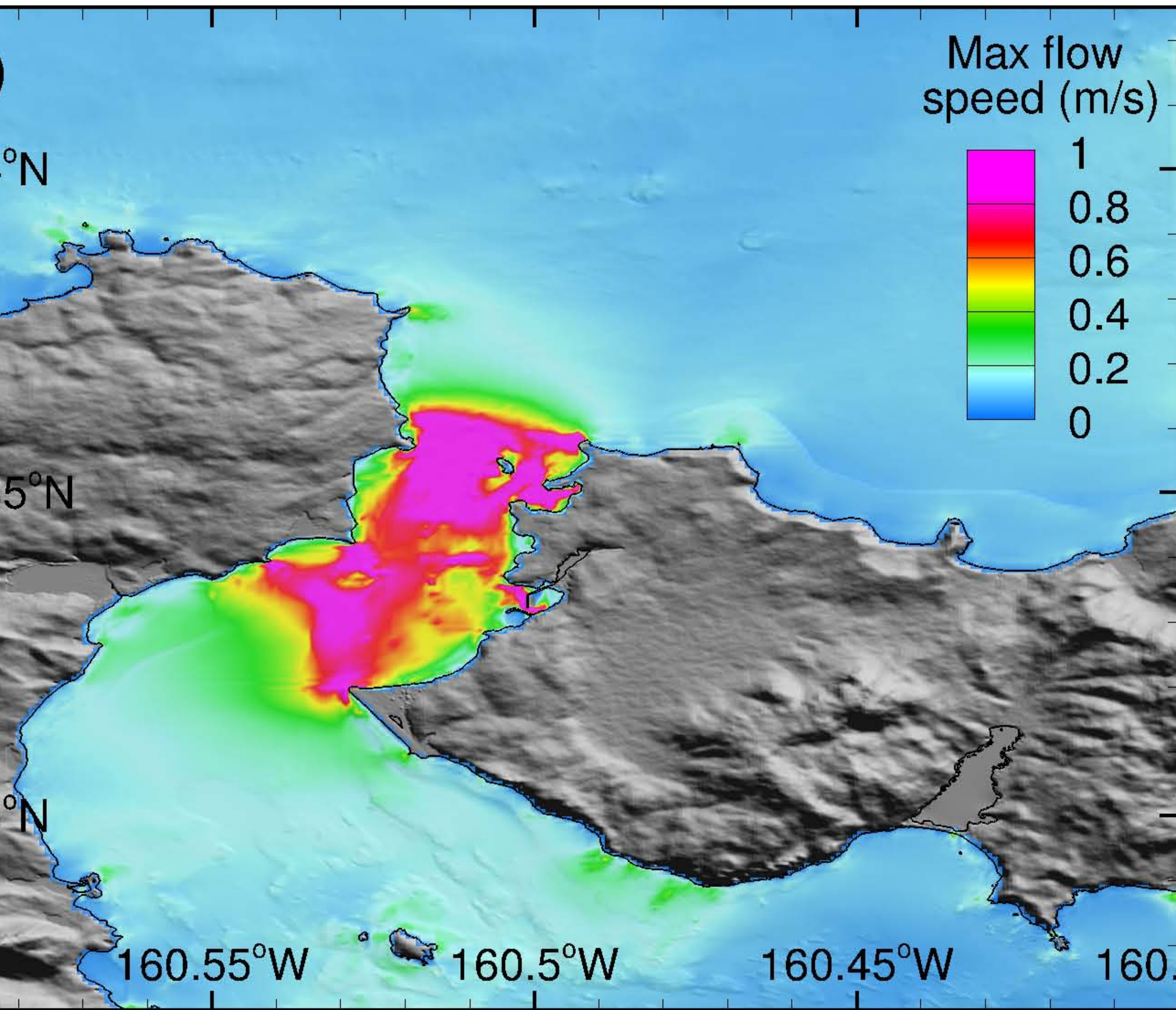
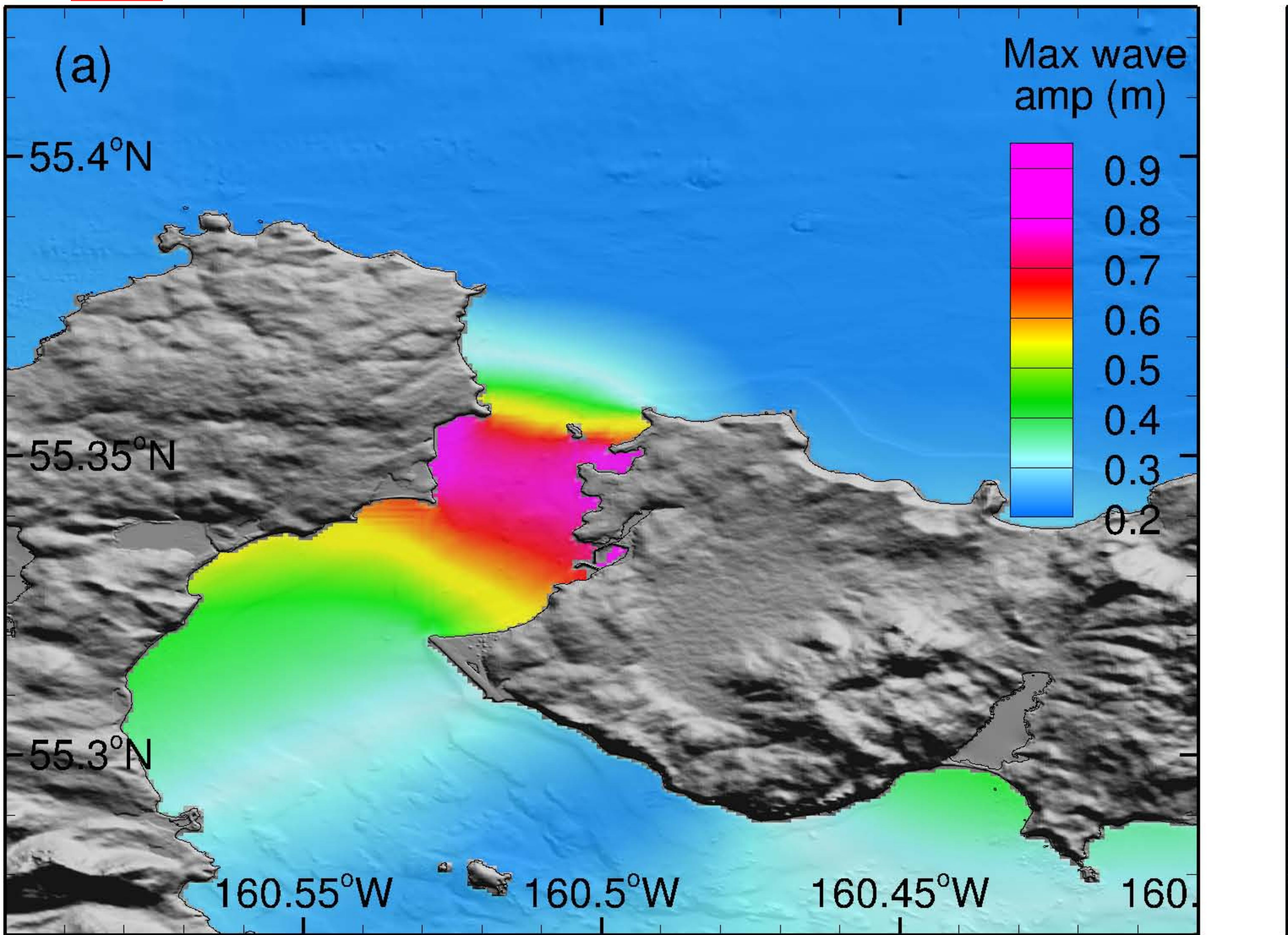


Figure 36

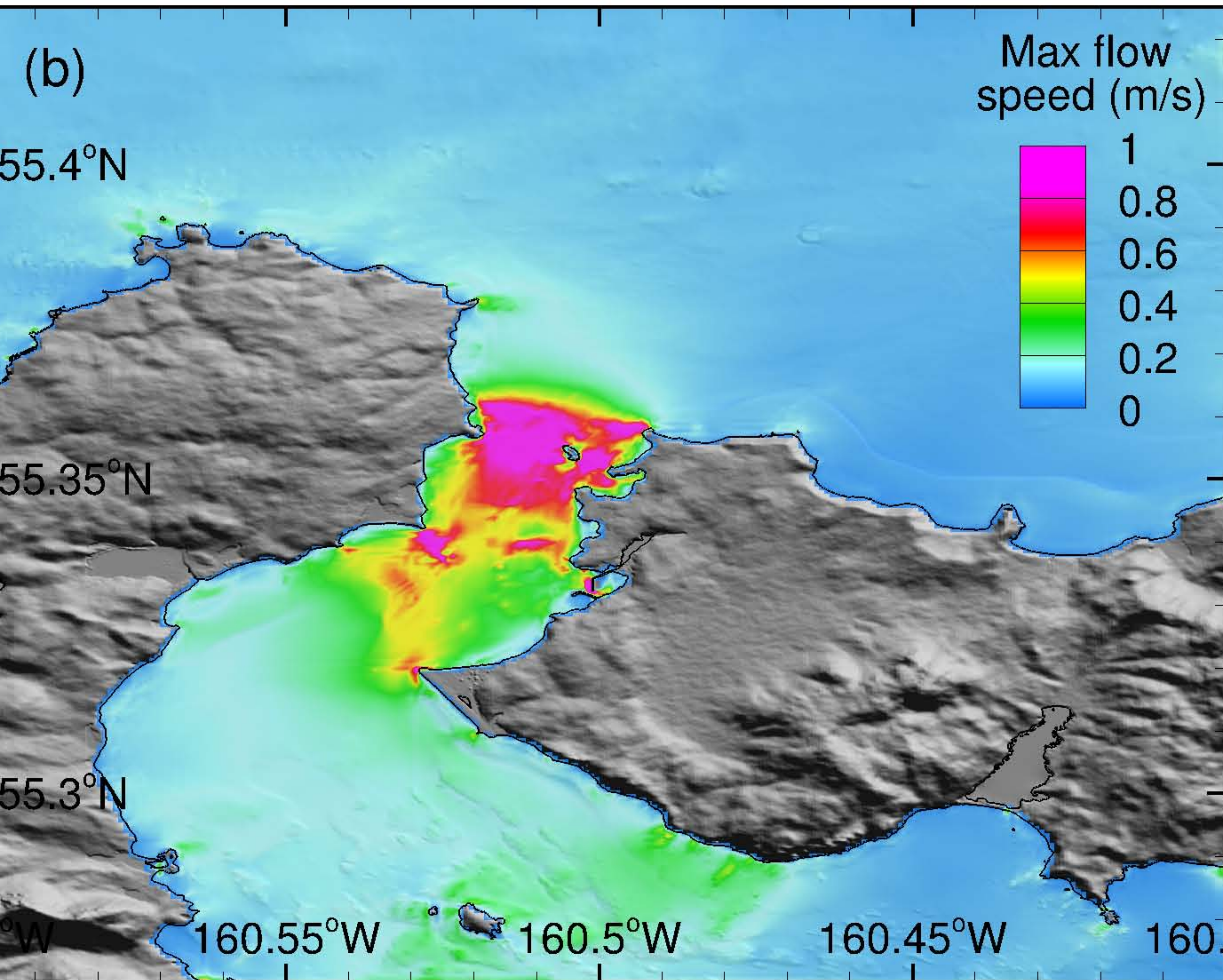
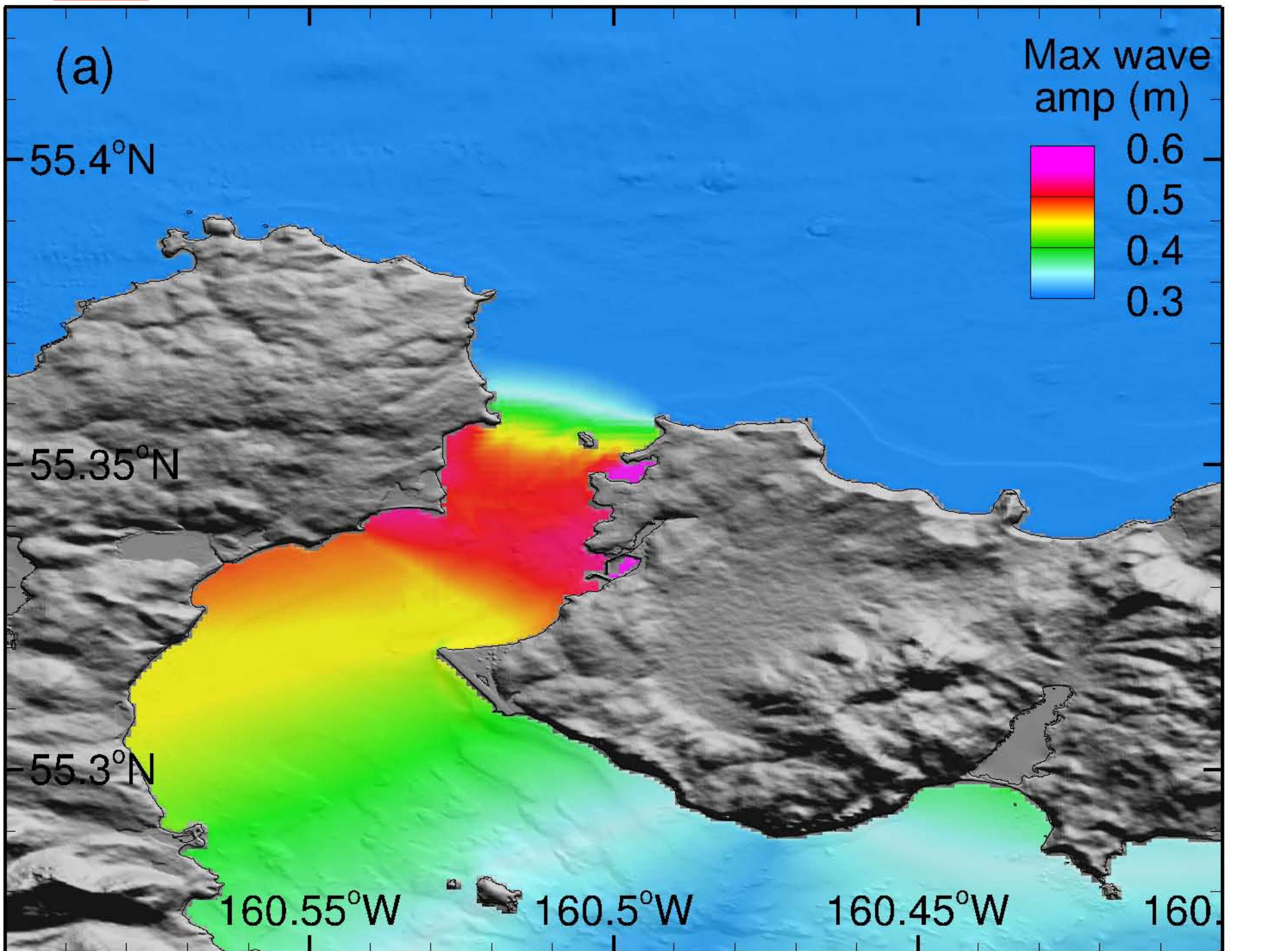


Figure 37

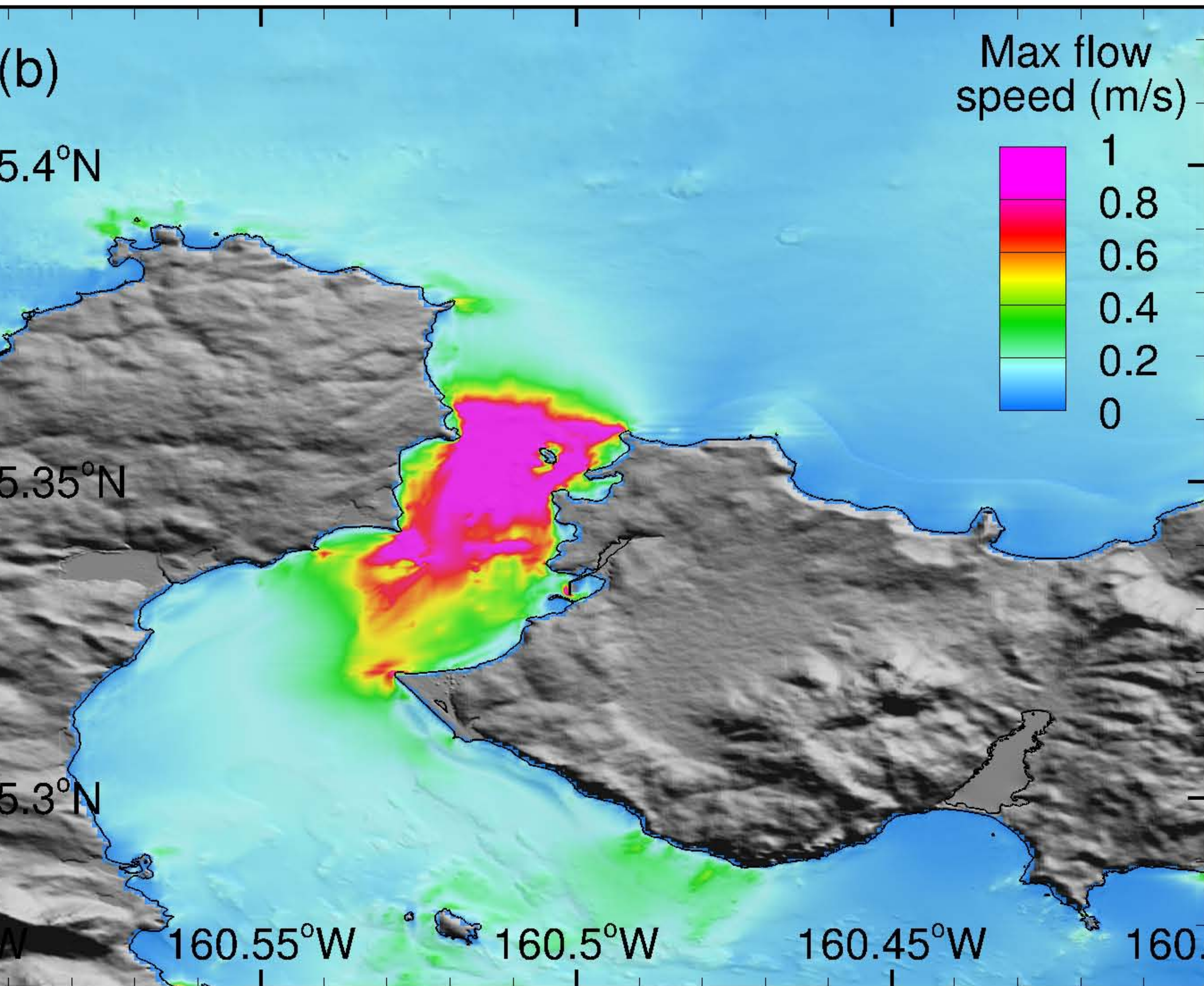
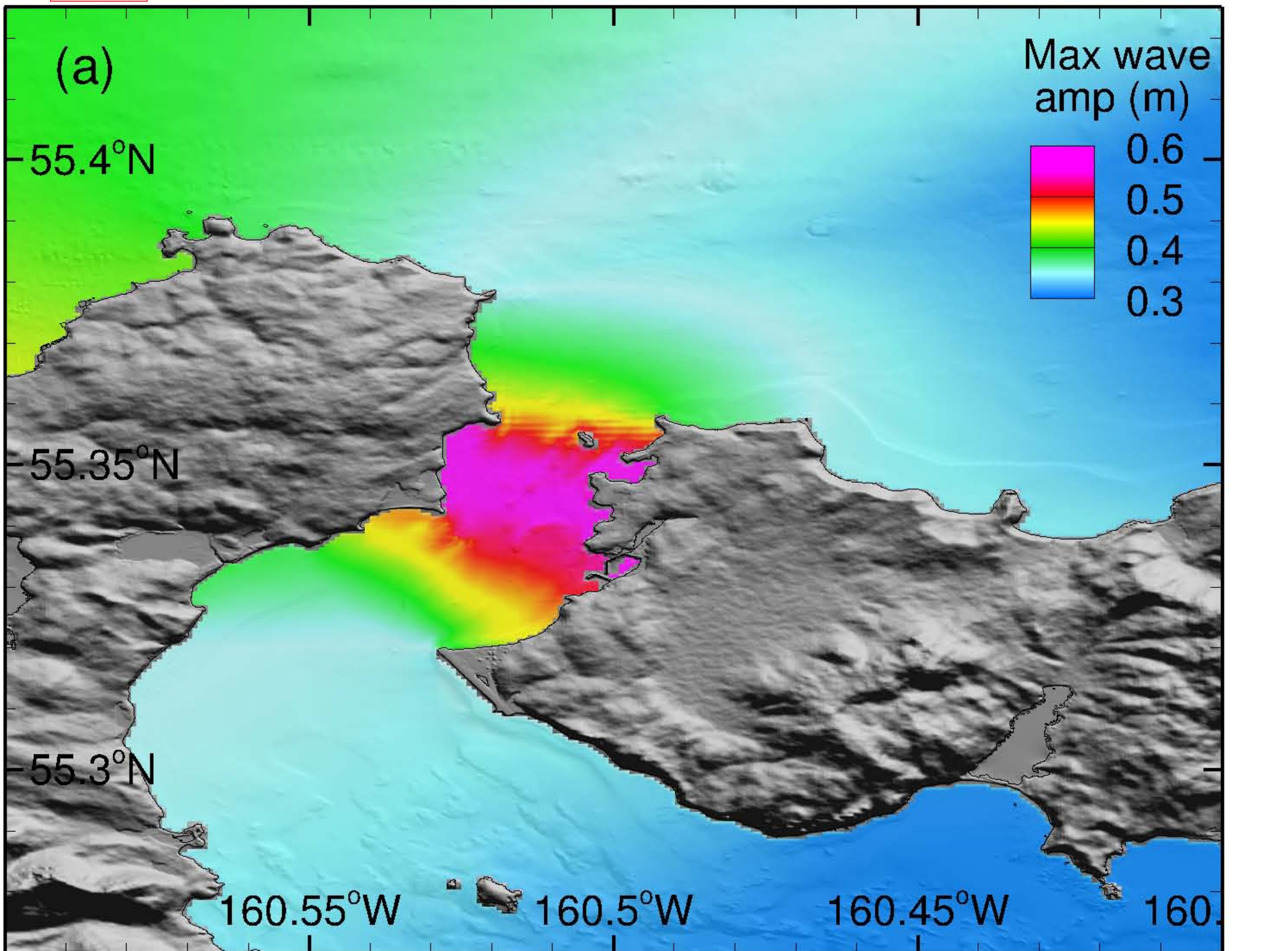


Figure 38

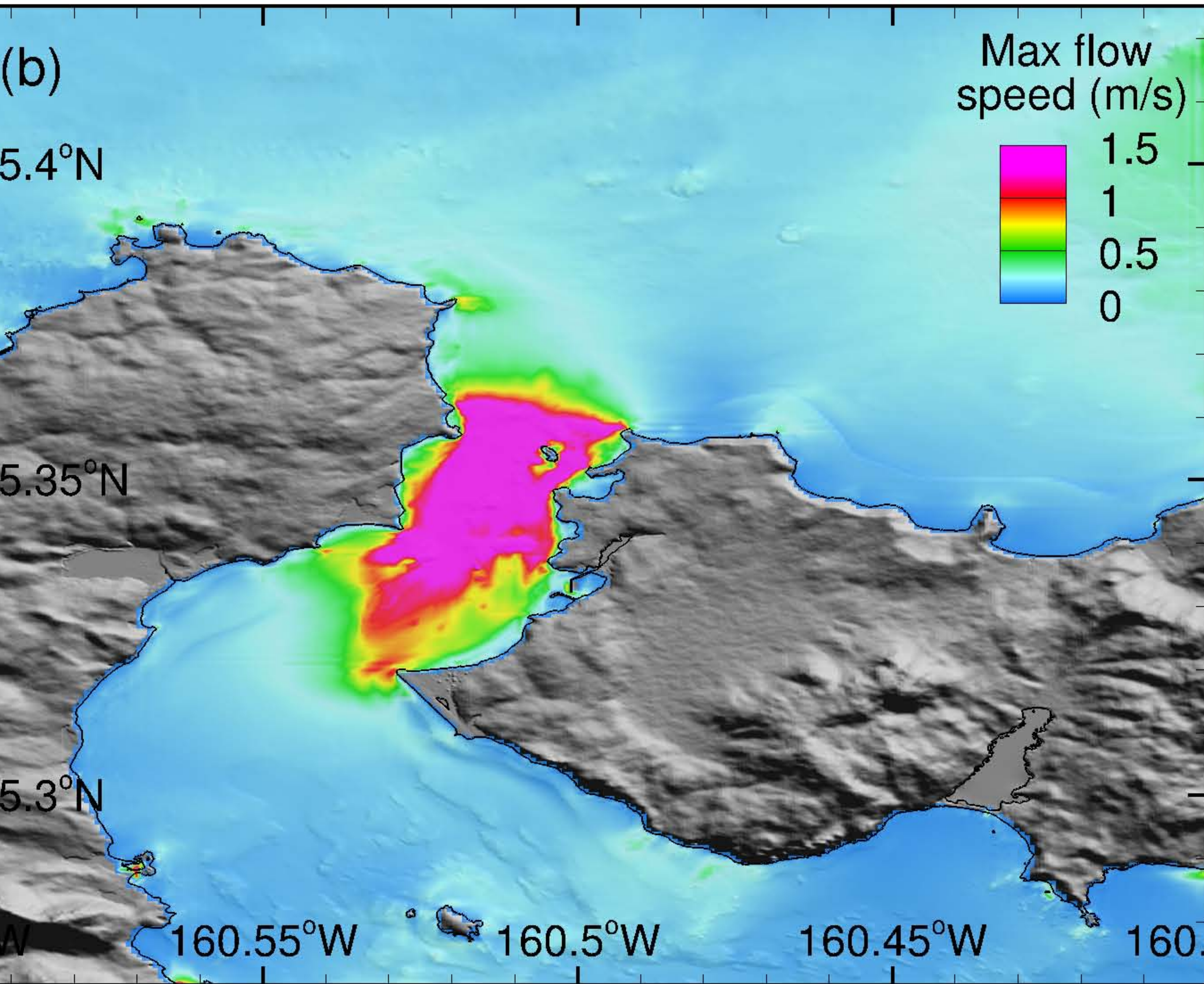
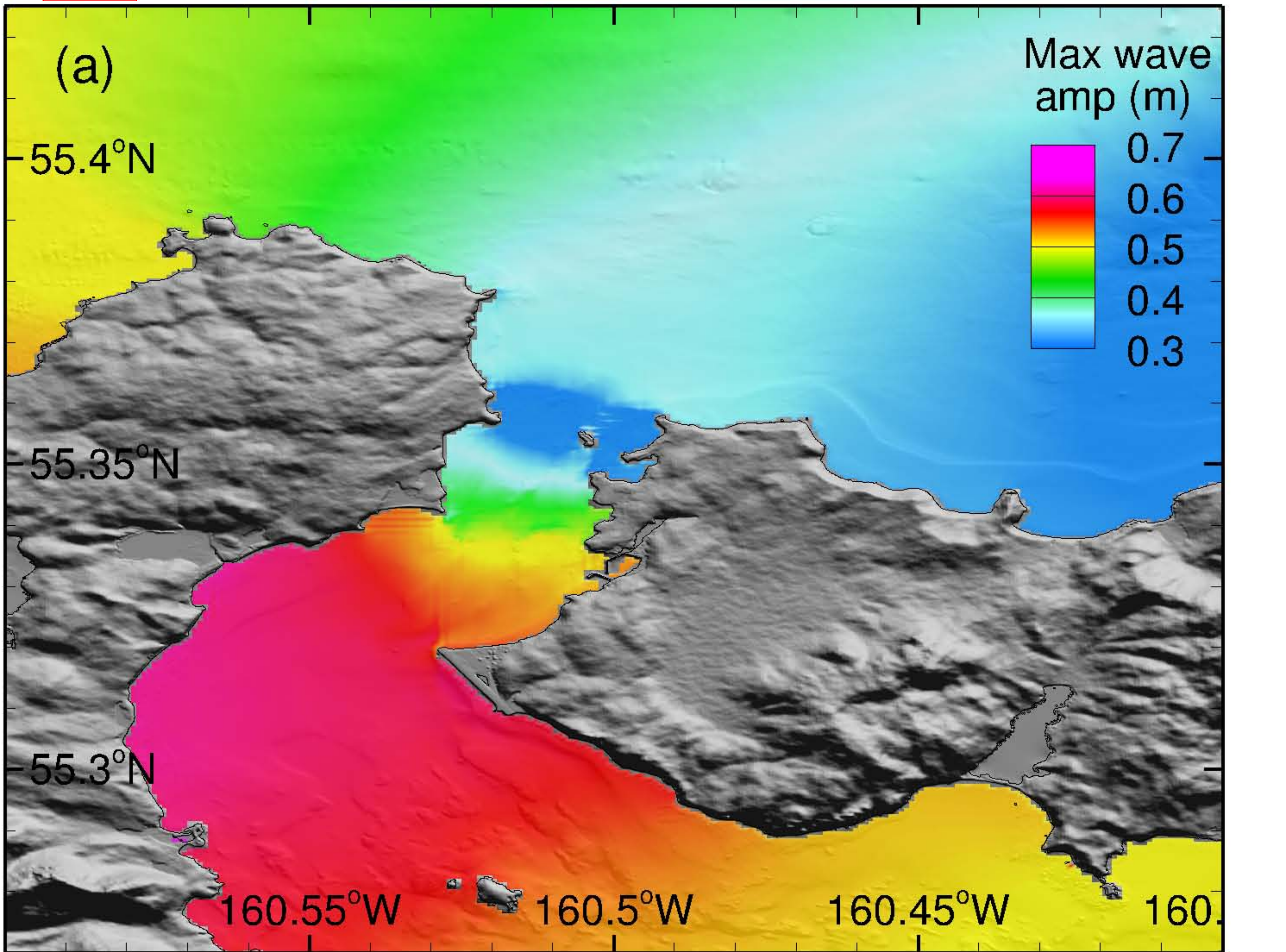


Figure 39

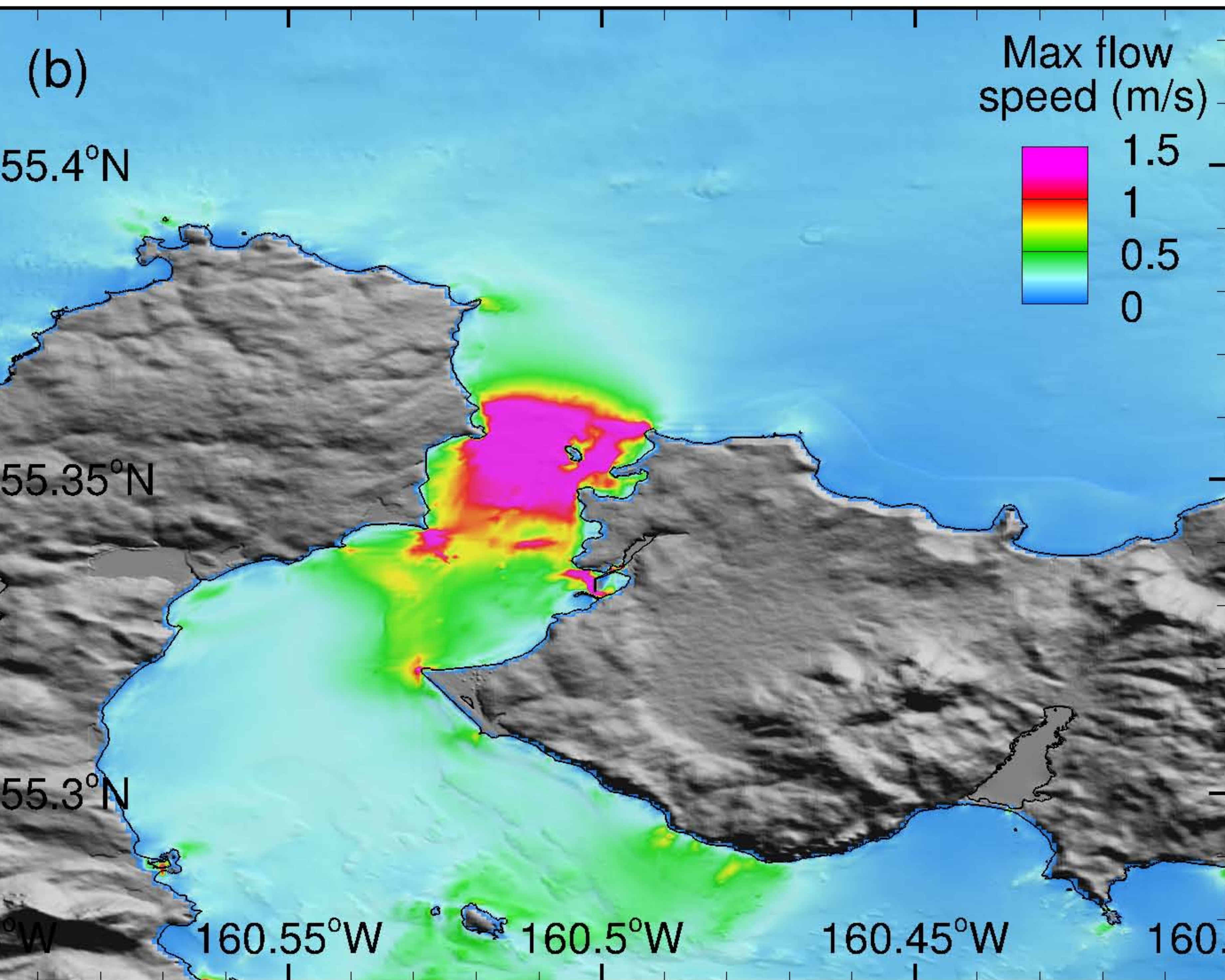
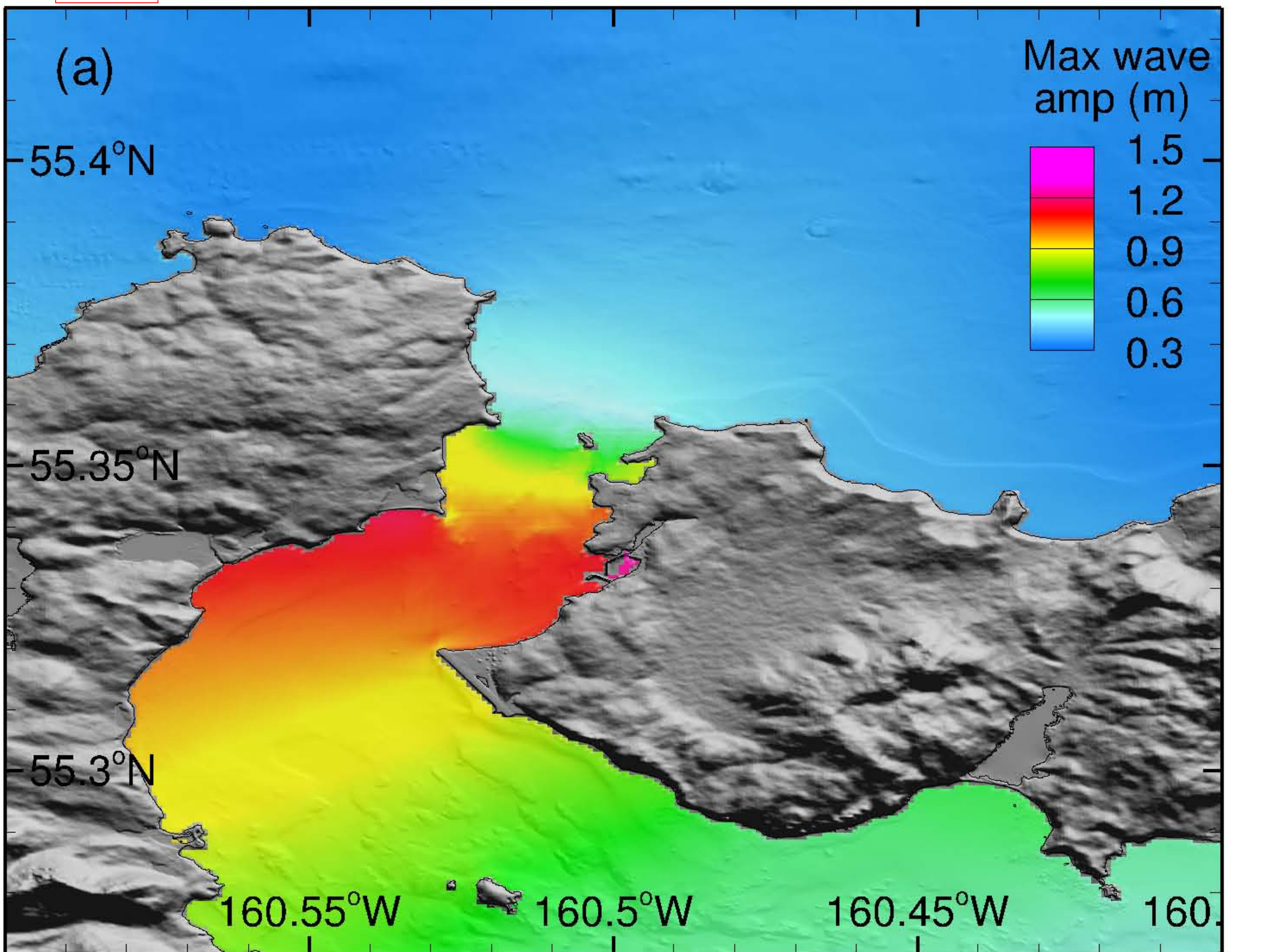


Figure 40

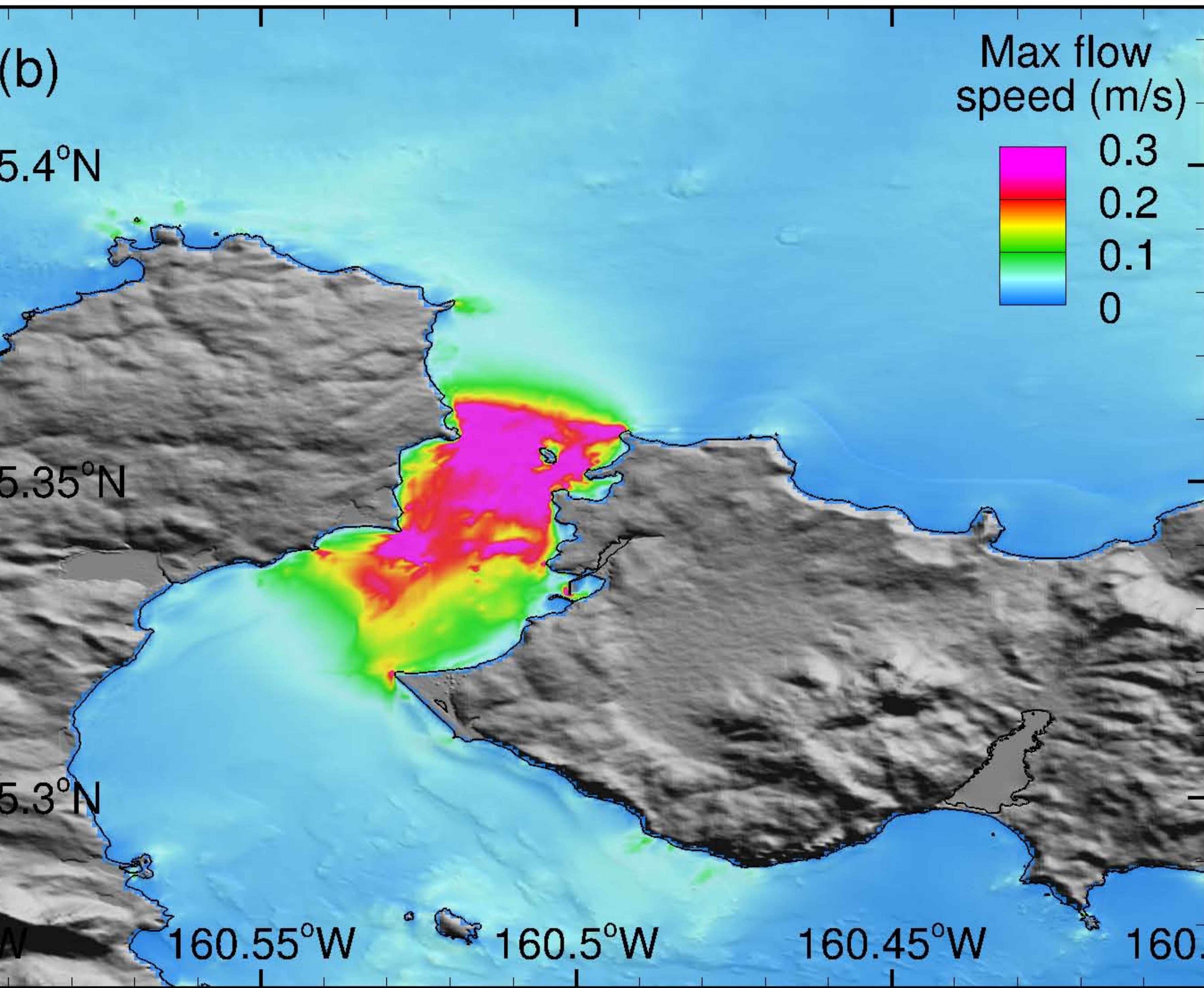
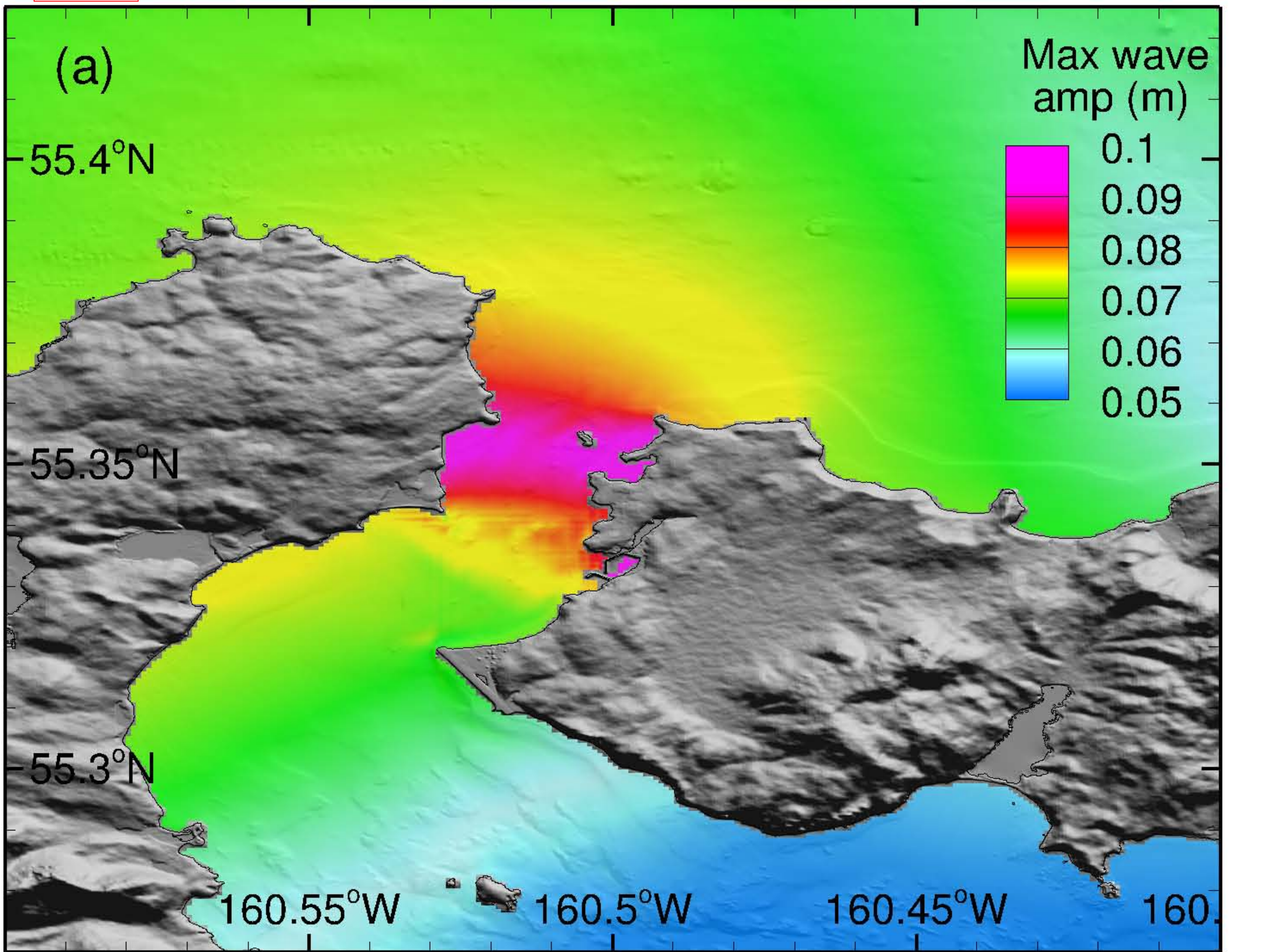


Figure 41

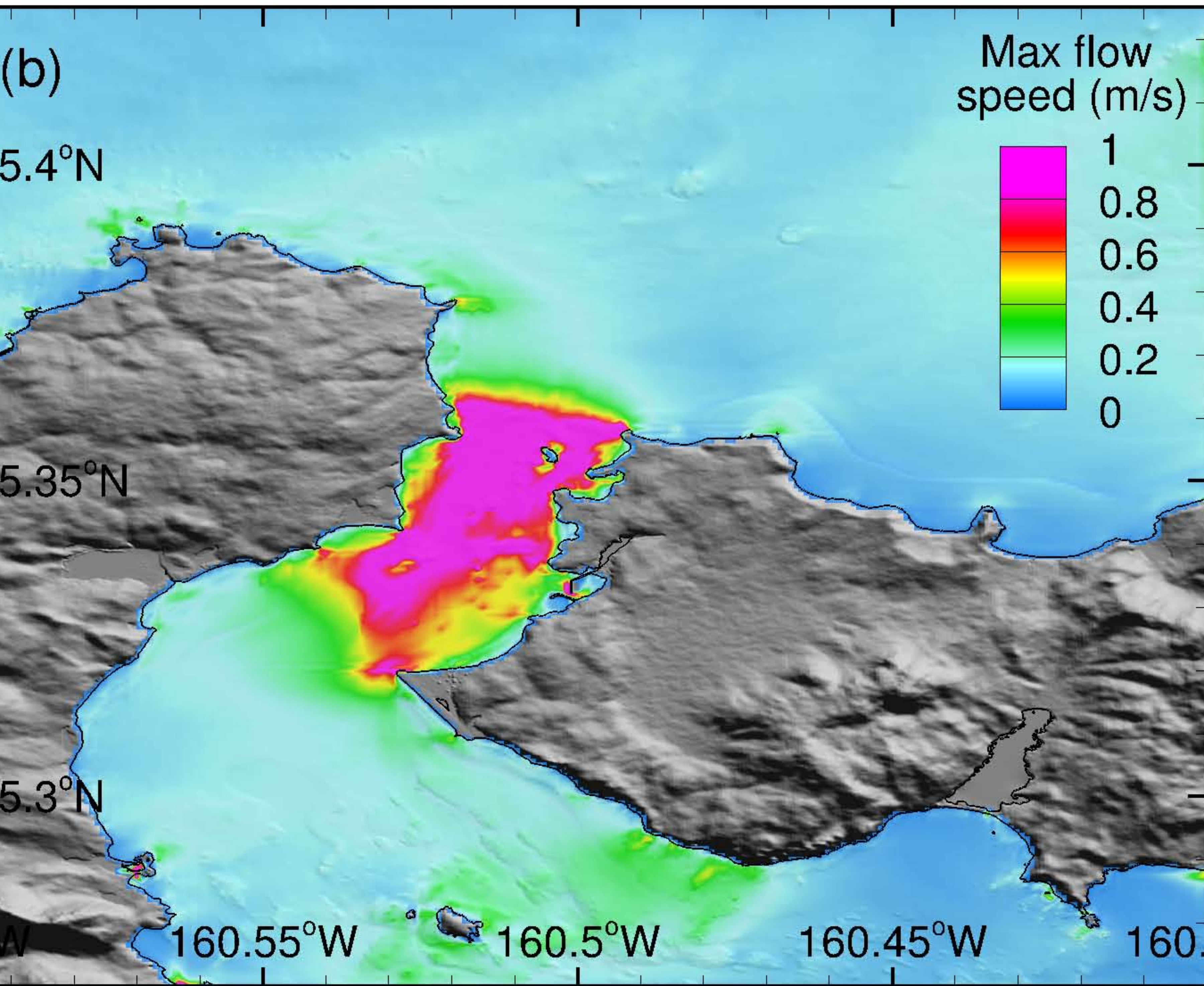
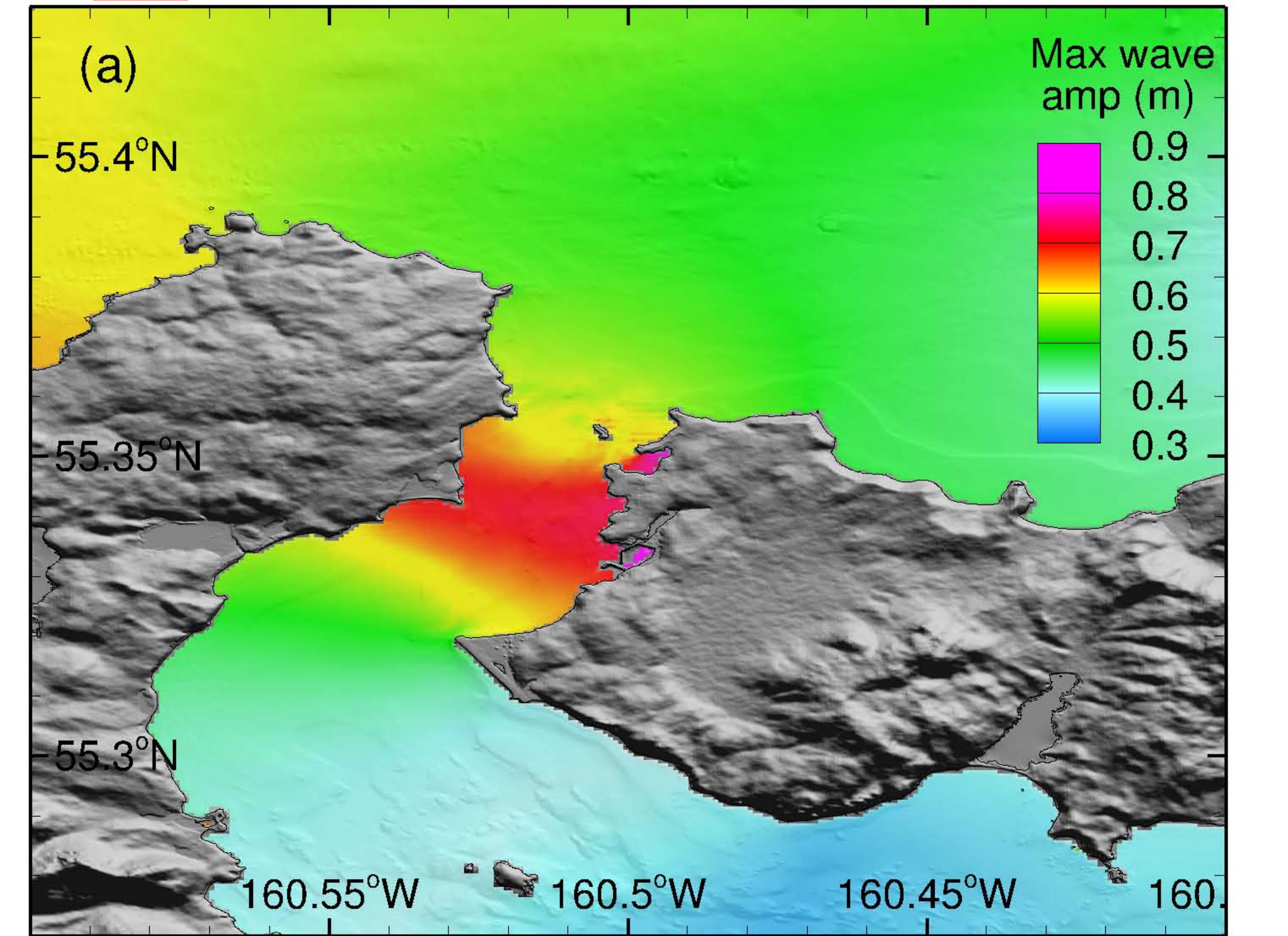
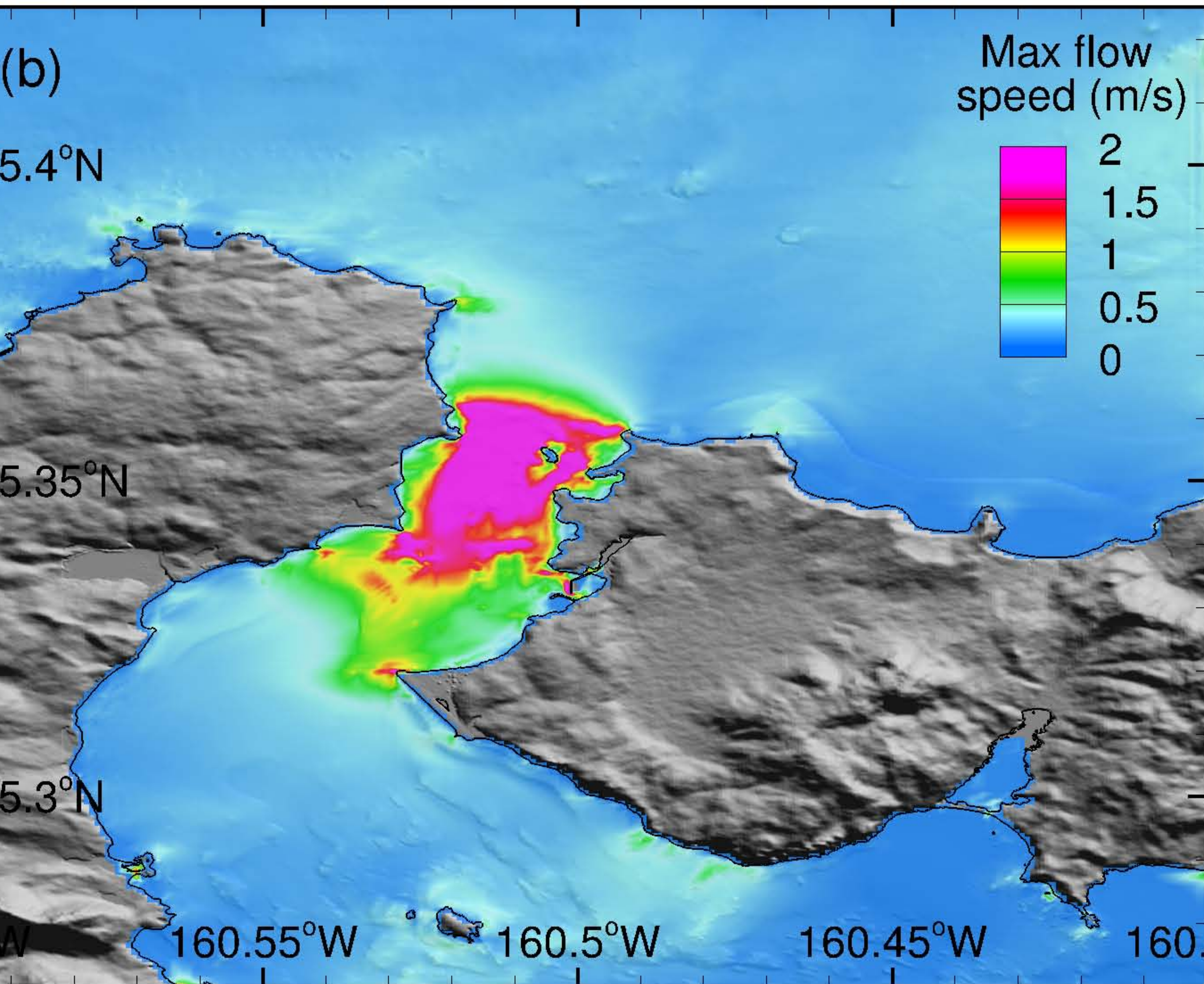
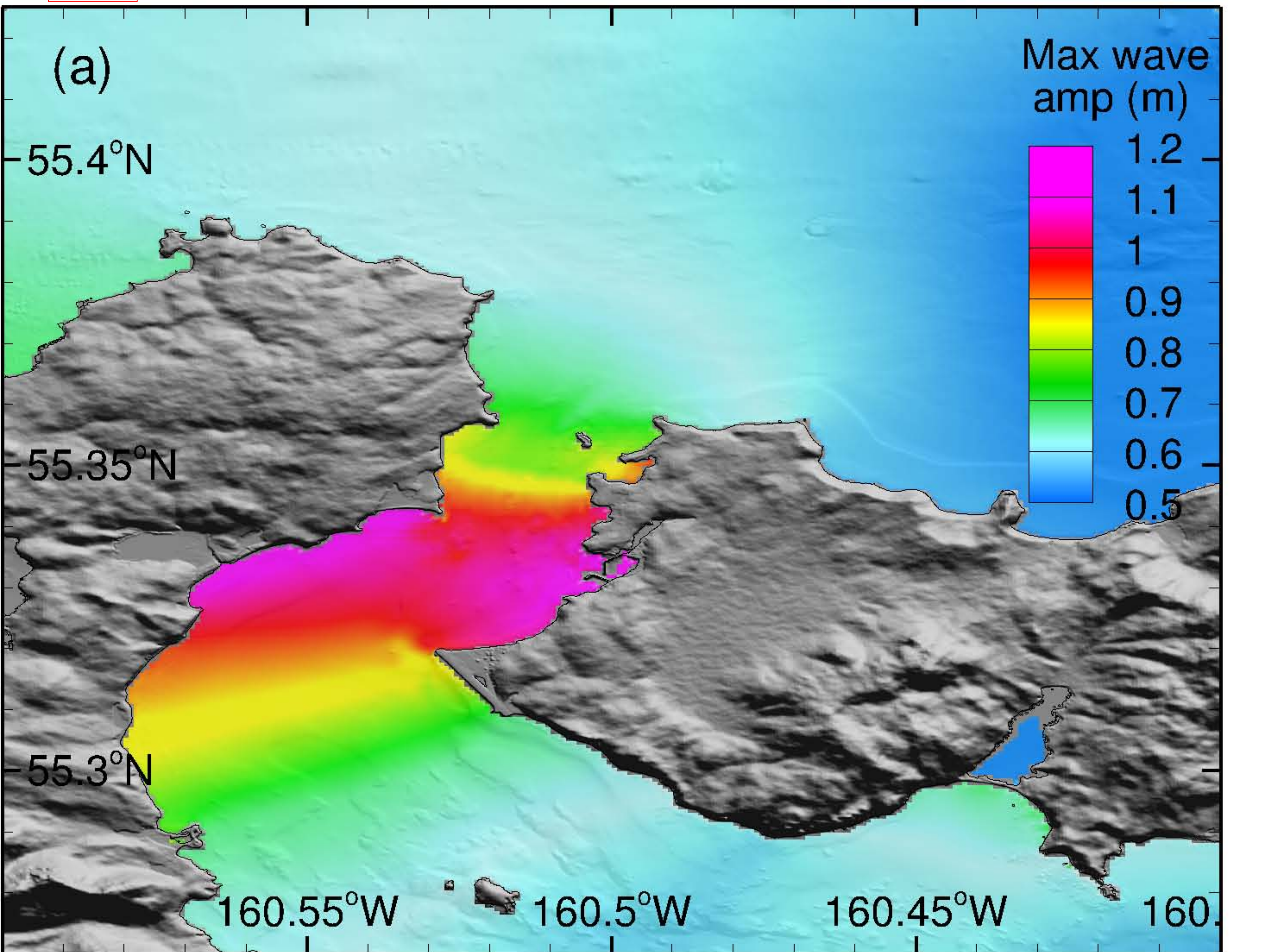


Figure 42

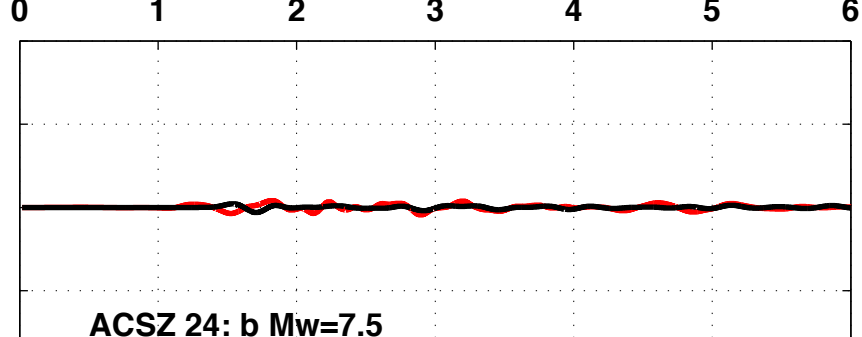
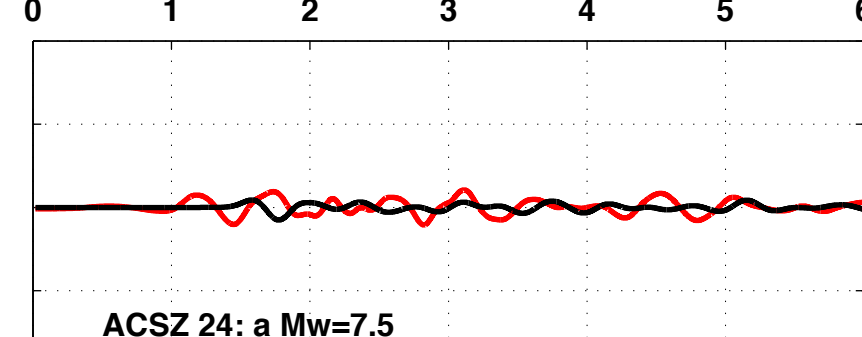
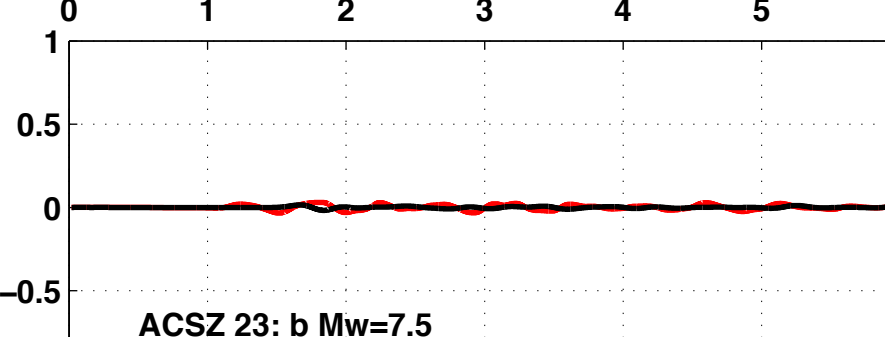
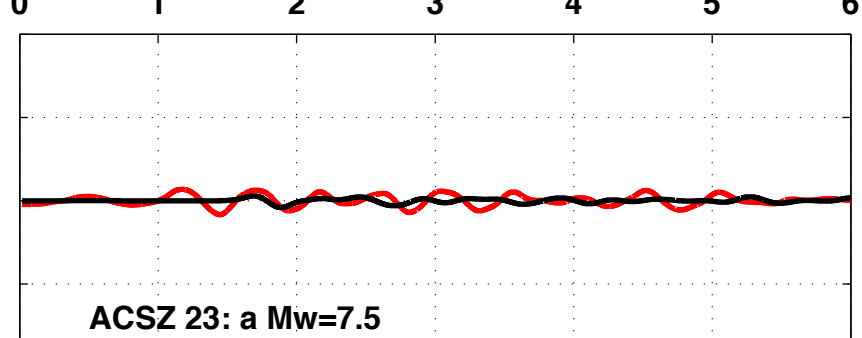
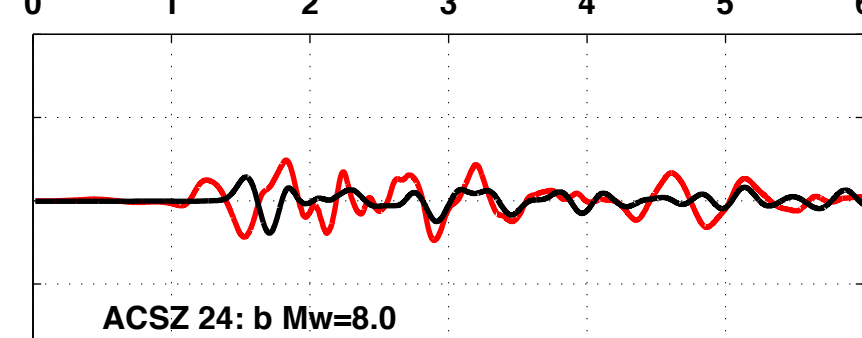
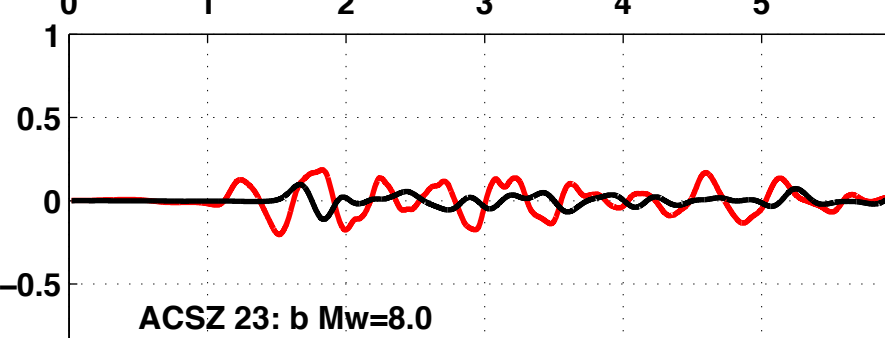
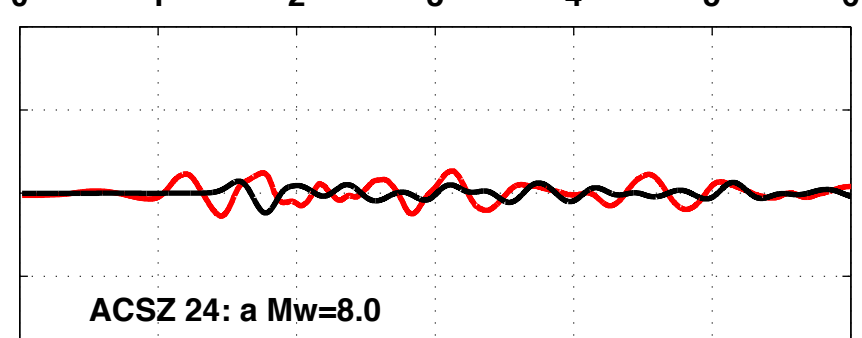
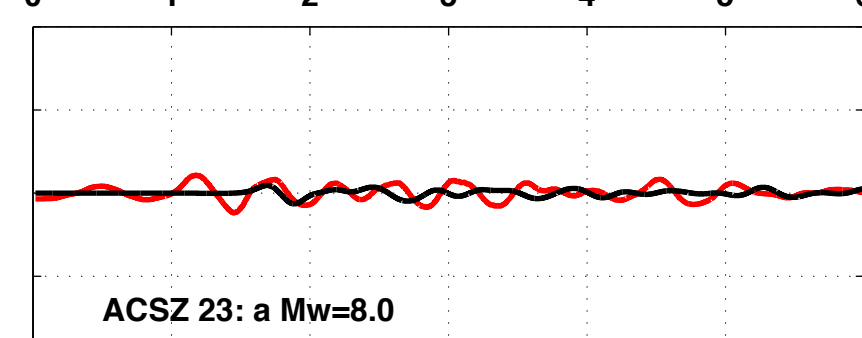
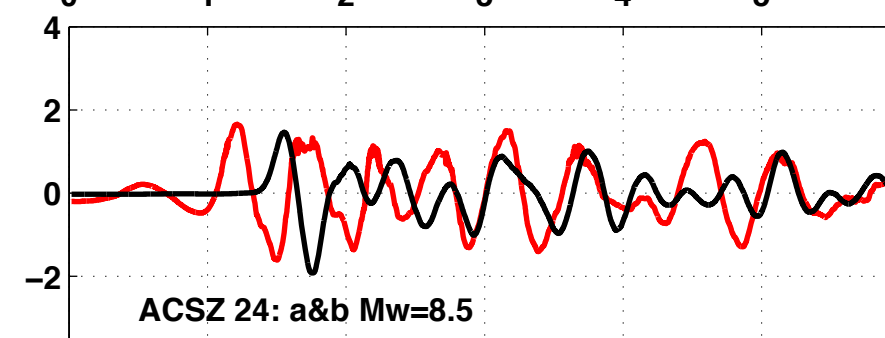
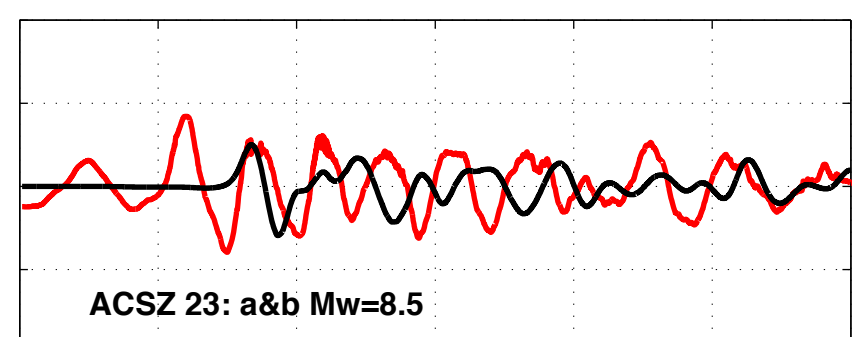
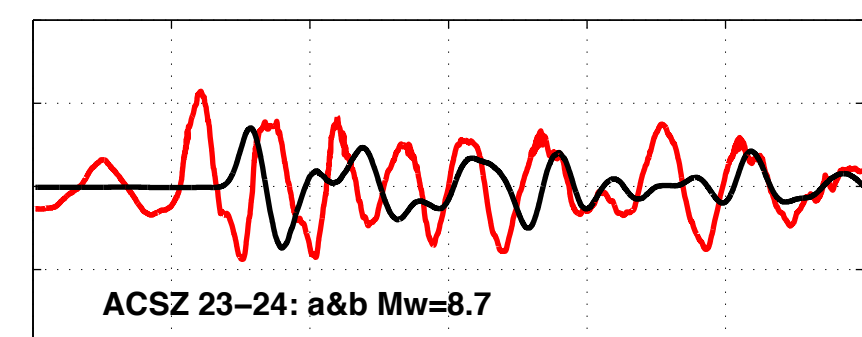
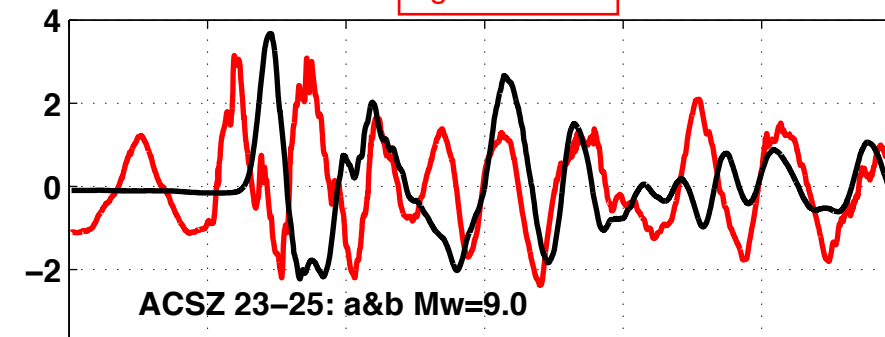


Water Elev. (m)

Figure 43

Unalaska Tide Station

Sand Point Tide Station



Time (hrs. after earthquake)

Water Elev. (m)

Figure 44

— Unalaska Tide Station — Sand Point Tide Station

